Copyright

by

Alexander James McAuley

2015

The Dissertation Committee for Alexander James McAuley Certifies that this is the approved version of the following dissertation:

Generation and Characterization of Flavivirus Receptor-Binding Domain Mutants and Chimeras

Committee:

David Beasley, PhD, Supervisor

Dennis Bente, DVM, PhD, Co-Supervisor

Alexander Freiberg, PhD

Robert Davey, PhD

Michael Holbrook, PhD

_____

Dean, Graduate School

Generation and Characterization of Flavivirus Receptor-Binding Domain Mutants and Chimeras

by

Alexander James McAuley, MBiol

Dissertation

Presented to the Faculty of the Graduate School of

The University of Texas Medical Branch

in Partial Fulfillment

of the Requirements

for the Degree of

Doctor of Philosophy in Microbiology and Immunology

The University of Texas Medical Branch

November, 2015

Acknowledgements

I would firstly like to thank my family and friends who have supported me through the last six years, and have kept me relatively sane. Particular thanks to my understanding wife, Kristen, who has tolerated occasional grumpiness and neglect with good humour, as well as my parents, John and Philippa McAuley, who were but a telephone call away whenever I questioned my life-choices.

Secondly, I would like to thank Dr David Beasley and Dr Dennis Bente for their help and support as my mentors. Their patience and guidance were invaluable, and I hope they are satisfied with the final product. In addition, I would like to thank my committee members, Dr Alexander Freiberg, Dr Robert Davey, and Dr Michael Holbrook, for their direction and feedback during the course of the project.

Finally, I would like to thank the James W McLaughlin Endowment and Jeane B Kempner Endowment for the predoctoral fellowships I received during the course of my studies, as well as the Department of Microbiology & Immunology and the Graduate School of Biomedical Sciences at the University of Texas Medical Branch for their financial support during the transitional stages between mentors.

Generation and Characterization of Flavivirus Receptor-Binding Domain Mutants and Chimeras

Publication No._____

Alexander James McAuley, PhD

The University of Texas Medical Branch, 2015

Supervisors: David Beasley & Dennis Bente

Abstract: Flaviviruses are positive-sense, single-stranded RNA viruses responsible for millions of infections annually. Primarily transmitted by ticks and mosquitoes, their associated diseases range from mild febrile infections to encephalitis and hemorrhagic fever. The molecular basis of the differences in disease presentation between genetically related viruses is uncertain, but potentially involves the putative receptor-binding domain of the envelope glycoprotein, domain III (EIII). In order to determine the tolerance for heterologous sequences, and to characterize the role of EIII in virus growth and tissue tropism, chimeric viruses were generated using the West Nile virus (WNV) infectious clone, into which EIIIs from a range of flaviviruses of increasing genetic diversity from WNV were substituted. Four versions of each chimera were generated using combinations of up- and downstream restriction sites. Of the constructs tested, chimeras containing EIII from Koutango virus (KOUV), Japanese encephalitis virus (JEV), St. Louis encephalitis virus (SLEV), and Bagaza virus (BAGV) were successfully recovered. Characterization of the chimeras *in vitro* and *in vivo* revealed differences in growth and virulence between the viruses. The JEV EIII chimeras behaved similarly to WNV both *in vitro* and *in vivo*. In contrast, the KOUV chimeras, despite

having greater EIII sequence identity, were more attenuated, failing to successfully infect organs other than the kidney, despite generating a strong WNV-like viremia, suggesting a significant change in tissue tropism. The SLEV chimeras were particularly attenuated, with low peak viremia, suggesting a poor infection of early targets, despite strong WNV-like growth *in vitro*. The BAGV chimeras were similarly attenuated, with temperature sensitivity assays suggesting lower particle stability than the other viruses. In addition to the chimeras, *in vivo* characterization of a WNV EIII single-site G331A mutant was performed. This virus was significantly attenuated, even in immunodeficient mice, suggesting that receptor-binding had been significantly impaired. Mutations present in isolates from mouse brains suggested that the G331A mutant could be compensated for, presumably through the alteration of receptor usage. Taken together, the data demonstrate that mutations and substitutions of EIII can significantly affect virulence and tissue tropism *in vivo*, in keeping with the hypothesis that this region is the flavivirus receptor-binding domain.

TABLE OF CONTENTS

List of Tables xii

List of Figures xiv

List of Abbreviations xviii

INTRODUCTION 1

Chapter 1: Introduction 1

Genome 2
Viral Proteins 13
Translation and Processing of the Flaviviral Polyprotein 16
Capsid Protein (C) 17
Membrane Glycoprotein (prM) 19
Envelope Glycoprotein (E) 22
Non-Structural Protein 1 (NS1) 24
Non-Structural Protein 1' (NS1') 27
Non-Structural Protein 2a (NS2a) 28
Non-Structural Protein 2b (NS2b) 29
Non-Structural Protein 3 (NS3) 30
Non-Structural Protein 4a (NS4a) 32
2K Protein 34
Non-Structural Protein 4b (NS4b) 35
West Nile Virus Alternative Reading Frame 4 (WARF4) 37
Non-Structural Protein 5 (NS5) 37
Lipids 41
Structure of the Virion 42
The Flavivirus Replication Cycle 46
Receptor Binding 47
Virus Entry 50
RNA Translation and Polyprotein Processing 53
RNA Replication and Packaging 53
Virus Maturation and Secretion 56

Antigenic Properties of Flaviviruses....57
Flavivirus Transmission....64
West Nile Virus....68
Animal Models for WNV....72
Flavivirus Chimeras....75
Project Rationale....80

MATERIALS AND METHODS....93

Chapter 2: Materials and Methods....93

Cell and Virus Procedures....93
Viruses and Infectious Clone Plasmids....93
Cells and Tissue Culture....94
Virus Culture....96
Virus Titration – Plaque Assay....97
Virus Titration – Immunostaining....98
Virus Growth Kinetics....99
Virus Neutralization Assays....100
Temperature-Sensitivity Assays....101
Molecular Procedures....103
RNA Purification – TRIzol....103
RNA Purification – QIAamp Viral RNA Mini Kit....104
Reverse Transcription....105
Polymerase Chain Reaction (PCR)....106
DNA Gel Electrophoresis....107
Purification of DNA Bands from Agarose Gel....108
Purification of PCR Products....109
pGEM Cloning of PCR Products....110
Transformation of Plasmids into Bacteria & Generation of Glycerol Stocks....110
Culture of Bacteria from Glycerol Stocks....111
Purification of Plasmids – Miniprep....112
Purification of Plasmids – Midiprep....112
Nucleic Acid Quantification....113

Restriction Digests 114
DNA Sequencing 114
Site-Directed Mutagenesis 116
Virus Recovery from Infectious Clone – pWN-AB & -CG System 118
Virus Recovery from Infectious Clone – pWNV System 122
Next-Generation Sequencing 124
Animal Procedures 126
Mouse Model 126
Assessment of Neurovirulence and Neuroinvasion 126
Serial Sacrifice Studies 127
Other Assays 129
Cytokine & Chemokine Determination – MilliPlex 129
Enzyme-Linked Immunosorbent Assay (ELISA) 130
Western Blot 131
Statistical Analyses 132

EXPERIMENTAL RESULTS 133

Chapter 3: Generation, Recovery, and *in vitro* Characterization of Chimeric Flaviviruses 133

Introduction 133
Modification of pWN-AB Infectious Clone Plasmid 134
Construction of Chimeric Viruses 136
Recovery of Chimeric Viruses 137
"Reverse Chimerization" of DENV-2 Constructs 139
Recovery and Passaging of Inviable Viruses in prM-E Expressing Cells 139
Vero Cell Growth Kinetics 140
C6/36 Growth Kinetics 142
Stability of Chimeric Sequences 143
Characterization of SLEV A Passage 1 146
Antigenicity of Chimeric Viruses 147
Discussion 149

Chapter 4: *in vivo* Characterization of Chimeric Viruses 185

Introduction.....185
Chimeric Virus Virulence Studies – Single Dose (100pfu) i.p.....186
Neurovirulence Studies with Chimera B-Forms.....187
Serial Sacrifice Studies with Chimera B-Forms.....188
Survival.....189
Temperatures & Weights.....189
Viremia and Virus Loads in Organs.....190
Hematology.....193
Cytokines and Chemokines.....195
Serial Sacrifice Comparison of JEV A- and JEV B-Forms.....199
Discussion.....201

Chapter 5: *in vivo* Characterization of WNV EIII Single-Site G331A Mutation.....225

Introduction.....225
Virulence in Swiss Webster Mice Following i.p. and i.c. Inoculation.....226
Serial Sacrifice Study with WNA G331A Following i.p. Inoculation (100pfu).....227
Virulence in IFNα/β Receptor Knock-out Mice.....228
Virulence of WNV G331A Adaptive Mutants in Swiss Webster and IFNα/β Knock-out Mice.....229
Discussion.....230

FINAL DISCUSSION 242

Chapter 6: Final Discussion, Summary, and Future Direction.....242

Discussion.....242
Summary and Conclusion.....255
Future Directions.....255

APPENDICES.....260

Appendix A: Primer List.....260

Mutagenesis Primers.....260
Sequencing Primers.....263

Appendix B: Antibody List....264

Mono- and Polyclonal Antibodies....264

Mouse Immune Ascitic Fluid....264

References....265

Vita....345

Education....345

Publications....345

Research Papers....346

Review Papers....347

Presentations....348

List of Tables

Chapter 1:

Table 1.1: Published Structural Protein Substitution Chimeric Flavivirus Studies ...91

Table 1.2: Candidate Flavivirus Receptors 92

Chapter 2:

Table 2.1: List of Donor Viruses with Strain Details and Material Source 94

Chapter 3:

Table 3.1: Mutations in the Chimeric Plasmids Compared to Published Sequences 174

Table 3.2: Chimeric Plasmids Generated and Viruses Recovered 175

Table 3.3: Mean Plaque Sizes and Statistical Comparison 176

Table 3.4: Statistical Comparison of Growth Kinetics in Vero Cells 177

Table 3.5: Statistical Comparison of Growth Kinetics in C6/36 Cells 179

Table 3.6: Mutations in Passage 0 Viruses 180

Table 3.7: Mutations in Passage 1 Viruses 183

Table 3.8: Neutralization of B-Form Chimeras with WNV-Specific Immune Sera and MIAF 184

Chapter 4:

No Tables in this Chapter

Chapter 5:

Table 5.1: Adaptive Mutations Present in WNV G331A Isolated from Mouse Brains 241

Chapter 6:

No Tables in this Chapter

List of Figures

Chapter 1:

Figure 1.1: Structure of WNV 5' and 3' UTRs 85

Figure 1.2: Structure of Flavivirus Genome and Polyprotein Maturation 86

Figure 1.3: Structure of WNV Envelope Glycoprotein 87

Figure 1.4: Structure of Mature Flavivirus Virion 88

Figure 1.5: Flavivirus Replication Cycle 89

Figure 1.6: Symptoms of Human West Nile Virus Infection 90

Chapter 2:

Figure 2.1: Thermocycler Settings for Polymerase Chain Reaction 107

Figure 2.2: Thermocycler Settings for Sequencing Sample Preparation 115

Figure 2.3: Thermocycler Settings for Site-Directed Mutagenesis 117

Chapter 3:

Figure 3.1: Location of Restriction Sites Engineered into pWN-AB 162

Figure 3.2: Comparison of Plaque Morphology and *in vitro* Growth Kinetics of WNV NY99 and the Four Restriction Site-Containing Backbone Virus 163

Figure 3.3: Insert Size and Composition Comparison for the Four Chimera Versions 164

Figure 3.4: Plaque Morphology of the Chimeric Viruses 165

Figure 3.5: Comparison of Virus Titer at 37°C and 41°C.....166

Figure 3.6: Generation of DENV-2 "Reverse Chimeras" 167

Figure 3.7: Growth Kinetics of Chimeric Viruses in Vero Cells 168

Figure 3.8: Growth Kinetics of Chimeric Viruses in C6/36 Cells 169

Figure 3.9: Characterization of SLEV A Passage 1 170

Figure 3.10: Antigenicity of Chimeric Viruses 171

Figure 3.11: Alignment of Donor EIII Amino Acid Sequences.....172

Figure 3.12: Correlation Between Chimera Metrics 173

Chapter 4:

Figure 4.1: Virulence of WNV 4 Sites Following i.p. Inoculation 213

Figure 4.2: Virulence of Chimeric Viruses Following i.p. Inoculation 214

Figure 4.3: Virulence of Chimera B-Forms Following i.c. Inoculation.....215

Figure 4.4: Survival, Temperature, and Weight Changes Following i.p. Inoculation with B-Form Chimeras 216

Figure 4.5: Organ Titers Following i.p. Inoculation 217

Figure 4.6: White Blood Cell Counts and Proportions Following i.p. Inoculation.218

Figure 4.7: Hematological Values Following i.p. Inoculation 219

Figure 4.8: Plasma Cytokine and Chemokine Concentrations Following i.p. Inoculation 221

Figure 4.9: Survival, Temperature, and Weight Changes Following i.p. Inoculation with JEV A and JEV B 223

Figure 4.10: Organ Titers Following i.p. Inoculation with JEV A and JEV B 224

Chapter 5:

Figure 5.1: Location of EIII Neutralization Escape Mutants 234

Figure 5.2: Survival Following i.p. and i.c. Inoculation with WNV NY99 and WNV G331A.....235

Figure 5.3: Survival, Temperature, and Weight Changes Following i.p. Inoculation 236

Figure 5.4: Organ Titers Following i.p. Inoculation with WNV NY99 and WNV G331A.....237

Figure 5.5: Survival Following i.p. Inoculation with WNV NY99, WNV L107F and WNV G331A in IFNα/β Receptor Knock-Out Mice 238

Figure 5.6: Survival Following i.p. Inoculation of Swiss Webster and IFNα/β Receptor Knock-Out Mice with WNV NY99 and WNV G331 Adaptive Mutants 239

Figure 5.7: Location of Adaptive Mutants in Relation to G331A.....240

Chapter 6:

Figure 6.1: Comparison of Chimera B-Form Growth Kinetics in Vero Cells 259

List of Abbreviations

2K	2K Protein
ADE	Antibody-Dependent Enhancement
AHFV	Alkhumra Hemorrhagic Fever Virus
anchC	Anchored Capsid Protein
ANOVA	Analysis of Variance
AST	Average Survival Time
ATPase	Adenosine Triphosphatase
BAGV	Bagaza Virus
BBB	Blood-Brain Barrier
BHK	Baby Hamster Kidney
BSL	Biosafety Level
C	Capsid Protein
CFA	Complement Fixation Assay
cHP	Capsid Coding Region Hairpin
CM	Convoluted Membranes
CMV	Cytomegalovirus
CNS	Central Nervous System
CPE	Cytopathic Effect
CS	Cyclization Sequence
CYC	Cyclization Sequence
DAR	5'-Downstream of the AUG Coding Region

DB	Dumbbell-Like Region
DENV	Dengue Virus
DHF	Dengue Hemorrhagic Fever
DNA	Deoxyribonucleic Acid
DNase	Deoxyribonuclease
dNTP	Deoxynucleotide Triphosphate
dpi	Days Post Infection
ds	Double-Stranded
DTV	Deer-Tick Virus
E	Envelope Glycoprotein
EDTA	Ethylenediaminetetraacetic Acid
EH	Envelope Stem-Helix
EI	Envelope Glycoprotein Domain I
EII	Envelope Glycoprotein Domain II
EIII	Envelope Glycoprotein Domain III
ELISA	Enzyme-Linked Immunosorbent Assay
EM	Electron Microscopy
Endo H	Endoglycosidase H
ER	Endoplasmic Reticulum
FASN	Fatty Acid Synthase
FCS	Fetal Calf Serum
G-CSF	Granulocyte Colony-Stimulating Factor
GM-CSF	Granulocyte Macrophage Colony-Stimulating Factor

GMP	Guanosine Monophosphate
GPI	Glycosylphosphatidylinositol
GTase	Guanylyltransferase
HI	Hemagglutination Inhibition
HRP	Horseradish Peroxidase
i.c.	Intracranial
i.p.	Intraperitoneal
IC	Infectious Clone
ICTV	International Committee on Taxonomy of Viruses
IFN	Interferon
IgG	Immunoglobulin Gamma
IGUV	Iguape Virus
IL	Interleukin
IP-10	Interferon Gamma-Induced Protein 10
IRES	Internal Ribosomal Entry Site
JEV	Japanese Encephalitis Virus
KFDV	Kyasanur Forest Disease Virus
KOUV	Koutango Virus
KUNV	Kunjin Virus
LD_{50}	50% Lethal Dose
LGTV	Langat Virus
LIV	Louping Ill Virus
M	Membrane Virus

mAb	Monoclonal Antibody
MCP	Monocyte Chemotactic Protein
MEM	Minimal Eagle's Medium
MIAF	Mouse Immune Ascitic Fluid
MIP	Macrophage Inflammatory Protein
MODV	Modoc Virus
MOI	Multiplicity of Infection
mRNA	Messenger RNA
MTase	Methyltranferase
MVEV	Murray Valley Encephalitic Virus
ncRNA	Non-Coding RNA
NS1	Non-Structural Protein 1
NS1'	Non-Structural Protein 1'
NS2a	Non-Structural Protein 2a
NS2b	Non-Structural Protein 2b
NS3	Non-Structural Protein 3
NS4a	Non-Structural Protein 4a
NS4b	Non-Structural Protein 4b
NS5	Non-Structural Protein 5
NTPase	Nucleotide Triphosphatase
OHFV	Omsk Hemorrhagic Fever Virus
ORF	Open Reading Frame
PBS	Phosphate Buffered Saline

PCR	Polymerase Chain Reaction
pfu	Plaque-Forming Unit
PK	Pseudoknot
PKG	Protein Kinase G
PKR	Protein Kinase R
PN	Pentanucleotide Motif
POWV	Powassan Virus
prM	Membrane Precursor Protein
$PRNT_{50}$	50% Plaque Reduction Neutralization Test
PS	Paracrystalline Structures
RANTES	Regulation on Activation, Normal T Expressed and Secreted
RdRp	RNA-Dependent RNA Polymerase
RF	Replicative Form
RNA	Ribonucleic Acid
RNAi	RNA Interference
RNase	Ribonuclease
RPM	Revolutions per Minute
RT	Reverse Transcriptase/Reverse Transcription
RTPase	Ribonucleotide Triphosphatase
SAM	S-Adenosyl-Methionine
SD	Standard Deviation
sfRNA	Subgenomic Flavivirus RNA
SHA	Slowly-Sedimenting Hemagglutinin

sHP	Small Hairpin
SL	Stem-Loop
SLEV	St Louis Encephalitis Virus
SMS	Smooth Membrane Structures
ss	Single-Stranded
TBEV	Tick-Borne Encephalitis Virus
TM	Transmembrane Domain
TMD	Transmembrane Domain
TMV	Tobacco Mosaic Virus
TNFα	Tumor Necrosis Factor α
UAR	5'-Upstream AUG Region
UTMB	University of Texas Medical Branch
UTR	Untranslated Region
VLP	Virus-Like Particle
VP	Vesicle Packets
WARF4	WNV Alternative Reading Frame 4
WBC	White Blood Cell
WNV	West Nile Virus
WT	Wild-Type
XRN1	Exoribonuclease 1
YFV	Yellow Fever Virus
ZIKV	Zika Virus

Chapter 1: Introduction

Flaviviruses have been found on almost every continent, and are responsible for significant global morbidity and mortality (Gubler, 2002). Indeed, dengue virus alone is estimated to infect over 390 million people a year, with nearly 4 billion people at risk (Bhatt et al., 2013, Brady et al., 2012, WHO, 2015). The genus *Flavivirus* fits into the family *Flaviviridae* alongside the *Hepacivirus*, *Pegivirus*, and *Pestivirus* genera, and are characterized by their Type 1 capped, single-stranded, positive-sense RNA genomes that lack poly-A tails, but code for a large polyprotein that is subsequently cleaved into its constituent proteins (ICTV, 2014, Gubler et al., 2007). The current listings by the International Committee on Taxonomy of Viruses (ICTV) show 53 different flavivirus species, with over 70 identified viruses (ICTV, 2014). Of the 53 species, 27 are mosquito-borne, 12 are tick-borne, and 17 have no known vector (Gubler et al., 2007). More than half have been shown to cause disease in humans.

Flaviviral diseases have been recognized for centuries. Some of the earliest written records of a dengue-like illness come from China prior to 992, although the exact date is uncertain (Gubler, 2014). Modern records of dengue appear to start in the 1635, when a dengue-like illness was described in Martinique and Guadeloupe, and in 1699 in Panama (Brathwaite Dick et al., 2012). Less equivocal outbreaks were described in 1779 in Cairo and Alexandria, Egypt, and in Batavia (Jakarta), Indonesia, with an outbreak in Philadelphia the following year, described by Rush (Bylon, 1780, Gubler, 2014, Rush, 1789). From then on, outbreaks were described frequently. The history of yellow fever is

similar, with one of the earliest outbreaks described in Barbados in 1647, and frequent occurrences thereafter (Creighton, 1883).

Phylogenetic analysis of the flaviviruses reveals clustering based upon vector association, with the mosquito-borne flaviviruses further grouping into *Culex*- and *Aedes*-associated clades (Gubler et al., 2007, Gaunt et al., 2001). For the most part, viruses within the *Culex* clade tend to be associated with avian or rodent hosts, and cause encephalitic disease in humans, while viruses in the *Aedes* clade tend to have primate hosts, and cause hemorrhagic or arthralgic disease in humans (Gaunt et al., 2001). Although the tick-borne flaviviruses are more closely related to one another genetically, their associated diseases are quite diverse, with high sequence similarity between encephalitis- (TBEV) and hemorrhagic fever- (OHFV) causing members (Gaunt et al., 2001). The exact mechanisms governing disease presentation are poorly understood.

GENOME

Most of the early studies into the nature and properties of the nucleic acid components of viruses were not conducted with the flaviviruses, but with tobacco mosaic virus (TMV) and bacteriophage. Viruses had been identified (and distinguished from bacteria) by the end of the 19th Century, primarily through the studies of Ivanovsky and Beijerinck. These researchers demonstrated that sap from plants infected with tobacco mosaic virus that had been filtered through Chamberland filter-candles, thus removing any bacteria or fungi, was still capable of infecting and causing disease in previously healthy plants (Beijerinck, 1898, Beijerinck, 1942, Ivanovsky, 1892, Ivanovsky, 1942). Despite these studies demonstrating a hitherto unknown class of pathogen, research into the chemical nature of viruses was limited in number during the first few decades of the 20th Century, mainly due to issues of isolation and purification. It was not until 1933 that

Max Schlesinger, working with the WLL bacteriophage of *Escherichia coli*, was able to purify by means of filtration and ultracentrifugation, a preparation of virus clean enough for chemical analysis (Schlesinger, 1933). Soon afterwards he published the first such analysis of a virus, demonstrating that it was in fact a nucleoprotein, consisting of both nucleic acid and protein and, two years later, demonstrated by means of the Feulgen reaction that the nucleic acid was of the thymonucleic acid type (deoxyribonucleic acid; DNA) (Schlesinger, 1936, Schlesinger, 1934).

These studies led other investigators to apply similar techniques to characterize the chemical nature of their own viruses of interest. In 1935, Wendell Stanley purified and crystallized tobacco mosaic virus, but concluded that it was an "autocatalytic protein" (Stanley, 1935). This was soon demonstrated to be incorrect by Bawden and Pirie, who showed that tobacco mosaic virus was indeed a nucleoprotein, and that the nucleic acid component was actually of the "yeast" type (ribonucleic acid; RNA) rather than the thymonucleic acid type (Bawden and Pirie, 1937). Thus, within the space of just four years, viruses had been purified, shown to be nucleoproteins, and to contain either DNA or RNA components.

The understanding of the role of viral nucleic acids took at great leap forward in 1952, as a result of experiments carried out by Alfred Hershey and Martha Chase. Their studies, using the DNA-containing bacteriophage T2, demonstrated that the majority of the sulphur-containing proteinaceous component of the virus is required only for the attachment to the cell surface, and the insertion of the viral DNA into the cytosol of the target cell (Hershey and Chase, 1952). These findings were significant not only to virologists, but to biologists in general, as the results strongly suggested that nucleic acids (in this case DNA), not proteins, were the hereditary genetic material.

For the RNA viruses, the role of the nucleic acid was still not clear. Four years later, in 1956, Schuster, Schramm & Zillig developed a technique for the extraction of RNA from viruses using phenol, and used this method to purify RNA from TMV (Schuster et al., 1956). Gierer & Schramm demonstrated that, even after the removal of the protein component of the virus, the purified RNA remained infectious (Gierer and Schramm, 1956b, Gierer and Schramm, 1956a). Studies carried out by Fraenkel-Conrat *et al*. at the same time supported these findings (Fraenkel-Conrat, 1956, Fraenkel-Conrat et al., 1957). This discovery further cemented the hypothesis that the nucleic acid components of viruses served as the template for the production of viral progeny.

Soon after these studies were published, the phenol extraction technique for RNA purification was used on a number of different RNA-containing viruses. One of the first was West Nile virus (WNV). Colter *et al*. demonstrated that RNA purified from WNV-infected cells was infectious after intracranial inoculation in mice, suggesting that, similar to tobacco mosaic virus, the RNA alone is sufficient for the production of progeny viruses (Colter et al., 1957). Similar studies demonstrated infectious RNA for tick-borne encephalitis virus (TBEV) (Sokol et al., 1959), dengue virus (DENV) (Ada and Anderson, 1959a), Murray Valley encephalitis virus (MVEV) (Ada and Anderson, 1959b, Anderson and Ada, 1959), Japanese encephalitis virus (JEV) (Igarashi et al., 1963, Nakamura, 1961), and yellow fever virus (YFV) (Nielsen and Marquardt, 1962). Ribonuclease sensitivity, and a lack of base pairing indicative of double-stranded base complementarity, suggested that the RNA was single-stranded (Stollar et al., 1966, Russell et al., 1980). The infectious nature of the RNA indicated that it was a positive-sense strand, fitting into Group IV of the Baltimore classification (Baltimore, 1971).

Sedimentation analysis of RNA from flavivirus virions revealed coefficients ranging from 38 to 45 S, from which a molecular weight range of $3\text{-}4\text{x}10^6$ was estimated

(Igarashi et al., 1964, Stollar et al., 1966, Trent et al., 1969, Boulton and Westaway, 1972, Nishimura and Tsukeda, 1971). When similar analyses were run using RNA from infected cells, two other species were identified with coefficients of about 20 and 26 S (Stollar et al., 1967, Trent et al., 1969, Nishimura and Tsukeda, 1971). These species were determined to be RNase resistant, indicative of a double-stranded form of viral RNA. This view was further supported by the observation that denaturation of the 20 S moiety with dimethylsulphoxide resulted in a shift in the sedimentation coefficient to 45 S, similar to that of the single-stranded, genomic RNA. It was concluded that the 20 and 26 S RNAs are replication intermediates generated during the infectious cycle (Stollar et al., 1967, Trent et al., 1969, Nishimura and Tsukeda, 1971). Polysomes (clusters of ribosomes associated with RNA) isolated from SLEV- and DENV-2-infected cells were demonstrated to be associated with the 45 S RNA species, indicating that the genomic RNA behaved directly as messenger RNA (mRNA) within the cells, fitting with the previous demonstration that the genomic RNA alone is sufficient for viral replication (Cleaves et al., 1981, Naeve and Trent, 1978, Cleaves and Schlesinger, 1977). These findings were further confirmed by *in vitro* translation studies with the genomic RNA of TBEV (Svitkin et al., 1978, Svitkin et al., 1981, Svitkin et al., 1984), WNV (Wengler et al., 1979) and KUNV (Monckton and Westaway, 1982).

In eukaryotic cells, mRNA is recognized as usually having a 5'-modified-guanine cap, and a 3'-poly-adenylated tail (Latchman, 2005, Shatkin, 1976). These are believed to be important for the initialization of translation and for mRNA stability, respectively (Latchman, 2005). The demonstration of the role of the flavivirus genomic RNA as a functional mRNA led researchers to determine whether these features were present. Studies by Wengler *et al*. and Cleaves & Dubin showed that for both WNV and DENV-2, the majority of genomic RNAs had an $m^7G(5')ppp(5')AmpN_1$ "Type 1" cap, with a minority containing the further methylated $m^7GpppAmpN_1mpN_2$ "Type 2" cap (Shatkin,

1976, Cleaves and Dubin, 1979, Wengler et al., 1978). The inability of WNV genomic RNA to bind to oligo-d(T)-cellulose chromatography columns demonstrated a lack of a poly(A) tail, a feature that distinguished flavivirus genomic RNA from that of the related alphaviruses (Russell et al., 1980, Wengler et al., 1978). To make up for the lack of a poly(A) tail, flaviviral RNA forms stable secondary structures in the 3'-terminal sequence ensuring that the last 4-5 nucleotides are hydrogen bonded, and reducing the sensitivity to exonuclease digestion (Deubel et al., 1983, Grange et al., 1985, Rice et al., 1985, Wengler and Wengler, 1981, Westaway, 1987).

A number of studies to determine the length of a flavivirus genome in nucleotide terms focused on YFV. Deubel *et al*. estimated that the genome of the 17D vaccine strain of YFV was approximately 11,000 nucleotides in length, by comparing the physical length of the RNA, as determined by electron microscopy, with genomes of known length from different bacteriophages (Deubel et al., 1983). A more definitive sequence length, as well as the sequence itself, was determined for YFV 17D by Rice *et al*. in 1985 (Rice et al., 1985). The first published flavivirus genome sequence, they demonstrated that Deubel *et al*.'s estimation was impressively close: 10,862 nucleotides in length (Rice et al., 1985). By 1990, genome lengths and sequences had been determined for a number of different flaviviruses, including DENV-2 (Deubel et al., 1988, Hahn et al., 1988), DENV-3 (Osatomi and Sumiyoshi, 1990), DENV-4 (Mackow et al., 1987), JEV (Hashimoto et al., 1988, Sumiyoshi et al., 1987), KUNV (Coia et al., 1988), MVEV (Dalgarno et al., 1986, Lee et al., 1990), TBEV (Mandl et al., 1989, Pletnev et al., 1990), WNV (Castle et al., 1986, Castle et al., 1985, Wengler et al., 1985, Castle and Wengler, 1987, Wengler and Castle, 1986, Wengler and Wengler, 1981) and YFV (Rice et al., 1985, Hahn et al., 1987a).

In addition to providing the first published genome sequence for a flavivirus, the 1985 Rice *et al*. paper helped to answer a few questions about the structure of the genome, and the mechanisms governing protein expression. Previous studies that focused on the *in vitro* transcription of the flavivirus genome (Monckton and Westaway, 1982, Svitkin et al., 1978, Svitkin et al., 1984, Svitkin et al., 1981, Wengler et al., 1979) had essentially ruled out the production of a flavivirus polyprotein, and it was believed that independent initiation of translation of individual proteins occurred from the genomic RNA (Westaway, 1977, Westaway and Shew, 1977, Shapiro et al., 1973b). Rice *et al*. demonstrated that, starting from the first AUG codon, the YFV genome contains an extremely long open reading frame (ORF), 10,233 nucleotides in length, potentially coding for a polyprotein of 380,763 Daltons (Rice et al., 1985). It was concluded that the five other potential ORFs were unlikely to code for proteins due to the presence of multiple stop codons. There was therefore "no reason to expect that any protein is translated from yellow fever RNA other than the polyprotein encoded by the long open reading frame" (Rice et al., 1985). This study also demonstrated another feature of the flavivirus genome: 3'- and 5'-untranslated regions (UTRs).

The 3'- and 5'-UTRs are poorly conserved regions at the terminal ends of the flavivirus genomic RNA, flanking the single, large ORF (Figure 1.1). The 5'-UTR is reasonably short, ranging from about 90nts in DENV-2 to about 130nts in TBEV (Markoff, 2003). The 3'-UTR is a little longer, ranging from around 380nts in DENV-4 to about 760nts in TBEV (Markoff, 2003). While the sequence of the 5'-UTR is not well conserved between different species of flaviviruses (although intraspecies sequence variation seems to be low), there appear to be structurally conserved regions indicative of a functional role (Brinton and Dispoto, 1988, Thurner et al., 2004). Within this region there are three main structural features known as SLA (stem-loop A), SLB (stem-loop B), and cHP (capsid coding region hairpin) (Brinton and Dispoto, 1988, Dong et al., 2008,

Thurner et al., 2004, Lodeiro et al., 2009, Gritsun and Gould, 2007, Alvarez et al., 2008, Cahour et al., 1995). A number of studies employing phosphorodiamidate morpholino oligomers targeting parts of the 5'-end of the genome have demonstrated that disruption of these regions significantly inhibits translation (Deas et al., 2005, Holden et al., 2006, Kinney et al., 2005, Lindenbach et al., 2007). A further potential role for the 5'-UTR lies in its structure in the negative-sense strand. Studies by Cahour *et al*. demonstrated that, while certain deletions in the 5'-UTR did not affect translation, replication of the virus did not occur. It was therefore hypothesized that these mutations affect the generation of positive-sense strands from the complementary strand, stopping viral replication (Cahour et al., 1995).

The 3'-UTR has a more complex secondary structure (Figure 1.1). The very end of the genome has a conserved CU_{OH} dinucleotide, shown to function as the recognition site for the viral RNA-dependent RNA polymerase (RdRp) (Rice et al., 1985, Brinton et al., 1986, Wengler and Wengler, 1981, Khromykh et al., 2003, Nomaguchi et al., 2003). At the terminal end of the 3'-UTR is a stem-loop (3'-SL) structure containing a pentanucleotide motif (PN; 5'-CACAG-3') that is conserved throughout the arthropod-borne flaviviruses (Brinton and Basu, 2015, Brinton et al., 1986). The importance of these nucleotides seems to vary between virus species. In WNV, two bases within and one adjacent to the PN are required for viral replication, but not translation (Khromykh et al., 2003, Elghonemy et al., 2005, Tilgner et al., 2005). In contrast, only the fifth nucleotide of the PN is essential for YFV replication, although mutation of the others reduces fitness of the virus when competing with a WT sequence (Silva et al., 2007). Adjacent to, and upstream of, the 3'-SL is a small hairpin (sHP) containing a highly conserved octanucleotide sequence known as the 3'-cyclization sequence (3'-CS or CYC). An exactly complementary sequence is present in the 5'-end of the genome, at the downstream base of the cHP (Hahn et al., 1987b). Basu and Brinton demonstrated that,

while up to three adjacent mismatches may be tolerated, albeit with reduced replication efficiency, five mutations were lethal (Basu and Brinton, 2011). With the viable mutants, revertants and adaptive mutants were readily generated (Basu and Brinton, 2011). In addition to the CYC, two other regions of complementarity exist in the 5'- and 3'-terminal regions: a 5'-upstream AUG region (UAR) that interacts with a complementary sequence in the sHP-3'-SL linker region; and one (DENV) or two (WNV) 5'-downstream of the AUG coding region (DAR) sequences that interact with complementary sequences found in the sHP structure of the 5'-UTR (Alvarez et al., 2005b, Zhang et al., 2008, Dong et al., 2008, Friebe and Harris, 2010). A number of studies have shown that the three regions of complementarity between the 5'-and 3'-ends of the flavivirus genome are important for the cyclization of the genome, and thence the initiation of negative-strand synthesis (Khromykh et al., 2001, Corver et al., 2003, Lo et al., 2003, Alvarez et al., 2005a). Studies by Polacek *et al*. demonstrated that mutation of the 3'-UAR disrupted hybridization with it complement in the 5'-end, but did not affect hybridization of the CYCs. Conversely, mutation of the 3'-CYC ablated both CYC and UAR hybridization (Polacek et al., 2009). Friebe *et al*. further demonstrated that the DAR sequence is also required for genome cyclization and replication (Friebe et al., 2011). Taken together, it has been proposed that the data demonstrate that the 5'-3' RNA-RNA interactions follow a temporal order, with the 5'- and 3'-CYC regions interacting first, followed by the DAR sequences, and finally the UAR features (Brinton and Basu, 2015). The mechanisms requiring these interactions have started to be elucidated. Filomatori *et al*. demonstrated that, prior to 3'→5' negative-sense RNA synthesis, the viral RdRp interacts with SLA in the 5'-UTR, a finding confirmed by Dong *et al*., therefore necessitating genome cyclisation for replication (Filomatori et al., 2006, Dong et al., 2008). Studies by Blackwell & Brinton demonstrated that phosphorylated eukaryotic elongation factor-1 (eEF1A) binds to the 3'-SL region of the WNV genome (Blackwell and Brinton, 1997), while Davis *et al*. demonstrated that this interaction is conserved amongst YFV, DENV-2

and TBEV (Davis et al., 2007). Mutation of the binding region within the 3'-SL region that decreased eEF1A association led to a decrease in the amount of negative-sense viral RNA within the cell, while other studies suggested that eEF1A may play a role in recruiting the viral RdRp to the 5'-SLA (Davis et al., 2007).

Within the cell, there is an asymmetrical accumulation of positive- and negative-sense viral RNAs, with the genomic, positive-sense strands often up to ten-fold more numerous (Cleaves et al., 1981, Lindenbach et al., 2007). The cause is thought to be multifaceted, but likely includes the complexity of negative-strand synthesis (described above), and the exponential production of positive-sense RNA from a negative-sense template once replication is occurring within replication vesicles (Chu and Westaway, 1987). The exact mechanisms governing the accelerated positive-strand synthesis are unknown, but are thought to involve the rearrangement of the 3'-end of the negative-sense strand to form a stem-loop structure capable of interacting with a number of cellular proteins including TIAR/TIA-1 and GAPDH which likely aid in the recruitment of the viral RdRp to the complex (Brinton and Basu, 2015, Li et al., 2002, Yang et al., 2009a, Blackwell and Brinton, 1995, Shi et al., 1996).

In addition to 3'-SL and sHP, the 3'-UTR contains a number of other "dumbbell-like" (DB) and stem-loop (SL) structures, predicted to form pseudoknots (PKs) (Brinton and Basu, 2015). These structures are less well conserved throughout the flavivirus genera than 3'-SL and sHP, and mutations of individual structures, while often significantly reducing replication and translation efficiency, are usually non-lethal (Brinton and Basu, 2015, Manzano et al., 2011). Within the WNV 3'-UTR there are four conserved stem-loop structures located upstream of the dumbbell-like structures, denoted SL-I, SL-II, SL-II and SL-IV, and similar structures are present in other flavivirus genomes, although the nucleotide sequences in these areas are not well conserved

(Brinton and Basu, 2015). These RNA structures have been shown to be important in the generation of flaviviral non-coding RNA (ncRNA) species (Clarke et al., 2015, Funk et al., 2010, Silva et al., 2010, Chapman et al., 2014a, Pijlman et al., 2008). To date, two different non-coding RNAs have been demonstrated to be derived from the 3'-UTR of the flavivirus genome: subgenomic flavivirus RNA (sfRNA) and a flavivirus-derived microRNA (KUN-miR-1) (Roby et al., 2014, Pijlman et al., 2008, Clarke et al., 2015, Bidet and Garcia-Blanco, 2014, Hussain and Asgari, 2014, Hussain et al., 2012).

sfRNA has been demonstrated to be generated as a result of incomplete digestion of the viral genomic RNA by the cellular 5'→3' exoribonuclease-1 (XRN1) (Chapman et al., 2014a, Funk et al., 2010, Pijlman et al., 2008, Roby et al., 2014). XRN1 is a cellular ribonuclease important in the RNA degradation pathway, where it usually degrades de-capped mRNA (Sheth and Parker, 2003). Flaviviral RNA is similarly treated within the cell, although the de-capping mechanism has yet to be determined, with XRN1 degrading the RNA from the 5'-end. Unlike most mRNAs, flavivirus genomic RNA forms a complex tertiary structure in the 3'-UTR, resulting from a ring-like pseudoknot generated by the interaction of a short region at the top of SL-II with a complementary sequence immediately downstream of the same stem-loop (Funk et al., 2010, Silva et al., 2010). This structure stalls the progress of XRN1, leading to the generation of an approximately 525nt sfRNA (Funk et al., 2010, Silva et al., 2010). Mutations or deletions to the SL-II region in WNV lead to the generation of a smaller sfRNA (sfRNA2; approximately 365nts in length) hypothesized to be generated after XRN1 stalling at SL-IV (Chapman et al., 2014b, Funk et al., 2010, Pijlman et al., 2008). Successively smaller sfRNAs have been generated following mutations in the pseudoknot structures in the WNV 3'-UTR (Funk et al., 2010, Pijlman et al., 2008). While similar apparent redundancy is also found in DENV-2, a secondary stalling point does not appear to exist in YFV.

To date, three different roles have been attributed to sfRNAs: inhibition of mRNA degradation pathways; inhibition of immune responses; and contributions towards *in vitro* and *in vivo* pathogenesis. Infection of Vero cells with WNV mutants unable to generate sfRNA let to significantly reduced CPE generation, even after 6-8 days (Funk et al., 2010, Pijlman et al., 2008). Similar observations were made with mutant DENV-2 (Liu et al., 2014). Liu *et al*. demonstrated that DENV-2 sfRNA inhibits the phosphorylation of Akt, leading to decreased levels of Bcl-2, thus inhibiting apoptosis (Liu et al., 2014). Within a mouse model, WNV mutants allowing only the production of sfRNA2 or sfRNA3 were significantly attenuated (Schuessler et al., 2012, Funk et al., 2010, Pijlman et al., 2008). In addition to inducing cellular apoptosis, sfRNA has been shown to inhibit XRN1 function and endogenous mRNA turnover by sequestering it in a complex with the sfRNA (Chapman et al., 2014a, Chapman et al., 2014b, Moon et al., 2012). Schnettler *et al*. demonstrated that sfRNA from a number of flaviviruses inhibits arthropod and mammalian cell RNAi responses by inhibiting Dicer activity (Schnettler et al., 2012, Schnettler et al., 2014), while Chang *et al*. demonstrated that sfRNA from JEV inhibits nuclear translocation of interferon regulatory factor 3 (IRF-3), thus inhibiting interferon activation (Chang et al., 2013). This finding supported those of Schuessler *et al*., who demonstrated that, while sfRNA-deficient WNV was attenuated in wild-type mouse embryonic fibroblasts, the virus grew readily in cells lacking IRF-3 and -7 (Schuessler et al., 2012). A potential fourth role for sfRNAs has been proposed by Fan *et al*., who showed that an sfRNA from JEV inhibited viral negative-sense RNA synthesis, suggesting that for JEV, sfRNA may play a role in minimizing negative-sense RNA build-up (Fan et al., 2011). The same studies demonstrated that JEV sfRNA may also inhibit translation.

In addition to sfRNA, KUNV has been shown to encode a miRNA (KUN-miR-1) required for efficient viral replication within mosquito cells (Hussain et al., 2012). This

miRNA was shown to upregulate the GATA4 transcription factor, and its inhibition reduced viral titers and RNA levels 10-fold (Hussain et al., 2012). The same group reported a miRNA-like small RNA derived from the DENV-2 3'-UTR whose role appears to be in limiting virus replication in mosquitoes, presumably to prevent the virus from killing its vector (Hussain and Asgari, 2014). When this miRNA, denoted vsRNA-5, was inhibited, viral replication was increased nearly 10,000-fold. Target prediction studies suggested that vsRNA-5 binds to the NS1 region of the viral genome, regulating viral replication (Hussain and Asgari, 2014).

VIRAL PROTEINS

Soon after the purification and initial characterization of the RNA component of the virion, studies were undertaken to investigate flaviviral proteins. The first studies, by Stollar and Westaway & Reedman, were focused on the structural proteins of the virion (Stollar, 1969, Westaway and Reedman, 1969). Stollar's work with DENV-2 demonstrated three proteins, which he labeled VSP-1, -2, and -3, and which had molecular weights of 7,700; 15,500; and 59,000 Da, respectively (Stollar, 1969). Westaway & Reedman, working with KUNV, identified four peaks by polyacrylamide gel electrophoresis, with molecular weights of 13,000; 18,000; 65,000; and 120,000 Da, although the latter peak was very small and, although not concluded by the original authors, was likely an artifact (Westaway and Reedman, 1969). Further studies with SLEV and JEV demonstrated three structural proteins each of 8,500; 18,000; and 63,000 Da for SLEV, and 8,700; 13,500; and 53,000 Da for JEV (Shapiro et al., 1971, Trent and Qureshi, 1971). Shapiro *et al*. characterized the virions of eight additional mosquito- and tick-borne flaviviruses, and showed that they all had a similar complement of structural proteins (Shapiro et al., 1972b). The nomenclature for the proteins varied somewhat depending on the study, although by the mid-1970s a designation of V1, V2 and V3 was

widely used for the small, medium and large proteins, respectively (Russell et al., 1980). Treatment of the virions with non-ionic detergent revealed that V1 and V3 were envelope proteins, while V2 was associated with the nucleocapsid (Trent and Qureshi, 1971, Westaway and Reedman, 1969). Studies looking at intracellular virions, and virions released from cells in the presence of Tris, demonstrated viral particles that appeared to contain a cell-associated viral protein, NV2, rather than V1. The data suggested that NV2 was a precursor of V1 (Shapiro et al., 1972a, Westaway and Shew, 1977, Russell et al., 1980).

In addition to structural proteins present in the virion, investigations were made to determine viral proteins present in the cell during infection. In their studies with KUNV, Westaway & Reedman identified three potential viral proteins in the cytoplasm of infected cells when lysates were run on polyacrylamide gels, but had difficulty discerning some of the peaks over the background noise of cellular proteins (Westaway and Reedman, 1969). Trent & Qureshi, working with SLEV, and Shapiro *et al*., working with JEV, were able to distinguish the three structural proteins and five virus-specific non-structural proteins in BHK cells following actinomycin and cycloheximide treatment to inhibit host RNA transcription and, later, protein translation. These proteins had molecular weights of 10,500; 19,000; 45,000; 71,000; and 93,000 Da (Trent and Qureshi, 1971, Shapiro et al., 1971). By 1973, the number of identified viral proteins within flavivirus-infected cells had risen to nine: two structural proteins (V2 and V3), and seven non-structural proteins (including NV2): NV1 (10,300 Da); NV2 (19,000 Da); NV2½ (21,000 Da); NVX (32,000 Da); NV3 (44,000 Da); NV4 (70,500 Da); and NV5 (98,000 Da) (Westaway, 1973). Westaway *et al*. demonstrated that, within the cytoplasm, the V2 core protein of KUNV is present as a smaller peptide, denoted NV1½, within the cytoplasm (Wright and Westaway, 1977, Westaway et al., 1977). Studies to determine glycosylation of flavivirus proteins showed that the V3 protein of DENV-2, as well as

NV2 and NV3, are glycoproteins (Stollar, 1969, Shapiro et al., 1972a, Shapiro et al., 1973a, Westaway, 1975).

Early studies into the translation of viral proteins resulted in some confusion regarding the specific mechanisms of viral protein production from the RNA genome. Comparisons between flavivirus protein synthesis and that of other positive-sense viruses led to the expectation that pre-cleavage protein precursors indicative of a polyprotein would be detected within the infected cell, but none could be found (Westaway, 1980, Westaway, 1973, Westaway and Shew, 1977). In addition, the different proportions of the viral proteins present during infection suggested that some sort of translational control was occurring (Shapiro et al., 1971, Westaway and Reedman, 1969, Westaway and Shew, 1977). Tryptic mapping of some of the larger and smaller proteins revealed that they were not related to one another (i.e. no pre-cleaved polyproteins), and the working hypothesis was that, unlike other positive-sense animal RNA viruses, translation of flaviviral proteins is mediated by "multiple and independent internal initiation", with the genome acting as a polycistronic messenger (Westaway, 1980, Wengler et al., 1979, Wright and Westaway, 1977, Wright et al., 1977).

In 1980, Westaway *et al.* proposed to rename the flaviviral proteins. The structural proteins V1, V2 and V3 were redesignated M, C and E, respectively, for Membrane, Core (later renamed Capsid) and Envelope (Westaway et al., 1980). The non-structural proteins were renamed based upon their molecular weight (in kilodaltons), and prefixed by a P, or GP if a glycoprotein (Westaway et al., 1980). With the publication of the complete genome sequence for YFV in 1985, and the identification of a single, large open reading frame, it was possible to sequence the N-terminal amino acids of the identified viral protein, and map them to the genome (Bell et al., 1985, Rice et al., 1986a, Rice et al., 1986b). This demonstrated that the viral proteins are indeed translated as a

polypeptide and, further, showed the order of the protein coding regions within the genome. In addition, it demonstrated the actual number of proteins coded for within the flavivirus genome: three structural proteins, and seven non-structural proteins. It also showed that the non-structural protein NV2 contained the coding sequence of the mature M protein at the C-terminal, suggesting that NV2 is a precursor to M, a hypothesis proposed earlier based upon the observation that M is not present within the infected cell (Shapiro et al., 1972a, Rice et al., 1986b). Based upon the genome/protein map for YFV, Rice *et al*. proposed another renaming of the flavivirus proteins. Starting from the 5' end of the genome, the three structural proteins, C, prM (membrane precursor; contains M), and E, then the non-structural proteins, NS1, NS2a, NS2b, NS3, NS4a, NS4b and NS5 (Rice et al., 1986b). Expression of randomly-generated JEV cDNAs covering 83% of the protein-coding region in E. coli by Mason *et al*. confirmed the expression of a polyprotein by the viral genome. They also demonstrated that, for JEV, an extra protein was expressed, NS1' (Mason et al., 1987). To date, NS1' expression has been demonstrated in only a handful of viruses within the JE complex, including JEV, MVEV and WNV (Mason et al., 1987, Blitvich et al., 1999, Blitvich et al., 1995).

TRANSLATION AND PROCESSING OF THE FLAVIVIRAL POLYPROTEIN

Translation of the flaviviral polyprotein is dependent upon the recognition of the 5'-cap structure by host ribosomes, and scanning by the ribosome for the start codon (Lindenbach et al., 2007). Unlike host mRNAs, the flavivirus genomic RNA does not contain a consensus Kozak sequence around the start codon, instead, Clyde & Harris demonstrated that cHP in the capsid coding region appears to direct the ribosome to the correct AUG by slowing the scanning complex as it approaches (Clyde and Harris, 2006).

Once transcribed, the flavivirus polyprotein is approximately 3,000aa long. It is processed into its ten constitutive proteins, as well as a small peptide known as 2K (Lin et al., 1993), by a combination of host and viral proteases (Figure 1.2). A signal sequence between C and prM targets prM, E and NS1 to the endoplasmic reticulum, whilst the rest of the proteins remain in the cytoplasm (Kümmerer, 2006, Markoff, 1989). Cleavage between C and prM, prM and E, and E and NS1, as well as between 2K and NS4b, is carried out by a host signalase (Nowak et al., 1989, Rice et al., 1986b, Lin et al., 1993). Most of the cleavage within the non-structural protein region, as well as between C and its anchor peptide, is mediated by the viral NS2b/NS3 protease (Kümmerer, 2006). Interestingly, the cleavage of C from its signal peptide is required for efficient cleavage of prM from the other terminal of the peptide (Lobigs et al., 2010). The protease responsible for separating NS1 and NS2a has yet to be identified, but is thought to be located within the endoplasmic reticulum (Falgout and Markoff, 1995). The expression of NS1', an NS1 sequence-derived protein with an additional 52aa at the C-terminal, has been shown to occur through a -1 ribosomal frame-shift during translation (Melian et al., 2010, Firth and Atkins, 2009).

CAPSID PROTEIN (C)

The capsid protein (C) is a non-glycosylated protein of about 13,000 Da (Russell et al., 1980). Compared to other flavivirus proteins, it is lysine-rich, giving it a highly basic chemistry thought to be important in its interaction with the negatively-charged genomic RNA (Lindenbach et al., 2007, Russell et al., 1980, Boege et al., 1983). The charged residues are not uniformly dispersed throughout the protein, but are clustered at the N- and C-termini separated by a hydrophobic region involved in membrane integration (Lindenbach et al., 2007, Ma et al., 2004, Markoff et al., 1997). Following translation and initial cleavage of the polyprotein, the capsid protein is found as an

anchored precursor (anchC) with a hydrophobic C-terminal localization sequence, a component of the polyprotein involved in the ER translocation of prM. Release of C from its transmembrane anchor is mediated by the viral NS2b/NS3 protease complex, and is highly dependent upon the presence of host membranes (Lobigs, 1993, Lobigs et al., 2010, Kurz et al., 2012). As alluded to above, the cleavage of prM from the other end of the localization sequence by a host signalase appears to be inefficient until C has been released from the anchoring sequence (Lobigs et al., 2010, Lobigs, 1993, Stocks and Lobigs, 1995). This sequential cleavage has been shown to be required for virus growth, with mutations in the signal region that uncoupled cleavage coordination having a lethal effect on YFV, and a significant shift towards VLP production with MVEV (Lee et al., 2000, Lobigs et al., 2010, Lobigs and Lee, 2004). The capsid protein folds into a tight, multi alpha-helical structure that forms homodimers stabilized by salt-bridges (Jones et al., 2003, Ma et al., 2004, Zhan et al., 2013). These dimers are such that hydrophobic and positively-charged surfaces form at opposite ends, delineating the RNA-binding and membrane-interacting faces (Ma et al., 2004). Loss of 16aa within the hydrophobic middle region of C was shown by Kofler *et al*. to be tolerated, albeit with an increase in production of empty particles (Kofler et al., 2002). Occasionally, C proteins are found in WNV-infected cells lacking 16aa of the N-terminus, due to initiation of translation from the second in-frame AUG, although it is unclear whether this form of C is functional (Castle et al., 1985, Nowak et al., 1989, Chambers et al., 1990a). Studies by Kiermayr *et al*. demonstrated that purified capsid protein dimers assemble themselves into capsid-like structures *in vitro* when viral RNA or single-stranded DNA is present (Kiermayr et al., 2004).

Extra-virion roles of C within the infected cells are poorly understood. Although flaviviral replication occurs within the cytoplasm, studies have shown significant amounts of C present within the nucleus during infection, with translocation being

dependent upon C being phosphorylated (Bulich and Aaskov, 1992, Sangiambut et al., 2008, Bhuvanakantham et al., 2010a). Once in the nucleus, flavivirus C protein interacts with a number of host factors including: DAXX, for the induction of Fas-mediated apoptosis (Netsawang et al., 2010); HDM2, activating p53-mediated apoptosis through sequestration of HDM2 to the nucleolus (Yang et al., 2008); and I2PP2A, although the significance of this interaction has yet to be established (Hunt et al., 2007). Colpitts *et al*. have demonstrated an interaction between C and four core histones, H2A, H2B, H3, and H4. The interactions with the histones led to DNA binding and disruption of nucleosomes, presumably affecting host gene expression to favour the virus (Colpitts et al., 2011).

Within the cytoplasm, WNV and DENV-2 C proteins have been demonstrated to interact with the host protein Sec3, reducing Sec3 levels within the cell by targeting it to the 20S proteasome for degradation (Bhuvanakantham et al., 2010b, Bhuvanakantham and Ng, 2013). Reducing cellular levels of Sec3 is important, as the protein inhibits viral RNA replication and translation through sequestration of eEF1A, whose role in viral RNA replication has been described above (Bhuvanakantham et al., 2010b). Additional studies into the non-structural properties of C have demonstrated a role in inhibiting early apoptosis during infection through the activation of the PI3K/Akt pathway, suggesting a Janus-like approach to apoptosis modulation (Urbanowski and Hobman, 2013). An interaction between C and Hsp70 has also been demonstrated, but the purpose of this interaction has yet to be established (Oh and Song, 2006).

MEMBRANE GLYCOPROTEIN (PRM)

The membrane precursor protein (prM) is an approximately 19-25kDa (depending upon glycosylation state) glycoprotein, and is the second peptide derived from the N-

terminal region of the flavivirus polyprotein (Lindenbach et al., 2007, Rice et al., 1986b). N-linked glycosylation of prM occurs, but the specific numbers and locations of potential glycosylation sites vary between different flavivirus species. For instance, the prM proteins of members of the JE complex are singly glycosylated at Asn-15, while YFV prM is glycosylated at Asn-13 and Asn-29, with additional potential sites at Asn-51 and Asn-55, although these sites are unlikely to be modified due to steric effects (Kim et al., 2008, von Lindern et al., 2006, Chambers et al., 1990b). As mentioned above, within the polyprotein, prM is connected to a signal sequence located between its N-terminal and the C-terminal of C. This signal sequence is required for the targeting of prM, E and NS1 to the endoplasmic reticulum. The release of prM from the peptide requires the host signalase enzyme, with the reaction being inefficient unless C is released first (Lobigs, 1993, Lobigs et al., 2010, Stocks and Lobigs, 1995).

The main roles for prM are to aid in the proper folding of E, and the protection of E during viral release. Konishi & Mason demonstrated via expression of JEV structural proteins in mammalian cells from a vaccinia vector that, in the absence of prM, JEV E folded improperly, and would not be incorporated into flavivirus sub-viral particles (Konishi and Mason, 1993). These findings were further supported by Lorenz *et al.*, working with TBEV, who showed that, in the absence of prM, E was still able to form disulphide bonds, but did not present specific conformational epitopes, suggesting a mis-folding of the protein (Lorenz et al., 2002). prM itself was shown to fold very quickly, and independently of other viral proteins (Lorenz et al., 2002). The molecular basis of the chaperone activity of prM has not been determined. During virion assembly, prM is incorporated into the virus particle, protecting E from rearranging into its acid-induced fusion form, which would render the virions inviable for infection (Guirakhoo et al., 1992, Heinz et al., 1994). Structural analysis of the prM-E complex demonstrated that the pr component of prM covers the fusion loop of E, therefore preventing fusion with host

membranes (Li et al., 2008). During movement through the secretory pathway, prM is cleaved by furin in the Golgi, which allows for the release of the pr peptide and the reorganization of the E glycoproteins into dimers, resulting in the release of mature virions from the cell (Stadler et al., 1997, Stiasny et al., 1996, Wengler and Wengler, 1989b). Inhibition of the cleavage of prM leads to the release of immature, non-infectious particles (Elshuber et al., 2003, Guirakhoo et al., 1992). Interestingly, mutations in TBEV prM resulting in trypsin-dependent maturation yielded viruses that were capable of low-level infection when directly inoculated into the brain of mice (Elshuber et al., 2003, Elshuber and Mandl, 2005). Adaptive mutations acquired by the virus after replication in the brains of these mice led to a change in the number of cysteine residues within prM, presumably affecting the shape of the molecule (Elshuber and Mandl, 2005). These mutants would not grow in BHK cells at 37°C, but one grew to a very low titer at 28°C (Elshuber and Mandl, 2005). Chymotrypsin-dependent mutants were not neurovirulent, but were stable for six passages without adaptations (Fischl et al., 2008).

Extra-virion roles for prM are poorly characterized, with studies to date limited to effects on the induction of apoptosis. Studies with mature M from a range of flaviviruses, particularly DENV, have demonstrated a pro-apoptotic effect localized to nine amino acids in the C-terminal (Catteau et al., 2003a). Further studies have demonstrated that this peptide sequence induces apoptosis through the permeabilization of mitochondrial membranes, and the activation of caspase-3 (Brabant et al., 2009, Catteau et al., 2003b). Studies to identify potential binding partners for prM within the cell have identified a number of candidates, including vacuolar ATPase and claudin-1 (Duan et al., 2008, Che et al., 2013, Gao et al., 2010). These interactions were suggested to be important in virus entry and release, but the exact mechanisms are poorly understood.

ENVELOPE GLYCOPROTEIN (E)

The envelope glycoprotein (E) is the third, and largest, of the flavivirus structural proteins, with a molecular weight of approximately 53-56kDa (Lindenbach et al., 2007, Rice et al., 1986b). Flavivirus E contains 12 conserved cysteine residues, which are important for generating disulphide bonds (Nowak and Wengler, 1987). For many flaviviruses, glycosylation of E occurs within the E_0F_0 loop (residue 154 for WNV), with residue 67 in DENV also glycosylated (Bryant et al., 2007, Lee et al., 2010). While beneficial to the virus (loss of glycosylation often results in decreased virus titers *in vitro* and lower virulence *in vivo*) glycosylation of E is not necessary for viral viability. Studies with DENV and WNV have suggested a role for the glycan in DC-SIGN and CD209L interaction (Alen et al., 2012, Davis et al., 2006a). Studies by Lee *et al*. with DENV-2 showed that loss of the glycosylation of E enhanced infection of mosquito cells, but adversely affected virion release (Lee et al., 2010). Some flaviviruses, including a number of isolates of SLEV and WNV, lack glycosylation of E without seemingly affecting *in vitro* growth kinetics, although disease severity may be reduced (Adams et al., 1995, Beasley et al., 2004a, Berthet et al., 1997, May et al., 2006, Post et al., 1992, Vorndam et al., 1993). Beasley *et al*. and Shirato *et al*. demonstrated that the loss of glycosylation of E could attenuate the neuroinvasiveness of WNV NY99, and Vorndam *et al*. demonstrated that lack of glycosylation of SLEV E reduced infectivity for mammalian cells (Vorndam et al., 1993, Beasley et al., 2005, Shirato et al., 2004b). As discussed above, correct folding of E and protection from premature conformational changes are highly-dependent upon prM (Guirakhoo et al., 1992, Heinz et al., 1994, Lorenz et al., 2002).

Structurally, E is composed of three distinct domains: Domain I, II, and III (Figure 1.3). Domain I (EI) has an eight-stranded β-barrel structure containing two

disulphide bonds, and is formed from three sections of the polypeptide chain (residues 1-51, 137-189 and 285-302 for TBEV, 1-51, 132-197 and 282-298 for WNV) (Rey et al., 1995, Kanai et al., 2006, Nybakken et al., 2006). Domain II (EII) is an elongated region of the glycoprotein composed of a number of β-sheets, and two α-helices (residues 52-136 and 190-284 in TBEV; 52-132 and 198-281 in WNV). It is important for dimerization of the glycoproteins on the surface of the virion, and contains a hydrophobic sequence in the cd loop at the distal end that is highly conserved between all flaviviruses, and is required for pH-dependent fusion (Rey et al., 1995, Allison et al., 2001). The third domain of E, Domain III (EIII), has an IgC-like fold similar to some host proteins (Bork et al., 1994, Rey et al., 1995). Indeed, the Arg-Gly-Asp/Glu (RGD/RGE) motif present in the FG loop of Domain III of a number of JE-complex flaviviruses has been implicated in binding of cellular proteins to integrins like the Fibronectin type III receptor (Rey et al., 1995, Ruoslahti and Pierschbacher, 1987). A number of flaviviruses have been shown to bind to integrins via EIII, although inhibition of these interactions, while reducing viral infection, do not fully stop it, suggesting that interaction with multiple cellular targets is important (Chu and Ng, 2004b, Hurrelbrink and McMinn, 2001). Interactions with glycosaminoglycans also seem to involve EIII, but again these seem to be dispensable for cell entry, and in some cases may be artifacts of tissue culture adaptation (Lee and Lobigs, 2000). Downstream of EIII are two antiparallel alpha helices that lie flush with the lipid envelope, which constitute the stem of E, followed by two hydrophobic transmembrane domains, TM1 and TM2 (Allison et al., 1999, Zhang et al., 2003a). The two stem-helices, EH1 and EH2, have been shown to be important for virion entry and particle assembly, with EH2 mediating interactions between prM and E during the heterodimerization process; and EH1, along with TM1 and TM2, playing a necessary role in the pH-dependent trimerization of E in the endosomes (Allison et al., 1999, Fritz et al., 2011, Lin et al., 2011).

A major role for E is in the pH-dependent fusion of the viral envelope with the endosomal membrane allowing for the release of the viral genome into the cytoplasm. When exposed to the acidic environment of the endosome, the E dimers that are normally lying parallel to the envelope dissociate into monomers, which interact with the target membrane (Allison et al., 1995, Stiasny et al., 1996). These monomers then trimerize, and draw the envelope and endosomal membranes together (Fritz et al., 2008, Stiasny et al., 2002, Stiasny et al., 2004). This conformational change requires significant rearrangement of the structure of E.

Extra-virion effects of the flavivirus envelope glycoprotein are poorly understood. Chiu *et al*. demonstrated an interaction between E of DENV-2 and the sumoylating enzyme Ubc9, with an overexpression of Ubc9 leading to reduced plaque formation (Chiu et al., 2007). Shyu *et al*. demonstrated that EIII from DENV-2 activates the MEK/ERK signaling transduction pathways, leading to the expression of plasminogen activator inhibitor type-1 (PAI-1), a factor also upregulated by YFV (Shyu et al., 2010, Woodson et al., 2013), findings that were further confirmed by Chen *et al*. (Chen et al., 2010). Due to its role in the modulation of the coagulation cascade, expression of this factor may contribute to the coagulatory dysregulation observed in viral hemorrhagic syndromes.

NON-STRUCTURAL PROTEIN 1 (NS1)

Non-structural protein 1 (NS1) is an approximately 46kDa glycoprotein that, with prM and E, is translocated to the ER after synthesis, where the E-NS1 junction is cleaved by a host signalase, and the NS1-NS2a junction is cleaved by an as yet undetermined protease (Lindenbach et al., 2007, Falgout and Markoff, 1995, Falgout et al., 1989). Structurally, NS1 has three domains: a hydrophobic β-roll (residues 1-29); an α/β "wing"

(residues 38-151), with a RIG-I-like structure; and a central β-ladder with an accompanying "spaghetti loop" structure behind (residues 181-352) (Akey et al., 2015, Akey et al., 2014). The domains are connected by a three-stranded β-sheet linker. The protein contains two or three N-glycosylation sites depending on the virus: YFV NS1 has glycosylation sites at residues 130 and 208, while MVEV NS1 has an additional site at residue 175 (Rice et al., 1986b). Soon after synthesis, NS1 dimerizes generating a hydrophobic "inner face" capable of associating with cellular membranes, and a hydrophilic outer face containing the glycosylation sites (Akey et al., 2015, Akey et al., 2014, Edeling et al., 2014). In addition to the membrane-associated dimer form, NS1 can be found as a secreted, lipid-associated hexamer (Akey et al., 2015, Flamand et al., 1999). The differences in localization appear to be dependent upon the modification of the oligosaccharides of the protein (Flamand et al., 1999). Monoclonal antibodies raised against NS1 are capable of inducing complement-mediated lysis of infected cells, suggesting that NS1 protein may be found on the cell membrane (Rice et al., 1986b).

NS1 appears to have an important role in flavivirus RNA replication, as it associates with the RNA replication complex, although the exact role is uncertain (Brinton, 2009, Mackenzie et al., 1996, Westaway et al., 1997). Trans-complementation experiments with YFV lacking NS1 demonstrated that neither positive- or negative-sense RNA accumulated, suggesting a role in early RNA synthesis (Brinton, 2009, Lindenbach and Rice, 1997). An inability of the NS1-lacking YFV to use NS1 from DENV suggested a necessary interaction with other viral proteins, with further studies identifying an interaction between NS1 and NS4a (Brinton, 2009, Lindenbach and Rice, 1999).

Jacobs *et al*. demonstrated that DENV NS1 could be glycosyl-phosphatidylinositolated to anchor it at the cell surface. This GPI-anchored form was shown to be capable of phosphorylating tyrosines on cellular proteins, indicative of signal

transduction, following binding with an anti-NS1 antibody, although the role this activity may play in infection is unknown (Jacobs et al., 2000). Chua *et al*. demonstrated that recombinant NS1 from DENV-2 interacts with STAT3β in cytoplasmic vesicles, and that the expression of NS1 leads to increased production of TNF-α and IL-6 (Chua et al., 2005). There are contradictory studies regarding the interaction with and/or inhibition of the host pattern-recognition receptor TLR3 by NS1 from WNV and other flaviriruses. Wilson *et al*., working with HeLa cells stably expressing WNV NS1, suggested that expression of WNV NS1 inhibits TLR3 signal transduction by stopping the induction of nuclear translocation of IRF3 and NF-κB (Wilson et al., 2008). Baronti *et al*. rebuffed those findings, reporting that NS1 from a number of flaviviruses, including WNV, had no inhibitory effect on TLR3 signaling in the same cell type (Baronti et al., 2010). However, the controversy has continued with the recent publication of papers by Crook *et al*. and Morrison & Scholle who proposed that secreted NS1 may have a TLR3-inhibiting effect on uninfected cells, and that the inhibitory effect could be abrogated by mutation of amino acids in the C-terminal (Crook et al., 2014, Morrison and Scholle, 2014).

Secreted NS1 appears to potentially have a number of extracellular functions. Recombinant NS1 has been shown to interact with a number of components of the complement system, including Factor H, C1s, C4, and C4b-binding protein (Chung et al., 2006, Avirutnan et al., 2010, Avirutnan et al., 2011). In addition, antibodies generated against DENV NS1 appear to cross-react with fibrinogen, thrombin and plasminogen, potentially contributing to the hemorrhagic manifestations observed in some DENV infections (Falconar, 1997, Chuang et al., 2014).

Non-Structural Protein 1' (NS1')

Some members of the JE complex of flaviviruses express an eleventh viral protein known as NS1' (approximately 58kDa). This protein is a form of NS1 elongated by 52aa, with additional sequence at its C-terminus derived from the NS2a coding region, although the sequence is not that of NS2a (Mason et al., 1987). Studies to determine the mechanism governing the production of NS1 have identified a -1 frameshift that occurs near the start of the NS2a coding sequence during translation, arising from a slippery heptanucleotide sequence and a nearby pseudoknot structure (Melian et al., 2010, Firth and Atkins, 2009, Sun et al., 2012). Mutational studies of the pseudoknot structure in NS2a, particularly an A30P mutation in KUNV, demonstrated that viruses lacking NS1' production permitted persistent non-cytopathic replication in mammalian cells, although it is not clear what additional role the mutation in NS2a may play (Melian et al., 2010). Other studies have demonstrated that SA14-14-2, the live, attenuated vaccine strain of JEV, does not produce NS1' due to a silent mutation in the same region of NS2a (Sun et al., 2012, Ye et al., 2012).

The role of NS1' in infection at both the cellular and organismal level is poorly understood. Young *et al*. demonstrated that NS1 and NS1' co-locate to the same sites within the cell, with NS1' capable of complementing key NS1 functions (Young et al., 2013). Sun *et al*. demonstrated that the elongated C-terminus can be recognized and cleaved by host caspases, but the role for this cleavage, and the effects of the products within the cell, is still unknown (Sun et al., 2012). Finally, Takamatsu *et al*. showed that NS1' appears to facilitate JEV infection in avian cells and embryonated chicken eggs, suggesting that it may play a role in the replication within the avian host (Takamatsu et al., 2014).

NON-STRUCTURAL PROTEIN 2A (NS2A)

Non-structural protein 2a (NS2a) is an approximately 22kDa non-glycosylated, hydrophobic viral protein (Lindenbach et al., 2007, Rice et al., 1986b). It is unclear which of the previously-named proteins NS2a was, due to a number of viral factors running similarly by polyacrylamide gel electrophoresis (PAGE) (Rice et al., 1986b). The structure of NS2a has not yet been determined, but the protein is thought to be membrane associated as it is cleaved at the N-terminus by an as yet unidentified ER-resident protease, and at the C-terminus by the cytoplasmic NS2b-NS3 protease complex (Lindenbach et al., 2007). Indeed, recent studies by Nemésio & Villalaín have demonstrated that a particular region of NS2a, located towards the N-terminus, interacts with membranes, with preference for those containing a large proportion of lipid molecules with a negative charge. Xie *et al*. have carried out a topographical analysis of DENV NS2a, showing that it possesses five transmembrane domains, and a sixth that associates with, but does not cross, the membrane (Nemésio and Villalaín, 2014, Xie et al., 2013). In addition to cleaving the NS2a-NS2b junction, the viral protease is also capable of digesting NS2a at an internal site to generate a truncated form known as NS2aα (Lindenbach et al., 2007, Chambers et al., 1990b, Nestorowicz et al., 1994). Mutation of that internal NS2aα cleavage revealed that blocking NS2aα production also stopped the production of infectious particles, but that this block did not occur at the RNA replication stage (Kümmerer and Rice, 2002). It was further shown that this block could be overcome by a compensating mutation in NS3, suggesting that both proteins together contribute to the assembly and release of infectious viral particles (Kümmerer and Rice, 2002). Studies by Liu *et al*. have supported a role for NS2a in virus assembly, as the introduction of an NS2a I59N mutation completely blocked virion production by a KUNV strain. This block could be overcome by complementing with WT NS2a *in trans*, but replicon RNA with the mutant NS2a could not be packaged when the KUNV

structural proteins were expressed *in trans* (Liu et al., 2003). Mutational analysis of the YFV NS2a N-terminus revealed a cluster of basic amino acids shown to be important in efficient virion production (Voßmann et al., 2015). Work by Leung *et al*. suggested that part of the role of NS2a in assembly may involve the biogenesis of viral membranes (Leung et al., 2008). In addition to a role in virus assembly, studies have shown NS2a to be associated with viral RNA replication complexes, where it interacts with NS3, NS5 and the 3' UTR, although the role it may play is unknown (Mackenzie et al., 1998).

Separate from virus replication, NS2a has been shown to play a role in minimizing the innate immune responses following infection (Muñoz-Jordan et al., 2003). Studies by Dalrymple *et al*. have demonstrated that NS2a, in combination with NS4b, can inhibit interferon-β induction by inhibiting TBK1 and IRF3 phosphorylation, in turn stopping RIG-I/MAVS signal transduction (Dalrymple et al., 2015). Liu *et al*. demonstrated that NS2a could significantly inhibit interferon-β promoter-driven gene transcription, and that a single mutation in NS2a, A30P, could dramatically reduce this inhibition (Liu et al., 2004, Liu et al., 2006).

NON-STRUCTURAL PROTEIN 2B (NS2B)

Non-structural protein 2b (NS2b) is a small membrane-associated protein with a molecular weight of about 14kDa (Clum et al., 1997, Lindenbach et al., 2007). Its main function appears to be as a co-factor for the viral protease NS3, as a number of studies have shown both a role in the activation of the NS3 protease precursor and in its enzymatic activity (Falgout et al., 1991, Clum et al., 1997, Zuo et al., 2009, Erbel et al., 2006). Other roles for NS2b are poorly understood, but studies by Yu *et al*. have demonstrated that NS2b appears to interact with NS2a, NS4a and NS4b, in addition to

NS3, suggesting that it may play a role in complexing viral membrane-associated non-structural proteins with the cytosolic NS3 and NS5 (Yu et al., 2013).

NON-STRUCTURAL PROTEIN 3 (NS3)

Non-structural protein 3 (NS3) is a large, cytoplasmic, non-glycosylated viral protein of approximately 70kDa (Lindenbach et al., 2007, Rice et al., 1986b). Structurally, NS3 contains a number of functional enzymatic domains. Expression of the N-terminal 184aa has demonstrated that this region codes for the protease domain, while the C-terminus possesses helicase, nucleotide triphosphatase (NTPase) and RNA triphosphatase (RTPase) activity (Chappell et al., 2005, Gorbalenya et al., 1989, Wengler and Wengler, 1991, Li et al., 1999). One of its primary roles is as the viral protease (Bazan and Fletterick, 1989, Lindenbach et al., 2007, Chambers et al., 1990c, Gorbalenya et al., 1989). As mentioned previously, this domain is produced as a protein precursor that requires the NS2b co-factor for activation (Clum et al., 1997, Erbel et al., 2006, Falgout et al., 1991, Zuo et al., 2009). NS2b appears to contribute a β-strand to the chymotrypsin-like fold, and provides a negatively-charged surface for substrate recognition, requirements that can be overcome by artificially fusing the necessary regions of NS2b with the NS3 protease domain (Erbel et al., 2006, Chappell et al., 2005, Yusof et al., 2000). Studies by Aleshin *et al*. have demonstrated that the interaction of WNV NS2b with NS3 can take two different forms, with one conformation leading to protease activation, and the other seemingly inhibiting the protease, presumably as a control mechanism (Aleshin et al., 2007). Similarly to NS2a, NS3 may be cleaved within itself by the NS2b/NS3 protease, resulting in a truncated form known as NS3' (Arias et al., 1993, Pugachev et al., 1993, Pugachev et al., 1992). The role of NS3' in infection has not been determined. The protease has a preference for sequences containing two basic amino acids followed by an amino acid with a short side chain (Yusof et al., 2000). As a

result of its rather non-specific cleavage requirements, it is logical to think that host factors may also be cleaved. Indeed, Lin *et al*. have recently demonstrated that the NS2b/NS3 protease is capable of cleaving IκB-α and –β, leading to the activation of NF-κB, and ultimately cell death (Lin et al., 2014).

The helicase activity of NS3 appears to be important for virus replication, with mutations abolishing helicase activity inhibiting the production of infectious virions (Matusan et al., 2001). The exact role of the helicase in virus replication is uncertain, but is thought to be important for unwinding double-stranded RNA during NS5-mediated RNA synthesis, particularly in the 3' UTR (Sampath et al., 2006, Chen et al., 1997a). The NTPase domain of NS3 appears to overlap with that of the helicase, and is likely involved generating the energy required for the helicase activity (Benarroch et al., 2004, Brinton, 2009). The RTPase activity is thought to be important for the dephosphorylation of the 5' terminus of the flavivirus genomic RNA prior to cap addition (Wengler and Wengler, 1993). The three non-protease activities of NS3 appear to require the same Walker B motif in the helicase core, although the main functional domain for the RTPase activity is located in the C-terminus (Benarroch et al., 2004, Bartelma and Padmanabhan, 2002).

NS3 has been shown to interact with a number of other flaviviral proteins, including NS4a, NS4b and NS5, as part of the replication complex (Zou et al., 2015a, Kapoor et al., 1995). Binding of NS4b appears to improve the specificity of the helicase domain of NS3 by reducing the affinity for single-stranded RNA, while NS4a appears to regulate the NTPase activity (Umareddy et al., 2006, Shiryaev et al., 2009). The interaction between NS3 and NS5 has been shown to enhance the activity of the NTPase and RTPase domains, suggesting that the association of the cytoplasmic non-structural

proteins within the replication complex is necessary for full efficiency replication-related activity (Cui et al., 1998, Yon et al., 2005).

In addition to its roles in virus replication and polyprotein processing, NS3 has been shown to induce apoptosis in the cell through both caspase-dependent and -independent pathways (Yiang et al., 2013, Shafee and AbuBakar, 2003, Ramanathan et al., 2006). The protease domain induces apoptosis to a significantly higher level than either the whole NS3 protein, or the helicase domain on its own (Yiang et al., 2013). Interestingly, for JEV NS3, caspase-dependent apoptosis appears to rely upon the activation of caspase-3 and -9, but not caspase-8 as had been described for Langat and other flaviviruses (Yiang et al., 2013, Prikhod'ko et al., 2002, Ramanathan et al., 2006, Yang et al., 2009b).

Finally, NS3, along with all of the cytoplasmic non-structural proteins except NS5, has been shown to inhibit IFN-α signaling and STAT2 translocation into the nucleus, although the mechanisms are unknown (Liu et al., 2005). In addition, García Cordero *et al*. have demonstrated that the NS2b/NS3 protease complex is associated with lipid rafts, and that NS3 directly interacts with caveolin-1 (García Cordero et al., 2014).

NON-STRUCTURAL PROTEIN 4A (NS4A)

Non-structural protein 4a (NS4a) is a small (approximately 16kDa), non-glycosylated viral protein with a number of roles during infection (Lindenbach et al., 2007). Structurally, NS4a is thought to have three membrane-associating domains (TMD1-3), with TMD1 and 3 crossing the ER membrane, and TMD2 associating with the internal face of the membrane (Lee et al., 2015, Miller et al., 2007). The first transmembrane domain has been shown to be important for NS4a oligomerization,

although mutations to inhibit oligomerization also reduced protein stability, so the observed decrease in viral replication cannot be attributed solely to the lack of oligomerization (Lee et al., 2015).

NS4a has been shown to interact with a number of other viral and host proteins. One of the major roles of NS4a in virus replication is in the generation of the replication complex, where, in combination with NS2a, NS2b and NS4b, it serves as a scaffold (Mackenzie et al., 1998, Zou et al., 2015b). Specific interactions have been demonstrated between NS4a and NS4b, NS4a and NS3, and NS4a and NS1 (Shiryaev et al., 2009, Zou et al., 2015b, Li et al., 2015, Lindenbach and Rice, 1999). Within the replication complex, NS4a appears to be important for the membrane rearrangements required for optimal replication. Studies by Miller *et al*. demonstrated that, in the absence of the 2K peptide, recombinant NS4a is capable of inducing cytoplasmic membrane alterations similar to those seen during virus infection, although Roosendaal *et al*. suggested that the presence of the 2K peptide on NS4a led to the more viral-like membrane rearrangements, and that removal of 2K resulted in NS4a being redistributed to the Golgi (Miller et al., 2007, Roosendaal et al., 2006). Since these studies used proteins from different flaviviruses (DENV and WNV, respectively), it is possible that subtle differences occur in the mechanisms employed by the different viruses. Teo & Chu demonstrated that interaction between NS4a and cellular vimentin appears to be intrinsically linked with the generation of the replication complex and its localization at the perinuclear area (Teo and Chu, 2014).

In addition to its roles in virus replication, NS4a has been shown to exert effects on a number of cellular factors involved in immune responses and autophagy. Lin *et al*. demonstrated that NS4a from JEV is capable of inhibiting interferon signaling by reducing the amount of STAT1 and STAT2 activation following IFN treatment (Lin et

al., 2008). The same study demonstrated an interaction between NS4a and the host RNA helicase DDX42, but the significance of this interaction is still unknown (Lin et al., 2008). Studies by Ambrose & Mackenzie demonstrated that NS4a and NS4b are capable of potently inducing the cellular unfolded protein response, which facilitates virus replication and extends the inhibition of the interferon response (Ambrose and Mackenzie, 2011). The effects of NS4a are not restricted to interferon inhibition; McLean *et al*. have shown that in certain cell types, NS4a is important for inducing autophagy through a PI3K-dependent process (McLean et al., 2011). This protects the cells from death during infection, and enhances virus replication. Finally, Chen *et al*. have demonstrated that NS4a from DENV interacts with the host eukaryotic initiation factor 4AI (eIF4AI). This interaction appears to be important in sequestering eIF4AI, as a knock-down of the factor significantly increased replication and decreased the activation of PKR (Chen et al., 2015).

2K Protein

The 2K protein, named after its molecular weight, is a small peptide located between NS4a and NS4b within the flavivirus polyprotein (Lin et al., 1993). 2K is generated through the cleavage at the C-terminus of NS4a by the viral NS2b/NS3 protease, followed by cleavage of the 2K/NS4b region by a host signalase (Lin et al., 1993). The role of 2K is unclear. Studies looking at NS4a-induced membrane rearrangements during DENV and WNV infection presented contradictory requirements for the presence of 2K attached to NS4a (Roosendaal et al., 2006, Miller et al., 2007). Drug studies have revealed a little light on 2K. Work by Zou *et al*. demonstrated that a single amino acid change in 2K (V9M) reduced the efficiency of the antiviral lycorine (Zou et al., 2009a). The authors concluded that 2K plays a role in viral replication, stating that the mutant grew to higher titers than wild-type (WT) WNV, although the differences

were a matter of 3-fold, barely over the level of variability of the assay (Zou et al., 2009a). Further studies with the 2K V9M mutant showed that 2K may have a role in preventing superinfection – infection of cells secondarily to an initial infection – since the 2K V9M mutant grew better than WT WNV in cells that were already expressing a WNV replicon (Zou et al., 2009b). This mutation has been independently observed by Mertens *et al*., who showed that the same V9M mutation promoted resistance to the antiviral effects of 2', 5'-oligoadenylate synthetase 1b (Mertens et al., 2010). Studies have demonstrated that this mutation occurs in a number of WNV isolates from mosquitoes and crows, and Campbell *et al*. determined that the mutation in 2K appears to increase the dissemination rate in mosquitoes, and outcompeted WT WNV at superinfection (Campbell et al., 2014, Armstrong et al., 2011, Pesko et al., 2012). However, during co-infection of mosquitoes with WT WNV, the 2K V9M mutant was moderately less fit (Campbell et al., 2014).

NON-STRUCTURAL PROTEIN 4B (NS4B)

Non-structural protein 4b is a 27kDa, hydrophobic protein located within the membrane of the endoplasmic reticulum (Lindenbach et al., 2007). Structurally, NS4b is thought to contain five transmembrane domains (TMD1-5), although membrane topographical studies suggest that the first two domains (TMD1 and 2) are actually not membrane-associated, and are instead resident in the ER lumen (Miller et al., 2006). NS4b has two predicted N-linked glycosylation sites, but the data are contentious as to whether the protein is actually glycosylated within infected cells (Miller et al., 2006, Zou et al., 2014, Naik and Wu, 2015). A recent study by Naik & Wu, who mutated the putative glycosylation sites on DENV NS4b, demonstrated that N→Q mutations, which would ablate glycosylation but should maintain structure, reduced RNA replication (Naik

and Wu, 2015). Studies by Zou *et al*. have demonstrated that NS4b likely forms homodimers, but the functional role of dimerization is unknown (Zou et al., 2014).

Similar to the other small non-structural proteins, NS4b is thought to be an integral part of the flavivirus replication complex (Miller et al., 2006). Studies looking at the interactions between NS4b and other viral proteins have shown that it interacts with NS4a and NS3, with the interaction with NS3 increasing the affinity of the NS3 helicase for double-stranded RNA (Zou et al., 2015a, Zou et al., 2015b, Umareddy et al., 2006). Youn *et al*. demonstrated that NS4b and NS1 can physically interact, presumably within the ER lumen, and suggested that this may be a mechanism for NS1-induced signal transduction across the ER membrane (Youn et al., 2012).

In addition to its roles in virus replication, NS4b has been shown to have a number of additional effects within infected cells. Similar to NS4a, Blázquez *et al*. have shown that mutations in WNV NS4b can affect the induction of autophagy, demonstrated for other flaviviruses to prolong the survival of infected cells and allow replication to higher titers (Blázquez et al., 2014), and Ambrose & Mackenzie have shown that both NS4a and NS4b are potent inducers of the unfolded protein response (Ambrose and Mackenzie, 2011). Studies by Kakumani *et al*. have revealed that DENV-2 NS4b is a potent suppressor of RNA interference (RNAi) mechanisms within mammalian cells, with a downregulation of host micro RNAs and factors involved in generating miRNAs (Kakumani et al., 2013). It has not yet been demonstrated whether similar inhibition of RNAi occurs in the arthropod vector, where RNAi appears to play a more significant immune-related role. Kelley *et al*. have demonstrated that NS4b appears to be responsible for the induction of dengue hemorrhagic fever (DHF)-related immunomodulators in THP-1 monocytes, and that these factors lead to permeabilization of endothelial cell monolayers, potentially contributing to the hemorrhagic aspects of DHF (Kelley et al., 2012, Kelley et al., 2011). Finally, Muñoz-Jordan *et al*. have demonstrated that the N-

terminal 125aa of NS4b is capable of partially blocking IFN-α/β signaling by inhibiting STAT1 activation. They also showed that the presence of the 2K peptide is required for this IFN antagonism, but that it can be replaced by an unrelated signal peptide (Muñoz-Jordan et al., 2005).

West Nile Virus Alternative Reading Frame 4 (WARF4)

Studies to look for alternative reading frames within the genome of flaviviruses have been limited, primarily due to the dogma that the large polyprotein-coding region is the single ORF in the genome, and the lack of demonstrable internal ribosomal entry sites (IRES). Nevertheless, as seen with NS1', products from alternative reading frames have been observed, usually resulting from frame-shifts during translation. Another such potential protein is West Nile Virus Alternative Reading Frame 4 (WARF4). Faggioni *et al*. demonstrated that a hypothesized 148aa peptide could be derived from an alternative reading frame in the NS4b/NS5 region of lineage I WNV isolates (Faggioni et al., 2009). Expression of a recombinant form of the potential peptide, followed by screening of WNV-infected horse serum demonstrated that a third of the samples had antibodies that reacted with the sequence (Faggioni et al., 2009). Further studies of the protein led to the generation of a monoclonal antibody specific to the peptide (Faggioni et al., 2012). Using this antibody, it was demonstrated that Lineage I WNV strains express WARF4 during infection of Vero cells, but that Lineage II strains do not. It was hypothesized that, similar to NS1', WARF4 is produced as a result of a ribosomal -1 frame-shift, but the cause of this shift and the role of the peptide within infected cells have not been determined (Faggioni et al., 2012).

NON-STRUCTURAL PROTEIN 5 (NS5)

Non-structural protein 5 (NS5) is the largest of the flaviviral proteins, with a molecular weight of approximately 104kDa (Lindenbach et al., 2007, Rice et al., 1986b). The structure of NS5 is such that it has two main domains, each with different enzymatic activity (Zhao et al., 2015). The N-terminal region of NS5 has a methyltransferase (MTase) and RNA guanylyltransferase (GTase) domain approximately 265aa in size, while the C-terminal domain of about 300aa is the RNA-dependent RNA polymerase (RdRp) (Zhao et al., 2015, Saeedi and Geiss, 2013, Issur et al., 2009, Grun and Brinton, 1986).

The capping of the 5'-terminal of viral genomic RNA is necessary for RNA stability and translation. Early studies on the methyltransferase domain of NS5 demonstrated that it possesses homology with S-adenosyl-methionine (SAM)-dependent methyltransferases, a large family of enzymes responsible for methylating a range of molecules within the cell, including the 5'-cap of mRNA, which suggested that the N-terminal of NS5 may be responsible for capping genomic RNA (Loenen, 2006, Chiang et al., 1996, Koonin, 1993). Later studies by Egloff *et al*. suggested that the SAM-dependent methyltransferase activity of NS5 was direct towards pre-capped RNA, raising doubt about the capping activity of the protein (Egloff et al., 2002). However, recent studies by Issur *et al*. have shown convincingly that a combination of activities by NS3 and NS5 are sufficient for *de novo* formation of a methylated cap structure (Issur et al., 2009). The working model is that, following the initiation of RNA synthesis by the RdRp domain of NS5, the 5'-triphosphate is hydrolyzed by the RNA triphosphatase activity of NS3. This modification of the RNA allows it to interact with the methyltransferase and RNA guanylyltransferase domain of NS5. The NS5 GTase then catalyzes the generation of a modified GMP, a process enhanced by the interaction with NS3, and the modified GMP is added to the RNA. The NS5 MTase then methylates the capped RNA to generate the appropriate Type 1 cap (Issur et al., 2009).

The other main role of NS5 in replication concerns its C-terminal RdRp domain. Early studies on flavivirus cell extracts had demonstrated the presence of RdRp activity, with this activity shown to be located in the membranes of the periplasmic ER (Tan et al., 1996, Chu and Westaway, 1987, Chu and Westaway, 1985, Lubiniecki and Henry, 1974). Sequence comparisons suggested that, based on homology with other positive-sense viruses, NS5 likely contained the RdRp domain (Koonin and Dolja, 1993, Lindenbach et al., 2007, Rice et al., 1985). *In vitro* studies with recombinant NS5 confirmed these suspicions (Ackermann and Padmanabhan, 2001, Guyatt et al., 2001, Tan et al., 1996). Studies with DENV-2 revealed two forms of RNA generated by the NS5 RdRp: full-length genomic RNA, and a hairpin RNA twice the size of the viral genome (Ackermann and Padmanabhan, 2001). The large, hairpin RNA was thought to be produced through self-priming by the template RNA, generating a single, large, palindromic sequence, while the full-length RNA product was thought to have been generated through *de novo* synthesis (Ackermann and Padmanabhan, 2001, Lindenbach et al., 2007). Interestingly, studies with the NS5 of KUNV produced only full-length RNA copies, rather than hairpins, suggesting that there may be a greater functional efficacy, or that RNA structural differences favored *de novo*, rather than self-priming, replication (Guyatt et al., 2001).

As mentioned previously, replication of the flavivirus genome requires cyclisation between the 5'- and 3'-UTRs. Within the UTRs there are three complementary regions that allow for the formation of an RNA ring, with the 5'- and 3'-termini coming into close proximity (Dong et al., 2008, Alvarez et al., 2005b, Friebe and Harris, 2010, Zhang et al., 2008). Prior to the generation of the negative-sense RNA, the NS5 RdRp recognizes and interacts with the 5'-SLA hairpin and the 3'-SL structure (Filomatori et al., 2006, Chen et al., 1997a). The negative-sense RNA synthesis then begins from the 3'-

terminus. Studies by Chen *et al*. demonstrated that the interaction with the 3'-SL involved both NS5 and NS3, an interaction discussed above (Chen et al., 1997a).

NS5 contains nuclear localization sequences that allow for importation into the nucleus by importin β1 and importin α/β (Brooks et al., 2002, Johansson et al., 2001). This importation appears to be dependent upon the phosphorylation state of NS5; with the majority of nuclear NS5 being hyperphosphorylated, and accordingly unbound to NS3 (Johansson et al., 2001). Inhibition of nuclear localization of NS5 by the drug Ivermectin demonstrated that this importation is important for infection (Tay et al., 2013, Wagstaff et al., 2012). Kumar *et al*. have shown that nuclear import of NS5 does not strictly correlate with viral replication and inhibition of interferon, so the role of NS5 in the nucleus remains unclear (Kumar et al., 2013).

One of the main non-replication roles for NS5 is inhibiting host interferon signaling, and therefore reducing antiviral immune responses. A number of studies have demonstrated that NS5 from tick- and mosquito-borne flaviviruses inhibit interferon signaling by targeting the Jak/STAT pathway, particularly STAT2 (Best et al., 2005, Lin et al., 2006, Park et al., 2007, Ashour et al., 2009, Laurent-Rolle et al., 2010, Mazzon et al., 2009, Werme et al., 2008). Studies into the mechanism of NS5-mediated IFN inhibition have demonstrated that, for YFV, NS5 binds to STAT2, but only in cells that have already been stimulated with IFN (Laurent-Rolle et al., 2014). This binding appears to require the IFN-induced phosphorylation of STAT1, and the polyubiquitinylation of NS5.

Studies looking at DENV-2 in mosquitoes have demonstrated that the mosquito protein kinase G (PKG) is capable of phosphorylating NS5 and its own regulatory domain *in vitro*, and that increasing PKG activity in mosquitoes alters flight behavior by

increasing wing activity during the day and flight activity at night. It was hypothesized that the observed increased flight activity may aid in the transmission of the virus (Keating et al., 2013).

Finally, NS5 has been implicated in modulating the expression of a number of chemokines, including IL-8 and RANTES. Both of these chemokines have been shown to be induced by DENV NS5, with IL-8 expression primarily resulting from activation of the CAAT/enhancer binding protein, and RANTES through NF-κB (Medin et al., 2005, Khunchai et al., 2015). It is thought that the expression and release of these chemokines from infected cells may aid in the dispersal of the virus throughout the host by recruiting immune cells to the site of infection (Lindenbach et al., 2007).

LIPIDS

The flaviviruses are enveloped viruses, and thus contain a lipid bilayer around the nucleocapsid in which the M and E glycoproteins are anchored. Early studies into the composition of flaviviruses determined that the particles contain approximately 10-20% lipid (Russell et al., 1980). Although much of the lipid content of the viral envelope is similar to that of the membrane of the endoplasmic reticulum from which it was derived, some differences have been observed in the proportions of lipid components. Trent (1980) demonstrated that, for SLEV, the percentage of sphingomyelin in the envelope was substantially higher than in the host cell membranes, a finding supported by Martín-Acebes *et al*., who showed that the levels of sphingomyelin can be 2-3 times higher than that of the average for host cell membranes (Martín-Acebes et al., 2014). In addition, phosphatidylcholine levels were shown to be lower in virions compared to host membranes, although data from Trent suggests this may be cell type-specific (Martín-Acebes et al., 2014, Russell et al., 1980).

A number of studies have investigated the role of lipids in virus replication. Work by Tang *et al*. demonstrated that the host factor Rab18, a member of the Rab GTPase family involved in membrane trafficking, is necessary for proper interaction of fatty acid synthase (FASN) and DENV NS3, and that inhibition of Rab18 reduced virus replication (Tang et al., 2014). Studies by García Cordero *et al*. have shown that NS3 interacts with caveolin-1 in cholesterol-rich lipid rafts, and that disruption of these detergent-resistant membranes reduced NS3 protein levels and particle release, suggesting that lipid rafts are important for proper polyprotein processing (García Cordero et al., 2014).

Finally, a number of studies have demonstrated a preferential interaction between C and endoplasmic reticulum-derived lipid droplets. Samsa *et al*. demonstrated that the capsid protein from DENV binds to the outer surface of lipid droplets in the cytoplasm (Samsa et al., 2009). This interaction appears to play important roles in sequestering the capsid proteins, and for acting as a scaffold for the association between C and the viral RNA (Samsa et al., 2009). Studies by Carvalho *et al*. demonstrated that the interaction between C and lipid drops is potassium-dependent, and is mediated by the host protein perilipin 3, found on the lipid drop surface (Carvalho et al., 2012). Martins *et al*. showed that the positively-charged N-terminal of C promotes interaction with the negatively-charged membranes of the lipid drops, leading to a conformational change in C which allows for the integration of the hydrophobic domain into the membrane (Martins et al., 2012).

STRUCTURE OF THE VIRION

The filterable nature of flaviviruses has been known for over a hundred years. In 1902, Reed & Carroll demonstrated that blood from patients suffering from yellow fever that had been filtered to remove bacteria could still cause the disease when administered

to healthy volunteers (Reed, 1902, Reed and Carroll, 1902). They concluded, "yellow fever… is caused by a micro-organism so minute in size that it might be designated as ultra-microscopic". Similar findings were made of the agent responsible for dengue in 1907 by Ashburn & Craig (Ashburn and Craig, 1907). They concluded, "the parasite causing dengue fever is ultramicroscopic in size", and that "a living organism is present in the filtrate, rather than a toxin" because of the delay before the development of symptoms.

It was not until the late 1960s, with the employment of electron microscopy techniques, that a clearer picture of the size and structure of the flavivirus virion arose. A number of early studies were carried out with JEV and DENV, and showed that the virions were spherical, approximately 50nm in diameter, and contained a lipid envelope approximately 35-45nm in diameter (Smith et al., 1970, Brandt et al., 1970, Matsumura et al., 1971, Matsumura and Hotta, 1971, Yoshinaka and Hotta, 1971, Kitaoka et al., 1971, Nishimura et al., 1968, Kitano et al., 1974). Similar studies with WNV (Chippaux-Hyppolite et al., 1970), TBEV (Weckström and Nyholm, 1965, Slávik et al., 1967, Slávik et al., 1970), POWV (Abdelwahab et al., 1964) and LGTV (Boulton and Webb, 1971, Boulton et al., 1971) were performed around the same time with similar results. Sedimentation analysis showed that mature, infectious virions had buoyant densities of around 1.23g/cm^3 (Smith et al., 1970, Stevens and Schlesinger, 1965, Heinz and Kunz, 1977, Shapiro et al., 1971). In addition to infectious virions, smaller subviral particles were identified and denoted as slowly sedimenting hemagglutinin (SHA) (Brandt et al., 1970, Smith et al., 1970). These particles were shown to also have a buoyant density of 1.23g/cm^3, similar to infectious viruses, but a diameter of only about 14nm, and a "doughnut-like" appearance by EM (Brandt et al., 1970, Smith et al., 1970).

Chemical analysis of infectious virions demonstrated that they were made of three proteins: C, M and E (known at the time as V2, V1 and V3, respectively); and were associated with a ribonucleic acid genome and a lipid envelope (Stollar, 1969, Westaway and Reedman, 1969, Westaway, 1975, Shapiro et al., 1972b, Shapiro et al., 1973a). Treatment of the virions with non-ionic detergent effectively solubilized E and M, indicating their presence as membrane-bound proteins on the surface, while leaving C associated with the viral RNA (Stollar, 1969, Shapiro et al., 1971). Analysis of SHA revealed that they were composed of M and E, as well as NV-2 (likely uncleaved prM), but lacked a nucleocapsid (Shapiro et al., 1972b, Shapiro et al., 1971, Cardiff et al., 1971). Accordingly, by 1980, the basic size and composition of flaviviruses and associated subviral particles were known, but details of the structure and inter-protein interactions were still left wanting.

A clearer understanding of the structure of the flavivirus remained lacking until the late 1990s and early 2000s. In 1995, Rey *et al*. published the structure of E of TBEV, derived from x-ray crystallographic analysis of the extracellular region of the glycoprotein that was purified following trypsinization of virions (Rey et al., 1995). The crystal structure suggested that, rather than forming spikes on the surface of the virion like many other viruses, E lies parallel to the envelope of the virion in dimers, and that the proteins likely form a lattice covering the surface (Rey et al., 1995). These hypotheses were confirmed by Kuhn *et al*. who, using cryoelectromicroscopy and fitting the known structure of E into the electron map, published the first 3D structure of the complete flavivirus at a resolution of 24Å (Kuhn et al., 2002). This revealed that the virions do indeed have a rather smooth surface, with only EIII forming minor protrusions from the surface, owing to the arrangement of the body of E parallel to the lipid envelope. Covering the surface of the virion is a “herringbone” lattice of 90 E dimers (180 copies of E in total) giving the virion an icosahedral structure. The M proteins (180 copies per

virion) are associated with the E near the fusion loop of EII. Within the envelope, the nucleocapsid forms a cage-like structure, although this structure appears to be flexible and less well-defined than the E lattice, likely due to less restrictive interactions with the envelope affecting cryo-EM resolution (Kuhn et al., 2002) (Figure 1.4).

The structure of the immature, prM-containing virions is substantially different. Within the envelope, the structure of the nucleocapsid is the same, but on the surface the arrangement of the E and prM molecules is distinct from that of mature, infectious particles. Zhang *et al*. demonstrated that on the surface of immature particles, three prM/E heterodimers group together to form a spike whose axis lies perpendicular to the envelope (Zhang et al., 2003b). As mentioned previously, the pr portion of prM is associated with the fusion loop located in EII, protecting it from premature pH-induced changes and fusion with target membranes. During maturation of the particles, prM is cleaved by cellular furin releasing pr from the virions. This maturation process is highly pH dependent. After immature virions have budded into the endoplasmic reticulum, where the pH is a reasonably neutral 7.2, they are transported to the Golgi, where the pH steadily drops to about 6.0 (Yu et al., 2008). Yu *et al*. have shown that this drop in pH leads to a conformational change in the structure of the immature virion, smoothening the surface to a conformation similar to that of the mature virion. It is at this stage that the low pH-dependent furin-mediated cleavage of prM occurs. Despite being cleaved, under the low pH conditions of the secretory exosome, the pr peptide remains associated with E, protecting it from forming the fusion state. The release of pr appears to be pH-dependent, and does not occur until the virion has been released from the cell (Yu et al., 2008).

The structure of the fusion trimer of E has been determined, and shares some similarity to the spikes seen on the surface of immature virions, albeit without the

protective prM caps (Modis et al., 2004). The exposure of the mature virion to the low pH of the endosome leads to the dissociation of the E dimers on the surface, and to a conformational change in E with an associated trimerization resulting in the bodies of E lying perpendicular to the envelope (Fritz et al., 2008, Stiasny et al., 2002, Stiasny et al., 2004). This structure allows for the hydrophobic fusion loop at the far end of EII to punch into the endosomal membrane, allowing for fusion of the envelope and endosomal membranes, and release of the nucleocapsid into the cytoplasm (Sultana et al., 2009).

THE FLAVIVIRUS REPLICATION CYCLE

The flavivirus replication cycle may be divided into several stages (Figure 1.5). Replication starts with the virus binding to receptors on the cell surface, followed by internalization into clathrin-coated endosomal vesicles. The lowering of pH in these vesicles results in a conformational change in the envelope proteins on the virion, leading to fusion between the viral envelope and the endosomal membrane, allowing for the viral RNA to be released into the cell. The genomic RNA is translated by host ribosomes to generate viral polyproteins, which are cleaved into constituent proteins by host and viral proteases. Rearrangement of ER membranes leads to the generation of replication complexes, in which new copies of the genomic RNA are produced. The genomic RNA associates with C proteins to form nucleocapsids, which are incorporated into prM-E-coated virions budding into the ER. The immature virions are secreted through the Golgi, where the lowering of the pH results in furin-mediated cleavage of prM, leading to virus maturation. Once the virions are released from the cell they are in a mature form capable of infecting other target cells. Each of these steps in the replication cycle is described in more detail below.

Receptor Binding

The initial stage of viral replication involves the interaction with, and binding to, receptors on the surface of the cell. The cell surface receptor is unknown for most flaviviruses; indeed a number of studies suggest that flaviviruses may use multiple receptors to gain entry to the cell, with the particular receptors used dependent upon the target cell type (Cruz-Oliveira et al., 2015). On the virus, attachment appears to be mediated by the domain III of the envelope glycoprotein (Cruz-Oliveira et al., 2015). The evidence for EIII being the receptor-binding domain is mostly indirect, but quite compelling. Crill & Roehrig demonstrated that antibodies targeting EIII of DENV were the most potently neutralizing, by blocking adsorption of the virus to the surface of Vero cells (Crill and Roehrig, 2001). Volk *et al*. showed that antibodies against EIII of WNV could neutralize the virus with a 3.7-$\log_{10}$ reduction in virus titer, while Nybakken *et al*. demonstrated that the potently WNV-neutralizing antibody E16 binds to a large region of EIII encompassing three structural loops, helping to narrow down the potential receptor-binding regions within EIII (Nybakken et al., 2005, Volk et al., 2004).

Further evidence for the role of EIII as the receptor-binding domain comes from binding competition assays between infectious virus and recombinant EIII molecules. A number of studies have demonstrated that recombinant EIII molecules can effectively inhibit viral entry, presumably through direct competition for cell surface receptors. Hung *et al*. demonstrated that recombinant EIII from DENV could effectively inhibit adsorption of the virus to the surface of BHK-21 and C6/36 cells, with a greater than 95% reduction in plaque number compared to the control, although this inhibition was only effective against the four DENV serotypes, with JEV infection only minimally inhibited, results that were further supported by Chin *et al*. (Hung et al., 2004, Chin et al., 2007). Similar observations were made for WNV, suggesting that the role of EIII applies

broadly to flaviviruses, and not just DENV (Chu et al., 2005). Chen *et al*., using recombinant DENV E fused to the Fc domain of IgG, demonstrated that for Vero, CHO, endothelial, and glial cells, receptor binding was mediated by amino acids within the 281-423 region of E, which corresponds to EIII (Chen et al., 1996). For monocytes and U937 cells, the Fc-Fc receptor interactions were more prevalent (Chen et al., 1996).

The cellular factors involved in flavivirus binding are a little less well defined. The RGD/RGE motif found within the EIII of a number of flaviviruses is a common amino acid triad found in adhesive proteins and demonstrated to mediate binding to integrins on the cell surface (Ruoslahti and Pierschbacher, 1987, Rey et al., 1995, Brinton, 2009). Studies with WNV and YFV have shown that EIII may interact with $\alpha_V\beta_3$ integrin, but that this interaction appears dispensable for infection, as recombinant $\alpha_V\beta_3$ integrin molecules failed to effectively inhibit virus entry, and mutation of the RGD motif in YFV did little to reduce infectivity (van der Most et al., 1999). Mutations of the final D/E in the motif have been observed following passaging in tissue culture for a number of flaviviruses including WNV and MVEV. Lee *et al*. targeted this residue for mutational analysis with MVEV and demonstrated that substitution of the negatively-charged residue for Gly, Ala or His led to increased inhibition by heparin and, for Gly and His, an attenuated phenotype in mice (Lee and Lobigs, 2000). Follow-up studies demonstrated that binding to glycosaminoglycans (GAGs) is important for flavivirus entry but that overreliance on this binding led to attenuation of the virus (Lee et al., 2004). It appears that the interaction between EIII and GAGs is non-specific, and functions to provide an initial attachment to the surface to allow for more specific receptor interactions to occur (Lindenbach et al., 2007, Grove and Marsh, 2011).

Specific flavivirus receptors have not been identified. Candidate mammalian and arthropod cell receptors include highly-sulphated heparan sulphate (heparin) (Chen et al.,

1997b, Germi et al., 2002, Hilgard and Stockert, 2000, Kroschewski et al., 2003, Lee et al., 2006, Okamoto et al., 2012), the glycosphingolipid nLc_4Cer (Galβ1-4GlcNAcβ1-3Galβ1-4Glcβ1-1'Cer) (Aoki et al., 2006, Wichit et al., 2011), DC-SIGN/L-SIGN (Navarro-Sanchez et al., 2003, Tassaneetrithep et al., 2003, Davis et al., 2006b, Mondotte et al., 2007, Davis et al., 2006a, Dejnirattisai et al., 2011), CD14 (Chen et al., 1999), HSP70 and HSP90 (Chen et al., 1999, Reyes-Del Valle et al., 2005, Das et al., 2009, Zhu et al., 2012, Thongtan et al., 2012, Salas-Benito et al., 2007, Vega-Almeida et al., 2013), mannose receptor (Miller et al., 2008), CLEC5A (Chen et al., 2008, Chen et al., 2012, Wu et al., 2013), mosGCTL-1 (Cheng et al., 2010), GRP78 (BiP) (Jindadamrongwech et al., 2004, Upanan et al., 2008, Cabrera-Hernandez et al., 2007, Vega-Almeida et al., 2013), high-affinity laminin receptor (Thepparit and Smith, 2004, Tio et al., 2005, Sakoonwatanyoo et al., 2006), Prohibitin (Kuadkitkan et al., 2010), TIM/TAM (Meertens et al., 2012, Jemielity et al., 2013), Integrin $\alpha_V\beta_3$ (Chu and Ng, 2004b, Chu and Ng, 2003), scavenger receptor class B type I (Li et al., 2013), claudin-1 (Che et al., 2013, Gao et al., 2010), NKp44 receptor (Hershkovitz et al., 2009), and unknown proteins of 29, 34, 43, 44, 65 and 74kDa molecular weights (Ramos-Castañeda et al., 1997, Martínez-Barragán and del Angel, 2001, Wei et al., 2003) (Table 1.1). The problem with all of these factors is that they are dispensable: no single receptor appears to be critical for flavivirus binding.

For some flaviviruses, particularly DENV and, to a lesser extent, WNV, virions can enter the cell by opsonization. In these instances, sub-neutralizing antibodies against viral structural proteins E and M, as well as the membrane protein precursor, prM, bind to the surface of the virion and mediate interaction between the virus and host cell through the immunoglobulin Fc receptors (Luo et al., 2015, Halstead, 1970, Peiris and Porterfield, 1979, Schlesinger and Brandriss, 1983, Schlesinger et al., 1983, Halstead and O'Rourke, 1977a, Halstead and O'Rourke, 1977b, Halstead et al., 1977, Schlesinger and Brandriss,

1981). This “antibody-dependent enhancement” (ADE) of infection relies upon the presence of pre-existing antibodies, and is particularly problematic in DENV, where antibodies generated against one serotype often cross-react with other serotypes in a sub-neutralizing manner allowing for enhanced infection and, potentially, the development of more severe symptoms such as those seen in dengue hemorrhagic fever (DHF) and dengue shock syndrome (DSS) (Guzman et al., 2013). Antibodies targeting prM (as opposed to M) may be particularly effective for ADE, as they allow for infection with immature virions that would otherwise be non-infectious (Dejnirattisai et al., 2010, Luo et al., 2015, Rodenhuis-Zybert et al., 2010, Chan et al., 2012).

Virus Entry

Following receptor binding, the next step in the replication cycle is entry. The binding of the virus to the receptor is followed by endocytosis via the formation of clathrin-coated pits (Gollins and Porterfield, 1985, Gollins and Porterfield, 1986c, Ishak et al., 1988, Nawa, 1998, Ng and Lau, 1988, Chu and Ng, 2004b, Chu et al., 2006, Chu and Ng, 2004a). Because the exact receptors used for flavivirus binding are uncertain, the steps between receptor-binding and endocytosis are unclear. Traditionally, the invagination of the membrane following receptor activation was thought to result from the recruitment of the host cellular protein AP2 to the plasma membrane, either through the binding to Yxxϕ (Tyr-any residue-any residue-bulky hydrophobic residue) motifs in the cytoplasmic tails of membrane-associated receptors, or through the interaction with the plasma membrane-specific lipid phosphatidylinositol-4,5-bisphosphate (McMahon and Boucrot, 2011, Ohno et al., 1995, Höning et al., 2005). Recent studies have suggested that AP2 may be recruited to the sites of endocytosis later than initially thought. Instead, the simultaneous binding of the virus to multiple receptors likely distorts the membrane slightly, causing it to curve. This curve in the membrane is recognized by the F-BAR

domain of FCH domain only (FCHO) proteins (Henne et al., 2010, Reider et al., 2009). In addition to FCHO proteins, EGFR pathway substrate 15 (EPS15) and intersectins associate with the curved membrane to generate a "nucleation module" that recruits AP2 and a number of receptor-specific adaptor proteins (McMahon and Boucrot, 2011, Henne et al., 2010, Reider et al., 2009, Stimpson et al., 2009). AP2 serves as a hub to which clathrin and other accessory proteins, such as epsins, bind to promote further membrane curvature (McMahon and Boucrot, 2011, Saffarian et al., 2009). The clathrin forms a cage-like structure around the developing endosome, which stabilizes the curvature. As the endosome formation nears a close, a number of BAR domain-containing proteins, including amphipysin, endophilin and sorting nexin 9 (SNX9) bind to the neck of the endosome, recognizing the sharp curve of the membrane (McMahon and Boucrot, 2011, Wigge et al., 1997, Ferguson et al., 2009, Sundborger et al., 2011). Dynamin is recruited to these proteins, and the vesicle detaches from the plasma membrane in a GTP-dependent manner, although the exact mechanism is uncertain (Hinshaw and Schmid, 1995, Sweitzer and Hinshaw, 1998, Stowell et al., 1999, Roux et al., 2006, Bashkirov et al., 2008). The endocytic process takes a matter of minutes, and ends with the vesicle being uncoated of its clathrin shell by the ATPase heat shock cognate 70 (HSC70) protein with one of its cofactors, auxilin or cyclin G-associated kinase (GAK) (Schlossman et al., 1984, Ungewickell et al., 1995, Greener et al., 2000). The uncoating procedure allows for the recycling of clathrin, and results in an uncoated vesicle containing the virus particle.

Following endocytosis, the next step in the entry process is the pH-dependent fusion of the viral envelope with endosomal membranes. The acidification of endosomes is dependent upon the vacuolar proton pump, or V-type H^+-ATPase (Van Dyke, 1996). This protein complex is capable of changing the pH within the endosome by 1.01ΔpH/min, although the rate at which the pH drops appears to be biphasic, with an initial fast drop to pH 6.0-6.2, and from there a more gentle drop to below 5.5 (Van Dyke,

1996, Van Dyke, 1993, Roederer et al., 1987). Gollins & Porterfield initially demonstrated that the lysosomotropic agents chloroquine, methylamine and ammonium chloride could inhibit viral entry by causing a build-up of virus in endosomes, without fusion and release of the nucleocapsid (Gollins and Porterfield, 1985, Gollins and Porterfield, 1986c, Gollins and Porterfield, 1984, Gollins and Porterfield, 1986b). Subsequently, Nawa showed that the treatment of Vero and C6/36 cells with bafilomycin A1, a specific inhibitor of the V-type H^+-ATPase, prevented viral fusion with the virions accumulating in the endosomes as demonstrated by gradient ultracentrifugation (Nawa, 1997, Nawa, 1998).

The reduction in pH within the endosome is necessary for the rearrangement of the envelope glycoproteins on the surface into a fusion conformation. Allison *et al*. demonstrated that a decrease in pH to about 6.5 led to the dissociation of the E homodimers on the surface of the virion, and to the formation of homotrimers (Allison et al., 1995). The conformational change allows for the presentation of the hydrophobic fusion loop of EII on the tip of the E trimers, which incorporates into the endosomal membrane (Allison et al., 2001, Stiasny et al., 2002). Recent studies by Chao *et al*. into the kinetics of fusion have shown that the threshold for fusion of WNV virus-like particles (VLPs) is about pH 6.4, with mean time to hemifusion of around 50 seconds following a drop in pH (Chao et al., 2014). The fact that fusion is efficient at pH 6.0-6.25 indicates that the conformational changes in E are optimally suited to the rapid drop to pH 6.0-6.2 in the endosome. In addition to pH, the efficiency of the fusion between the envelope and endosomal membranes appears to be dependent on the lipid composition of the target membrane, with membranes rich in cholesterol and oleic acid enhancing fusion, and lyophosphatidylcholine inhibiting it (Stiasny and Heinz, 2004, Stiasny et al., 2003). Once fusion has occurred, the nucleocapsid is released into the cytoplasm, where the capsid protein dissociates from the RNA allowing translation and replication to occur.

RNA Translation and Polyprotein Processing

As described previously, the genomes of flaviviruses are positive-sense, single-stranded RNA with a 5'-Type 1 $m^7G(5')ppp(5')AmpN_1$ cap structure and no poly(A) tail (Russell et al., 1980, Stollar et al., 1966, Cleaves and Dubin, 1979, Shatkin, 1976, Wengler et al., 1978). Translation is cap-dependent, with the ribosome recognizing the 5'-cap and then scanning for the AUG start codon (Lindenbach et al., 2007). Since the flavivirus RNA lacks a Kozak consensus sequence near the start codon, as is usual for eukaryotic mRNAs, it relies upon the secondary structure of the RNA within the 5'-UTR to direct the ribosome to the appropriate AUG (Clyde and Harris, 2006, Deas et al., 2005, Holden et al., 2006, Kinney et al., 2005).

The result of translation is a large polyprotein that is cleaved into the constituent mature proteins by a combination of host and viral proteases (Kümmerer, 2006, Lin et al., 1993, Nowak et al., 1989, Rice et al., 1986b). Three of the viral proteins, prM, E and NS1, are targeted to the endoplasmic reticulum, while the rest are either released into the cytoplasm, or are located on the cytoplasmic side of the ER membrane (Kümmerer, 2006, Markoff, 1989).

RNA Replication and Packaging

Within infected cells, three different forms of viral RNA have been demonstrated. Stollar *et al*. showed that during infection with DENV-2, the two major forms of viral RNA sediment at 45S and 20S, with a third, minor 26S component (Stollar et al., 1967). RNase sensitivity indicated that the 45S RNA was the single-stranded genomic form, while the 20S and 26S moieties were double-stranded replicative form (RF) and replicative intermediate (RI) (Cleaves et al., 1981, Stollar et al., 1967). The RF appears to be a true double-stranded RNA intermediate, while the RI is thought to be actively

replicating, with multiple new copies being generated simultaneously, which accounts for the slightly lower resistance to RNase compared to the RF (Chu and Westaway, 1985, Cleaves et al., 1981). The asymmetrical nature of the genome replication, which can lead to 10-fold excess in positive-sense RNA compared to negative-sense, ensures that the functional strand of viral RNA is preferentially generated so as to minimize resource waste through generation of the intermediary negative strand (Cleaves et al., 1981, Muylaert et al., 1996).

Infection of cells by flaviviruses leads to significant reorganization of host membranes. About 8 hours into KUNV infection of Vero cells, the rough ER starts to proliferate (Ng and Hong, 1989). After about 9 hours, clusters of smooth membrane structures (SMS) or vesicle packets (VP), ranging in size from 50nm to 200nm, start to appear around the nucleus (Ng and Hong, 1989). For JEV, the SMS start to appear about 15 hours after infection, and are localized within the cisternae of the ER (Leary and Blair, 1980). In addition to the SMS, convoluted membranes (CM) and paracrystalline structures (PS) form near the endoplasmic reticulum (Leary and Blair, 1980, Westaway et al., 1997, Ng and Hong, 1989). The CM and PS form late in infection, and are associated with numerous SMS, which led Leary *et al*. to hypothesize that they arise as by-products of SMS production (Leary and Blair, 1980). Studies to look for the source of the membranes in the virus-induced structures have shown that the CM and PS membranes are derived from intermediate compartments, as determined by the presence of ERGIC-53, while membranes of the SMS/VP are derived from the *trans*-Golgi, as they contain GalT (Mackenzie et al., 1999). The differences in sources of the membranes indicate that the CM and PC are not by-products of SMS generation, but are distinct, virally-induced membrane structures.

Studies to look for the localization of viral proteins and RNA with these membrane structures led the demonstration that the viral NS2b/NS3 protease is strongly associated with the CM/PS membranes, and these structures potentially play a role as polyprotein processing factories for optimal virus replication (Westaway et al., 1997). The SMS/VP are thought to be the main sites of RNA replication, as a number of viral non-structural proteins are localized there in complexes with double-stranded viral RNA (Westaway et al., 1997, Uchil and Satchidanandam, 2003a, Westaway et al., 1999). The localization of the replication complex within SMS/VP appears to protect it from protease activity, and allows for only the bare minimum of replicase proteins to be required, as previous studies demonstrated that protease treatment of JEV-infected cells resulting in the destruction of most NS3 and NS5, still possessed RdRp activity *in vitro* (Uchil and Satchidanandam, 2003a, Uchil and Satchidanandam, 2003b).

Replication of viral RNA is dependent upon the interaction between complementary cyclisation sequences in the 5'- and 3'-UTRs (Alvarez et al., 2005a, Alvarez et al., 2005b, Corver et al., 2003, Khromykh et al., 2001, Lo et al., 2003). The circularization of the genome allows for the interaction between NS5 and SLA in the 5'-UTR prior to 3'→5' negative-sense RNA synthesis (Dong et al., 2008, Filomatori et al., 2006). The roles of the viral proteins in RNA replication have been outlined above. *In vitro*, most of the newly synthesized RNA appears to be self-primed extensions of the template RNA leading to a large hairpin-like RNA molecule, which could account for the large quantity of 20S double-stranded RF RNA within the infected cell. However, a mechanism for processing the hairpin-like RNA into two, separate complementary copies has not been described (You and Padmanabhan, 1999). *De novo* generation of viral RNA has been demonstrated *in vitro*, but often as a minor occurrence (Chu and Westaway, 1987, Chu and Westaway, 1985, Ackermann and Padmanabhan, 2001, Nomaguchi et al., 2003). Generation of positive-sense RNA from the negative-sense template appears to be

efficient, with multiple copies being generated simultaneously (Chu and Westaway, 1987, Brinton, 2014).

The positive-sense genomic RNA generated within the replication complexes is released into the cytoplasm, where it is able to interact with ribosomes for further protein expression, and viral capsid protein for packaging into new virions. The capsid proteins, cleaved from the viral polyprotein into their mature form, associate with lipid droplets in the cytoplasm (Samsa et al., 2009). This association appears to act as a scaffold for holding the capsid proteins together to allow the viral RNA to associate with the positively-charged region of the protein. These lipid drop-nucleocapsids are thought to then interact with the endoplasmic reticulum, resulting in a conformation whereby the capsid-RNA is associated with the cytoplasmic face of the ER, and the viral prM and E proteins are present in the membrane on the luminal side of the ER. Studies expressing prM and E alone have shown that budding of viral and virus-like particles is dependent upon the interactions between prM/E heterodimers within the ER (Allison et al., 2003, Lorenz et al., 2003, Schalich et al., 1996). The observation of the production of slowly sedimenting haemagglutinin during infection suggests that the incorporation of nucleocapsids may be somewhat passive, and is dependent upon their presence on the cytoplasmic face of the ER membrane. The scarcity of observed viral budding by electron microscopy suggests that the process is rapid (Lindenbach et al., 2007).

Virus Maturation and Secretion

Once the immature, prM-containing virions have been produced and are present within the lumen of the ER, they are exported from the cell via the Golgi by the cell's secretory pathway (Lindenbach et al., 2007, Mackenzie and Westaway, 2001). Studies by Mackenzie & Westaway demonstrated that the secretion of particles late in infection

could be reduced by the addition of brefeldin A, a drug that inhibits the anterograde transportation of vesicles between the ER and Golgi (Klausner et al., 1992, Mackenzie and Westaway, 2001). Trafficking through the Golgi is important for the processing of the glycans of prM, E and NS1, as well as for the maturation of the virions as they pass through conditions of different pH (Rini et al., 2009, Yu et al., 2008). The process of virion maturation has been discussed in the virus structure section. During the maturation process through the Golgi, prM is cleaved to the mature M-form by furin in a pH-dependent manner (Yu et al., 2008). The mature viruses are released into the intracellular space allowing them to go forth and infect other cells.

ANTIGENIC PROPERTIES OF FLAVIVIRUSES

Early studies to distinguish between viruses, and to group them into genera and families, were heavily dependent upon cross-reactivity with serum from infected individuals, as well as mono- and polyclonal antibodies. Some of the earliest investigations were concerned with determining the identity of hitherto unknown viruses such as SLEV. During the outbreak that struck St Louis and Kansas City, MO, in 1933, studies to determine the etiological agent relied upon the demonstration that, whilst serum from SLEV-infected patients protected mice from intracranial inoculation with SLEV, serum from JEV-, LIV- and MVEV-infected patients did not, indicating that the virus was different from those previously described (Webster and Fite, 1934, Webster et al., 1935). Further studies by Kuttner & Ts'Un, confirmed by Webster, demonstrated that serum from a 27-year-old American woman, living in China, neutralized both JEV and SLEV (Kuttner and Ts'Un, 1936, Webster, 1938). The conclusion was drawn that JEV and SLEV were closely related. However, as the woman had travelled to China in 1933 (the year of the SLEV outbreak) it is possible that she encountered SLEV prior to emigrating. Nevertheless, a relationship between JEV and SLEV was suspected.

Investigations using rabbit immune serum raised against JEV and SLEV tended to support the suspicion. Kudo *et al*. demonstrated that, whilst serum from rabbits inoculated with SLEV neutralized SLEV, it was not successful at neutralizing JEV. Conversely, serum generated against JEV occasionally cross-neutralized SLEV, but this cross-neutralization appeared to be dependent upon the particular strain of JEV employed for generating the immune serum (Kudo et al., 1937).

Similar studies were carried out following the identification of West Nile virus by Smithburn *et al*. in 1940 (Smithburn et al., 1940). Cross-neutralization assays run soon after the initial isolation demonstrated that WNV was strongly neutralized by serum from a JEV-infected monkey, partly neutralized by serum from a human LIV infection, and barely neutralized at all by serum from an SLEV-infected monkey (Smithburn et al., 1940). Follow-up studies by Smithburn, Casals and Lennette & Koprowski further elucidated the antigenic similarities between a number of presumed-similar viruses. These results demonstrated that cross-neutralization occurred to some extent between JEV, SLEV and WNV viruses using immune serum, suggesting that all three viruses were closely related (Lennette and Koprowski, 1946, Casals, 1944, Smithburn, 1942). YFV serum and virus failed to neutralize, or be neutralized by, any of the other test materials (Lennette and Koprowski, 1946).

The development and use of complement fixation assays proved to be a more sensitive approach to determining cross-reactivity of antibodies, as it allowed for a determination of sub-neutralizing antibody binding. This assay was used by Casals to show that an antigenic relationship existed between Russian encephalitis (TBEV) and LIV, as well as between JEV, SLEV and WNV, but that no cross-reactivity occurred between these groups (Casals, 1944). Similar studies conducted by Sabin demonstrated that different dengue virus strains would differentially neutralize one another, with the

results clearly dividing them into two groups now known as Type 1 and Type 2 (Sabin, 1950). Within the same study, it was demonstrated that serum from DENV-infected patients cross-reacted with JEV, WNV and YFV, but not SLEV (Sabin, 1950).

A rather complicated picture was starting to develop regarding the relationships between viruses. Hirst had demonstrated in 1941 that red blood cells from chick embryos had a tendency to agglutinate when they came into contact with allantoic fluid following infection of the embryo with influenza virus (Hirst, 1941). It was concluded that this hemagglutination was virally-induced, and led other researchers to determine whether it was a broad effect of a range of viruses. Work by Hallauer, Lahelle & Horsfall and Olitsky & Yager demonstrated that a number of viral agents, including YFV, mousepox virus, and mengovirus were also capable of inducing hemagglutination (Lahelle and Horsfall, 1949, Olitsky and Yager, 1949, Hallauer, 1946). A large number of the early studies on flavivirus hemagglutination were carried out by Casals, MacDonald, and Sabin and associates. They demonstrated that hemagglutination efficacy was highly sensitive to the pH of the assay buffer, but that most of the as then-ungrouped flaviviruses were capable of hemagglutination (Casals and Brown, 1954, Sabin and Buescher, 1950, Chanock and Sabin, 1953c, Chanock and Sabin, 1953b, Chanock and Sabin, 1953a, Chanock and Sabin, 1954, MacDonald, 1952, Sabin, 1951, Sweet and Sabin, 1954). The ability to hemagglutinate erythrocytes, and the inhibition of this reaction by virus-directed antibodies, allowed for a detailed determination of the antigenic relationships between arboviruses. Given that hemagglutination inhibition (HI) tests were less specific than neutralization and complement fixing assays, it allowed for more distant relationships to be determined. A study by Casals & Brown, which looked at 21 different viruses, including 19 arboviruses, demonstrated that the majority of arboviruses tested by HI could be split into two main groups, Group A and Group B (Casals and Brown, 1954). Group A contained the viruses now known as the alphaviruses, including Eastern and

Venezuelan encephalitis viruses, as well as Sindbis, while Group B contained the viruses now known as the flaviviruses. Their studies demonstrated that the Group B arboviruses were all antigenically related to one another, but that the strength of cross-reactivity (determined by HI titer) varied, indicating a range of similarity (Casals and Brown, 1954). Further studies by Casals expanded the number of members in each group such that, by 1957, Group A contained 7 viruses, Group B contained 17, and a new Group C contained 3 (Casals, 1957). By 1975, and the publication of the second edition of the International Catalogue of Arboviruses, the combination of HI, complement fixation and neutralization assays had allowed for the demonstration of antigenic relationships between 57 different flaviviruses (Berge, 1975).

A reasonably comprehensive cross-neutralization study by De Madrid & Porterfield looked at serum from rabbits that had been immunized with one of forty-two different flaviviruses to determine homologous and heterologous neutralization titers (De Madrid and Porterfield, 1974). This study clearly revealed a grouping of flaviviruses by their ability to be cross-neutralized by various immune sera. Many of the tick-borne flaviviruses were neutralized by serum raised against other tick-borne flaviviruses, the exception being POWV. Additionally, what is now known as the JE complex of viruses, which includes JEV, WNV, SLEV and MVEV, was shown to possess high levels of cross-reactivity (De Madrid and Porterfield, 1974).

Studies to determine the structure and components of flaviviruses revealed the envelope glycoprotein to be the major contributor to the antigenic differences between otherwise closely related viruses and, due to its roles in virus binding and entry, the major neutralizing target of host antibodies (Roehrig, 2003, Cardiff et al., 1971, Eckels et al., 1975, Shapiro et al., 1971, Shapiro et al., 1973a, Shapiro et al., 1972b, Trent and Qureshi, 1971, Trent, 1977, Kitano et al., 1974, Heinz et al., 1981, Takegami et al., 1982). The

development of monoclonal antibodies (mAbs) allowed researchers to gain insight into the structure of E prior to the publication of the crystal structure of the TBEV envelope protein in 1995, and also to map the antigenic sites within the protein (Roehrig, 2003).

Many of the early studies to characterize the antigenic structure of the flaviviral E glycoprotein were carried out by Heinz and colleagues. Their work with monoclonal antibodies against TBEV E demonstrated the presence of three antigenic domains A, B and C, within which were epitopes that were mostly conformationally dependent, and some that were recognized by antibodies that effectively neutralized the virus (Heinz et al., 1982, Heinz et al., 1983b, Heinz et al., 1983a, Guirakhoo et al., 1989). Similar domains were demonstrated for DENV-2, however studies with SLEV and JEV E failed to demonstrate the three domains (Roehrig, 2003, Kimura-Kuroda and Yasui, 1983, Roehrig et al., 1983, Roehrig et al., 1998). The publication of the structure of the TBEV envelope glycoprotein revealed that the three antigenic domains were also structural domains, with antigenic domains A, B and C being structural domains II, III and I, respectively (Rey et al., 1995).

Detailed epitope mapping has been carried out for the envelope glycoprotein of a number of flaviviruses using a combination of approaches including sequencing of escape mutants, determining reactivity of mAbs with protease-derived fragments of the proteins, and the reactivity of mAbs with synthetic peptides (Roehrig, 2003). These studies have shown that neutralizing epitopes are present on all three of the domains of E, but antibodies targeting EIII are particularly effective at inhibiting viral adsorption to cells (Crill and Roehrig, 2001). In addition to inhibiting receptor interactions, neutralization of flaviviruses is thought to occur through the inhibition of fusion between the envelope and endosomal membranes. Antibodies that target the fusion loop within EII, such as the monoclonal antibody 4G2, also inhibit infection and, due to the

conserved nature of the EII fusion region, tend to be cross-reactive with other flaviviruses (Gollins and Porterfield, 1986a, Butrapet et al., 1998, Roehrig et al., 1998, Henchal et al., 1982). Studies into characterizing the binding site of neutralizing monoclonal antibodies have demonstrated that they tend to be around 500-900Å^2, and involve 15-20 contact residues, but are dependent upon the structure of the protein being in a mature conformation (Gubler et al., 2007, Davies et al., 1990), which accounts for the lack of strong reactivity of many neutralizing anti-flavivirus antibodies with denatured protein and synthetic peptides (Wengler and Wengler, 1989a, Guirakhoo et al., 1989, Holzmann et al., 1993, Roehrig et al., 1989).

Recent studies have demonstrated that, at physiological temperatures, cryptic epitopes, those that are not usually readily available for binding, may be revealed for recognition by reactive antibodies, often leading to virus inhibition (Kuhn et al., 2015). These findings have suggested that the surface of some flaviviral particles may be somewhat dynamic, as work by Lok *et al*. showed that the anti-DENV mAb 1A1D-2 potently neutralizes DENV-1, -2 and -3, but that this neutralization occurs at 37°C and not at 4°C (Lok et al., 2008). Binding studies revealed that the antibody binds to an epitope that includes the β-strand of EIII, a region of the protein that, based on the structure of mature virions, should not be readily accessible (Lok et al., 2008). The conformational changes required to permit antibody binding are not trivial, so led researchers to look at the structure of particular DENV serotypes at physiological temperatures. These investigations demonstrated that at 37°C, DENV-2 has a more fluid surface structure than anticipated, owing to the rotation of E-dimers outward from the surface, forming a "bumpy" configuration that allows antibodies to access regions of the protein otherwise concealed (Fibriansah et al., 2013, Zhang et al., 2013). Other studies have suggested that less-infectious partially mature virions, those with some residual, uncleaved prM, may behave differently to mature viruses with regards to antibody-

mediated neutralization (Plevka et al., 2011, Oliphant et al., 2006, Pierson et al., 2007, Nelson et al., 2008).

In addition to the envelope glycoprotein, small numbers of flavivirus neutralizing antibodies have been demonstrated targeting prM/M (Roehrig, 2003, Takegami et al., 1982, Holbrook et al., 2001, Bray and Lai, 1991b). Bray & Lai demonstrated that vaccination of mice with vaccinia viruses expressing DENV-4 prM and M could protect them from subsequent viral challenge, whereas a vaccinia virus expressing the pr peptide fragment could not (Bray and Lai, 1991b). Interestingly, similar vaccination with prM from DENV-2 was not protective. Work by Holbrook *et al*. demonstrated that antiserum raised against M from Langat virus was cross-protective against LGTV and POWV, but not against DENV-4, JEV or YFV, indicating that neutralizing epitopes on M are not strongly conserved throughout the flaviviruses (Holbrook et al., 2001).

Finally, a number of studies have shown that antibodies against NS1 are often generated to high levels during infection. Due to the fact that NS1 is not resident in the virion, these antibodies cannot be classed as neutralizing, but passive transfer of anti-NS1 antibodies has been demonstrated to protect against subsequent viral challenge (Roehrig, 2003, Gould et al., 1986, Henchal et al., 1988, Iacono-Connors et al., 1996, Schlesinger et al., 1985, Schlesinger et al., 1986, Schlesinger et al., 1987). Owing to the protective, but non-neutralizing nature of many anti-NS1 antibodies, detailed studies have been carried out to map the epitopes on DENV NS1, which has revealed that the majority, as for E, are conformation dependent (Falconar and Young, 1991, Henchal et al., 1987, Young et al., 1993, Bletchly, 2002). Similar epitope maps have been generated for NS1 from MVEV (Hall et al., 1990). Interestingly, the majority of the epitopes appear to be serotype-specific, with little cross-reactivity between antibodies raised against NS1 from one virus when targeted against another (Hall et al., 1990, Henchal et al., 1987). Immunogenicity

of NS1 appears to be dependent upon the physical state of NS1, with dimers generating a stronger immune response than monomers, and secreted NS1 being more immunogenic than its cell-associated form (Falconar and Young, 1991). A number of studies have suggested that sequence similarity between NS1 and certain endothelial cell molecules may lead to binding of anti-NS1 antibodies to these host factors, causing endothelial cell damage, and potentially contributing to hemorrhage seen in DENV infection (Lin et al., 2002, Lin et al., 2005). Indeed, there has been a suggestion that high circulating levels of NS1 early in DENV infection may be correlated with severe outcomes such as dengue hemorrhagic fever and dengue shock syndrome (Libraty et al., 2002).

FLAVIVIRUS TRANSMISSION

In humans, members of the *Flaviviridae* are responsible for a variety of diseases including acute febrile disease with painful arthralgia during DENV infection, encephalitis with WNV and JEV infection, and hemorrhagic fever with Omsk hemorrhagic fever virus (OHFV) and YFV. Most of the flaviviruses are arthropod-borne viruses (arboviruses), vectored by either mosquitoes or ticks, although a few have no known vector (Gubler et al., 2007). Both the mosquito- and tick-borne groups contain members that cause encephalitic and hemorrhagic fever infections.

The mosquito-borne flaviviruses include the majority of those that cause significant global mortality and morbidity, such as DENV, WNV, JEV, and YFV (Gubler et al., 2007). The potential for transmission of flaviviruses by mosquitoes was first proposed by Finlay in 1881, and by 1899 he had demonstrated that a mild, febrile illness could be induced in patients who had been fed upon by an infected mosquito a few days after that same mosquito had fed upon a YFV-infected patient (Finlay, 1881, Finlay, 1899). At the same time, he proposed, based upon the studies by Smith & Kilborne,

working on Texas Fever in ticks, that vertical transmission of the agent of yellow fever may occur from adult mosquitoes to their offspring, a mechanism that was only demonstrated experimentally for flaviviruses in 1976 by Coz *et al*. using KOUV (Coz et al., 1976). Following Finlay's inconclusive results with mosquito transmission, Reed *et al*. attempted the experiments again in 1900, using materials supplied by Finlay, this time increasing the time between feeding of the mosquito on an infected patient, and its subsequent feeding on a naïve one, with more success than Finlay's original study (Reed et al., 1900, Anon, 1900, Finlay, 1881). The mosquitoes used for the studies were *Culex fasciatus* (now named *Aedes aegypti*), and led to the conclusion that if the mosquitoes were eradicated, so too might the disease. Under this assumption, Gorgas and officials in Cuba proceeded to muster teams to drain areas of standing water, including drains and ditches, where possible, and cover the water with a layer of oil where drainage was not feasible. This, combined with the sealing of barrels of water, lead to a drop in yellow fever cases in Havana from 603 in 1897 to just 3 in 1901 (Gorgas, 1901). Gorgas later went on to employ similar techniques to rid the Canal Zone in Panama of yellow fever and malaria, scourges that had plagued the workers building the Panama canal (Gorgas, 1915).

For dengue, the realization of its transmission by mosquitoes followed a couple of years later than for yellow fever. Interestingly, one of the earliest accounts of bilious remitting fever (now known as dengue fever), written by Rush in 1789, specifically states in a footnote that the mosquitoes were particularly bad at the time of the outbreak in 1780, however, a connection between mosquitoes and outbreaks was not made for nearly 100 years (Rush, 1789). Graham was the first to demonstrate that DENV could be transmitted by mosquitoes, although he purported to have used *Culex fatigans* (*Culex quinquefasciatus*), which subsequent studies have shown not to support transmission of DENV (Graham, 1902, Graham, 1903, Siler et al., 1925, Rosen et al., 1985). Further

studies by Bancroft demonstrated that *Stegomyia fasciata* (*Aedes aegypti*), the same vector demonstrated by Finlay and Reed *et al*. to transmit YFV, was capable of transmitting DENV, although concluded that "the organism lives but a few days in the mosquito" (Bancroft, 1906). Ashburn & Craig, working with *Culex fatigans* struggled to see transmission of DENV, indeed only one of the subjects developed dengue-like symptoms (Ashburn and Craig, 1907). Cleland & Burton were able to confirm transmission by *Stegomyia fasciata*, demonstrating that DENV was indeed a mosquito-borne disease, but that only certain mosquitoes were able to transmit it (Cleland and Bradley, 1918). Later studies revealed that a number of *Aedes* species mosquitoes were efficient vectors of DENV (Siler et al., 1925, Simmons et al., 1931, Snijders et al., 1931, MacKerras, 1946, Rosen et al., 1954).

Other mosquito-borne flaviviruses, such as JEV, SLEV and WNV, were shown to be effectively transmitted by *Culex* mosquitoes, although transmission by other species, such as *Mansonia spp*. (JEV), *Aedes normanensis* (MVEV), and *Aedes spp*. (WNV) has been demonstrated (Gubler et al., 2007). In addition to *Aedes aegypti*, YFV has been shown to be transmitted by a range of *Aedes* species, and has even been isolated from eggs and larvae of a hard tick, *Amblyomma variegatum* (Gubler et al., 2007, Saluzzo et al., 1980).

The tick-borne flaviviruses include some of the more pathogenic viruses for humans, such as TBEV, OHFV, KFDV and AHFV, as well as POWV and LIV (Gubler et al., 2007). One of the earliest demonstrations of tick-borne transmission was with LIV. It had been suspected since the 1880s that louping ill, a disease primarily of sheep, was associated with ticks, as most infected animals were heavily infested (Williams, 1883). By 1897, Williams had determined epidemiologically that "where there are no ticks, there is no louping-ill", but experimental evidence was still sparse due to the difficulties of

experimentally infecting ticks and, subsequently, sheep (Williams, 1897). The identification of the filterable nature of the etiological agent by Pool *et al*. allowed for a more thorough investigation into the transmissibility by ticks (Pool et al., 1930). By 1932, the experimental evidence of tick-borne transmission had been attained: virus could be isolated from *Ixodes ricinus* ticks that had fed on an infected sheep, and the disease could be transmitted to naïve sheep by female ticks and nymphs that had been infected at the nymphal or larval stage, respectively (Macleod and Gordon, 1932).

Tick-borne encephalitis was first described by Schneider in 1931, after noticing an increase in cases of aseptic meningitis during the summer months in Austria and Germany (Schneider, 1931). However, it wasn't until the late 1930s, during an expedition to the Far East of the Soviet Union, that a viral agent was identified (Chumakov and Seitlenok, 1940, Smorodintseff, 1940, Silber, 1939). During the same expedition, it was shown that TBEV was transmitted by the ixodid tick, *Ixodes persulcatus* (Chumakov and Gladkikh, 1939, Shubladse and Serdiukova, 1939). Soon afterwards, TBEV was discovered in the European part of the USSR, with subsequent studies revealing that in this area, *Ixodes ricinus* ticks were the principle vectors, similar to LIV (Chumakov and Seitlenok, 1940, Gubler et al., 2007). Subsequent studies have shown that a number of *Ixodes* ticks, as well as *Dermacentor* and *Haemaphysalis* ticks, are capable of transmitting the virus (Gubler et al., 2007).

Whilst most mammalian tick-borne flaviviruses are transmitted by hard ticks, such as *Ixodes ricinus*, many of the seabird tick-borne flavivirus complex members are transmitted by soft ticks, such as *Ornithodoros (Alectorobius) maritimus*, although there are exceptions (Gubler et al., 2007, Chastel et al., 1985).

Transmission of both mosquito- and tick-borne flaviviruses is biological rather than mechanical. As such, the virus replicates within tissues of the arthropod, allowing for increased titer and efficient transmission (Gubler et al., 2007). Within mosquitoes, initial infection occurs in the epithelial cells lining the wall of the midgut after it imbibes a blood meal from an infected host. The titer of the virus increases until it reaches a threshold whereby it can escape into the haemocoel and spread to the salivary glands. Infection of the salivary glands allows for a high titer of virus to be present in the saliva, and permits transmission of the virus when the mosquito feeds on a naïve host (Gubler et al., 2007, Gubler and Rosen, 1977).

For ticks, the route of infection is similar: through the epithelial cells of the midgut. However, within the tick midgut, the virus has longer to infect the cells, as the blood meal remains undigested for an extended period of time (Nuttall and Labuda, 2003). The infection of midgut epithelial cells appears to be a limiting factor in vector competence for ticks, however if this early infection occurs, spread to the salivary glands is common (Nuttall and Labuda, 2003, Nuttall et al., 1994).

WEST NILE VIRUS

West Nile virus (WNV) is an encephalitic flavivirus first isolated in 1937 from a patient in Uganda (Smithburn et al., 1940). Early studies demonstrated that it was a filterable agent, and that it was antigenically strongly related to JEV (Smithburn et al., 1940). WNV activity remained low until the mid-1950s, when cases were reported in Egypt and Israel, with further serological evidence in South Africa, India, Sudan, Kenya, Uganda and the Belgian Congo (Melnick et al., 1951, Bernkopf et al., 1953, Weinbren, 1955, Smithburn and Jacobs, 1942, Smithburn et al., 1954). At the same time, studies were being presented showing that the virus was mosquito-borne, spread by a number of

Culex and *Aedes* species (Kitaoka, 1950, Philip and Smadel, 1943, Taylor et al., 1953). In the early 1950s, there were even experimental infections with WNV in patients with advanced neoplastic disease, with a view to determining whether it had anti-neoplastic effects, with a secondary investigation into experimentally controlled infections (Southam and Moore, 1951, Southam and Moore, 1954b, Southam and Moore, 1954a, Southam and Moore, 1952, Newman and Southam, 1954). Suffice to say, the oncolytic properties of the virus were minimal.

Over the following few decades, WNV remained something of an inconvenience rather than a significant public health problem, with occasional outbreaks of dengue-like illness (Gubler et al., 2007). By 1999 it was prevalent throughout Africa, the Middle East, the Mediterranean, West Asia and parts of Europe, with some reports of neuroinvasive disease, but was often overlooked by researchers in favor of more common viruses such as DENV. Indeed, between 1943 and 1999, there was an average of only 16 WNV research papers published per year, with a maximum of 35 in 1986. The events of 1999 ensured that there was a seismic shift in focus towards WNV.

In the late August of 1999, a small cluster of cases of encephalitis was observed in northern Queens, NY. Patients were presenting with a febrile illness followed by a change in mental state, with a few cases showing signs of flaccid paralysis (Nash et al., 2001). The combination of prevalent *Culex* mosquitoes, and a propensity for the patients to work outdoors in the evening led epidemiologists to suspect an arbovirus. Serological screening of the patients revealed positive results against SLEV, and a hypothesis of an atypical SLEV outbreak was proposed (Nash et al., 2001). A concurrent epizootic was killing substantial number of bird around New York but, due to the low pathogenicity of SLEV in birds, it was assumed the two outbreaks were unrelated. A month after the first human cases were reported, a virus was isolated from tissue specimens from American

crows and a Chilean flamingo, which later turned out to be WNV (Steele et al., 2000). Sequencing of samples amplified from the brains of five human infections revealed a WNV-like virus to be the culprit (Briese et al., 1999). Since 1999, there has been an average of 366 WNV-focused papers published each year.

The emergence of WNV in the Americas has been impressive. In the years following 1999, the virus spread quickly and relentlessly across the United States, and into Canada and Mexico. After the initial cases in 1999, the virus moved south and west, akin to the pioneers of old. By the end of 2000, prevalent viral activity had been observed across the North East (particularly New York State). By 2002, human and non-human WNV activity was being reported across the Eastern two-thirds of the United States, with additional WNV-positive mosquito, equine, and bird samples in Ontario, Canada, and Mexico (Roehrig, 2013, PHAC, 2015, Estrada-Franco et al., 2003). 2003 saw a further push west, and a peak number of reported cases at 9,862, with 2,866 cases of neuroinvasive disease, although this peak may be somewhat overrepresented by increased surveillance (CDC, 2015). Aside from a lull between 2008 and 2011, the number of neuroinvasive cases of WNV infection has remained fairly steady, with about 1,200 cases (min 386 (2009), max 2,873 (2012)) per year in the US (CDC, 2015). Amongst the contiguous 48 states, all reported at least one human case of neuroinvasive disease between 1999 and 2012 (CDC, 2015).

Phylogenetically, WNV may be divided into two lineages. Lineage I viruses appear to be more widely distributed than Lineage II, with strains isolated from Africa, Australia, India, the Middle East, the Americas, and Europe, while Lineage II viruses appear to be mostly restricted to Africa and Madagascar, although they have been implicated in some recent outbreaks in Europe (Gubler et al., 2007). The majority of WNV epidemics have been caused by Lineage I viruses, which have historically been

more virulent than their Lineage II relatives, although recent outbreaks suggest that this may be changing (Lanciotti et al., 1999, Murgue et al., 2002, Gubler et al., 2007).

Studies by Work and colleagues in Egypt demonstrated that WNV could be isolated from birds in the Nile delta, including hooded crows and rock pigeons, and proposed that wild birds may be reservoir hosts for the virus (Work et al., 1955, Work et al., 1953, Hurlbut et al., 1956). Subsequent studies confirmed that West Nile virus is primarily maintained in nature by an enzootic cycle involving the mosquito vectors and a variety of bird species (Gubler et al., 2007). WNV is particularly promiscuous, having been isolated from over 300 different bird species, as well as over 30 species of non-avian animals, including alligators and small mammals (Komar, 2003). While WNV infection in many North American birds is lethal, high-level viremia in passerine birds, such as crows and sparrows, is sufficient to readily infect feeding mosquitoes (Komar, 2003).

In humans, the majority of WNV infections are subclinical (Figure 1.6). Estimates place the proportion at around 80%, but exact numbers are uncertain (Gubler et al., 2007). Of the remaining 20%, the vast majority will have a mild to severe dengue-like illness, with less than 1% of infections leading to a neuroinvasive disease (Hayes and Gubler, 2006, Hayes et al., 2005). Of this 1%, a tenth of infections are usually fatal. As with many pathogenic flavivirus infections, symptomatic WNV infection often has a biphasic presentation and is usually characterized by fever, headache, generalized myalgia, vomiting, diarrhea and anorexia (Gubler et al., 2007, Asnis et al., 2000, Ceauşu et al., 1997, Chowers et al., 2001, Emig and Apple, 2004, Jeha et al., 2003, Nash et al., 2001, Pepperell et al., 2003, Sayao et al., 2004, Sejvar et al., 2003a, Weiss et al., 2001). About half of cases present with a roseolar or maculopapular rash. Neuroinvasive WNV infection is often characterized by aseptic meningitis, encephalitis or flaccid paralysis;

with other symptoms including altered mental status, fatigue, and tremors (Gubler et al., 2007, Asnis et al., 2000, Gadoth et al., 1979, Sejvar et al., 2003b, Sejvar et al., 2003a, Jeha et al., 2003).

ANIMAL MODELS FOR WNV

During the initial isolation of the virus by Smithburn *et al*. the investigators demonstrated that it was virulent in mice via intracranial, intranasal and intraperitoneal inoculations, although the particular mouse strain used is not noted (Smithburn et al., 1940). In rhesus macaques, intracranial and intranasal inoculation often led to signs of encephalitis, but the infection was not always lethal, and intravenous inoculation led to seroconversion, but not clinical disease (Smithburn et al., 1940). Rabbits, guinea pigs, hedgehogs and African green monkeys showed no clinical signs of infection, even after intracranial inoculation, but did seroconvert (Smithburn et al., 1940). The isolation of WNV from a human patient in Egypt led to another round of inoculations in a range of animals including mice, hamsters, monkeys, chimpanzees and chick embryos (Melnick et al., 1951). In most of these a viremia was detected, however monkeys only developed clinical signs of encephalitis following intracranial inoculation, and subcutaneous inoculation of chimpanzees led to an asymptomatic infection (Melnick et al., 1951). Reagan *et al*., using 3-week old female Swiss Webster mice and cave bats (*Myotis lucifugus*), demonstrated symptomatic infection in both animals when 10^6 mouse lethal doses of virus was administered by one of eight routes (intraperitoneal, rectal, intradermal, intracardiac, intramuscular, intralingual, intracerebral and intranasal) (Reagan et al., 1952b). As the mice were euthanised upon the first sign of neurological infection, mortality was not determined.

Throughout the 1950s, a number of investigators studied WNV infections with the B956 or Egypt-101 strains in a range of animals. Reagan *et al*. carried out experimental infections in chicks and young dogs, Mauelidis studied the neuropathology of WNV in monkeys, while Lavillaureix *et al*. focused on gerbils and mice (Reagan et al., 1952a, Reagan et al., 1953, Manuelidis, 1956, Lavillaureix et al., 1958). Schmidt & Elmansoury demonstrated natural and experimental infection in horses (Schmidt and Elmansoury, 1963).

By the late 1960s, detailed studies were starting to be carried out to characterize animal models with respect to the effects of age on susceptibility, and the virus titers and virus-induced pathology within the brain (Eldadah and Nathanson, 1967, Eldadah et al., 1967, Haahr, 1968). Following intraperitoneal inoculation with the Egypt-101 strain, lethal infection was observed in mice less than 6 weeks old, while intracranial inoculation remained lethal in the oldest mice (12 weeks). In rats, 10-day-old and younger animals were susceptible to intraperitoneal inoculation, while animals older than two weeks were resistant to intracranial inoculation (Eldadah et al., 1967). Subsequent investigations have involved the experimental infection with WNV NY99 and determination of pathology in wild birds, domestic geese, hamsters, non-human primates, and various strains of mice (Pérez-Ramírez et al., 2014, Sá E Silva et al., 2013, Kimura et al., 2010, Holbrook and Gowen, 2008).

The susceptibility of young mice (<8 weeks) to WNV by a variety of inoculation routes makes them a useful model for virulence and pathogenesis studies, and is accordingly by far the most commonly used model for WNV infection. A number of different inbred and outbred strains are frequently used, including C57BL/6, BALB/c, NIH Swiss and Swiss Webster and, while subtle differences may occur between different strains, the disease produced in sensitive mice following infection is usually comparable,

with more variation seen between virus strains than mouse strains (Beasley et al., 2002, Kimura et al., 2010, Nalca et al., 2003, Shirato et al., 2004a).

Following intraperitoneal (i.p.) inoculation with 100-1,000 pfu of WNV NY99 (a highly-virulent WNV isolate from the original New York outbreak in 1999) in the 3-4 week old Swiss Webster mouse model, clinical signs of infection are undetectable for the first seven days. Death usually occurs between Days 8 and 11 post infection. Death at the earlier timepoints (8-9 dpi) is often not preceded by any overt clinical signs, but mice who survive until the later times often present with a slightly dishevelled appearance, hypoactivity, hunched posture, and occasionally tremors and hind limb paralysis. Mice may often be found prostrate on the floor of the cage, unable to move, requiring immediate euthanasia. The more severe clinical signs often coincide with very low body temperatures (<30°C) and a weight loss of 20%. Very occasionally mice may be observed with a very gaunt appearance associated with a protruding spinal column. Since the i.p. 50% lethal dose (LD_{50}) for WNV NY99 in 3-4 week old Swiss Webster mice is very low (1.3 pfu (Zhang et al., 2010)), 100% mortality after inoculation with 10-1,000 pfu of virus is common.

Similar to other reports, Swiss Webster mice show interesting signs of intestinal swelling during the latter stages (7 dpi, onwards) of WNV NY99 infection, signs that are even more pronounced with some mutant viruses (Kimura et al., 2010, Nagata et al., 2015). Swelling appears to be restricted to the small intestine and stomach, but can be so substantial as to make the walls of the organs appear transparent (Kimura et al., 2010). The small intestine often contains a runny, black-colored, gritty-looking fluid, while the stomach is filled with a combination of air and green-colored liquid.

Serial sacrifice studies have also allowed for the determination of virus titers in important organs through the normal course of WNV infection in mouse models. In Swiss Webster mice, viremia usually peaks at day 3 post infection, with titers up to 10^5 pfu/ml (Peña et al., 2014). The viremia is rapidly cleared, such that while some virus may be detectable on Day 5, no detectable virus is present at later timepoints. Within the brain, virus is usually detectable from Day 5 onwards, with titers increasing until Day 9, where they often reach 10^8 pfu/100mg tissue. Peak peripheral organ titers tend to be around Day 5, with virus levels in the spleen, lung and kidney reaching 10^4-10^5 pfu/100mg tissue (Peña et al., 2014). Virus is rarely detected in the liver.

Studies of WNV distribution in the CNS of C3H/HeN mice revealed that viral antigen first appeared in neurons of the ventral horn of the lumbar spinal cord seven days after inoculation into the footpad (Kimura et al., 2010). Subsequently, virus was detected in the brainstem, cerebral cortex, caudate putamen, and cervical spinal cord (Kimura et al., 2010). Whilst the majority of WNV-infected cells in the CNS are neuronal, some astrocytes also appeared to be infected (Kimura et al., 2010).

FLAVIVIRUS CHIMERAS

Chimeric flaviviruses, whereby genomic sequence from one virus is incorporated into another, have been around for nearly 25 years. A list of studies involving the generation of whole structural protein chimeras can be found in Table 1.2. The first flavivirus chimeras were constructed by Bray & Lai, and consisted of the substitution of the structural protein (C-prM-E) coding region from DENV-1 and DENV-2 into a DENV-4 backbone (Bray and Lai, 1991a). In addition to demonstrating the feasibility of chimeric flaviviruses, intracranial (i.c.) inoculation of the chimeric and donor viruses into suckling mice demonstrated that the addition of the structural proteins from DENV-2

increased the neurovirulence of the resulting chimera, shifting the mortality rate closer to that of the DENV-2 donor virus than the DENV-4 parent (Bray and Lai, 1991a). Conversely, the chimeric virus with C-prM-E from DENV-1 in the DENV-4 backbone killed no mice after i.c. administration, similar to the DENV-1 donor virus (Bray and Lai, 1991a).

Follow-up studies involved the generation of chimeras between more distantly-related viruses: TBEV and DENV-4 (Pletnev et al., 1992). This time, C-prM-E or prM-E from TBEV was substituted into the DENV-4 infectious clone. The prM-E chimera was more readily recoverable, and was used for further characterization. In LLC-MK2 cells, the chimeric virus grew better than the DENV-4 backbone virus, with peak titers of 10^8 pfu/ml compared to 10^5 pfu/ml, and a larger plaque size. In C6/36 mosquito cells, however, the chimera grew less well, with a peak titer of $2x10^3$ pfu/ml compared to 10^6 pfu/ml for DENV-4. In 3-day-old BALB/c mice, the chimeric virus had 100% mortality after i.c. inoculation, compared to 12.5% mortality with DENV-4. Neither the chimera nor the backbone virus had associated mortality following i.p. inoculation, but the chimera-infected mice were protected against a subsequent TBEV challenge (Pletnev et al., 1992).

Until the late 1990s the use of chimeric flaviviruses use was limited to one group of researchers, but were helpful for demonstrating determinants of infection for mouse-adapted DENV-4 (T155I and F401L in E), as well as similar determinants in mouse-adapted DENV-2 (E71D and E126K in E) (Kawano et al., 1993, Bray et al., 1998).

The ability to immunize against the structural protein donor virus using a chimeric viral construct was appealing. Bray *et al*. demonstrated that monkeys inoculated with the DENV-4 chimeric viruses containing structural proteins from either DENV-1 or DENV-2

generated immune responses that would protect against subsequent challenge with the homologous virus corresponding to the structural proteins (Bray et al., 1996). Indeed, inoculating with both constructs protected against challenge with both viruses. The possibility of a chimeric vaccine against TBEV seemed promising with the demonstration that the addition of prM-E from Langat virus (LGTV) into DENV-4 resulted in a virus that lacked neuroinvasion, even after administration of 10^7 pfu i.p. into SCID mice, and was at least 5,000 times less neurovirulent than WT LGTV (Pletnev and Men, 1998). The residual neurovirulence was, however, a potential problem.

Safe and effective live-attenuated vaccine virus strains for JEV and YFV have existed for a number of decades and, while the live-attenuated SA14-14-2 JEV vaccine is only licensed in parts of Asia, the YFV vaccine has a widespread distribution. With this in mind, Chambers *et al*. developed a chimeric vaccine candidate whereby the YFV 17D vaccine strain was used as a backbone virus into which prM-E from either the JEV SA14-14-2 vaccine strain or a pathogenic JEV Nakayama strains were substituted (Chambers et al., 1999). Chimeras containing C-prM-E from JEV in the YFV backbone were not recoverable. When administered i.c. to mice, the chimera with the attenuated JEV sequences showed no neurovirulence, even after inoculation with 10^6 pfu of virus. Conversely, inoculation with the JEV Nakayama sequence-containing chimera led to neurovirulence at a similar level to YFV (Chambers et al., 1999). Inoculation of NHPs with the SA14-14-2 version demonstrated that the virus still lacked neurovirulence, but that it generated a robust, protective immune response (Monath et al., 1999).

This chimeric vaccine approach was used to generate vaccine candidates for a range of flaviviruses, including DENV (Caufour et al., 2001, Guirakhoo et al., 2002), WNV (Pletnev et al., 2002, Langevin et al., 2003), TBEV/LGTV (Pletnev and Men, 1998, Pletnev et al., 2001), and SLEV (Blaney et al., 2008, Pugachev et al., 2004).

Similar vaccine candidates have been made using a modified DENV-4 backbone containing an attenuating deletion of 30nts in the 3'-UTR with prM-E substitutions with sequences from other DENV serotypes, SLEV, WNV, JEV and LGTV (Durbin et al., 2001, Men et al., 1996, Whitehead et al., 2003, Blaney et al., 2004, Blaney et al., 2007, Blaney et al., 2008, Durbin et al., 2013, Pletnev et al., 2003, Gromowski et al., 2014). Of the chimeric vaccine candidates generated, a number have entered clinical trials, but to date only the ChimeriVax-JE construct has completed them, although a tetravalent chimeric DENV vaccine has completed Phase 3 trials and is pending licensure. The ChimeriVax-JE vaccine was licensed for human use in Australia in 2010, and in Thailand in 2012 (Halstead and Thomas, 2011).

In addition to vaccine candidates, chimeric flaviviruses have been used to try to determine the role of particular viral genomic regions and mutations in growth, virulence, and antigenicity. Studies by Tumban *et al*. demonstrated that replacing the whole 3'-UTR from mosquito-borne DENV-4 with the equivalent sequences from tick-borne LGTV or Modoc virus (MODV), a flavivirus with no known vector, resulted in constructs that were inviable, but that substituting the pentanucleotide or variable regions within the 3'-UTR gave viable virus, but did not alter vector competence (Tumban et al., 2013, Tumban et al., 2011). These studies followed on from work by Charlier *et al*. and Engel *et al*., who showed that substitution of prM-E from MODV into a YFV or DENV-2 backbone, and TBEV prM-E into a DENV-4 backbone, did not alter vector specificity, indicating a non-structural basis for vector competence (Charlier et al., 2010, Engel et al., 2011). Further studies by Charlier *et al*., showed that the chimera with MODV prM-E in a YFV 17D backbone gained neuroinvasiveness in SCID mice, suggesting that the structural proteins may play a more important role in growth within mammalian hosts than arthropod vectors (Charlier et al., 2004).

Studies by Audsley *et al*., looking at virulence determinants between WNV NY99 and KUNV, generated a range of chimeras particularly focused on the 5'- and 3'-UTRs, as well as the non-structural proteins. Their data showed that the chimeric KUNV constructs with NY99 UTRs and parts of the non-structural protein coding regions were more virulent that the original KUNV, indicating a non-structural and non-coding component to WNV virulence (Audsley et al., 2011). Maharaj *et al*., using complementary prM-E chimeras with SLEV and WNV, have demonstrated that, for the most part, growth kinetics of the chimeric viruses in mammalian cells were most similar to those of the backbone virus, although SLEV with WNV prM-E appeared to grow to higher titers in Vero cells than the SLEV control (Maharaj et al., 2012). This improved growth was extended to C6/36 cells.

A more limited number of chimeric flaviviruses have also been generated using highly-pathogenic flaviviruses. Yoshii *et al*. generated a series of chimeras using infectious clones for OHFV and TBEV to characterize determinants of neurological disease (Yoshii et al., 2014). Their studies demonstrated that four amino acids at the N-terminus of NS5 were responsible for the development of neurological signs, although these amino acids had no effect on growth kinetics *in vitro* or virus titers in the brain. Structural protein chimeras, whereby prM-E from TBEV was substituted in to OHFV significantly increased neuroinvasion, with virus detectable in the brain on Day 5, similar to TBEV, compared to Day 7 for OHFV (Yoshii et al., 2014). Interestingly, TBEV with prM-E from OHFV had similar neuroinvasion to WT TBEV, suggesting that prM-E are not the only viral factors mediating neuroinvasion, but can be sufficient. Studies in PC12 cells demonstrated that the four amino acids in NS5 affected neurite outgrowth, which was hypothesized to be a factor in the differences in clinical presentation between the viruses (Yoshii et al., 2014).

Whilst most flavivirus chimeras generated to date have involved the substitution of prM-E from a donor virus into a backbone, some constructs have involved generating antigenic chimeras, particularly between DENV serotypes. One such study, by Apt *et al*., used a DNA shuffling technique to generate chimeric DENV envelope proteins containing sequences from the four DENV serotypes, which allowed for antibodies to be generated against all four serotypes (Apt et al., 2006). While these chimeric proteins were not incorporated into a full-length infectious clone for virus recovery, they were expressed as Virus-Like Particles (VLPs) when combined with DENV-3 prM, although it is unclear whether true VLPs actually formed (Apt et al., 2006). A different epitope transplantation study was carried out by Lisova *et al*., who demonstrated that the DENV pan-serotype cross-reactive mAb4E11 could neutralize unrelated flaviviruses after substituting epitope-associated residues for those found in DENV (Lisova et al., 2007). Studies by Bielefeldt-Ohmann *et al*. demonstrated the feasibility of flavivirus envelope structural domain chimeric proteins, by expressing E protein from DENV-2 containing EIII from DENV-3 (Bielefeldt-Ohmann et al., 1997). Although incorporation of the resulting chimeric protein into an infectious virion was not attempted, antigenicity studies suggested that the protein folded sufficiently well to react with conformation-dependent monoclonal antibodies (Bielefeldt-Ohmann et al., 1997).

PROJECT RATIONALE

Previous studies have shown that chimeric flaviviruses containing prM-E proteins from genetically related donor viruses are usually viable, and often display different properties *in vitro* and *in vivo* when compared to the backbone virus. Early studies using chimeric DENV with alternative serotype prM-E substitutions into a DENV-4 backbone demonstrated increased virulence in mice when pathogenic DENV-2 prM-E was used, and increased attenuation when low-pathogenicity DENV-1 proteins were substituted

(Bray and Lai, 1991a). Similarly, DENV-4 with prM-E from TBEV showed increased neurovirulence compared to the backbone virus, while OHFV with prM-E from TBEV showed *in vivo* kinetics and organ titers more similar to TBEV than the OHFV backbone (Pletnev et al., 1992, Yoshii et al., 2014). These results strongly suggest that, for flaviviruses, the targeting of organs and growth in mammalian cells may, in part, be associated with the structural proteins present on the surface of the virion.

One of the major roles of the structural proteins is in mediating the interaction between the virion and the surface of target cells. While the target receptors on the surface of mammalian cells are poorly understood for most flaviviruses - no single receptor described to date has been shown to be indispensible - a better understanding of receptor interaction exists for the virus side. Studies by Chen *et al*. demonstrated that, for DENV, the receptor-binding domain mapped to a region of the envelope glycoprotein between amino acids 281 and 423 (Chen et al., 1996). With the publication of the crystal structure of E for TBEV the previous year, this region was shown to correspond to structural domain III (EIII) (Chen et al., 1996, Rey et al., 1995). Further studies provided more evidence of the receptor-binding role of EIII, including the demonstration that recombinant EIII molecules could effectively inhibit virus adsorption to cell surfaces, and that EIII-targeting antibodies are particularly effective at neutralizing viral particles (Chin et al., 2007, Crill and Roehrig, 2001, Cruz-Oliveira et al., 2015, Hung et al., 2004, Nybakken et al., 2005, Volk et al., 2004).

Owing to the complexities of intra- and intermolecular interactions, the vast majority of chimerization studies involve the substitution of whole proteins, or even groups of proteins, rather than individual structural domains within a protein. As seen with some C-prM-E chimeras, even substitution of whole proteins is no guarantee of viral viability (Chambers et al., 1999). Few studies have focused on the generation of chimeric

proteins, and those that have done so have often been carried out under the guise of DNA-based vaccines, where the requirement for correctly folded, functional proteins is secondary to antigenicity, or have focused on the expression of secreted, recombinant proteins (Apt et al., 2006, Sjatha et al., 2014, Bielefeldt-Ohmann et al., 1997).

Other studies have attempted to investigate the regions of EIII that may be responsible for receptor binding. Characterization of neutralization escape mutants has identified four residues in EIII that allow for reduced levels of neutralization if mutated: K307; T330 and T332 within the BC loop; and A367 within the DE loop (Beasley and Barrett, 2002, Choi et al., 2007, Zhang et al., 2010, Zhang et al., 2009). The fact that two of these residues are located within the same surface loop indicates that this region may be important for interactions between the virus and the cell surface, likely through the mediation of receptor binding. Other studies have shown that in mosquito cells, the FG loop, residues 380 and 389, of DENV E plays a significant role in cell binding, but that this region apparently plays a less significant role in binding to BHK cells (Hung et al., 2004). The equivalent sequence in WNV contains the RGE integrin-binding motif discussed previously, a motif lacking in DENV E, which, while shown to allow for interactions between EIII and cellular integrins, is not obligatory for cell binding (Chu and Ng, 2004b, Hurrelbrink and McMinn, 2001). Indeed, mutation of E390 of WNV EIII, the terminal residue in the RGE triad, increases binding to glycosaminoglycans but does not abrogate cell entry, suggesting instead a skewing of the receptor usage in these mutant viruses (Lee et al., 2004, Lee and Lobigs, 2000).

Since the BC loop appeared to be overrepresented in the neutralization escape mutant studies, Zhang *et al*. investigated this region further by mutating all of the residues in this loop to determine the effect on antigenicity and virulence (Zhang et al., 2010). It was shown that T330 and T332, the two residues identified in the neutralization

escape studies, could be mutated with little effect on virus growth *in vitro* or mouse virulence *in vivo*, but that such mutations had significant effects on antigenicity and the strength of antibody-mediated neutralization. By contrast, mutation of residues 331 and 333 had a more significant effect on virulence, with LD_{50} values >1,000pfu following i.p. inoculation, compared to an LD_{50} of 1.3pfu for the parental WNV NY99 (Zhang et al., 2010). While both residues appear critical for WNV virulence, residue 333 is rather variable between flaviviruses, suggesting a less critical role across the genus. By contrast, G331 is highly conserved amongst tick- and mosquito-borne flaviviruses, indicating that it may have a broader criticality with regards to efficient receptor-binding and successful infection.

The *goal* of this project was three-fold: to determine whether WNV would tolerate EIII substitutions from increasingly diverse flaviviruses; to determine whether these substitutions would affect the phenotypic characteristics of the viruses, including their growth *in vitro* and their virulence and tropism phenotype *in vivo*; and to further characterize the EIII single-site G331A mutant as a possible critical residue for WNV receptor binding. The *hypothesis* was that the **substitution of the putative flavivirus receptor-binding domain from related flaviviruses into WNV would result in chimeric viruses that would behave differently to the WNV backbone with respect to *in vitro* growth and *in vivo* pathogenesis**. In addition, it was *hypothesized* that **the G331A mutation within EIII of WNV attenuates the virus by significantly impeding receptor binding**.

The two related hypotheses were tested by the completion of the following *specific aims*:

1. Generation of chimeric flaviviruses using the WNV NY99 infectious clone system and donor EIIIs from a range of related flaviviruses
2. Characterization of the chimeric viruses *in vitro* with respect to growth kinetics in Vero and C6/36 cells, as well as particle stability and antigenicity
3. Determination of the pathogenesis of the chimeric viruses *in vivo* within the WNV mouse model
4. Characterization of the pathogenesis of the WNV G331A mutant in immunocompetent and IFNα/β receptor knock-out immunodeficient mice.

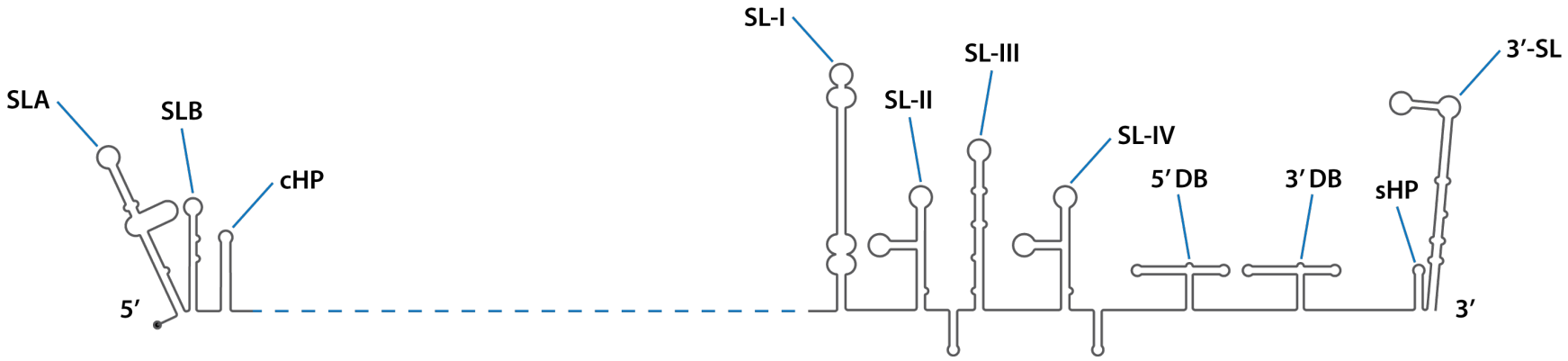

Figure 1.1: Structure of WNV 5’ and 3’ UTRs. The un-translated regions (UTRs) of the flavivirus RNA genome have complex secondary structures involved in the cyclisation of the genome for replication, as well as regulating transcription. The 5’ UTR has three main structures: stem-loop A (SLA), stem-loop B (SLB), and capsid coding region hairpin (cHP). The 3’ UTR has a more complex secondary structure, with four upstream stem-loops (SL-I to IV), two “dumbbell” structures (5’ DB & 3’ DB), a small hairpin (sHP), and a 3’ stem-loop (3’-SL).

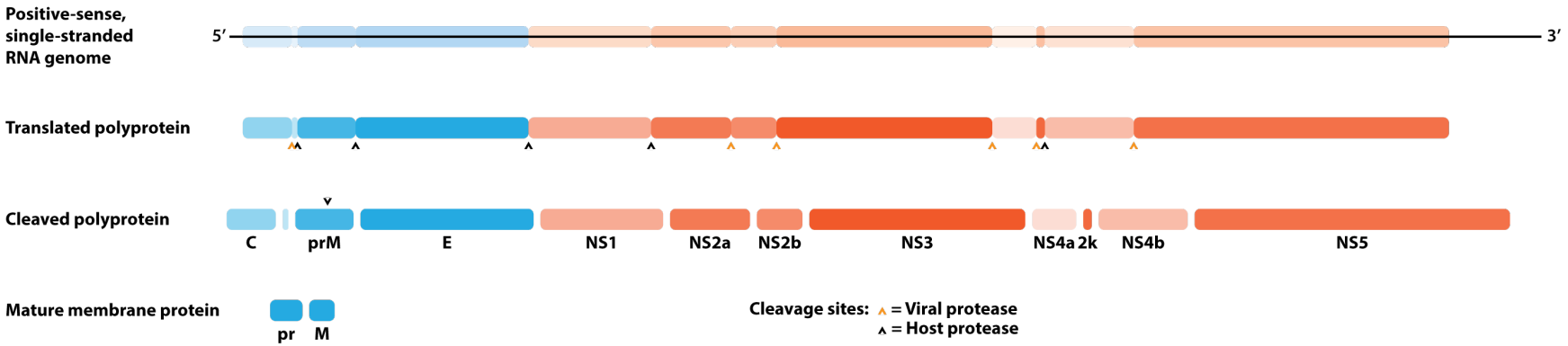

Figure 1.2: Structure of Flavivirus Genome and Polyprotein Maturation. Flaviviruses have a single-stranded RNA genome ranging from 9.5kb to 11kb that contains a large open-reading frame (ORF). This ORF codes for a single polyprotein that is subsequently cleaved into its constituent parts by host and viral proteases.

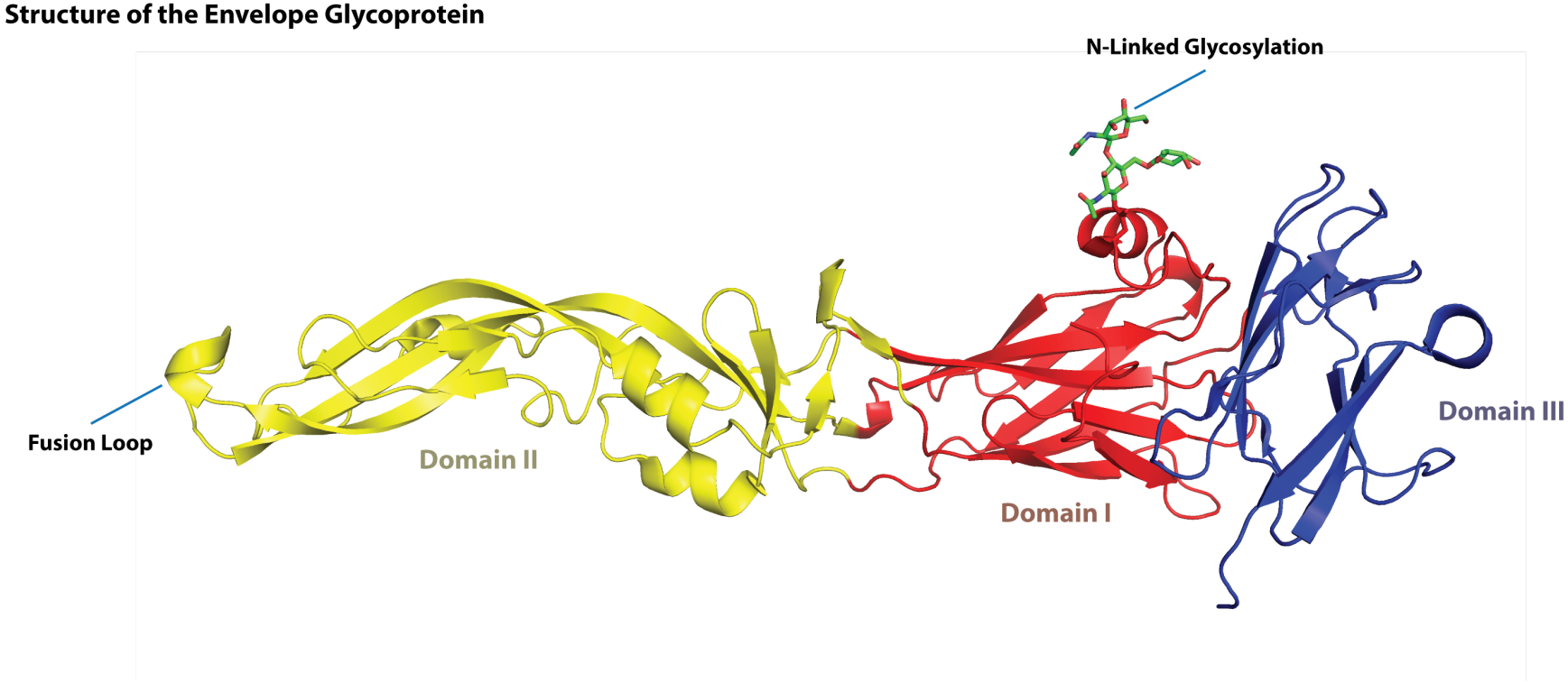

Figure 1.3: Structure of WNV Envelope Glycoprotein. The envelope glycoprotein is composed of three main structural domains: domain I (EI), domain II (EII), and domain III (EIII). The hydrophobic fusion loop, conserved amongst flaviviruses and necessary for virus entry, is located at the distal end of EII. The single N-linked glycosylation site, at residue 154, is located in EI, and the putative receptor-binding domain, EIII, is present as a semi-distinct entity adjacent to EI. Not shown are the two stem-helices or the transmembrane domains due to the inability of the protein to be successfully crystallized with these regions. (Figure is based on PDB 2I69)

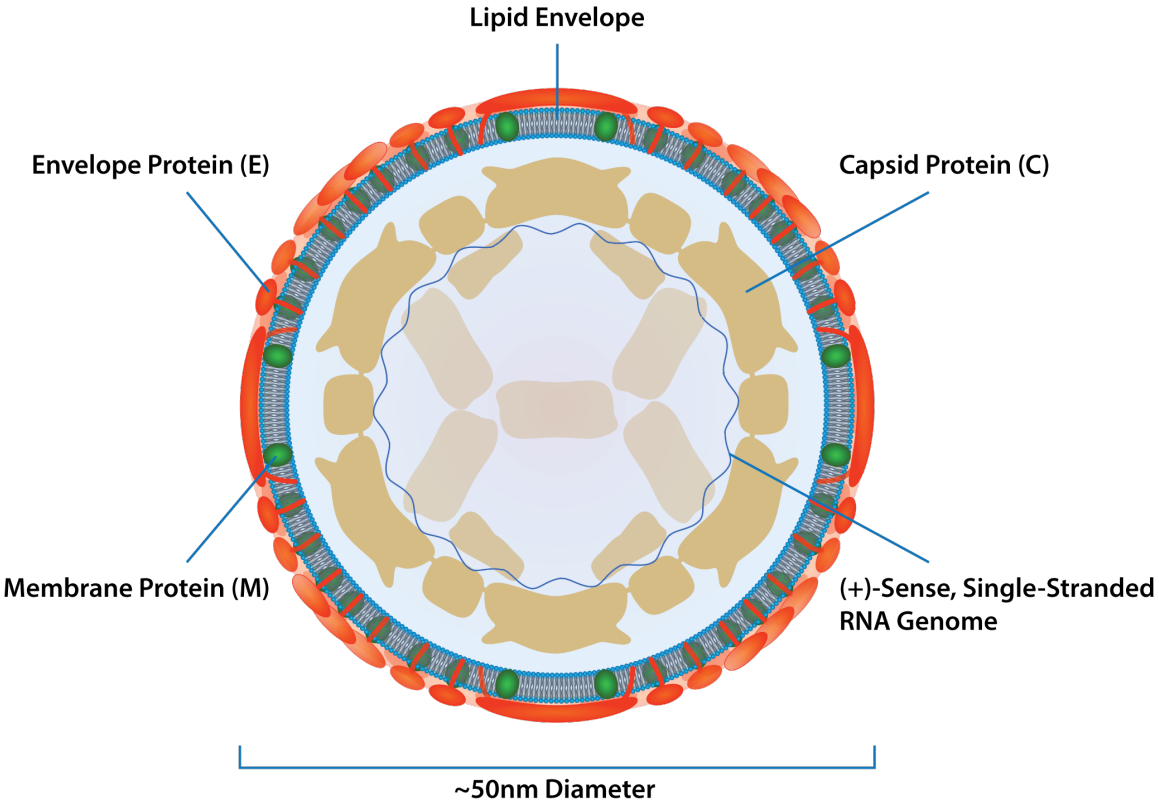

Figure 1.4: Structure of Mature Flavivirus Virion. Flavivirus virions are approximately 50nm in diameter, and are composed of three viral proteins: the capsid protein (C), which associates with genomic RNA to for the nucleocapsid; the membrane protein (M), which remains in the lipid envelope after cleavage of the precursor protein (prM) during maturation; and the envelope protein (E), which is the predominant protein on the surface of the virion and is responsible for binding and entry of the virus into host cells.

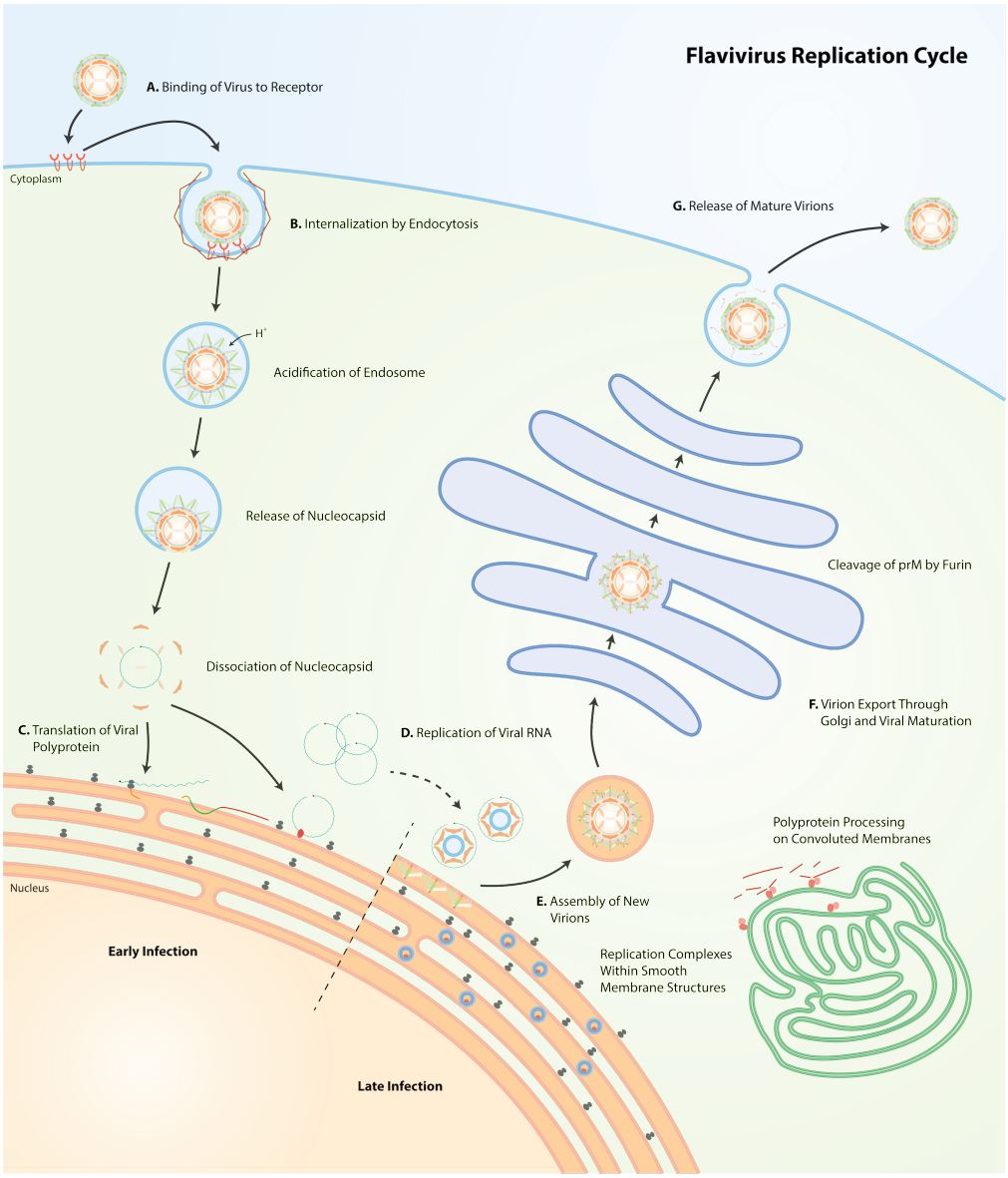

Figure 1.5: Flavivirus Replication Cycle. *A*) The virus binds to receptors on the cell surface through interactions mediated by EIII. *B*) Following attachment the virus is internalized by clathrin-mediated endocytosis, where the decreased pH leads to a conformational change in the E proteins on the surface, resulting in the fusion of the envelope and endosomal membranes, and the release of viral RNA into the cell. *C*) The positive-sense RNA genome functions as a mRNA molecule, allowing for the generation of viral polyproteins, which are cleaved by host and viral proteases. *D*) Viral proteins forming replication complexes amplify the viral genome, which associates with capsid proteins. *E*) The nucleocapsids associate with prM-E dimers in the ER membrane, resulting in budding and the formation of immature viral particles. *F*) Immature virions are exported from the cell via the Golgi, where they mature via the cleavage of prM by furin under acidic conditions. *G*) Mature virions are released from the cell.

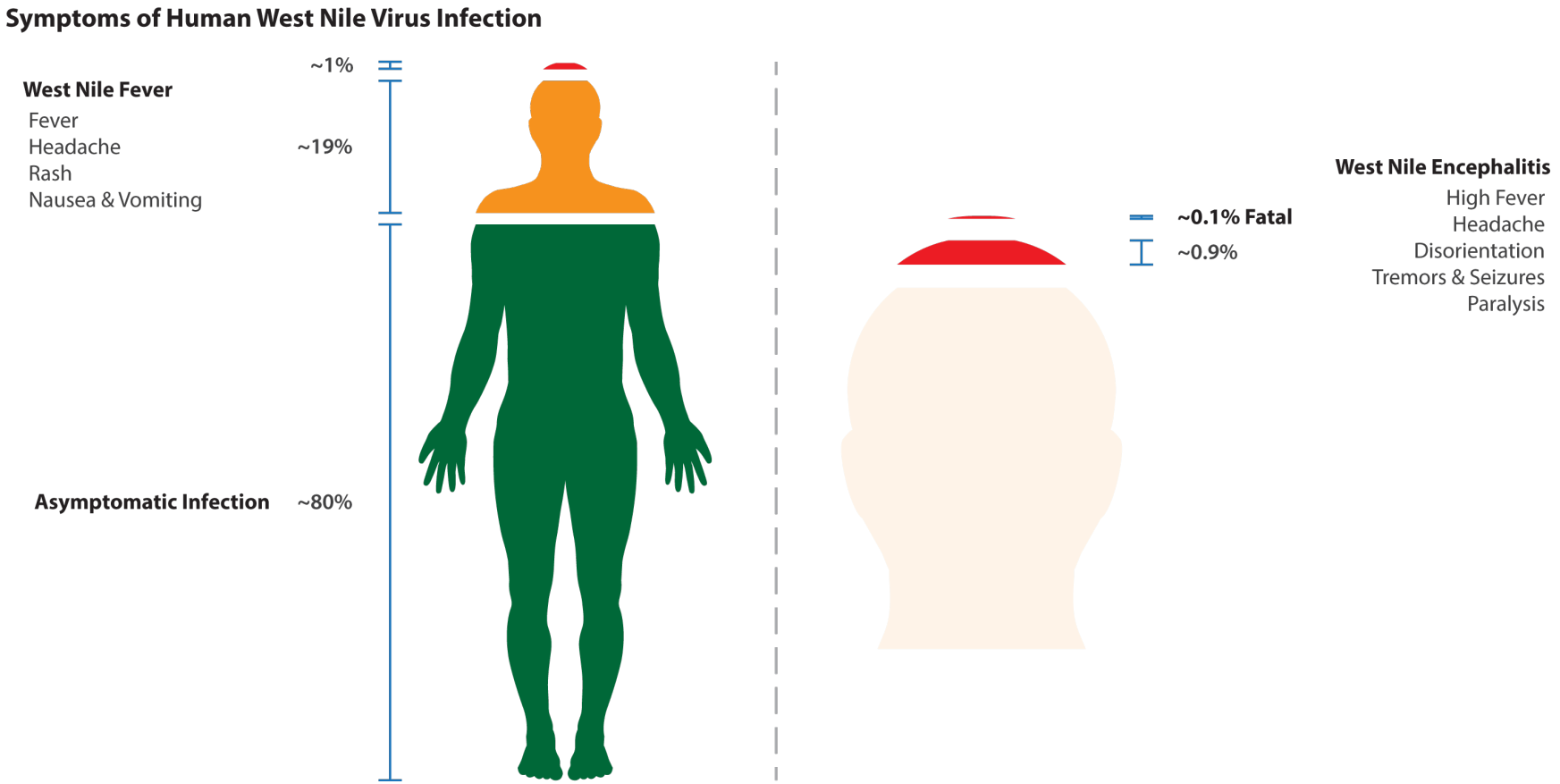

Figure 1.6: Symptoms of Human West Nile Virus Infection. In humans, the majority (~80%) of WNV infections are asymptomatic, as the virus is cleared without outward signs of infection. In approximately 19% of cases, patients suffer from West Nile Fever, a transient flu-like syndrome. In approximately 1% of cases, the infection proceeds to the brain, where West Nile Encephalitis develops. This neurological infection is characterized by high fever, headache, disorientation, tremors and seizures, and paralysis. In 10% of encephalitis patients (~0.1% of total WNV infections), the infection has a fatal outcome.

Candidate Flavivirus Receptors

Receptor	Virus	Cell Type	References
Heparan Sulphate (Heparin)	DENV-2	Vero	Chen et al., 1997b
	DENV-1	Huh-7	Hilgard and Stockert, 2000
	DENV-2 & YFV	Vero	Germi et al., 2002
	TBEV	BHK-21	Kroschewski et al., 2003
	JEV, WNV, & MVEV	BHK-21	Lee et al., 2006
	DENV-2	K562	Okamoto et al., 2012
nLc_4Cer	DENV-2	K562 & BHK-21	Aoki et al., 2006
	DENV-2	LLC-MK2	Wichit et al., 2011
DC-SIGN/L-SIGN	DENV-1, -2, -3, & -4	Immature Human MDDC	Navarro-Sanchez et al., 2003
	DENV-1, -2, -3, & -4	THP-1	Tassaneetrithep et al., 2003
	WNV	K562/DC-SIGN(R)	Davis et al., 2006a/b
	DENV-2	Huh-7 & Vero	Mondotte et al., 2007
	DENV-2	Human MDDC	Dejnirattisai et al., 2011
CD14	DENV-2	Primary Human Monocytes	Chen et al., 1999
HSP70 & HSP90	DENV-2	Primary Human Monocytes	Reyes-Del Valle et al., 2005
	DENV-2	C6/36	Salas-Benito et al, 2007
	JEV	Neuro2a	Das et al., 2009
	JEV	Huh-7	Zhu et al., 2012
	JEV	BV-2	Thongtan et al., 2012
	DENV-4	C6/36	Vega-Almeida et al., 2013
Mannose Receptor	DENV-1, -2, -3, & -4	MDDC	Miller et al., 2008
CLEC5A	DENV-2	Primary Human Monocytes	Chen et al., 2008
	JEV	Primary Human Monocytes	Chen et al., 2012
	DENV-2	Primary Human Macrophages	Wu et al., 2013
mosGCTL-1	WNV	Mosquitoes	Cheng et al., 2010
GRP78 (BiP)	DENV-2	HepG2	Jindadamrongwech et al., 2004
	DENV-4	C6/36	Vega-Almeida et al., 2013
High-Affinity Laminin Receptor	DENV-1	HepG2	Thepparit and Smith, 2004
	DENV-1, -2, -3	PS	Tio et al., 2005
	DENV-3 & -4	C6/36	Sakoonwatanyoo et al., 2006
Prohibitin	DENV-2	C6/36 & CCL-125	Kuadkitkan et al., 2010
TIM/TAM	DENV-1, -2, -3, & -4	Huh7.5.1 & A549	Meertens et al., 2012
	DENV & WNV	293T, 3T3, & Huh-7	Jemielity et al., 2013
Integrin $\alpha_v\beta_3$	WNV	Vero	Chu and Ng., 2003
	WNV	CS-1	Chu and Ng., 2004b
Scavenger Receptor B1	DENV-2	Various Mammalian	Li et al., 2013
Claudin-1	DENV	Huh-7	Gao et al., 2010
	DENV-1, -2, -3, & -4	Huh-7.5	Che et al., 2013
NKp44	DENV & WNV	NK	Hershkovitz et al., 2009

Table 1.1: Candidate Flavivirus Receptors. A number of candidate receptors have been identified for flaviviruses in a range of cell types, although none have been demonstrated to be indispensible for virus infection.

Published Structural Protein Substitution Chimeric Flavivirus Studies

Backbone Virus	Donor Virus	Type of Chimera	References
Dengue 4 Virus	Dengue 1 & 2 Viruses	C-prM-E	Bray and Lai, 1991
Dengue 4 Virus	Tick-Borne Encephalitis Virus	C-prM-E & prM-E	Pletnev et al., 1992
Dengue 4 Virus	Dengue 3 Virus	C-prM-E	Chen et al., 1995
Dengue 4 Virus	Langat Virus	prM-E	Pletnev and Men, 1998
Yellow Fever Virus*	Japanese Encephalitis Virus*	prM-E	Chambers et al., 1999
Yellow Fever Virus*	Japanese Encephalitis Virus*	prM-E	Monath et al., 1999
Dengue 2 Virus*	Dengue 1 Virus	C-prM-E	Huang et al., 2000
Yellow Fever Virus*	Dengue 2 Virus	prM-E	Caufour et al., 2001
Yellow Fever Virus*	West Nile Virus	prM-E	Arroyo et al., 2001
Dengue 4 Virus	West Nile Virus	prM-E	Pletnev et al., 2002
Yellow Fever Virus*	Dengue 1, 2, 3, & 4 Viruses	prM-E	Guirakhoo et al., 2002
Yellow Fever Virus*	Dengue 2 & 4 Viruses	prM-E	Chambers et al., 2003
Yellow Fever Virus*	Modoc Virus	prM-E	Charlier et al., 2004
Japanese Encephalitis Virus	Dengue 4 Virus	prM-E	Mathenge et al., 2004
Yellow Fever Virus*	St Louis Encephalitis Virus	prM-E	Pugachev et al., 2004
Dengue 2 Virus*	West Nile Virus	prM-E	Huang et al., 2005
Japanese Encephalitis Virus	Dengue 2 Virus	prM-E	Chambers et al., 2006
Yellow Fever Virus	Dengue 4 Virus	prM-E	McGee et al., 2008
Dengue 2 Virus	Modoc Virus	prM-E	Charlier et al., 2010
Murray Valley Encephalitis Virus	Alfuy Virus	prM-E	Prow et al., 2011
West Nile Virus	St Louis Encephalitis Virus	prM-E	Maharaj et al., 2012
St Louis Encephalitis Virus	West Nile Virus	prM-E	Maharaj et al., 2012
Japanese Encephalitis Virus*	West Nile Virus	prM-E	Li et al., 2013a
Japanese Encephalitis Virus*	Dengue 2 Virus	prM-E	Li et al., 2013b
Omsk Hemorrhagic Fever Virus	Tick-Borne Encephalitis Virus	prM-E	Yoshii et al., 2014
Tick-Borne Encephalitis Virus	Omsk Hemorrhagic Fever Virus	prM-E	Yoshii et al., 2014
Japanese Encephalitis Virus*	Tick-Borne Encephalitis Virus	prM-E	Wang et al., 2014
Japanese Encephalitis Virus*	Dengue 4 Virus	prM-E	Li et al., 2014
Modoc Virus	West Nile Virus	C-prM-E & prM-E	Saiyasombat et al., 2014
Dengue 4 Virus	Japanese Encephalitis Virus	prM-E	Gromowski et al., 2014

Table 1.2: Published Structural Protein Substitution Chimeric Flavivirus Studies. A number of studies have been carried out to determine the effect of structural protein substitution on virus viability and growth. To date, all have involved whole C-prM-E or prM-E substitutions, with prM-E substitutions allowing for viable chimeras with all of the tested combinations. Many of the chimeras have been generated with attenuated backbone and/or donor sequences (denoted in the table with an *).

Chapter 2: Materials and Methods

CELL AND VIRUS PROCEDURES

Viruses and Infectious Clone Plasmids

The infectious clone used for the construction of chimeric viruses was the two-plasmid WNV clone originally developed at the Centers for Disease Control and Prevention, Division of Vector-Borne Infectious Diseases, and described previously (Beasley et al., 2005). Briefly, a derivative of pBRUC-139S was engineered that contained, as DNA, nts 1-2495 of the WNV NY99 genome preceded by a T7 polymerase promoter. This plasmid was denoted pWN-AB. A second plasmid, pWN-CG, contained nts 2496-11029. The two plasmids contained NgoMIV restriction sites, at the downstream end of the genome sequence in pWN-AB, and upstream of the sequence in pWN-CG, to allow for ligation into a full-length version for *in vitro* transcription of genome-equivalent RNA. The two plasmids were available in the laboratory pre-transformed into DH5α *Escherichia coli* bacteria in glycerol stocks. A modified pWN-AB containing PstI (nts 1859-1864 of WNV) and StuI (nts 2183-2188 of WNV) restriction sites had already been generated via sequential PCR-based site-directed mutagenesis of the wild-type pWN-AB plasmid using the QuikChange XL kit (Agilent Technologies, Santa Clara, CA) and primers encoding the necessary nucleotide substitutions.

For the attempted recovery of inviable viruses in BHK cells expressing WNV prM-E, a different DNA-launched infectious clone system with expression controlled by a CMV promoter was used (Lin et al., 2012). Similar to the infectious clone described

above this system contains two plasmids. The first, pWNV backbone, contains the 5' UTR and part of the capsid coding region, as well as the non-structural proteins. The second plasmid, pWNV complement, contains the remainder of the capsid coding region, as well as the coding sequences for prM and E. The chimeric constructs were generated using unique BssHII and DraIII restriction sites present in the pWNV plasmid. Chimeric sequences were amplified from the pWN-AB plasmids, digested, and ligated into digested pWNV complement plasmid. The plasmids were transformed into Stbl2 *E. coli* bacteria (Life Technologies, Waltham, MA), as described below.

Nine flaviviruses were used as EIII donors. The particular isolates, with the accession numbers for their sequences are listed below:

Donor Virus	Strain	Source
Koutango Virus (KOUV)	Dak Ar D 5443	Viral RNA
Japanese Encephalitis Virus (JEV)	Nakayama	Viral RNA
St Louis Encephalitis Virus (SLEV)	Parton	Viral RNA
Bagaza Virus (BAGV)	DakAr B209	Viral RNA
Zika Virus (ZIKV)	MR 766	Synthetic Construct
Iguape Virus (IGUV)	SPAn 71686	Viral RNA
Dengue 2 Virus (DENV-2)	New Guinea C	Viral RNA
Yellow Fever Virus (YFV)	Asibi	Viral RNA
Deer Tick Virus (DTV)	IPS-001	Viral RNA

Table 2.1: List of Donor Viruses with Strain Details and Material Source

The donor RNA was reverse transcribed and amplified as described below. The resultant cDNA was stored at -80°C until needed.

Cells and Tissue Culture

Vero cells (ATCC #CCL-81; ATCC, Manassas, VA), derived from African green monkey kidney, were used as the primary cell type for virus recovery, titration, growth,

and passaging. Cells were cultured at 37°C with 5% CO_2 in MEM (Corning, Manassas, VA) containing 8% fetal calf serum (FCS; HyClone, Logan, UT), 10ml 50x penicillin/streptomycin solution (Corning, Manassas, VA), 5ml 100x L-glutamine (Life Technologies, Waltham, MA), and supplemented with 5ml non-essential amino acid solution (HyClone, Logan, UT). Cells were kept below passage 30, as later passages adversely affected development of plaques. Cells were passaged when confluent by removing the culture medium, and washing with 1x DPBS (Corning, Manassas, VA). The PBS was removed, and 2ml 0.25% trypsin solution (Corning, Manassas, VA) was added to dissociate the cells from the culture flask. Once the cells had separated, 18ml MEM culture medium was added (for a T-75 flask) to generate a 1x cell suspension. The cells were further diluted 1:5 in medium, and were plated in a new tissue culture vessel (e.g. 4ml 1x cells with 16ml culture medium for a T-75 flask).

C6/36 mosquito cells (ATCC #CRL-1660; ATCC, Manassas, VA), derived from larvae of *Aedes albopictus* mosquitoes, were used for determining growth kinetics of the viruses. Cells were cultured at 28°C without CO_2 in MEM (Corning, Manassas, VA) containing 8% FCS, 1x penicillin/streptomycin solution, 1x sodium pyruvate (Sigma Aldrich, St Louis, MO), and autoclaved 5% tryptose phosphate buffer (29.5g TPB powder in 500ml ddH_2O; Sigma Aldrich, St Louis, MO). Cells were passaged when confluent by carefully removing the culture supernatant, and washing with 10ml 1x DPBS. The PBS was removed, and the fresh culture medium was added to the same volume as that previously removed: 20ml for a T-75, 40ml for a T-150. The cells were dissociated using a cell scraper (Corning, Manassas, VA). They were diluted 1:3 with culture medium (approximately 7ml cells with 13ml medium for a T-75 flask), and were transferred to a fresh culture vessel.

Baby hamster kidney (BHK) cells stably transfected to express WNV prM/E were kindly provided by Dr. Gregg Milligan. These cells were used to recover and passage chimeras that were unviable in Vero cells. They were cultured at 37°C with 5% CO_2 in DMEM (Gibco-Life Technologies, Waltham, MA) containing 8% FCS, 1x penicillin/streptomycin solution, 1x L-glutamine, and 1x non-essential amino acids, as well as 20μg/ml gentamycin (Corning, Manassas, VA) and 10μg/ml puromycin dihydrochloride (Corning, Manassas, VA) as selection antibiotics to maintain prM/E expression. Cells were passaged when confluent by removing the culture medium, and washing with 1x DPBS. The PBS was removed and, for a T-75 flask, 20ml fresh culture medium was added. The cells were dissociated using a cell scraper, and clumps were broken up by gently pipetting the medium up and down with a 10ml serological pipette (Fisher Scientific, Pittsburgh, PA). The resuspended cells were further diluted 1:3 with culture medium (approximately 7ml cells with 13ml fresh medium for a T-75), and were transferred to a fresh culture vessel.

Virus Culture

Resuspended Vero cells from near-confluent tissue culture flasks were plated in T-25 or T-75 culture flasks at a dilution of 1:2.5 (8ml cells with 12ml medium for a T-75 flask) for use the following day. Once confluent, the cells were washed with PBS, and virus-containing supernatant/organ homogenate was added at a dilution of 1:50-1:1,000, in a volume one tenth that of the usual culture medium volume (e.g. 2ml for a T-75). The flask was rocked to ensure even distribution of the inoculum, and was placed in a 37°C incubator with 5% CO_2, with further rocking every 10mins to ensure that the cell monolayer did not dry out. After 30min, culture medium containing 2% FCS and a standard concentration of supplements, was added to the flask to the volume usually employed for cell culture. The flask was incubated at 37°C until early signs of cytopathic

effect (CPE) were visible, usually 3-4 days after inoculation. The culture supernatant was dispensed into 15ml tubes, and then centrifuged for 5mins at 3,200g, to remove cell debris. The cleared supernatant was dispensed into 0.5ml and/or 1ml aliquots, which were frozen at -80°C until required.

For virus culture in BHK cells expressing WNV prM-E, the same protocol was used, with the exception of the medium. For these cells, DMEM (Life Technologies, Waltham, MA) containing 2% FCS, 1x penicillin/streptomycin, 1x L-glutamine, 1x non-essential amino acids, and 10mM HEPES buffer (Life Technologies, Waltham, MA) was used.

For virus passaging in both Vero and BHK prM-E cells, infections were carried out as described above. Supernatant was harvested on Day 3 or 4, and was stored at -80°C until cells were ready for the next round of growth. This was repeated until the requisite number of passages had occurred.

Virus Titration – Plaque Assay

Vero cells from a confluent tissue culture flask were plated in 6- or 12-well plates (1:2.5 for use the next day, 1:5 for the day after). Once >90% confluent, the plates were transported to the BSL-3 laboratory for use. A 10-fold dilution series of virus stock, or organ homogenate, was prepared in a 96-well plate, usually from 10^{-1} to 10^{-8}, although a 10^{0} starting concentration was occasionally used for samples expected to have no or very low quantities of infectious virus present. The serial dilutions were made using 25µl sample in 225µl medium to ensure sufficient volume for infecting the wells. Once the dilution series was prepared, the medium was removed from the culture plates, and the wells were washed with 1x DPBS. The PBS was removed, and 100µl (for 12-well plates)

or 200µl (for 6-well plates) of diluted virus sample was added to the appropriate well, starting from the lowest virus concentration, and working up. The plates were rocked to ensure even distribution of the sample, and then incubated at 37°C in 5% CO_2 for 30mins, with repeated rocking every 10mins to ensure the cell monolayers did not dry out. After 30mins, an MEM/agar overlay (2ml/well for 12-well plates, 4ml/well for 6-well plates) was applied to the wells (2% agar (Sigma Aldrich, St Louis, MO) mixed 1:1 with 2x MEM (Quality Biological, Gaithersburg, MD) containing 4% FCS, 2x penicillin/streptomycin, 2x L-glutamine, and 2x non-essential amino acids). The plates were then incubated for two days at 37°C with 5% CO_2. After two days, a neutral red overlay (2% agar and 2x MEM with 2ml neutral red (Sigma-Aldrich, St Louis, MO) per 100ml) was applied, using 1ml/well for 12-well plates, and 2ml/well for 6-well plates. The plates were wrapped in foil, and returned to the incubator for another 24hrs. After the incubation, the plates were removed, and plaques were counted with the aid of a white light transilluminator. The number of plaques and the dilution of the sample were recorded for the wells in which plaques were quantifiable. Virus titers were determined by multiplying the number of plaques in the well by the reciprocal of the dilution value, and adjusted based upon the input volume (x5 for 6-well plates, x10 for 12-well plates) to give a titer per ml of sample.

Virus Titration – Immunostaining

Titration plates were prepared as described above for plaque assays. Plates with samples that failed to produce visible plaques by 4dpi, or that were known to plaque inefficiently, were fixed for an hour at room temperature with 10% buffered formalin (3.75% formaldehyde in phosphate-buffered water; Fisher Scientific, Pittsburgh, PA). The formalin was discarded, and the agar plugs were removed. Fresh formalin was added to the wells, and the plate was incubated for a further 10mins at room temperature. The

formalin was removed, and the plate was washed twice with 1x PBS. The cells were permeabilized by incubating them at -20°C for 30mins in 500µl per well of 70% ethanol (Fisher Scientific, Pittsburgh, PA). The ethanol was removed, and the plate was washed twice with PBS. The PBS was removed, and 200µl per well of primary antibody diluted in PBS with 0.5% I-Block (Thermo Scientific, Pittsburgh, PA) was added. The plates were incubated at room temperature for 90mins with gentle rocking, followed by a further two washes with PBS. 200µl of secondary antibody (Sigma-Aldrich, St Louis, MO) diluted 1:5,000 in PBS with I-Block was added per well, and the plate was incubated for 1hr at room temperature with rocking. The cells were washed again, and 200µl per well of True Blue HRP substrate (KPL, Gaithersburg, MD) was added. The plate was incubated for 10-15mins, until foci became apparent, and was then rinsed with distilled water. Finally, the plates were left to air-dry overnight before foci were counted. Virus titers were determined from foci counts using the same methodology as described above for the determination of titers from plaque assays.

Virus Growth Kinetics

Vero and C6/36 cells were plated in T-25 tissue culture flasks, as previously described. Three flasks were prepared for each virus, to allow for triplicate data. 6-well plates were also prepared for back-titrations of the infecting virus material. Once approximately 90% confluent, the flasks were inoculated with 1ml medium containing 1000pfu of a virus of interest; this quantity equates to an MOI of approximately 0.0005. This quantity of virus was chosen as some of the virus stocks had particularly low titers. The flasks were rocked to distribute the sample, and were then incubated for 40mins at 37°C with 5%CO_2. After the incubation, 6.5ml of culture medium with 2% FCS was added to each flask. The medium was washed over the monolayer, after which 0.5ml was removed from each replicate flask for a Day 0 timepoint sample. The samples were

stored at -80°C, and the flasks were returned to the incubator. The inoculum was serially diluted and titrated on Vero cells using a variation of the plaque or immunostaining methods described above to ensure that the virus quantity was correct. Three wells were used per virus, with expected plaque counts of 100, 10, and 1. To prepare the back titration samples, 150µl of inoculum was added to 150µl of medium to generate a target dilution of 100pfu per 200µl, the volume to be added to the back titration well. 10-fold dilutions were prepared from this sample by transferring 25µl into 225µl medium. The back titration plate was washed with PBS, and 200µl of diluted sample was added to the appropriate well of the plate. The plate was rocked, and incubated for 30mins at 37°C. From then on, the plate was treated as described above for plaque assays, with the number of plaques in the well compared to the expected number (10^2, 10^1, or 10^0) to determine the amount of virus added to the original flask.

500µl aliquots of supernatant were removed from the flasks daily from Days 1-5, with the volume replaced with fresh medium. The aliquots were centrifuged for 5mins at 20,000g to pellet cell debris, and the supernatant was removed and stored at -80°C until needed. Virus titers were determined for all of the samples by plaque assay, described above.

Virus Neutralization Assays

12-well plates were seeded with Vero cells at approximately $1.2x10^5$ cells/ml for use the following day. Serial 2-fold dilutions of sera/MIAF were prepared in a 96-well plate in duplicate starting at 1:20 and proceeding to 1:2560, giving a final sample dilution range of 1:40 to 1:5120 after subsequent 1:1 addition of diluted virus. To achieve this, 108µl/well of MEM with 2% FCS was added to the first row of the plate, with 60µl/well added to the subsequent wells. 12µl of serum/MIAF was added to the first row, and the

contents were mixed by pipetting. Serial transfer and mixing of 60µl per sample was carried out down the plate, with the 60µl from the last row discarded, leaving a volume of 60µl in each well of the 96-well plate. Previously-titrated virus stocks were diluted to give a final concentration of approximately 1,000pfu/ml, which would give about 40 plaques per well. 60µl of diluted virus was added to each well of the 96-well plate (giving a total volume of 120µl), and mixed by pipetting, using a fresh tip for each addition. The plate was then incubated at room temperature for 1hr to allow for neutralization. After incubation, media was removed from the previously-prepared 12-well cell plates, and the wells were washed with PBS. 100µl of each serum/virus sample was added to the appropriate well of the plate, with a control well containing 50µl of diluted virus and 50µl medium run per plate. The plates were incubated at room temperature for 30mins to allow for virus attachment and infection, and afterwards 1ml of agar overlay (1:1 dilution of 2% agar and 2x MEM with 4% FCS) was added to each well. The plates were incubated at 37°C with 5% CO_2 for two days before being formalin-fixed and immunostained as described above. $PRNT_{50}$ values were determined for each serum/MIAF sample by determining the dilution value that led to a 50% reduction in plaque count compared to the mean of the control wells.

Temperature-Sensitivity Assays

Plaque assays were performed in 12-well plates using the method described above. Virus dilutions were prepared with a total volume of 225µl for each dilution. Each virus was prepared in triplicate, with 100µl of each diluted sample added to duplicate plates. After incubation at 37°C for 30mins and the application of the agar overlay, one plate of each duplicate pair was placed at 37°C, while the other was incubated at 41°C. The plates were incubated for three days at each respective temperature, with neutral red

overlay applied on Day 2. Plaque counts and morphology differences were noted for each virus at each temperature to determine the effect of higher temperature on virus growth.

MOLECULAR PROCEDURES

RNA Purification – TRIzol

Cell culture supernatant or homogenized mouse organs were centrifuged at 10,000g for 5mins at room temperature to pellet debris. 200µl of the cleared sample was added to 800µl TRIzol reagent (Life Technologies, Waltham, MA) and incubated at room temperature for 15mins, or at 4°C overnight, for virus lysis. RNA was purified from TRIzol using the Direct-zol RNA MiniPrep kit (Zymo Research, Irvine, CA). A 1:1 volume of 100% Ethanol (Fisher Scientific, Pittsburgh, PA) was added to the RNA in TRIzol, and the tube was briefly vortexed to mix. 700µl of Ethanol/TRIzol was added to a supplied Zymo-Spin IIC column, and centrifuged for 1min at 20,000g at room temperature (Eppendorf 5410 Centrifuge, Eppendorf AG, Hamburg, Germany). The eluted TRIzol waste was discarded, an additional 700µl of sample was added to the column, and the tube was re-spun. Once again, the TRIzol waste was discarded, and the remainder of the Ethanol/TRIzol sample added to the tube and spun. The waste TRIzol was discarded, and 400µl of RNA Wash Buffer was added. The tube was again spun for 1min at 20,000g at room temperature. While the column was spinning, DNase I master mix was prepared as follows:

Per tube:

• DNase I (1U/µl)	5µl
• 10x DNase I Reaction Buffer	8µl
• DNase/RNase-Free Water	3µl
• RNA Wash Buffer	64µl
Total Volume	**80µl**

The waste wash buffer was discarded, and 80µl of diluted DNase I master mix was added to the column. The column was incubated at room temperature for 15mins, and then centrifuged for 30secs at 20,000g. The waste DNase I was discarded, and 400µl Direct-zol RNA PreWash was added to the column. The column once again spun for 1min at 20,000g at room temperature, and the waste wash buffer was discarded. The addition of Direct-zol RNA PreWash, and subsequent centrifugation was repeated. 700µl of RNA Wash Buffer was added to the column, and the tube was centrifuged for 1min at 20,000g. The flow-through was discarded, and the empty column was spun again for 2mins at 20,000g. The column was placed into a clean, RNase-free tube (Life Technologies, Waltham, MA), and 50µl of DNase/RNase-free water was added. The column was left to sit for 1min, before being centrifuged for 1min at 20,000g. The eluted RNA was stored at -80°C until needed.

RNA Purification – QIAamp Viral RNA Mini Kit

RNA extraction from cell culture supernatants using the Qiagen QIAamp Viral RNA Mini kit (Qiagen, Germantown, MD) was performed according to the manufacturer's instructions. Cell culture supernatant was centrifuged at 10,000g for 5mins at room temperature to pellet debris. 140µl of cleared supernatant was added to 560µl AVL buffer, and was left to inactivate for 10mins at room temperature. 560µl of 100% Ethanol (Fisher Scientific, Pittsburgh, PA) was added to the RNA/AVL buffer, and the tube was vortexed to mix. 630µl of sample was applied to a QIAamp mini column, and was centrifuged for 1min at 20,000g. The waste was discarded, and the remainder of the sample was applied to the column and re-spun. The flow-through was discarded, and 500µl of AW1 buffer was added to the column. The column was centrifuged again for 1min at 20,000g. The waste was discarded, and 500µl AW2 buffer was added to the column, followed by a centrifugation for 1min at 20,000g. The waste was removed, and

the empty column was spun for a further 2mins at 20,000g. The column was placed into an RNase-free tube (Life Technologies, Waltham, MA), and 40µl of AVE buffer was applied to the membrane. The column was incubated for 1min at room temperature to allow the RNA to dissolve in the buffer, and was then centrifuged for 1min at 20,000g. The eluted RNA was stored at -80°C until needed.

Reverse Transcription

Purified RNA (purification described above) was used for cDNA synthesis. Reverse transcription was carried out using AMV Reverse Transcriptase (New England Biolabs, Ipswich, MA; or, Roche, Indianapolis, IN). Random hexamer primers (Roche, Indianapolis, IN) were used to prime the reaction. dNTPs (Roche, Indianapolis, IN) were used for cDNA synthesis. The reaction mix was as follows:

• Viral RNA	10µl
• AMV RT Buffer (10x)	5µl
• Random Hexamer Primers	2µl
• dNTP Mix	2µl
• Molecular Grade Water	30µl
• AMV Reverse Transcriptase	1µl
Total Volume	**50µl**

The program AMVRTNEB on an Eppendorf Mastercycler Gradient (Eppendorf, Hamburg, Germany) PCR machine was used. This program consisted of a 42°C incubation for 1hour, followed by a 5min inactivation at 90°C. The cDNA was stored at -80°C until needed.

Polymerase Chain Reaction (PCR)

cDNA synthesized from viral RNA, or plasmid DNA, was used as a template for amplification by PCR. Amplification was carried out using the Roche High Fidelity PCR Master Mix (Roche, Indianapolis, IN). A list of primers used may be found in the Appendix. For amplification from cDNA, reactions were set up as follows:

- cDNA (from viral RNA) 5µl
- Forward Primer (100ng/µl) 1µl
- Reverse Primer (100ng/µl) 1µl
- Molecular Grade Water 18µl
- High Fidelity PCR Master Mix (2x) 25µl

  Total Volume **50ul**

For amplification from plasmid DNA, reactions were set up as follows:

- Plasmid DNA 0.1ul
- Forward Primer (100ng/µl) 1µl
- Reverse Primer (100ng/µl) 1µl
- Molecular Grade Water 23µl
- High Fidelity PCR Master Mix (2x) 25µl

  Total Volume **50µl**

The reactions were run on an Eppendorf Mastercycler Gradient (Eppendorf, Hamburg, Germany), with a standard annealing temperature of 58°C adjusted when necessary based upon the primer pairs used (See Appendix A). Elongation times varied

depending on the length of the amplicon, but were usually run at 1min per 1kb. The PCR cycle was as follows:

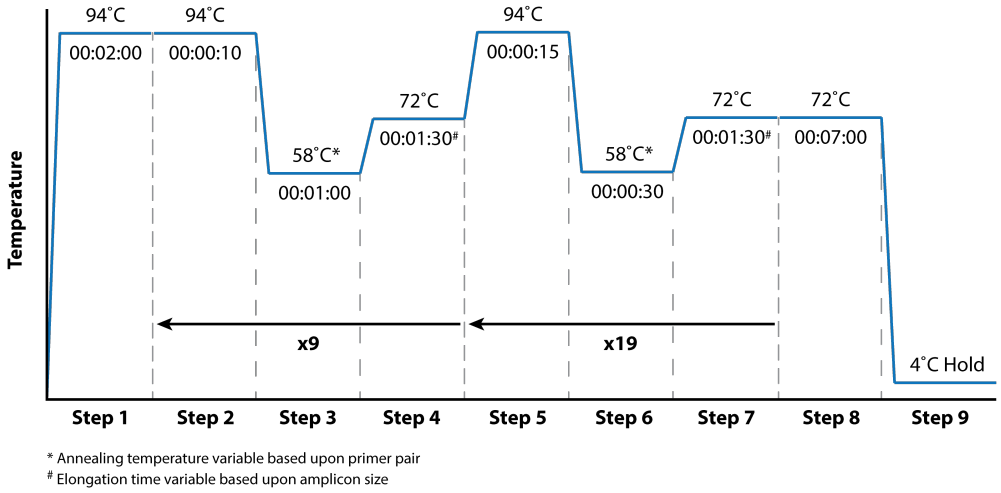

Figure 2.1: Thermocycler Settings for Polymerase Chain Reaction

The PCR products were stored at -20°C until needed.

DNA Gel Electrophoresis

DNA gels were prepared by dissolving and heating 1% agarose (Fisher Scientific, Pittsburgh, PA) in TAE buffer (Life Technologies, Waltham, MA). The volume of agarose/TAE solution prepared was determined based upon the number of samples to be run. In order to visualize the DNA bands, GelRed Nucleic Acid stain (Biotium, Hayward, CA) was added to the molten agarose/TAE at a 1:40,000 dilution (5µl per 200ml). The gel was poured into the appropriate-sized gel tray (8-, 12-, 20-, or 40-well) with a plastic comb installed to form sample wells, and was allowed to set. The gel and tray were then transferred to a horizontal DNA electrophoresis tank (Fisher Scientific, Pittsburgh, PA), which was filled with sufficient TAE buffer to cover the top of the gel by about 5mm. The well-forming comb was removed, and 2µl of 1kb DNA ladder (New England

Biolabs, Ipswich, MA) was added to the left-hand well. 2-30µl of DNA (PCR product or cut plasmid) prepared with 1x DNA loading dye (Qiagen, Germantown, MD) was added to adjacent wells as required. The lid of the gel tank was fitted, and a 100V electrical charge was applied to the gel for 120mins using a Bio-Rad PowerPac Basic (Bio-Rad, Hercules, CA), allowing for the separation of DNA bands by their size. The DNA bands were visualized using a UV transilluminator (Fisher Scientific, Pittsburgh, PA) or imaged using a Bio-Rad Gel Doc XR with Bio-Rad Quantity One v4.6.7 software (Bio-Rad, Hercules, CA).

Purification of DNA Bands from Agarose Gel

For samples intended for extraction, a 1% agarose gel was prepared as described above. A small portion of the sample in 1x sample buffer was added to the well adjacent to the ladder, while the remainder was added to a well elsewhere on the gel, ensuring at least two empty wells were left between the ladder group, and the wells intended for extraction. The gel was run as normal (100V for 120mins). Once finished, the gel was cut between the two empty wells left during loading. The portion of the gel containing the ladder group was taken to the UV transilluminator, where a scalpel was used to cut a groove in the gel to mark the location of the desired band. The removed gel portion was reunited with the other part and, based upon the location of the marked band, the equivalent area was removed from the lane that had not been exposed to UV light. The extracted gel fragment was placed into a clean 1.5ml tube. The whole gel was placed on the UV transilluminator to determine whether the bulk of the intended band had been removed. If not, the remainder of the desired DNA band was removed with the minimal UV exposure, or the gel was re-run. If the band extraction was successful, purification of the DNA from the gel fragment was undertaken using the Qiagen QIAquick Gel Extraction kit (Qiagen, Germantown, MD). The tube containing the gel fragment was

weighed after the balance had been zeroed using an empty tube. The weight of the gel fragment was recorded on the side of the tube. To the gel-containing tube, 3 volume-equivalents (100mg gel ≈ 100µl) of QG buffer were added. The agarose/QG buffer-containing tubes were either incubated at 50°C for 10mins, vortexing regularly, or at 4°C overnight. Once the gel had dissolved, 1 gel volume equivalent of 100% isopropanol (Fisher Scientific, Pittsburgh, PA) was added to the tube, and the sample was mixed. 700µl of sample was applied to a QIAquick column, and spun for 1min at 20,000g. The flow-through was discarded, and another 700µl of sample was added to the tube and spun. This was repeated until the entire sample had been run through the column. Once the flow-through had been discarded, 500µl of QG buffer was added to the column to ensure residual gel was removed. The tube was spun for 1min at 20,000g. The waste was discarded, 700µl of PE buffer was added, and the column was spun again for 1min at 20,000g. The flow-through was discarded, and the empty column was then spun for 2mins at 20,000g to remove residual ethanol. 50µl of molecular grade water was added directly to the membrane of the column, and left to sit for 1min to allow for the DNA to dissolve. The DNA was eluted into a clean 1.5ml tube, and was stored at -20°C until needed.

Purification of PCR Products

Before submitting samples for sequencing or digesting with restriction enzymes, PCR products were purified using the QIAquick Gel Extraction kit (Qiagen, Germantown, MD). The protocol followed was as stated above for gel extraction, with the exception of the first step. Instead of dissolving gel in QG buffer, 3 PCR reaction volume-equivalents of QG buffer were added to the PCR reaction. After the addition of 1 volume-equivalent of isopropanol, the purification proceeded as described above.

pGEM Cloning of PCR Products

When required in high concentration, PCR products were cloned into the pGEM-T Easy vector (Promega, Madison, WI) and transformed into bacteria for amplification. Purified PCR products were combined with pre-cut pGEM-T Easy plasmid and T4 ligase in the following manner:

• 2x Ligation Buffer	5µl
• pGEM-T Easy Vector	1µl
• Purified PCR Product	3µl
• T4 DNA Ligase	1µl
Total Volume	**10µl**

The ligation reaction was carried out overnight at 4°C.

Transformation of Plasmids into Bacteria & Generation of Glycerol Stocks

Chemically competent DH5α or Stble2 *E. coli* bacteria (Life Technologies, Waltham, MA) were previously dispensed into 50µl aliquots and stored at -80°C. For transformation, a vial of bacteria was thawed on ice, and 5µl of plasmid was gently added to the vial. The plasmid/bacteria were incubated on ice for 30mins to allow for interaction between the plasmid and the bacterial surface. In order to transform the bacteria, the vial was heat-shocked for 40secs at 42°C, before being returned to ice for 2mins. 800µl SOC medium (Life Technologies, Waltham, MA) was added to the vial, and the bacteria were incubated at 30°C for Stbl2 or 37°C for DH5α for an hour, shaking at 225RPM. LB Agar plates (2% LB (Sigma-Aldrich, St. Louis, MO) and 2% Agar (Sigma-Aldrich, St. Louis, MO)) containing ampicillin (100µg/ml; Sigma-Aldrich, St. Louis, MO) or kanamycin (50µg/ml; Sigma-Aldrich, St. Louis, MO), X-Gal (5µg/ml; Sigma-Aldrich, St. Louis,

MO), and IPTG (500μM; Sigma-Aldrich, St. Louis, MO) were used to culture the bacteria. 100-400μl of the bacteria was applied to the plate, and streaked using an L-shaped spreader (Thomas Scientific, Swedesboro, NJ). The plates were incubated upside-down for 16-18hrs at 30°C or 37°C with ambient humidity. Three colonies were picked from the plate, and were incubated for 16-18hrs in 15ml tubes containing 2ml of 2% LB medium with ampicillin at 30°C or 37°C, shaking at 225RPM. 500μl of culture was added to LB glycerol (a 1:1 ratio 2% LB (Sigma-Aldrich, St. Louis, MO) and glycerol (Sigma-Aldrich, St. Louis, MO) for creation of a glycerol stock, which was stored at -80°C. The remaining 1.5ml of the culture was centrifuged for 3mins at 20,000g, and the pellet used for plasmid purification by miniprep.

Culture of Bacteria from Glycerol Stocks

Depending on the quantity of plasmid required, 2-100ml of 2% LB with ampicillin or kanamycin was dispensed into an appropriately-sized culture vessel (e.g. 15ml tube or 500ml conical flask). The glycerol stock tube was removed from the -80°C, and a pipette tip was used to scrape a small (~5μl) portion of bacteria-containing sample. The sample was added to the LB/ampicillin, and an air-permeable covering was placed over the neck of the culture vessel. The bacteria were cultured for 16-18hrs at 30°C or 37°C with 225RPM shaking. After growth, the cultures were dispensed into centrifuge tubes for spinning at room temperature for 1min at 20,000g (for 1.5ml tubes), or at 4°C for 1hr at 3,200g (for 15ml and 50ml tubes). Plasmids were purified from the pelleted bacteria by mini- or midiprep.

Purification of Plasmids – Miniprep

Small (up to 2ml) bacterial cultures (grown as described above) were centrifuged for 3mins at 20,000g to pellet the plasmid-containing bacteria. Plasmid purification was carried out using the Qiagen QIAprep Miniprep kit (Qiagen, Germantown, MD). The LB was removed, and the pellet was re-suspended with 250µl of chilled P1 buffer containing RNase A and LyseBlue. Lysis was carried out by adding 250µl of P2 buffer, followed by inversion of the tube 6-times. 350µl of N3 buffer was added to neutralize the sample. The tube was centrifuged for 10mins at 20,000g to pellet the bacterial genomic RNA, and the supernatant was applied to a QIAprep spin column. The column was spun for 1min at 20,000g, and the flow-through was discarded. The column was washed by adding 500µl of PB buffer to the column, and centrifuging for 1min at 20,000g, and the waste was discarded. A second was performed with 700µl of PE buffer, followed by a further 1min centrifugation at 20,000g. The flow-through was discarded, and the tube was spun for a further 2mins at 20,000g to remove the residual ethanol. The column was transferred to a fresh 1.5ml tube, and 50µl of molecular grade water was added directly to the membrane. The column was left to sit for a minute, before being centrifuged for 1min at 20,000g. The eluted plasmid was stored at -20°C until needed.

Purification of Plasmids – Midiprep

Large, 100ml bacterial cultures were divided into two 50ml tubes, and centrifuged at 4°C for an hour at 3,200g. The medium was removed from the tubes, and the pellets were combined and resuspended in 4ml of P1 buffer containing RNase A and LyseBlue. 4ml of P2 lysis buffer was added to the tube, and the sample was thoroughly mixed by inversion 4-6 times. The sample was then left for 5mins, before 4ml of P3 neutralization buffer was added to the sample, and the sample was mixed by inverting the tube again 4-6 times. The entire contents were poured into a pre-stoppered filter syringe, and left for

10mins at room temperature. During the incubation step, a QIAGEN-tip 100 was equilibrated by adding 4ml of QBT buffer, and allowing it to run through. After the 10mins, the stopper was removed from the syringe, and the plunger was inserted to force the plasmid-containing supernatant through the filter into the equilibrated column, leaving the bacterial genomic RNA inside the syringe. The supernatant was allowed to run through the column, allowing the plasmid to associate with the membrane. Two washes with 10ml QC buffer were run, and the plasmid was eluted into a fresh 50ml tube with 5ml of QF buffer. 3.5ml of 100% isopropanol (Fisher Scientific, Pittsburgh, PA) was added to the tube, and the sample was mixed by inversion. The sample was divided into 1.5ml portions in 1.5ml tubes, and was centrifuged at 4°C for 1hr at 20,000g. The supernatant was removed, being careful not to disturb the pellet, and 400µl of 70% ethanol (Fisher Scientific, Pittsburgh, PA) was added to each tube. The tubes were spun again at room temperature for 10mins at 20,000g. The supernatant was carefully removed, and the tubes were left to air dry for 10mins at room temperature. 80µl of molecular grade water was added to the first tube, and the pellet was allowed to dissolve for approximately 10secs. The water was transferred to the next tube, and the pellet was again allowed to dissolve. This transfer was repeated until all of the pellets had been dissolved in the water. Finally, the plasmid sample was transferred to a new 1.5ml tube, where it was stored at -20°C until needed.

Nucleic Acid Quantification

Nucleic acids (RNA and DNA) were quantified using an Eppendorf Biophotometer Plus (Eppendorf AG, Hamburg, Germany). Samples were diluted 1:20 in molecular grade water (5µl nucleic acid with 95µl water). An Eppendorf UVette (Eppendorf AG, Hamburg, Germany) was loaded with plain molecular grade water to be

used as a blank. The water was removed, and the sample was added and read. The output concentration was multiplied by 20 to account for the dilution factor.

Restriction Digests

Plasmid DNA, or appropriately-amplified PCR products, containing specific restriction sites were digested using desired restriction enzymes (New England Biolabs, Ipswich, MA). Most of the digests used for this project were carried out with enzymes that cut at 37°C with NEB CutSmart buffer (Previously NEB Buffer 4 with BSA; New England Biolabs, Ipswich, MA). The volume of input DNA varied, but the general reaction mixture was thus:

- DNA (plasmid or PCR) Xµl
- CutSmart Buffer (10x) 3µl
- Restriction Enzyme 1µl
- Optional: Second Enzyme 1µl
- Molecular Grade Water (25-X)µl

Total Volume **30µl**

The digests were incubated for 12hrs at 37°C in a Mastercycler Gradient thermocycler (Eppendorf, Hamburg, Germany), and then held at 4°C until the next morning. Digested DNA was used as soon as possible.

DNA Sequencing

Plasmids or PCR products purified by one of the methods outlined above were used as templates for nucleotide sequencing. For plasmids, a concentration no greater

than 100ng/µl per sequencing reaction was used. For purified PCR products, the samples were typically used neat without specific quantification of the DNA. For either template type, 6µl of DNA sample was put into a 0.5ml tube, into which 1µl of primer (100ng/µl stock concentration) was added. The sample tube was then submitted to the Molecular Genomics core facility at UTMB for Sanger sequencing. After submission, the samples were prepared for sequencing in 96-well plates using the BigDye Terminator 3.1 Cycle Sequencing kit (Life Technologies, Waltham, MA) as follows:

- DNA/Primer Combination 6µl
- BigDye Buffer 1.5µl
- BigDye Terminator 3.1 1.5µl

  Total Volume **9µl**

The plates were capped and spun down. The sequencing reaction was carried out using a Bio-Rad DNA Engine Tetrad 2 thermocycler (Bio-Rad, Hercules, CA) with the following program:

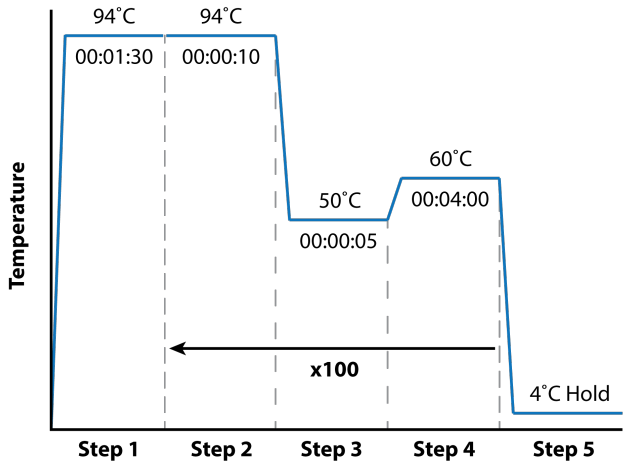

Figure 2.2: Thermocycler Settings for Sequencing Sample Preparation

Before running on the sequencer, the sample was precipitated and resuspended in formamide. To precipitate, 10µl of 125mM EDTA (Sigma-Aldrich, St Louis, MO) was added to the well, followed by 50µl of 100% ethanol (Fisher Scientific, Pittsburgh, PA). The sample was incubated at room temperature for 15mins, and then spun at 15°C for 5mins at 1,500g. The supernatant was removed from the well by inverting the plate onto a paper towel and briefly pulse-centrifuging. 50µl of 70% ethanol was added to the well, and the plate was centrifuged again for 5mins at 1,500g. The plate was again inverted on a paper towel and pulse-centrifuged to remove the ethanol. The sequencing reaction was resuspended in 10µl of formamide (Sigma-Aldrich, St Louis, MO), and vortexed for 15secs. The plate was heated to 90°C for 2mins, then allowed to cool. The sequencing septa was added to the plate, and the plate was run on an Applied Biosystems 3130XL sequencer (Life Technologies, Waltham MA). The output chromatographs were analyzed using Geneious 8 (Biomatters, Auckland, New Zealand).

Site-Directed Mutagenesis

Restriction sites were engineered into the West Nile virus infectious clone using the Agilent QuikChange Multi kit (Agilent, Santa Clara, CA). PstI (nts 1859-1864 of WNV) and StuI (nts 2183-2188 of WNV) sites had previously been added to the pWN-AB plasmid by Dr. Beasley. Primers were designed to engineer SalI and BamHI restriction sites into regions 1829-1834 and 2251-2256 of the WNV genome, respectively (primer sequences in appendix). These sites were added to the wild-type infectious clone plasmids, as well as the plasmid containing the PstI and StuI sites, in order to have a selection of three plasmids with a variety of insertion points. Template plasmids were grown in 2ml cultures from glycerol stocks, and DNA purified by miniprep, as described above. The mutagenesis reaction was set up as follows:

- QuikChange Multi Buffer (10x) 2.5µl
- Plasmid Template 2µl (100ng)
- SalI Primer (100ng/µl) 1µl
- BamHI Primer (100ng/µl) 1µl
- dNTP Mix 1µl
- QuikChange Multi Enzyme Mix 1µl
- Molecular Grade Water 16.5µl

Total Volume **25µl**

The mutagenesis reaction was run on Eppendorf Gradient Master thermocycler with the following program:

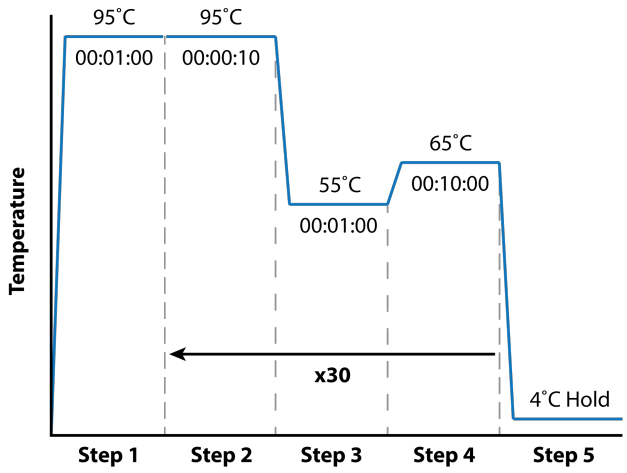

Figure 2.3: Thermocycler Settings for Site-Directed Mutagenesis

In order to remove the template DNA without the mutations, a DpnI digest was run to cleave methylated DNA. 1µl of DpnI was added to the reaction, the sample was mixed by pipetting, and the tube was incubated for 1hr at 37°C. The mutated plasmids were transformed into DH5α bacteria, plated, and grown as described above. Glycerol

stocks were made for each colony, with the remainder of the culture purified by miniprep. The purified plasmids were submitted for sequencing analysis as described above to confirm successful mutagenesis.

Virus Recovery from Infectious Clone – pWN-AB & -CG System

100ml cultures DH5α *E. coli* transformed with pWN-AB and pWN-CG plasmids were grown from glycerol stocks in LB medium containing 100µg/ml ampicillin (Sigma Aldrich, St Louis, MO) for 16-18hrs at 37°C with shaking at 225RPM. Plasmids were purified by midiprep and quantified, as described below. A volume X of pWN-AB containing 2µg of plasmids, and a volume Y containing 4µg of pWN-CG were digested with NgoMIV and XbaI (New England Biolabs, Ipswich, MA) with the following recipe:

• Plasmid Stock (pWN-AB or -CG)	X or Yµl
• CutSmart Buffer	3µl
• Molecular Grade Water	25-(X or Y)µl
• NgoMIV (10,000U/ml)	1µl
• XbaI (20,000U/ml)	1µl
Total Volume	**30µl**

The plasmids were digested for 12hrs at 37°C. The digested plasmids were run on a 1% agarose gel. The larger band for each sample was excised and DNA extracted as outlined in the gel extraction section below. The extracted DNA bands were each eluted in 40µl of molecular grade water, and combined into one tube for ligation with T4 ligase (New England Biolabs, Ipswich, MA). The ligation reaction was set up as follows:

- Purified pWN-AB Band 40µl
- Purified pWN-CG Band 40µl
- Molecular Grade Water 9µl
- T4 DNA Ligase Buffer (10x) 10µl
- T4 DNA Ligase (400,000U/ml) 1µl

  Total Volume **100µl**

The ligation reactions occurred during overnight incubation at 4°C. After the incubation, the ligase was inactivated by heating for 10mins at 70°C. The now full-length plasmid was linearized with XbaI as follows:

- Ligation Reaction 100µl
- Molecular Grade Water 32.0µl
- CutSmart Buffer 15µl
- XbaI (20,000U/ml) 2.5µl

  Total Volume **150µl**

The digestion was incubated at 37°C for 2hrs, after which 5µl of proteinase K (20mg/ml; New England Biolabs, Ipswich, MA) was added to the reaction. The reaction was incubated for a further 1hr at 37°C. 300µl of molecular grade water was added to the sample, followed by 500µl of phenol/chloroform/isoamyl alcohol (Roche, Indianapolis, IN). The sample was vortexed for 20secs, and incubated for 5mins at room temperature. The tube was centrifuged for 2mins at 16,000g to separate the organic and aqueous phases. The organic phase was removed, and was transferred to a clean 1.5ml tube. Another 500µl of phenol/chloroform/isoamyl alcohol was added to the tube, and the sample was vortexed for a further 20secs. The tube incubated for 5mins, and was spun again to separate out the phases, with the organic phase put into a fresh tube. 500µl of

chloroform (Fisher Scientific, Pittsburgh, PA) was added to the sample, which was then vortexed for 30secs. The tube was centrifuged for 1min at 16,000g. The aqueous phase was again transferred to a fresh tube, and 50µl of 3M potassium acetate (Sigma Aldrich, St Louis, MO) was added to the tube, followed by 1ml of 100% ethanol (Fisher Scientific, Pittsburgh, PA). The sample was mixed by inversion three times, and then incubated at -20°C overnight to precipitate the DNA. After incubation, the linearized plasmid was pelleted by centrifugation at 16,000g for 1hr at 4°C. The ethanol was carefully removed by pipetting without disturbing the pellet, and the DNA was allowed to dry for 5-10mins at room temperature. Once dry, the DNA was resuspended in 10µl molecular grade water and transferred to a fresh tube to minimize potential ethanol contamination. From the linearized infectious clone plasmid, full-length viral RNA was prepared by *in vitro* transcription. The RNA was generated using T7-Flash Ampliscribe kit (Epicentre, Madison, WI) with a m^7G(5')ppp(5')Amp Type I RNA cap (New England Biolabs, Ipswich, MA). The reaction was prepared as follows:

• Linearized IC Plasmid	10µl
• NTP mix (2.5mM A; 25mM C, G, U)	7.2µl
• AmpliScribe Reaction Buffer	2.5µl
• m^7G(5')ppp(5')Amp cap	1.8µl
• Dithiothreitol	2µl
• AmpliScribe T7	2µl
Total Volume	**25.5µl**

The reaction was incubated for 30mins at 37°C. While incubating, Vero cells were prepared for electroporation. A confluent T-150 is usually sufficient for two recoveries. The growth medium was removed from the cells, which were then washed with 10ml 1x DPBS. The PBS were removed, and the cells were trypsinized with 2ml 0.25% trypsin

solution. After detachment, the cells were resuspended in 18ml of growth medium. The cells were transferred to a 50ml tube, and were pelleted by centrifugation for 5mins at 3,500g and 4°C. The medium was removed from the tube, and the cell pellet was resuspended in 10ml of chilled, sterile PBS, and stored on ice. 10µl of cells were diluted in 990µl PBS to allow for cell counting with the Scepter 2.0 cell counter (Millipore, Darmstadt, Germany). To determine the cell concentration in the original 10ml PBS, the count was multiplied by 100. The target concentration was around $3x10^6$ cells/ml in the 10ml PBS. Cell concentration was adjusted until this was the case. The cells were then pelleted again by centrifugation at 3,500g for 5mins at 4°C. The PBS was removed, and the pellet was resuspended in 1ml of Buffer R of the Invitrogen Neon 100µl Transfection kit (Life Technologies, Waltham, MA) giving a final cell concentration of approximately $3x10^7$ cells/ml. After the 30min *in vitro* transcription reaction, the tubes were placed on ice. 15µl of RNA was combined with 135µl Vero cells and gently mixed by pipetting. 100µl of the cell-RNA mixture was taken up into a Neon electroporation tip, and the RNA was transfected into the Vero cells using the Invitrogen Neon Transfection System (Life Technologies, Waltham, MA) following the manufacturers protocol. The instrument was set up for a single 1100V pulse lasting 20ms. The 100µl of transfected cells were ejected into a T-75 flask containing 20ml of pre-warmed culture medium without antibiotics. The flasks were immediately transferred to the BSL-3, where they were incubated at 37°C with 5% CO_2. After 4hrs incubation, 400µl of 50x penicillin/streptomycin solution was added to the flask, and the cells were incubated overnight. The next morning the cells were checked to determine confluence. If the flask was more than 70% confluent, the culture medium was removed, and 20ml 2% FCS maintenance medium was added. The flasks were incubated for a further 3 days, with daily observations made to determine development of CPE. On Day 4 post electroporation, 10ml of supernatant was removed to a 15ml tube, and replaced with fresh

medium. The supernatant was centrifuged for 5mins at 3,500g to pellet the cell debris, and divided into 0.5ml and 1ml aliquots, which were stored at -80°C until needed.

Virus Recovery from Infectious Clone – pWNV System

The wild-type and chimeric pWNV complement plasmids, as well as the pWNV backbone plasmid, were grown from glycerol stocks for 18hrs in 100ml of 2% LB with 100µg/ml ampicillin (for pWNV backbone) or 50µg/ml kanamycin (for pWNV complement). Plasmids were purified by midiprep. Plasmids were quantified by spectrophotometry, and prepared for digestion as follows:

pWNV backbone:

• pWNV backbone plasmid	5µl
• CutSmart Buffer (10x)	2µl
• BssHII (25,000U/ml)	1µl
• BamHI (20,000U/ml)	1µl
• Molecular Grade Water	11µl
Total Volume	**20µl**

pWNV complement:

• pWNV complement plasmid	12µl
• CutSmart Buffer (10x)	2µl
• BssHII (25,000U/ml)	1µl
• BamHI (20,000U/ml)	1µl
• Molecular Grade Water	4µl
Total Volume	**20µl**

Digestion reactions were incubated at 37°C for 4hrs, followed by 50°C for a further 4hrs. The samples were then heat-inactivated at 80°C for 20mins. According to the developers of the IC system, purification of the correct plasmid bands is unnecessary, so ligation of the raw plasmid digests was performed:

• Digested pWNV backbone	15µl
• Digested pWNV complement	15µl
• T4 DNA Ligase Buffer (10x)	4µl
• T4 DNA Ligase (400,000U/ml)	1µl
• Molecular Grade Water	5µl
Total Volume	**40µl**

The plasmids were ligated overnight at 4°C. For virus recovery, Vero cells and BHK cells expressing WNV prM-E were plated the previous day in a 12-well plate to allow for duplicate recoveries of each construct. Once approximately 80% confluent, the cells were washed with PBS, and were given 1ml/well of fresh medium (DMEM with 2% FCS, 1x Pen/Strep, and 10mM HEPES buffer). Transfections were carried out using Lipofectamine LTX with PLUS Reagent (Life Technologies, Waltham, MA). Each Lipofectamine/DNA sample was prepared to ensure sufficient sample for two wells of a 12-well plate by diluting 10µl of Lipofectamine LTX in 140µl of Opti-MEM medium in a 1.5ml tube (Life Technologies, Waltham, MA). In a second 1.5ml tube, the complete ligation reaction was combined with 5µl of PLUS reagent and 105µl of Opti-MEM. The two 150µl volumes were combined and allowed to sit for 5mins at room temperature. After incubation, 150µl of the Lipofectamine/DNA mixture was added to each of two wells of the 12-well plate. This method was repeated for each chimeric plasmid, with five constructs run in duplicate per plate. Two of the wells were reserved as mock-transfected controls, whereby the transfection was carried out similar to the chimeric plasmids,

except for the addition of 40µl of PBS to the Opti-MEM instead of post-ligation plasmid DNA. The plate was transferred to the BSL-3 laboratory, where it was incubated for 4 days at 37°C with 5% CO_2. Successful recovery from the BHK prM-E cells was determined by a change in the color of the medium within the well compared to the mock-transfected wells, as even the wild-type WNV control failed to generate clear CPE. A 500µl aliquot of cleared supernatant was removed from each well and was frozen at -80°C for storage until cells were ready for subsequent infection to amplify any infectious virus present in each recovered supernatant.

Next-Generation Sequencing

Viral RNA was purified from clarified supernatant samples using the Qiagen QIAmp Viral RNA kit as outlined above. Samples were submitted to the Next Generation Sequencing Core Facility at UTMB for *de novo* determination of consensus sequences and single-nucleotide polymorphisms with >1% prevalence. After submission, the RNA was quantified using Qubit fluorescence analysis (Life Technologies, Waltham, MA). If deemed necessary by the core facility staff, background ribosomal RNA levels were reduced using a Ribo-Zero rRNA Removal Kit (Illumina, San Diego, CA). RNA libraries were generated using the Illumina TruSeq v2 kit (Illumina, San Diego, CA). This entails fragmenting 0.5-1.0µg of total RNA by heating the samples to 94°C for 8mins in the presence of divalent cations. cDNA synthesis was carried out on the RNA fragments using the Superscript II Reverse Transcriptase kit (Life Technologies, Waltham, MA) with random primers. The cDNA was converted to dsDNA, and was ligated into the adapter DNA molecules contained within the TruSeq kit. The adapter-flanked 'viral' DNA was amplified by PCR using primers specific to sequences found within the adapter regions. This RNA-Seq library was quantified and characterized using the Qubit fluorescence kit as well as with a DNA 100 chip using the Agilent 2100 Bioanalyser

(Agilent, Santa Clara, CA). Once determined to be appropriate, the samples were sequenced using an Illumina HiSeq 1500 instrument (Illumina, San Diego, CA). The output sequencing contigs were assembled *de novo* to give a consensus sequence for each virus using the Illumina BaseSpace package (Illumina, San Diego, CA). The sequencing contigs were then aligned to the consensus sequence using the bowtie2 package (Johns Hopkins University, Baltimore, MD) to allow for SNP determination using the VarScan2 programme (Washington University in St. Louis, St. Louis, MO). The output from this programme demonstrated SNPs compared to the consensus sequences, as well as the prevalence of said polymorphisms.

ANIMAL PROCEDURES

Mouse Model

Female, 3-4 week-old Swiss Webster mice (Harlan, Indianapolis, IN) were used as the outbred animal mode for WNV, due to their susceptibility following inoculation by various routes (see Chapter 1, section "Animal Models for WNV"). For the WNV G331A studies, male and female IFNα/β receptor knock-out mice were also used as an immunosuppressed mouse model. These mice were acquired from the breeding colony present at UTMB. All of the mice were housed in HEPA-filtered enclosures within the ABSL-3 facilities at UTMB, with an unlimited supply of food and water. All animal studies were conducted in accordance with approved IACUC protocols.

Assessment of Neurovirulence and Neuroinvasion

Groups of mice were inoculated i.p. or i.c. with 100µl or 50µl DPBS (Corning, Manassas, VA), respectively, containing 10 or 100pfu of virus. The inocula were tested by back titration to confirm the virus dose. The mice were checked daily for signs of infection, increasing to twice-daily once clinical signs started to develop. Mice were recorded as dead if they were found dead, or deemed too sick to continue, requiring euthanasia. Moribund mice were euthanised by CO_2 asphyxiation followed by cervical dislocation. After at least 21 days, surviving mice were bled by cardiac puncture under isofluroane anesthesia and then immediately euthanised. Blood samples were allowed to coagulate at room temperature, after which serum was prepared from the blood by spinning for 5mins at 10,000g. The serum was heat inactivated for 30mins in a waterbath set to 56°C before removal to the BSL-2 laboratory for ELISA testing to assess seroconversion.

Serial Sacrifice Studies

Two days prior to infection, groups of five mice were anaesthetized and implanted with subcutaneous IPTT-300 transponders (BMDS, Seaford, DE) to allow for identification and temperature measurements. Temperature and weight data were recorded daily throughout the course of the experiment. On Day 0, the chipped mice, and an additional 15 unchipped mice, were inoculated i.p. with 100µl of PBS containing 100pfu of virus. The virus titer in the inoculate was confirmed by back titration plaque assay on Vero cells. On Days 1, 3, 5, 7, and 9, groups of three mice were selected at random from the unchipped infected cages, anesthetized for blood collection via cardiac bleed, and then euthanized for tissue collection. Blood samples were dispensed into purple-topped EDTA-containing tubes (Sarstedt, Nümbrecht, Germany). The samples were thoroughly mixed immediately to prevent clotting. Hematological analysis was carried out on the whole blood using a Hemavet 950 (Drew Scientific, Miami Lakes, FL). Liver, kidney, spleen, lung, and brain samples were removed and deposited in pre-weighed 2ml homogenization tubes containing Lysing Matrix D (MP Biomedicals, Santa Ana, CA).

The blood samples were centrifuged for 5mins at 10,000g to separate out plasma, which was removed and stored at -80°C until needed. The organ-containing tubes were weighed, with organ weight determined by subtracting the empty tube weights from the filled weights. The organ weights were converted to volume equivalents (1mg ≈ 1µl), and the tubes were filled to an effective total volume of 500µl with MEM containing 2% FCS and 2x penicillin/streptomycin solution. The samples were homogenized at full speed for two cycles of 1.5mins using a Qiagen TissueLyser II (Qiagen, Germantown, MD). The samples were centrifuged for 5mins at 10,000g to spin down the contents. A further 500µl of medium was added to the tubes to give a total volume of 1ml. The brain samples

were mixed and re-centrifuged before storage at -80°C. The other organs were homogenized again at full speed for two 2min cycles. These samples were centrifuged again for 5mins at 10,000g, before being stored at -80°C. Virus titers in the organs and plasma were determined by plaque assay, as described above.

OTHER ASSAYS

Cytokine & Chemokine Determination – MilliPlex

Mouse plasma samples were collected during the serial sacrifice study, described above. Cytokines and chemokines within the samples were quantified using a Milliplex 25-plex mouse cytokine/chemokine magnetic bead kit (Millipore, Billerica, MA). Assay standards and controls were prepared as outlined in the assay handbook. To run the assay, 200µl of wash buffer was added to each of the wells of the 96-well assay plate. The plate was sealed, and was incubated at room temperature, shaking at 600RPM, for 10mins. The wash buffer was removed, and 25µl of controls and serially-diluted standards were added per well in duplicate. 25µl of assay buffer was added to the sample wells. Since plasma samples were being run, 25µl of serum matrix was added to each of the standard and control wells. 25µl of plasma samples (diluted 1:1 with assay buffer) were added in duplicate to pre-determined wells on the plate. The pre-mixed magnetic beads were vortexed for 1min, and 25µl was added to each well of the plate. The plate was sealed, and was incubated at room temperature for 2hrs, shaking at 600RPM. After incubation, the plate was attached to a Bio-Rad handheld magnetic plate washer (Bio-Rad, Hercules, CA), and the wells were washed twice with 200µl each of wash buffer. 25µl of detection antibody mix was added to each well, and the plate was sealed and incubated at room temperature for 1hr, shaking at 600RPM. After incubation, 25µl of streptavidin-phycoerythrin was added to each well, and the plate was sealed and incubated for a further 30mins. The plate was attached to the magnetic plate washer, and was washed twice with 200µl of wash buffer per well. The wash buffer was removed, and 150µl of instrument sheath fluid was added to each well. The plate was sealed, and shaken for 5mins at 600RPM to resuspend the beads, before being read with a Bio-Rad Bio-Plex 200 instrument with Bio-Plex Manager 4.1.1 software (Bio-Rad, Hercules, CA).

Enzyme-Linked Immunosorbent Assay (ELISA)

Nunc Maxisorp 96-well plates (Thermo Scientific, Waltham, MA) were coated with a pre-determined concentration of recombinant protein in 1.5M borate saline solution (pH9; Sigma-Aldrich, St. Louis, MO), 50µl per well. Background control wells were plated with borate saline solution alone. The plates were sealed and incubated overnight at 4°C to allow for adsorption of the protein. After the incubation, the coating buffer was removed, the plate was washed with PBS containing 0.5% Tween-20 (Thermo Scientific, Pittsburgh, PA), and the wells were blocked with 75µl of PBS-Tween containing 3% skimmed milk powder (Saco, Middleton, WI). The plate was sealed, and blocking was performed at room temperature for at least 1hr. Once blocked, the plate was washed twice with PBS-tween, and 50µl of serum diluted in PBS-tween was added to wells in duplicate. A positive control anti-WNV MIAF, and a negative control serum was run in duplicate on each plate. The plate was sealed and incubated for 60mins at room temperature. After incubation, the plate was washed three times with PBS-tween, and residual wash buffer was removed by sharply tapping the inverted plate on paper towels. 50µl of HRP-conjugated, anti-mouse IgG (Sigma-Aldrich, St Louis, MO) diluted to 1:5,000 in PBS-tween was added to each well, and the plate was sealed and incubated for 60mins at room temperature. The plate was washed three times with PBS-tween, and residual buffer was removed as before. To develop the ELISA, 50µl of TMB substrate (Sigma-Aldrich, St Louis, MO) was added per well, and left to incubate at room temperature for 10min, or until color developed. The reaction was stopped by the addition of 50µl per well of 3M hydrochloric acid (Sigma-Aldrich, St Louis, MO). The absorbance was read using a Tecan Sunrise microplate reader (Tecan, Männedorf, Switzerland) at 450nm, with a reference wavelength of 595nm. Samples were deemed positive if they had absorbances greater than the background plus three standard deviations in addition to the values for the negative control serum.

Western Blot

Cell lysates were prepared from T-25 flasks of Vero cells infected with WT or chimeric viruses. Supernatant was removed from the tissue culture flask and 500µl of NuPAGE LDS sample buffer (Life Technologies, Waltham, MA) was spread across the cell monolayer and incubated for 5mins at room temperature to ensure cell lysis. The sample buffer was removed to a fresh 1.5ml tube, and was heat inactivated at 95°C for 20mins. It was stored at -20°C until required.

The protein samples were thawed, and loaded onto a 15-well NuPAGE Novex 4-12% Bis-Tris protein gel (Life Technologies, Waltham, MA), with 5µl of Bio-Rad Precision Plus Protein Kaleidoscope protein standard in the first lane (Bio-Rad, Hercules, CA). The gel was run using NuPAGE MES SDS running buffer in an XCell SureLock Mini-Cell gel tank (Life Technologies, Waltham, MA) with a Bio-Rad PowerPac Basic power supply (Bio-Rad, Hercules, CA) set to 200V for 40mins. The proteins were transferred to a nitrocellulose membrane (GE Healthcare Life Sciences, Pittsburgh, PA) using an XCell II blot module (Life Technologies, Waltham, MA) with NuPage transfer buffer (Life Technologies, Waltham, MA) containing 20% methanol (Fisher Scientific, Pittsburgh, PA). The power pack was set to 100mA constant current for 90mins.

Following sample transfer, the western blot was run using the WesternBreeze Chemiluminescent kit (Life Technologies, Waltham, MA). The blot was blocked overnight with 10ml of the provided blocking buffer (2ml buffer A, 1ml buffer B, 7ml water), rocking at room temperature. The primary antibody (See Appendix B) was appropriately diluted in a further 10ml of blocking buffer, and incubated with the blot for 2hrs. The antibody was removed, and the blot was washed four times with wash buffer for 5mins each time. The wash buffer was discarded, and 10ml of secondary antibody

solution (AP-labeled, anti-mouse IgG) was added and incubated for 1hr. The blot was washed again four times with wash buffer for 5mins each, followed by two 2min washes with distilled water. 2.5ml of CDP-Star substrate, containing 125µl of NitroBlock was added to the membrane, and incubated for 5mins. The substrate was blotted off, and protein bands were determined using x-ray film (GE Healthcare Life Sciences, Pittsburgh, PA) developed using an x-ray film developer (Kodak, Rochester, NY).

Statistical Analyses

Statistical analysis of growth kinetics, plaque sizes, organ titer, hematology, and MilliPlex data was performed by ANOVA with Bonferroni post-hoc analysis using Stata 14 (StataCorp, College Station, TX). Values were determined to be significantly different for $p<0.05$. Hierarchical clustering of cytokine and chemokine data was performed using Mathematica 10 (Wolfram, Champaign, IL). Survival curve analysis was performed using a Log-rank (Mantel-Cox) test with GraphPad Prism v6.0g (GraphPad, La Jolla, CA).

EXPERIMENTAL RESULTS

Chapter 3: Generation, Recovery, and *in vitro* Characterization of Chimeric Flaviviruses

INTRODUCTION

As the major protein component of the surface of infectious virions, the flavivirus envelope glycoprotein plays a number of important roles during virus entry into target cells, including receptor-binding, and mediation of fusion between the viral envelope and cellular endosomal membranes. The recognition of receptor molecules on the surface of target cells, thought to be mediated by domain III of E (EIII), may play an important role in tissue tropism during infection by governing the particular cell types that the virus may bind to and enter.

Previous studies with chimeric viruses expressing whole prM-E from related donor viruses have demonstrated that the substitution of the structural proteins from one virus into another can significantly affect its growth in mammalian cells, but that growth in arthropod cells appears to be less significantly affected. The addition of prM-E from TBEV into a DENV-4 backbone resulted in a virus that grew significantly better in LLC-MK2 cells than DENV-4, with a peak titer 3-logs (1,000-fold) higher (Pletnev et al., 1992). The effects on growth in mammalian cells with prM-E chimeras appears to be variable, as similar substitutions between TBEV and OHFV showed growth kinetics more similar to the backbone virus than the donor virus (Yoshii et al., 2014). It is possible, however, that the similar growth kinetics and relative genetic similarity of TBEV and OHFV, compared to TBEV and DENV-4, meant that any effect of chimerization was less apparent.

Few previous studies have investigated chimeric proteins with respect to their incorporation into virions, and the maintenance of virulence of such particles. The aim of this project was to generate chimeric flaviviruses whereby the EIII from donor viruses was substituted into a WNV NY99 backbone. The donor viruses were selected based on their sequence diversity from WNV to allow for a determination of a limit for virus viability, with a number of donors additionally chosen for their differences in disease presentation and vector competence, compared to WNV.

Previous studies conducted in Dr. Beasley's laboratory had demonstrated that WNV containing a JEV SA14-14-2 EIII was viable, and grew reasonably similarly to WNV in Vero cells, suggesting that for genetically similar flaviviruses, EIII substitution may be tolerated quite well. The hypothesis was that the range of donor EIIIs permitting viable viruses could be extended further, and that EIII substitution from more genetically distinct flaviviruses would potentially affect the behavior of the chimera in tissue culture, as well as affect its antigenicity with respect to antibody binding and virus neutralization.

MODIFICATION OF PWN-AB INFECTIOUS CLONE PLASMID

In order to generate the chimeric viruses, restriction sites were engineered into the WNV IC at either side of the EIII coding region. A pWN-AB construct with an upstream PstI restriction site and a downstream StuI restriction site (at regions 1,849-1,854 and 2,183-2,188 of the genome, respectively) had been previously generated by Dr Beasley. These sites were created in regions of the genome that were highly conserved amongst the flaviviruses, and were such that the amino acid sequence was not altered. In order to provide a selection of insertion sites, and to determine whether the size of the insert affected the chimeric viruses generated, further modified pWN-AB plasmids were generated incorporating a SalI site (1,829-1,834) upstream of EIII and a BamHI site

(2,251-2,256) downstream, with the sites engineered into the wild-type IC plasmid, and also into the plasmid containing the other two sites, resulting in a construct containing all four insertion points (Figure 3.1). The SalI site is located within EI, upstream of the EI-EIII linker region, while the PstI site is located immediately upstream of the linker. Downstream of EIII, the StuI site is located immediately prior to the first of the stem-helices, while the BamHI site is located in the loop between the two stem-helical structures. The presence and identity of the sites were confirmed by sequencing. While the addition of the BamHI site did not affect the amino acid sequence of the protein, the addition of the SalI site led to a conservative valine to leucine substitution at position 290 (V290L) of the envelope glycoprotein. While not common, this mutation has been observed in a natural isolate from a symptomatic horse in Turkey in 2011 (Ergunay et al., 2015). The isolate, denoted T2 (GenBank accession no. KJ958922 (genome) and AJM13598 (polyprotein)), shared 99.6% amino acid identity with WNV NY99, and possessed no additional mutations within EIII. Indeed, across the whole polyprotein, there are only 15 amino acid differences including the V290L in the envelope glycoprotein.

In order to confirm that the SalI restriction site-induced amino acid change did not affect virus growth in mammalian (Vero) or mosquito (C6/36) cell lines, growth kinetics were determined and compared to those for WNV NY99. No significant differences were observed for either cell type as determined by ANOVA ($p>0.05$), and plaque morphology remained identical (Figure 3.2). Passaging of the virus ten times in Vero cells resulted in no sequence changes, with the V290L substitution maintained.

CONSTRUCTION OF CHIMERIC VIRUSES

Chimeric viruses were generated using the modified pWN-AB WNV IC plasmids described above. Nine different EIII donor viruses were chosen for their range of sequence diversity compared to WNV: KOUV, JEV, SLEV, BAGV, IGUV, ZIKV, DENV-2, YFV, and DTV. For eight of the viruses, RNA was acquired from the World Reference Centre for Emerging Viruses and Arboviruses at the University of Texas Medical Branch. For ZIKV, a synthetically-generated plasmid containing the EIII sequence of the MR766 strain was purchased. Where possible, the designated prototype strain, or an isolate known to be virulent, was used for each donor virus. For the seven donor viruses genetically most similar to WNV (KOUV, JEV, SLEV, BAGV, IGUV, ZIKV, and DENV-2), four different constructs were prepared using each combination of upstream and downstream restriction sites. These were denoted the A-, B-, C-, and D-forms (Figure 3.3). The A-, C-, and D-forms were generated using the pWN-AB plasmid containing all four restriction sites, while the B-forms were generated using the pWN-AB PstI-StuI plasmid. Based on the location of the restriction sites, the B-form (PstI-StuI) had the smallest insert, consisting solely of EIII, whereas the A-form (SalI-BamHI) was the largest substitution, containing part of EI upstream of the EI/EIII linker region, and the first stem-helix region downstream. The C- and D-forms (SalI-StuI and PstI-BamHI, respectively) had the additional upstream and downstream sequences, respectively.

For the SLEV A- and C-form chimeras, the use of a SalI restriction site led to the incorporation of a proline residue at position 290, which led to an unrecoverable virus, potentially due to the tendency of prolines to add a bend in the polypeptide chain. Instead, an XhoI site was used for the SLEV inserts, as this restriction enzyme generates an identical sticky-end to SalI, although the flanking bases are different. This allowed for

a valine at 290 instead, similar to that found in WT WNV. An XhoI site was also used for the BAGV A- and C-form construction, which also resulted in a valine at 290.

Following construction, the plasmids were sequenced to confirm the identity of the inserts, and to determine any sequence differences compared to published sequence for the donor viruses (Table 3.1).

RECOVERY OF CHIMERIC VIRUSES

Virus recovery was attempted for all of the chimeric viruses, with viability determined by the generation of CPE within the cells, and the presence of DNA bands on an agarose gel following RT-PCR of supernatant samples harvested after 4 days. Flasks that did not show CPE five days post electroporation were incubated until the cells were exhausted, to determine whether, given time, an adapted form could emerge. Before disposal, supernatant samples were taken from these flasks for RT-PCR testing to detect viral RNA. Of the nine donor viruses used, viable chimeras were generated for all four forms with EIIIs from KOUV, JEV, SLEV, and BAGV. None of the four forms resulted in viable viruses with EIIIs from IGUV, ZIKV, or DENV-2. The A-form YFV and DTV constructs were also unrecoverable (Table 3.2). Efforts to recover the inviable constructs were performed at least twice to rule out technical errors.

Distinct differences were seen in plaque morphology for some of the recovered viruses. Ten representative plaques were measured for each virus, with mean plaque size, standard deviations, and statistical comparisons determined by ANOVA with Bonferroni post-hoc analysis (Figure 3.4, Table 3.3). For the JEV chimeras, no significant differences in plaque size were observed either between the different forms, or between the chimeras and WNV NY99. For the KOUV chimeras, the plaques for all of the

constructs were significantly smaller than those of WNV, as determined by ANOVA, but there were no significant differences observed between the four different versions. Following initial virus recovery, the SLEV A-form failed to generate plaques at all in Vero cells, however small foci were visible following fixation and immunostaining of the plate. The SLEV B-form caused large plaques that were not significantly different to those of WNV NY99, however the plaques for the C- and D-forms were significantly smaller than either WNV NY99 or SLEV B. The BAGV A-form had very small plaques that were significantly different to either the WT or any of the other BAGV versions. The B-, C-, and D-forms of the BAGV chimeras had plaques that were significantly smaller than WNV NY99, but not significantly different from each other. Generally, based upon the plaque sizes, and the titer of virus present at day 4 of the recovery, the B-form inserts were deemed to be most well tolerated, with the A-forms least tolerated.

Stability assays run on all of the viable chimeras demonstrated that, with the exception of BAGV A, which showed a 5-fold decrease, the virus titers remained stable over the course of 2hrs incubation at 37°C. Temperature sensitivity assays comparing virus titers and plaque morphology when held at 37°C and 41°C, run on the A- and B-forms of each virus, revealed no differences for WNV NY99, the JEV chimeras, or the KOUV chimeras (Figure 3.5). SLEV A had titers below the limit of detection at both 37°C and 41°C, as determined by immunostaining, precluding effective comparisons, while SLEV B showed a non-significant 2-fold difference between the 37°C and 41°C plates, a change within the limits of variability of the plaque assay. BAGV A showed a significant 65-fold decrease in titer at 41°C compared to 37°C, whereas BAGV B showed little in the way of a titer drop, but the plaque size after 72hrs at 41°C was 4x smaller (~0.5mm diameter) compared to 37°C (1.95mm diameter), suggesting that both chimeras may be slightly unstable.

"Reverse Chimerization" of DENV-2 Constructs

In order to determine whether the inviability of some of the chimeric viruses, including DENV-2, was due to an incompatibility between other parts of E and particular regions of EIII, rather than EIII as a whole, "reverse chimeras" were generated, whereby particular regions of DENV-2 EIII were reverted to WNV sequence (Figure 3.6). Comparison of the crystal structures of EIII from WNV and DENV-2 suggested that the region from amino acids 362 to 372, which includes the DE loop, may protrude more towards EI with DENV-2 compared to WNV, potentially causing a clash between the two domains. In addition, interaction analysis carried out using the WNV E structure with the PDBePISA software indicated a region from 312 to 326 that may be involved in dimerization of E on the virion surface. Three synthetic DENV-2 EIII constructs with either or both of these regions returned to WNV sequence were generated, and plasmids for all four chimera versions were constructed. Since the B-forms had previously been determined to be most well tolerated for other constructs, recovery was attempted for these versions with all three "reverse chimera" constructs. Unfortunately none of the three allowed for recovery of viable viruses.

Recovery and Passaging of Inviable Viruses in prM-E Expressing Cells

The B-forms of the inviable IGUV, ZIKV, and DENV-2 chimeras, as well as WNV NY99 and JEV B as positive controls, were recovered in BHK cells stably expressing wild-type WNV NY99 prM-E. It was hypothesized that passaging the inviable viruses in these cells, without high selective pressure on E and allowing the packaging of chimeric genomes with wild-type as well as chimeric E proteins, would potentially allow for the generation of a quasispecies in which a range of mutations could occur, including in and around the chimeric region, that might allow for a viable mutant to emerge. Successful recovery of viruses was determined by alterations in the color of the medium,

compared to a mock-transfected control, as RT-PCR would amplify WT sequence derived from the cells. CPE generation was minimal even with the positive controls, but transfer of the supernatant from the control virus recoveries to Vero cells led to the generation of clear CPE, indicating that the recoveries were successful. However, even after five passages, none of the chimeric constructs had acquired the ability to grow in Vero cells.

VERO CELL GROWTH KINETICS

All sixteen viable chimeras were grown in Vero cells following an infection with 1,000pfu (an effective MOI of 0.0005) to determine growth kinetics (Figure 3.7, Table 3.4). As described above, the backbone virus containing the restriction sites, and the single amino acid substitution V290L grew identically to the WNV NY99 control. The four JEV chimeras grew similarly to one another (Figure 3.7A; Table 3.4A), although the peak virus titer for the A- C-, and D-forms at Day 2 was approximately 5-fold higher than for the WNV NY99 and JEV B, with statistical significance with JEV A ($p<0.001$) and D ($p<0.004$). The higher titers continued for the duration of the growth kinetics, with statistically significant differences (A: $p<0.003$; C: $p<0.047$; D: $p<0.004$) for all three versions on Day 3, and significant differences for JEV A ($p<0.008$) and C ($p<0.023$) on Day 4. The B-form grew like WNV NY99 over the course of the growth kinetics, with no significant differences.

Despite less genetic distance from WNV, compared to JEV, the KOUV EIII chimeras were more variable in their growth kinetics compared to the NY99 parental virus (Figure 3.7B; Table 3.4B). Although for the most part all four versions grew reasonably similarly to one another (there were no significant differences between the titers for all chimeras at any timepoint), there were significant differences in their growth

compared to WNV NY99. On Day 1, the B-, C-, and D-forms of the KOUV chimeras were significantly different to NY99 (B: $p<0.006$; C: $p<0.007$; D: $p<0.001$), whereas the difference between KOUV A and NY99 was not significant. For the remainder of the timecourse, all four versions were significantly different to WNV NY99.

The SLEV EIII chimeras showed the most variability between the different forms (Figure 3.7C; Table 3.4C). SLEV A, which had failed to plaque following recovery, had titers below the limit of detection, even by immunostaining, on Day 0 and Day 1. By Day 2 the virus appeared to have changed somewhat, as it reached a mean titer of nearly 10^4 pfu/ml, and acquired the ability to plaque, albeit with very small plaques. The titers determined by plaque assays and immunostaining were in agreement from Day 2 onwards, suggesting that a major proportion of the viruses in the sample possessed the plaquing phenotype. Throughout the growth kinetics, the SLEV A virus titers were significantly different to those of WNV NY99, and were different from SLEV B from Day 2 onward. Despite the apparent differences, SLEV A was not statistically significantly different from SLEV C and D at any time. Of the SLEV chimeras, the B-form grew most similarly to WNV NY99, although there were statistically significant differences on Days 1, 2, and 5. The largest difference, on Day 1, was a 5-fold lower titer, with a maximum of 2-fold differences at the other timepoints. The SLEV C-form grew second most similarly to WNV NY99; although the peak titer was 20-fold lower, and significant differences occurred throughout the growth period. Finally, SLEV D grew marginally less well than SLEV C, with a peak titer on Day 3, rather than Day 2. However, from Day 3 onward, SLEV C and D had almost identical titers.

All four of the BAGV chimeras grew to significantly lower titers than WNV NY99, although they grew quite similarly to one another, with no statistically significant difference in titer at any timepoint (Figure 3.7D; Table 3.4D). This is evident for the B-,

C-, and D-forms, but the A-form appeared to grow substantially less well, with a 250-fold lower titer on Day 2, compared to BAGV B.

C6/36 GROWTH KINETICS

Some previous studies with flavivirus prM-E chimeras and mutant EIIIs have shown differences in growth within arthropod cells. Accordingly, comparisons of growth kinetics in C6/36 mosquito cells were carried out for the A- and B-forms, as these were the versions that showed the clearest differences in their growth kinetics in Vero cells, as well as having largest differences in insert sizes (Figure 3.8, Table 3.5). The JEV A- and B-forms grew almost identically to one another and, although the titers at Day 4 and Day 5 were a little lower than those of WNV NY99, there were no significant differences (Figure 3.8A; Table 3.5A).

The KOUV A- and B-forms, while a little variable on Day 1, with a 5-fold difference in titer, also grew almost identically from Day 2 onward (Figure 3.8B; Table 3.5B). Interestingly, the slight shallowing of the curve seen at the later timepoints with the JEV chimeras is more noticeable with the KOUV chimeras, with significantly lower titers on Day 3 and Day 5. Indeed, whereas the WNV NY99 titers were still steadily increasing from Day 4 to Day 5, both of the KOUV chimeras seem to plateau at Day 4, with little additional virus on Day 5.

As seen with the growth kinetics in Vero cells, the SLEV chimeras were the most variable in C6/36 cells (Figure 3.8C; Table 3.5C). Over the first few days, the SLEV B-form outgrew the WNV NY99, despite starting with a similar input dose of 1,000pfu. The higher titers are statistically significant on Days 2 and 3, with the titer of SLEV B 5-fold higher than WNV NY99 on Day 2. By Days 4 and 5 WNV NY99 had caught up with

SLEV B, and the two viruses had similar titers. Conversely, SLEV A appeared to be completely attenuated in C6/36 cells, with a peak titer on Day 5 of just 50pfu/ml. Unlike in Vero cells, it appears the virus was unable to adapt to C6/36 cells during the 5 day period. RT-PCR run on purified RNA from the supernatant on Day 5 failed to produce enough sample for sequencing to determine any sequence changes.

Similar to the JEV and KOUV chimeras, the BAGV A- and B-forms grew reasonably similarly to each other throughout the growth kinetics, with no significant differences (Figure 3.8D; Table 3.5D). Following on from KOUV, the BAGV chimeras appeared to grow less efficiently compared to WNV NY99, and had a much shallower curve, with almost 100-fold lower titers on Day 4. The B-form appeared to grow a little better than the A-form towards the end of the experiment, with an almost 10-fold difference in titer at Day 5.

STABILITY OF CHIMERIC SEQUENCES

The apparent adaptation of the SLEV A chimera during the course of the Vero growth kinetics led to the question of sequence stability for the chimeric viruses. Deep sequencing was performed on the recovered viruses to determine the amount of variability in the stocks used for *in vitro* and *in vivo* characterization. As expected there were a number of minor nucleotide variants, but few non-synonymous changes with prevalence over 5% that were not detected in the original plasmids (Table 3.6).

The JEV chimeras had no significant changes to their sequences following recovery. KOUV A had two low frequency non-synonymous mutations, L325V in E (17.7% prevalence), and T390S in NS3 (6.62% prevalence), while KOUV B had four: Y43S in prM (6.2%), D390G in E (12.79%), I424V in NS3 (7.78%), and T165S in NS4b

(11.16%). KOUV C had only one non-synonymous mutation, M216V in NS2a (9.48%), while KOUV D had no non-synonymous mutations with prevalence greater than 5%.

Interestingly, the stocks of SLEV A harvested on Day 4 post electroporation were very homogeneous, likely due to the apparently poor replication efficiency of the virus. While SLEV B had a number of mutations, only one, an N222Y in E (11.29%), had prevalence above the 5% threshold. This same mutation was also the only significant non-synonymous mutation in SLEV C, although prevalent to a consensus level (>80% prevalence), with 98.24% frequency. Similarly in SLEV D, this previously observed N222Y mutation in E was highly prevalent (69.21%), with a further four minor variant non-synonymous mutations: M292I in E (5.29%), I481M in E (25.8%), L492V in E (7.45%), and I184V in NS1 (7.62%).

Similar to SLEV A, the BAGV A chimera had very little sequence diversity following the recovery, with no non-synonymous mutations. The N222Y mutation, prevalent in the SLEV chimeras, was prevalent to a consensus level in BAGV B (80.71%) and BAGV C (95.25%). Indeed, for BAGV C, this was the only non-synonymous mutation with frequency greater than 5%. BAGV B had an additional two non-synonymous mutations, a D423A in E (5.16%), and an M261L in NS3 (7.69%). BAGV D had no prevalent mutations.

In order to identify potential adaptions in the SLEV A and BAGV A chimeras (the most growth restricted of the viable chimeras) following a single passage in Vero cells, one of the three replicates for each virus from Day 5 of the Vero growth kinetics experiment was also submitted for deep sequencing (Table 3.7). Both the BAGV A and SLEV A P1 samples maintained reasonably low diversity. The N222Y in E was observed in both viruses, with a sub-consensus 23.87% frequency for BAGV A P1, and a

consensus 96.14% prevalence for SLEV A P1. This was the only non-synonymous mutation with prevalence greater than 5% in BAGV A P1, however SLEV A P1 had a further two prevalent, non-synonymous mutations, M144T in prM (26.35%), and H285Y in E (63.22%). No prevalent mutations were observed in the non-structural proteins.

In order to determine whether the H285Y mutation immediately upstream of the insert in SLEV A was common, the other two replicates from the Vero growth kinetics were sequenced by standard Sanger sequencing of E. Neither of these two replicates had detectable sequence differences at this site; however, the use of standard sequencing substantially limits the sensitivity. They did, however, have the N222Y mutation in E.

All sixteen of the chimeras, and the WNV NY99 control, were serially passaged up to Passage 10 in Vero cells. Passaging occurred in triplicate until Passage 7, after which the replicates were combined to give a single passaging sample for the remaining three passages. Each virus was sequenced in the E coding region by Sanger sequencing to look for adaptive mutations around the chimeric insert. The WNV NY99 control had one mutation, an E390G. The JEV A-, B-, and C-forms gained no mutations, but JEV D had a mixed sequence at 390 as determined from the chromatogram, with a proportion of the samples having a D390A substitution. None of the KOUV Passage 10 samples showed any sequence changes.

Sequencing of SLEV A Passage 10 revealed only the consensus level N222Y mutation, and an H398Y mutation that had reached consensus prevalence. The N222Y was also present in SLEV B, C, and D as the only detectable sequence change. All four of the BAGV chimeras possessed the N222Y mutation, with BAGV B having an additional conservative L311I substitution.

To determine the source of the H398Y mutation in the SLEV A Passage 10 sample, RNA was purified from all three replicates at Passage 5 and sent for sequencing within the E protein region via standard consensus sequencing. The first replicate, which had been deep sequenced after Passage 1, still contained the H285Y mutation with a frequency around 50%, judging by the chromatograph. It additionally contained the H398Y mutation discussed above as a minor variant. The second replicate lacked the H285Y of the first, but possessed the H398Y mutation at a frequency greater than 50%, although the chromatograph indicates that the mutation was not uniform. The third replicate failed to show either mutation, but this apparent homogeneity of E may have been due to the low sensitivity of Sanger sequencing. SLEV A Passage 8, the first passage following the pooling of the replicates, revealed that the H398Y mutation was still present at about 50% frequency, but that the H285Y mutation, only present in the first replicate, was no longer detectable.

CHARACTERIZATION OF SLEV A PASSAGE 1

The acquisition of a plaquing phenotype during the Vero cell growth kinetics with SLEV A, and the demonstration of the consensus N222Y sequence change and the two prevalent substitutions (prM M144T, and E H285Y) by deep sequencing, led to further characterization of this virus to determine its growth kinetics and plaque morphology in Vero cells, as well as its temperature sensitivity compared to the Passage 0 version (Figure 3.9). The Passage 1 virus formed clear and distinct plaques, with titers determined by immunostaining matching those of the plaque counts, suggesting that the majority of the viruses were, at this stage, of the plaquing form (Figure 3.9A). The Vero cell growth kinetics of SLEV A P1 showed a peak titer of 3.7×10^6 pfu/ml on Day 3, similar to that of SLEV A P0 on Day 4 (Figure 3.9B). The temperature sensitivity assay

showed a drop in titer of P1 below the limit of detection when incubated at 41°C, at least a 4,500-fold reduction (Figure 3.9C & D).

ANTIGENICITY OF CHIMERIC VIRUSES

Western blots were performed using cell lysates prepared from flasks from Day 5 of the Vero cell growth kinetics (Figure 3.10). The A- and B-forms, being the most diverse, were run alongside samples from mock and WNV NY99-infected cells. The 4G2 monoclonal antibody, a pan-flavivirus-reactive antibody that primarily targets the fusion region of EII (Rajamanonmani et al., 2009, Crill and Chang, 2004), reacted strongly with all of the samples, except the mock. Since EII is conserved between the chimeras and should thus allow for similar binding, normalization of loading volumes for each lysate was carried out using this antibody. The WNV EIII-specific monoclonal antibody, 3A3, unsurprisingly reacted strongly with the NY99 control, but substantially less strongly with the KOUV chimeras (Figure 3.10A). No reactivity was observed with the JEV, SLEV or BAGV chimera samples. The JEV EIII-specific monoclonal antibody ab81193 reacted strongly with the JEV chimeras, and partly with the KOUV chimeras, but not at all with the NY99, SLEV, or BAGV samples. Due to a dearth of monoclonal antibodies known to be specifically reactive with SLEV and BAGV EIII, similar experiments could not be run using antibodies against these. Interestingly, despite a very similar sequence, the KOUV EIII chimera E proteins appeared to have a slight reduction in molecular weight compared to the wild-type and most other chimeric proteins that could not be explained solely by differences in amino acid composition of the EIII. A potential explanation would be a loss of glycosylation, but Endo H digestion of the B-form samples, followed by a comparison of band sizes for the digested and non-digested samples indicated that this was not the case (Figure 3.10E). Interestingly, however, the digestion revealed that KOUV B was only partially digested, with two bands visible on

the blot. The fact that the digests were performed for 6hrs, and the other samples were fully digested, suggests that there may be a proportion of Endo H-resistant protein glycosylations. Since the activity of Endo H is restricted to high mannose-containing glycoslyations, and is incapable of digesting complex glycans, it is possible that such alternative glycosylation may be occurring on a proportion of the KOUV B E proteins. Western blots run with an anti-WNV membrane protein antibody revealed strong bands with the KOUV chimeras and fainter bands with the BAGV chimeras, but no visible bands with the other viruses (Figure 3.10D). This suggests a significant presence of mature virions in the KOUV chimera samples, potentially due to an inefficient release or a "sticky" virion leading to increased non-specific adhesion to cell surfaces.

In addition to monoclonal antibodies, polyclonal mouse immune ascitic fluid (MIAF) raised against WNV NY99 and each of the EIII donor viruses was used to characterize cross-reactivity (Figure 3.10B). MIAF raised against the Lineage I WNV Eg101 (#T-35570) was broadly cross-reactive with the different chimeras, whereas the anti-Lineage II WNV MIAF T-35345 had a lot greater specificity for the WNV NY99 control and the KOUV chimeras. The anti-JEV Nakayama MIAF, T-54119, was quite broadly-reactive, similar to the Lineage I WNV MIAF, while the anti-SLEV Parton MIAF T-34910 showed high reactivity with the SLEV chimeras and very little reactivity with the WNV NY99 control or JEV chimera viruses. It did, however, show rather clear reactivity with the KOUV and BAGV samples. Anti-BAGV Dak B-209 MIAF showed strong reactivity with the BAGV chimeras, but minimal reactivity with any of the other samples.

Two human serum samples from natural WNV infections were used to determine the contribution of anti-EIII antibodies to the complement generated during infection (Figure 3.10C). Strong responses were seen against WNV NY99 and KOUV B E, but

responses were substantially lower for the other chimeras, indicating that the sera contain a significant proportion of WNV EIII-specific antibodies.

Neutralization of the viruses with the anti-WNV MIAFs, rabbit serum raised against WNV EIII (Beasley et al., 2004b), and human sera from WNV-infected patients (Beasley et al., 2004b) also demonstrated antigenic variability amongst the different chimeras (Table 3.8). Of the sera and MIAF tested, the rabbit polyclonal serum showed the most specific WNV response, with strong neutralization of WNV NY99 and KOUV B, but significantly lower neutralization of any of the other chimeras. The anti-WNV Lineage I MIAF neutralized the KOUV B and BAGV B chimeras to a similar degree to WNV NY99, but JEV B and SLEV B were less well neutralized, with a 4-fold lower 50% neutralization titer. These differences were also seen with the Lineage II MIAF, although KOUV B was actually neutralized better than WNV NY99. The BAGV B chimera was less readily neutralized with the Lineage II MIAF than the Lineage I MIAF. The rabbit polyclonal serum raised against recombinant WNV EIII showed the least cross-reactivity with the chimeras, although as with the Lineage II MIAF, the KOUV B chimera was actually more readily neutralized than WNV NY99. Consistent with previous reports that human EIII antibodies are inefficient at neutralizing WNV, human serum 022 showed considerable cross-neutralization activity. However, neutralization by human serum 026 was rather more variable, with 8-fold lower neutralization titers for JEV B compared to WNV NY99 and KOUV B, although neutralization of SLEV B and BAGV B were not significantly different.

DISCUSSION

The generation and recovery of EIII chimeric flaviviruses demonstrate that, to a certain extent, EIII substitutions from other flaviviruses are tolerated without significant

modification to the remainder of the WNV E protein sequence. When generating the chimeras, the approach of engineering restriction sites into the WNV IC plasmid was preferred, as it allowed for a "cassette" approach to chimerization, whereby donor sequences could be cut-and-pasted into the plasmid with relative ease, as opposed to some of the more time-consuming, sequence-independent cloning methods (e.g. Gibson cloning). The downside to such an approach is that it is not always possible to maintain the original amino acid sequence of the mature proteins. Indeed, whilst three of the four restriction sites added to the IC plasmid were silent with regards the sequence of the translated peptide chain, the addition of one of the four, the SalI site, resulted in a valine to leucine substitution at position 290 of the envelope glycoprotein. This substitution is conservative: the side chain difference between valine and leucine is an extra methanediyl group (-CH_2-), elongating the side chain by one carbon atom. As such, the chemical and structural effects on the protein should be minimal. An alternative restriction site that could have been used at this position would have been an XhoI site, which would generate the same sticky ends as SalI. However, this site, while maintaining the valine at 290, would have generated a cysteine to serine substitution at position 288, a significantly more disruptive substitution since the cysteine is involved in the formation of a disulphide bridge that stabilizes the protein.

To ensure that the V290L substitution resulting from the SalI site had minimal effect on the backbone virus, it was first determined whether the mutation occurs in any natural WNV isolates. A recently published sequence from a Turkish WNV isolate, strain T2 (accession no. KJ958922), was found to have the particular V290L mutation induced by the restriction site (Ergunay et al., 2015). While there were three additional amino acid differences in the envelope glycoprotein of T2 compared to NY99, none were in or around EIII, or in close proximity to residue 290, suggesting that additional adaptive changes to tolerate the V290L substitution were not necessary. The fact that the T2 virus

was isolated from a horse that developed neurological signs of infection suggested that the mutation does not significantly affect virus growth or mammalian virulence. Nevertheless, detailed comparisons were made between the backbone virus containing the four restriction sites, and the parental NY99 strain. An initial indicator of phenotypic similarity was the lack of difference in plaque morphology between the two viruses when titrated in Vero cells. The mean plaque size for NY99 was 3.6mm (SD 0.52mm), and for the 4-site virus it was 3.45mm (SD 0.37mm). Growth kinetics of the two viruses in Vero and C6/36 cells were almost identical, suggesting that the V290L mutation had no appreciable effect on virus replication in either mammalian or mosquito cells. Passaging the virus ten times in Vero cells resulted in no detectable sequence changes within the envelope glycoprotein, with the SalI site preserved. The fact that the V290L mutation could revert with a single nucleotide C→G substitution suggests that there is no strong selective pressure to do so, further supporting the conclusion that the V290L mutation has little bearing on virus behavior *in vitro*.

For most of the EIII donor viruses, four different chimeras were generated, using each combination of the upstream and downstream insertion sites. The reasoning behind this was to assess whether the insertion location, and the size of the insert, played a significant role in the recoverability and growth characteristics of the chimeric viruses. With regards to viability, there was essentially an all-or-nothing outcome with the chimeras: for the four donor viruses that were capable of generating viable chimeras (JEV, KOUV, SLEV, and BAGV), all four versions were recoverable, albeit with varying phenotypic characteristics. The features of the chimeras that permit or prevent viability are hard to elucidate. One common feature of the recoverable viruses is that the donor EIIIs are the same nucleotide and amino acid length as that of WNV, while many of the inviable constructs have smaller EIIIs: IGUV EIII is two amino acids shorter, YFV and DENV-2 EIIIs are three amino acids shorter, and DTV EIII is six amino acids shorter.

The virus for which this observation fails is ZIKV. Its EIII is the same length as WNV and the other viruses for which chimeras were recoverable, but none of the ZIKV constructs were viable. Comparison of the amino acid sequence of ZIKV EIII and those of the viable chimeras reveals few significant differences, such as proline substitutions or charge changes, that could account for the lack of viability, suggesting that the inviability of the ZIKV chimeras may be a cumulative effect of the amino acid differences between its and WNV's EIII (Figure 3.11). This hypothesis is further supported by the fact that no viable mutant viruses emerged after repeated passage in cells stably expressing WNV prM-E, which would theoretically have allowed for a sampling of non-synonymous mutations that would naturally occur in replicating WNV genomes. The inviability of particular chimeras may potentially result from folding issues with the chimeric E proteins. Vero cells that were transfected with the DENV-2 B-form chimera failed to be stained with the conformation-specific, EII-targeting 4G2 antibody, while staining with an anti-WNV MIAF allowed for transfected cells to be identified. Since the MIAF contains a large amount of anti-NS1 antibodies, and likely conformation-independent E antibodies, it fits that MIAF would stain transfected cells even if E was not folding properly. Konishi & Mason, and Lorenz *et al*. demonstrated that proper folding of E requires prM to behave as a molecular chaperone (Lorenz et al., 2002, Konishi and Mason, 1993). The exact interactions between prM and E during this process are unknown, but it is conceivable that particular residues in EIII are required, and that the substitution of a non-WNV EIII with sequence divergence over a certain threshold would result in an E protein containing particular substitutions that preclude efficient formation of prM-E heterodimers and proper folding of E. Further, structural differences between flavivirus EIIIs may lead to potential interdomain clashes both within the protein and between E homodimers affecting protein stability and the likelihood of viable virus production. The phenotypic differences between SLEV A and B show that even subtle sequence differences (six amino acids in total, four of which are semi-conservative), can

significantly affect the stability and viability of the constructs, likely in a location-dependent manner.

In general the chimeras, particularly the B-forms in which only EIII has been substituted, are structurally stable. This is evidenced by the temperature sensitivity data comparing titer and plaque morphology at 37°C and 41°C, which showed for the B-forms that there was no reduced viability for the JEV, KOUV or SLEV chimeras. While the BAGV B chimera maintained a similar titer at the higher temperature, the plaque size was significantly smaller, indicating less efficient spread through the monolayer at the higher temperature. This suggests that BAGV B may be less structurally stable than the other B-form chimeras, with this instability being indicated by the reduced plaque size. Below a particular threshold of stability, as is seen with BAGV A and SLEV A P1, the temperature sensitivity manifests itself as a reduced titer, which indicates that the additional EIII-flanking sequences had a significant destabilizing effect on the chimeric E protein. In contrast to the BAGV A and SLEV A P1 chimeras, the JEV and KOUV A-forms showed no loss of particle stability, indicating that the additional sequences had no such adverse effect. The fact that BAGV A showed no sequence changes in and around EIII by Passage 10 when passaged in Vero cells at 37°C suggests that the stability issues are either less problematic at 37°C, such that adaptations are unnecessary, or that stabilizing the protein is more complicated than simply substituting one or two amino acids.

The growth of the chimeric viruses in Vero cells indicated that EIII may play a minor role in growth kinetics, but that for structurally stable chimeras, such as most of the B-forms, the effect of EIII substitution is minimal. Indeed, the chimeras that showed structural stability in the temperature sensitivity assays, JEV A & B, KOUV A & B, SLEV B, and to a certain extent BAGV B, grew similarly to WNV NY99, with peak

titers in Vero cells within 5-fold for the most stable chimeras, and within 10-fold for BAGV B. This is in contrast to the A-forms for SLEV and BAGV, which grew least well in Vero cells, and showed the greatest temperature sensitivity. These results would suggest that the growth kinetics for the chimeras is impacted more by the stability of the virion than the identity of EIII. This would fit with the proposed role of EIII as the flavivirus receptor-binding domain. Since the donor EIIIs came from viruses that are capable of growing in Vero cells, it implies that the donor EIIIs are still capable of binding to receptors on the cell surface, albeit potentially different ones to WNV NY99. If that is the main role of EIII in virus growth, and replication within the cell is a non-structural protein-driven process, one might expect that as long as particle stability remains similar to that of WNV NY99, the growth kinetics of the chimeric viruses should proceed similarly to the parental NY99 virus. That is not to say that in other cell types, where the complement of receptors on the cell surface may be different, there would not be clear differences in growth for the chimeric viruses.

There were, however, a few curiosities with the growth of some of the chimeras in Vero cells. Although growing very similarly to WNV NY99 for the first two days of the experiment, the titers of the KOUV chimeras appeared to drop more readily than the parental virus after the peak titer had been reached. The temperature sensitivity assays would suggest that this is not a particle stability issue. A potential explanation comes courtesy of the western blot run with the anti-WNV M polyclonal antibody. Mature M protein, with an apparent molecular weight between 8 and 10kDa, is found within mature virions following prM cleavage during viral maturation. Early studies with JEV demonstrated that minimal mature M is present within infected cells, an observation confirmed by the lack of a distinct M-band in the WNV NY99 cell lysate sample (Shapiro et al., 1972a, Shapiro et al., 1973a). Indeed, only the KOUV chimera lysates, and to a much lesser extent the BAGV chimera lysates, showed clear mature M bands.

The presence of this band would suggest that either final release of the mature virions, following furin-mediated cleavage of prM, is impaired, or that the virions have an increased adhesiveness resulting in non-specific interactions between the particles and the cell surface. If the former explanation were true, one would expect lower titers in the Vero cell growth kinetics due to reduced virus release into the supernatant. This was shown not to be the case, as the titers on Days 1 and 2 are similar to those for WNV NY99. The second explanation seems more feasible, and would go some way to explain the decline in titers observed for the KOUV chimeras on Days 3 to 5 compared to WNV NY99: if the virions are being pulled out of suspension, but are not being replaced because the cells are already exhausted, the titers will drop more readily than for viruses that are less "adhesive". The nature of glycosylation of proteins can affect their interaction with cell surfaces and extracellular matrix (Gu and Taniguchi, 2008). The Endo H digestion of the cell lysates suggest that the KOUV chimeras may have a mixed-identity glycosylation of the E protein, with a proportion of the proteins glycosylated with an Endo H-sensitive glycan, similar to WNV NY99 and the other chimeras, and a proportion glycosylated with Endo H-resistant glycans. This could account for their potentially increased adhesiveness, and thus the drop in titers at the later timepoints in the growth kinetics.

The different SLEV chimera versions showed the most variability of any of the viable construct groups. Significant differences were observed between the B-form, which contained the smallest insert and grew most similarly to WNV NY99, and the A-form, which contained the largest insert and failed to grow effectively until Day 2 of the growth kinetics. The C- and D-forms had intermediary growth kinetics, suggesting that the poor growth of the A-version may be a summative effect of both additional sequences. Within the additional upstream sequence, present in the C-form, there were only two amino acid differences, an M292L and an L295V. Both of these amino acid

differences are reasonably conservative, but appear to be sufficient to reduce the peak titer of the virus by approximately 10-fold. Although temperature sensitivity assays were not run for this or the D-form chimera, it is likely that these mutations affect the stability of the chimeric E protein by reducing the efficiency of the interaction of this SLEV region with the rest of WNV NY99 EI. Alternatively, the mutations in this region may be affecting the orientation of EIII. Studies by de Winspelaere & Yang demonstrated that mutations in the EI-EIII linker region can significantly impair virus particle assembly (de Wispelaere and Yang, 2012). Similarly, differences in the downstream SLEV stem-helix sequence present in the D-form may be reducing protein and virion stability leading to the decreased peak titer of this chimera compared to WNV NY99 and SLEV B. Compared to WNV NY99, there are four amino acid changes: an F408L, a T409A, a V412W, and an A420V. Some of these differences result in the addition or removal of bulky residues (i.e. F408L and V412W), or loss of polar residues (T409A), which may substantially affect the interaction between the first stem-helix and the second, as well as interactions between other regions of E. The A-form, which contained both of these additional sequences, was significantly attenuated. Sequencing of the Passage 1 SLEV A, which gained the ability to plaque, showed a consensus level mutation N222Y, which was prevalent across all of the SLEV and BAGV chimeras, as well as an H285Y substitution in a majority of the reads. This would suggest that one or the other of these mutations may be adaptive, potentially increasing the stability of the protein, although temperature sensitivity assays with this passaged virus showed that particle stability was still significantly impaired. The N222Y mutation is distant from any of the sequences changed by chimerization, but its location on the lower face of E suggests that it may play a role in compensating for some of the amino acid differences present downstream from EIII. By Passage 10, the H285Y mutation had been supplanted by an H398Y substitution, but the N222Y consensus mutation remained. Interestingly, the de Winspelaere & Yang paper that looked at disruptive mutations in the EI-EIII linker

region of DENV-2 showed that an introduced Y299F mutation could be compensated for by an additional Q400H mutation in the first stem-helix region of the protein (de Wispelaere and Yang, 2012). It is possible that the H398Y mutation performs a similar role with SLEV A.

Generally, the BAGV chimeras showed less variability in their growth kinetics than the SLEV chimeras but, as the temperature sensitivity data suggests, were generally less structurally stable than the other chimeras. Similar to SLEV A, the BAGV A chimera was restricted in Vero cells, but the BAGV C- and D-forms grew similar to BAGV B suggesting that the restriction of BAGV A was a cumulative effect of both additional sequences that appear to have minimal effects on their own. Similar to the KOUV chimeras, the titers of BAGV chimeras appeared to drop more readily than those for WNV NY99 at the later timepoints. The BAGV chimeras had faint mature M bands in the western blot, suggesting that they may have increased adhesiveness, but to a lesser extent than KOUV. This drop may therefore be explained by the combination of increased adhesion and reduced particle stability.

Compared to growth in Vero cells, the growth kinetics in C6/36 mosquito cells appeared to be less dependent on the size of the insert, and more dependent on the nature of EIII. For the JEV, KOUV, and BAGV chimeras, the growth of the A- and B-forms were very similar to one another, but the growth compared to WNV NY99 was increasingly restricted the more divergent the EIII sequence was. These observations fit with those seen previously for prM-E chimeras: SLEV with WNV prM-E grew almost identically to wild-type SLEV in C6/36 cells, suggesting that prM-E may play a less significant role in infection of arthropod cells than mammalian cells (Maharaj et al., 2012). Once again, the SLEV chimeras showed the most variability, with SLEV B growing like WNV NY99, while SLEV A barely grew at all: the titers of SLEV A had

barely reached 50pfu/ml by Day 5, so low that RT-PCR reactions on RNA purified from the supernatant failed to yield detectable levels of DNA. Interestingly, a correlation appears to exist between the Vero and C6/36 cell growth: the lower the peak titer in Vero cells, the lower the titer towards the end of the C6/36 growth kinetics.

Comparison of *in vitro* metrics, including peak Vero cell titers, plaque morphology, and percent EIII amino acid identity compared to WNV NY99, helps to reveal some trends in the data (Figure 3.12). Linear regression comparing mean plaque size and log-transformed peak titers in Vero cells showed a strong and significant positive correlation (Figure 3.12A; $p<0.000$, $R^2=0.8047$), suggesting that the smaller plaque size of some of the chimeras may be directly due to their reduced growth. Interestingly, a significant correlation also existed between plaque size and percent EIII amino acid identity (Figure 3.12B; $p<0.0154$, $R^2=0.3150$), although there are a number of outliers, such as SLEV B and BAGV A. When peak titer and percent EIII amino acid identity are compared, however, no statistical significance is observed, implying that the number of amino acid differences is less important than their identity with regards to virus growth (Figure 3.12C). This observation is accentuated by the previously-described differences between the SLEV A and B chimeras.

Serial passaging of wild-type WNV NY99 and the chimeras demonstrated that most were genetically stable in and around the insert regions. Two of the viruses gained mutations at position 390 in E (WNV NY99 E390G and JEV D D390A). This residue is the last in the RGD/E integrin-binding motif present in JEV complex viruses. The loss of the negative charge at this position has been implicated in increased binding to glycosaminoglycans for WNV and MVEV, and is deemed to be a tissue culture adaptation of the virus (Lee et al., 2004, Lee and Lobigs, 2000). The mutation appeared to be more prevalent in the WNV NY99 sequence, where it had reached consensus-level,

than in JEV D, which showed a mixed sequence on the chromatogram. The KOUV chimeras showed no sequence changes, while the SLEV and BAGV chimeras all had the N222Y mutation at a consensus level. The only additional mutations observed were the H398Y mutation in SLEV A discussed previously, and a conservative L311I mutation in BAGV B. Taken together it would imply that, with the possible exception of SLEV A, there was either little selective pressure on the viruses to adapt, or appropriate combinations of advantageous adaptations were not possible within ten passages of recovery.

The donor EIIIs appear to have maintained their antigenicity. 4G2, a monoclonal antibody that binds to flavivirus EII, reacted similarly with each chimeric E protein and was used to normalize the input volumes for each sample. The WNV EIII-specific monoclonal antibody reacts strongly with WNV NY99, but less efficiently against the KOUV chimeras, and not at all with the other chimeras. Similarly, the anti-JEV EIII monoclonal antibody reacts strongly with the JEV chimeras, but only very weakly with any of the others.

The MIAFs showed greatest cross-reactivity the closer the inoculating virus was to WNV NY99. This is not unexpected, as it is likely that such samples would have a large quantity of antibodies that recognize the other two domains of E. The more genetically distinct the donor flavivirus from WNV NY99, the more specific to that chimera the reactivity. This is taken to the extreme by the BAGV MIAF, which showed reactivity solely with the BAGV chimeras. Curiously, the KOUV chimeras showed quite substantial cross-reactivity, with the second strongest reactivity of all of the viruses with the SLEV MIAF. This may suggest that the KOUV EIII has quite broad antigenic properties, with potentially degenerate epitopes.

Cross-neutralization with the two anti-WNV MIAFs showed subtly different profiles than those of the reactivity in western blots, particularly with the BAGV chimera. In the western blots, the reactions with the BAGV chimera samples were some of the lowest, with similar band intensity to the JEV and SLEV chimeras. By contrast, in the neutralization assays, BAGV B is neutralized almost as well as WNV NY99 and KOUV B, whereas JEV B and SLEV B have at least 4-fold lower 50% neutralization titers. One potential explanation for this would be that the binding of the BAGV chimera to Vero cell receptors is less EIII-dependent than either the JEV or SLEV chimeras, thereby improving the relative efficacy of neutralization by the anti-WNV MIAFs despite loss of anti-EIII neutralizing activity. If binding mediated by another part of E, which would be WNV sequence in the chimeras, was more important for the BAGV chimera, it could explain the discrepancy between the western blot and neutralization data.

Differences between the western blot reactivity and virus neutralization also extend to the human serum samples. The western blots suggest that both human serum samples have strong anti-EIII reactivity, based on the lower band intensity for the non-KOUV chimeras. By contrast, human serum 022 neutralizes most of the viruses almost identically. This would suggest that for this sample, although a strong anti-WNV EIII antibody response was mounted, these antibodies have very poor neutralizing ability. Human serum 026, which was potently neutralizing against WNV NY99 and KOUV B showed much lower neutralizing ability against JEV B, suggesting that the neutralizing efficiency of human anti-EIII antibodies may be very variable. Previous studies have demonstrated that depletion of EIII-reactive antibodies in DENV human immune sera had little effect on neutralization of the virus, similar to the observations with human serum 022, but sample 026 would suggest that this is not the case for all human patients (Wahala et al., 2009, Dowd and Pierson, 2011). The strong neutralization of the SLEV B chimera with human serum 026 suggests that some antigenic regions common to WNV

NY99 and SLEV Parton EIII, but different in JEV Nakayama, may be important in neutralization with this serum. However, the only obvious residue difference that may account for this is 330, which is a threonine in WNV NY99 and SLEV EIII, but a serine in JEV EIII. Previous studies have demonstrated that this residue is important for monoclonal antibody recognition, but the particular T330S substitution has not been characterized (Zhang et al., 2010).

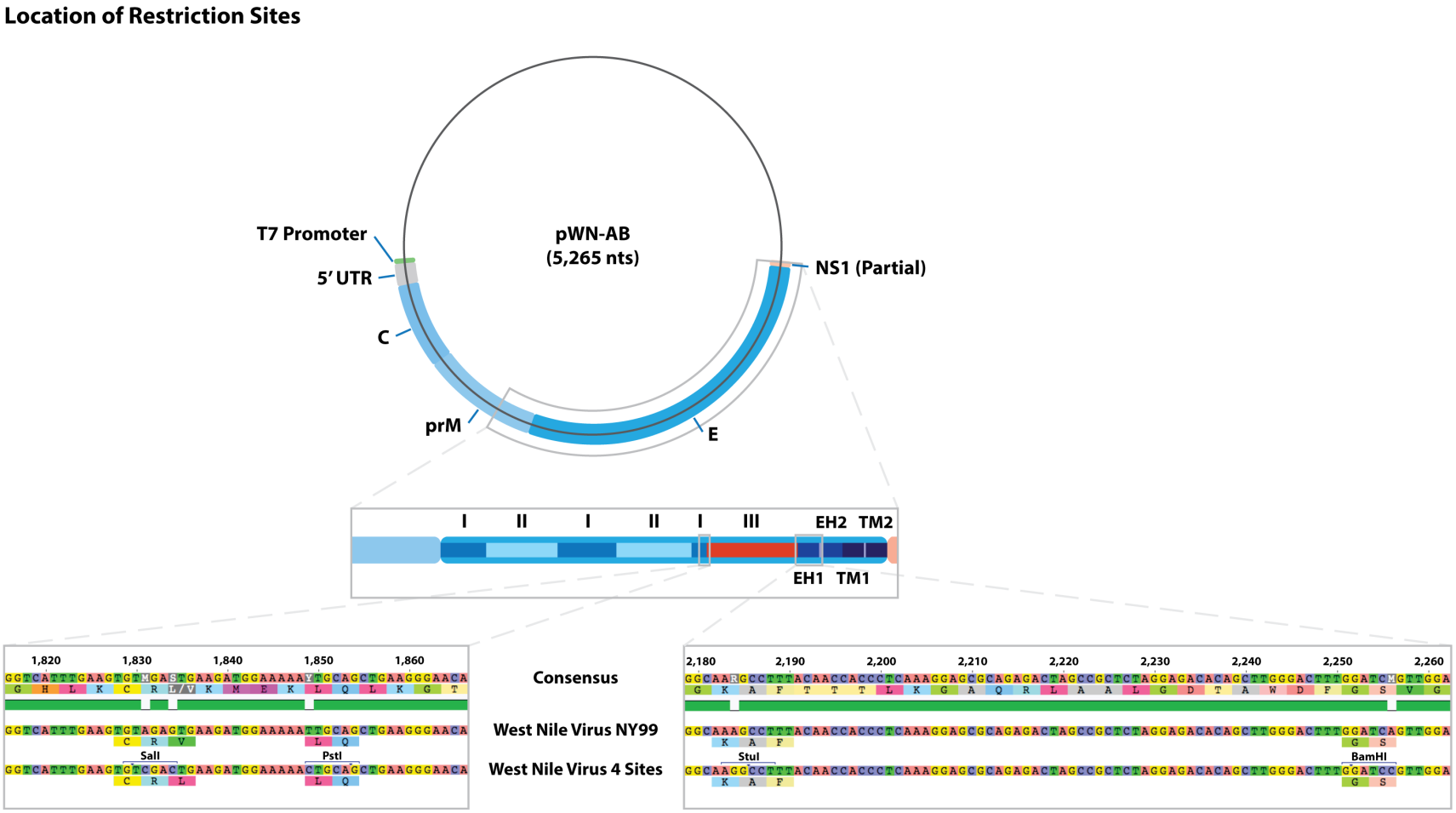

Figure 3.1: Location of Restriction Sites Engineered into pWN-AB. Restriction sites were engineered into the pWN-AB infectious clone plasmid by site-directed mutagenesis. Three of the four restriction sites resulted in no change to the amino acid sequence of the virus, however the SalI site led to a V290L substitution.

A) Plaque Morphology (72hrs Post Infection)

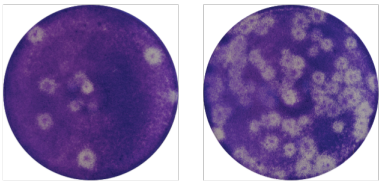

West Nile Virus NY99

Mean Plaque Size	Standard Deviation
3.60mm	0.52mm

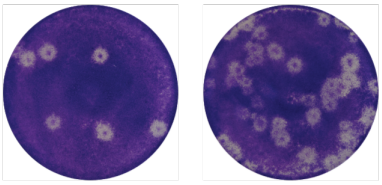

West Nile Virus 4 Sites

Mean Plaque Size	Standard Deviation
3.45mm	0.37mm

B) Vero Growth Kinetics

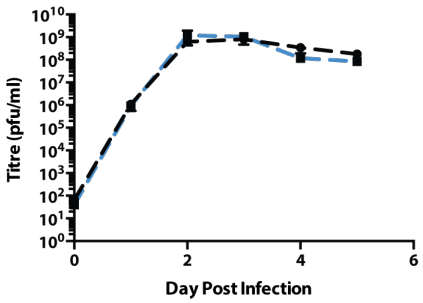

C) C6/36 Growth Kinetics

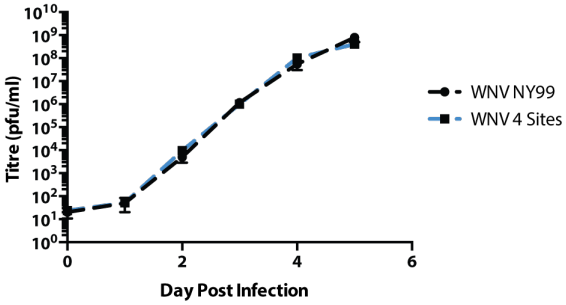

Figure 3.2: Comparison of Plaque Morphology and *in vitro* Growth Kinetics of WNV NY99 and the Four Restriction Site-Containing Backbone Virus. *A*: Both viruses were titrated and incubated at 37°C for 72hrs prior to formalin fixation and staining with crystal violet. Panels show 10-fold dilutions. Ten representative plaques were measured to give an average plaque size and standard deviation. Growth kinetics in Vero (*B*) and C6/36 (*C*) cells were performed in triplicate for both viruses. No significant differences were observed.

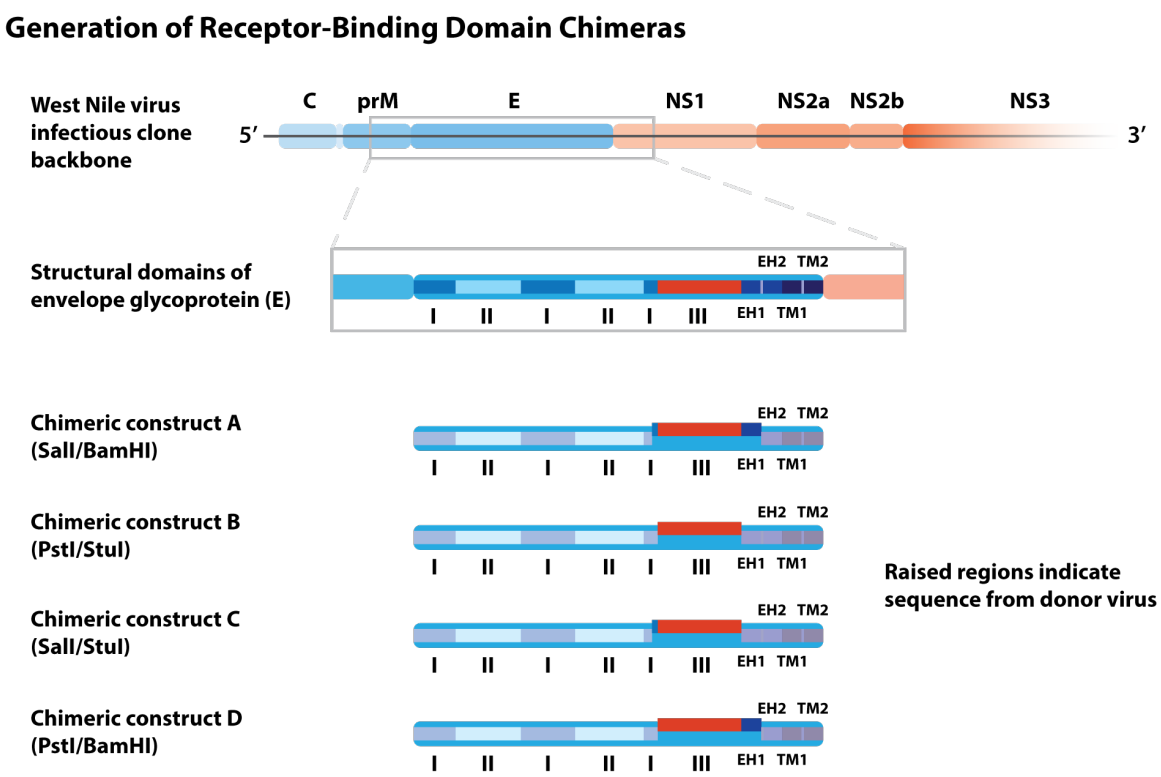

Figure 3.3: Insert Size and Composition Comparison for the Four Chimera Versions. The A-form had the largest insert including both a portion of EI upstream of EIII, and the first stem-helix region downstream of EIII. The B-form had the smallest insert, consisting solely of EIII. The C-form contained the additional upstream sequence in addition to EIII, while the D-form contained the downstream stem-helix region.

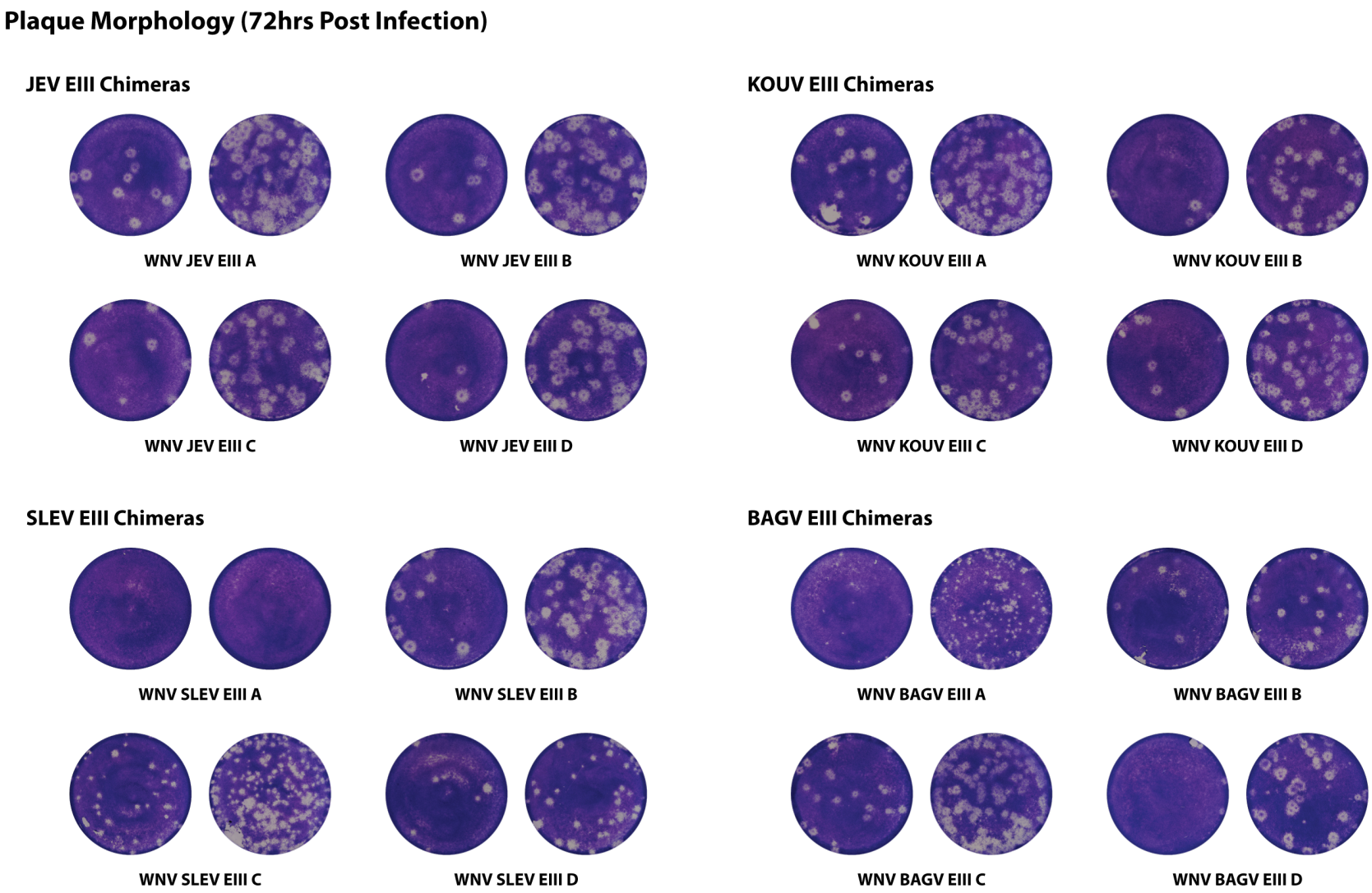

Figure 3.4: Plaque Morphologies of the Chimeric Viruses. Chimeric viruses were titrated and incubated at 37°C for 72hrs prior to formalin fixation and crystal violet staining. Panels show 10-fold dilutions.

A) Temperature Sensitivity

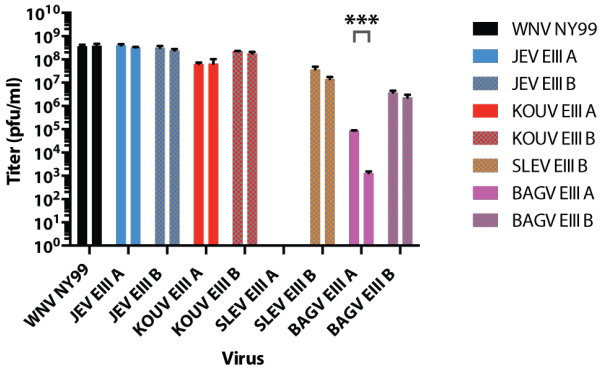

B) Log Fold Change and Statistical Analysis

Virus	37˚C Titer	41˚C Titer	Log_{10} Diff.	P-Value
WNV NY99	$3.73x10^8$	$3.85x10^8$	-0.013	0.418
WNV IC JEV EIII A	$4.00x10^8$	$3.27x10^8$	0.088	0.102
WNV IC JEV EIII B	$3.21x10^8$	$2.45x10^8$	0.118	0.146
WNC IC KOUV EIII A	$6.40x10^7$	$6.62x10^7$	-0.014	0.474
WNC IC KOUV EIII B	$2.27x10^8$	$1.78x10^8$	0.104	0.109
WNC IC SLEV EIII A (P0)	<LOD	<LOD	N/A	N/A
WNC IC SLEV EIII B	$3.70x10^7$	$1.45x10^7$	0.406	0.135
WNC IC BAGV EIII A	$8.67x10^4$	$1.32x10^3$	1.818	0.001
WNC IC BAGV EIII B	$3.80x10^6$	$2.30x10^6$ #	0.218	0.081

Average plaque size significantly smaller (<0.5mm) at 41˚C compared to 37˚C (1.95mm)

Figure 3.5: Comparison of Virus Titer at 37°C and 41°C. *A*: The A- and B-forms of the chimeras were titrated in triplicate at 37°C and 41°C to determine temperature sensitivity. Columns represent mean of triplicate values with standard error (*** $p<0.001$) *B*: Mean titers for each virus were compared at the two temperatures, with a log_{10} change determine for each. Statistical significance was determined by two-way Student's t-test.

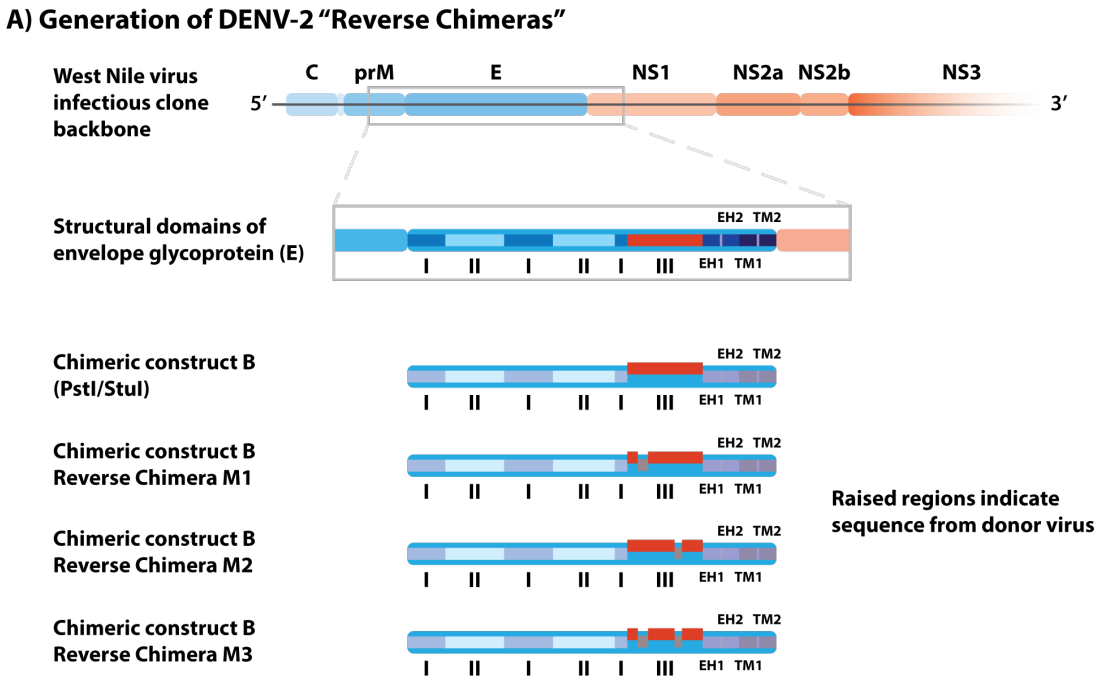

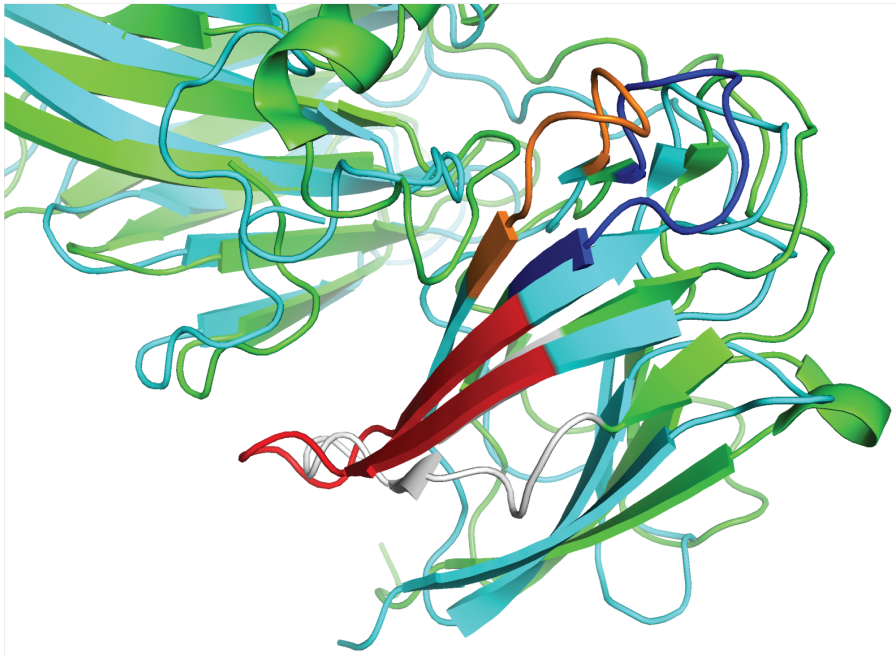

Figure 3.6: Generation of DENV-2 EIII "Reverse Chimeras". *A*: Location of sequences reverted to WNV in the chimeras. *B*: In the M1 and M3 chimeras, DENV-2 chimera residues 312-326 (red) were returned to a WNV sequence (grey). In the M2 and M3 chimeras, DENV-2 chimera residues 362-372 (orange) were substituted for those of WNV (blue; figure is based on PDB 2I69).

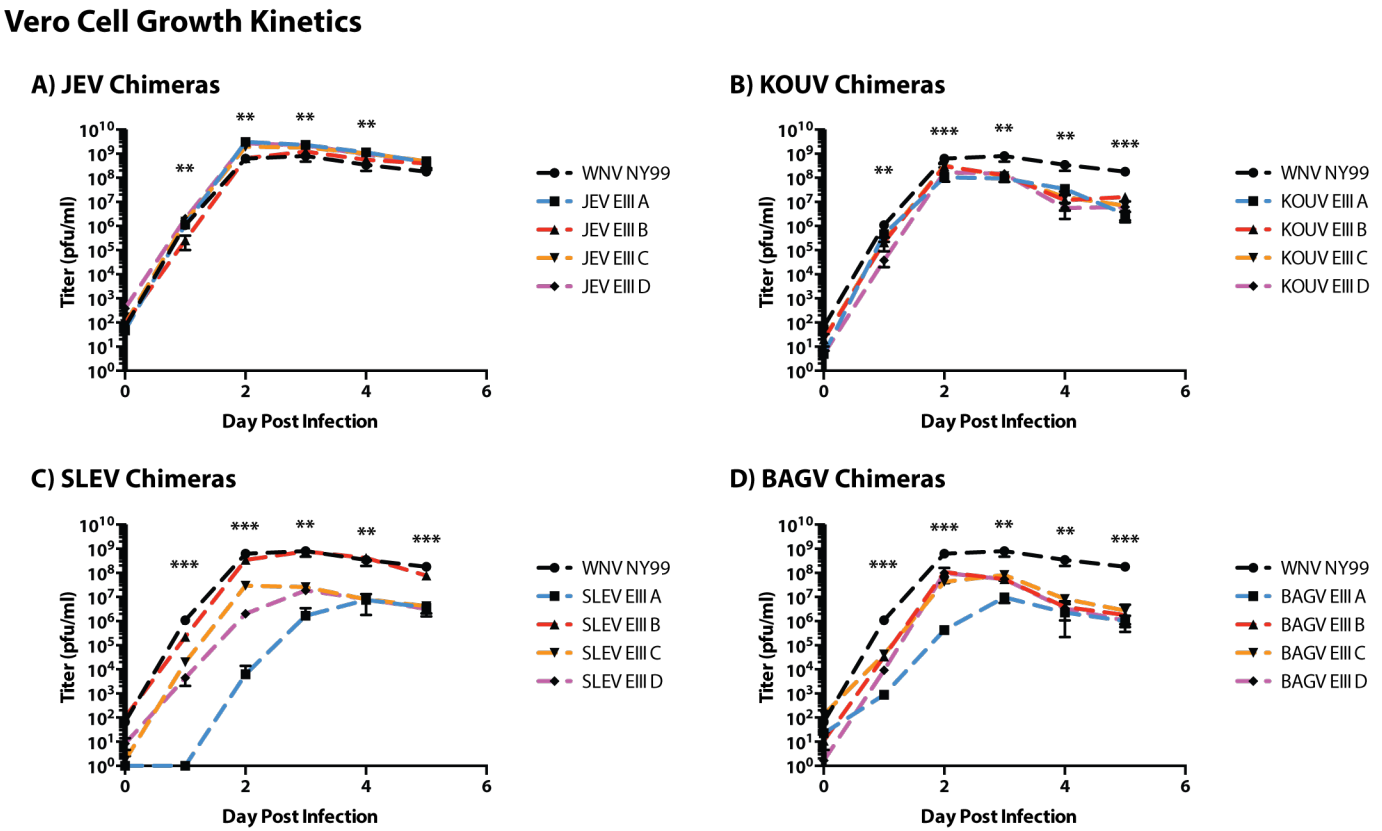

Figure 3.7: Growth Kinetics of Chimeric Viruses in Vero Cells. *A*: Growth kinetics were determined for all four JEV EIII chimeras. *B*: Growth kinetics were determined for all four KOUV EIII chimeras. *C*: Growth kinetics were determined for all four SLEV EIII chimeras. SLEV A gained a plaquing phenotype by Day 2. *D*: Growth kinetics were determined for all four BAGV EIII chimeras. All growth kinetics were performed in triplicate. Statistical significance was determined by ANOVA for all viruses (* $p<0.05$; ** $p<0.01$; *** $p<0.001$). Graphs show mean values with standard error.

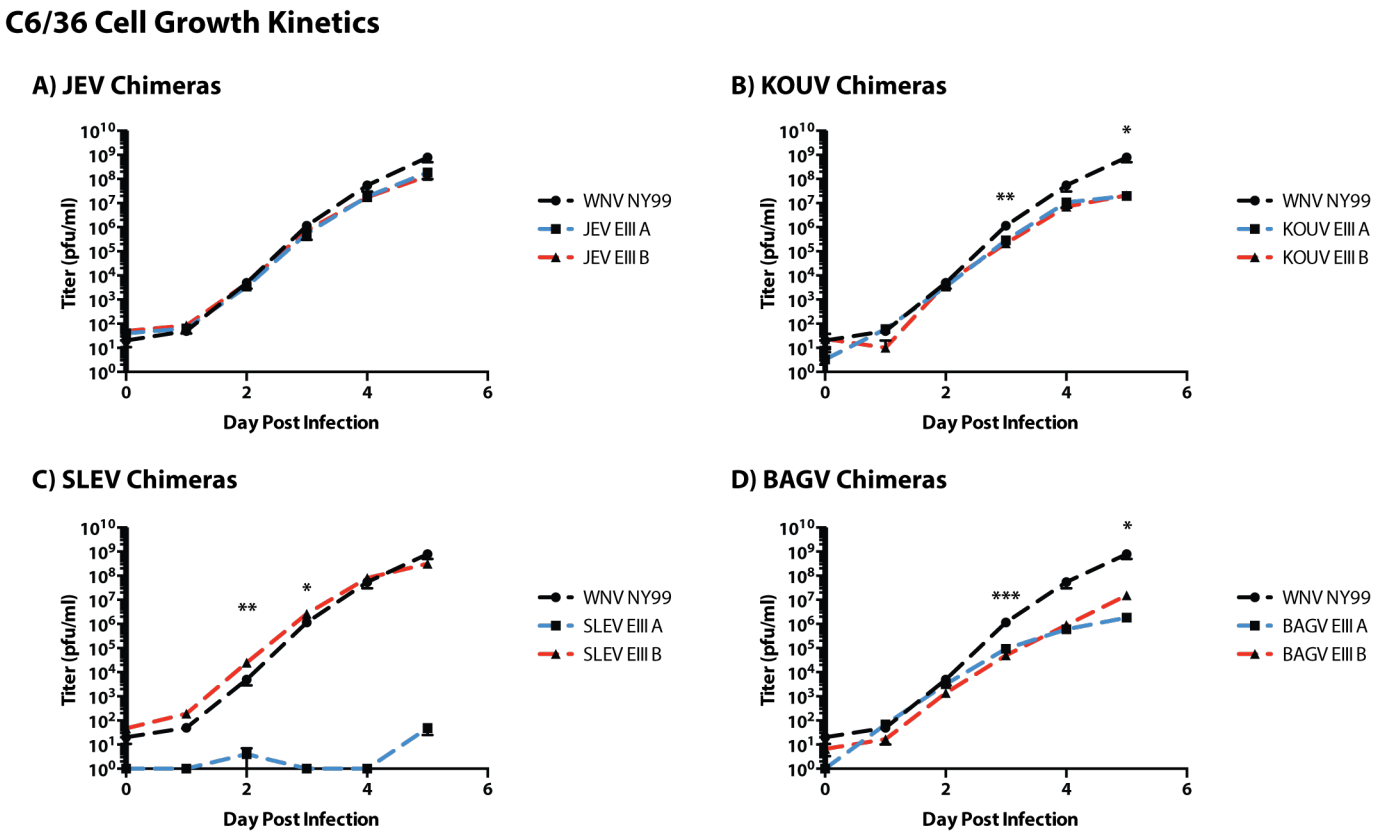

Figure 3.8: Growth Kinetics of Chimeric Viruses in C6/36 Cells. *A*: Growth kinetics were determined in triplicate for JEV EIII A & B chimeras. *B*: Growth kinetics were determined in triplicate for KOUV EIII A & B chimeras. *C*: Growth kinetics were determined in triplicate for SLEV EIII A & B chimeras. SLEV A failed to grow, with a titer of only 50pfu/ml on Day 5. *D*: Growth kinetics were determined in triplicate for all four BAGV EIII chimeras. All growth kinetics were performed in triplicate. Statistical significance was determined by ANOVA for all viruses (* $p<0.05$; ** $p<0.01$; *** $p<0.001$). Graphs show mean values with standard error.

A) Plaque Morphology (72hrs Post Infection)

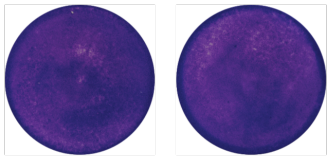

SLEV EIII A (P0)

Mean Plaque Size	Standard Deviation
0.00mm	0.00mm

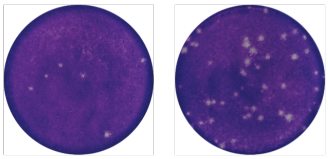

SLEV EIII A (P1)

Mean Plaque Size	Standard Deviation
1.05mm	0.28mm

B) Vero Growth Kinetics

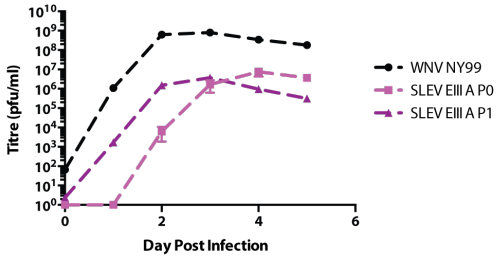

C) Temperature Sensitivity

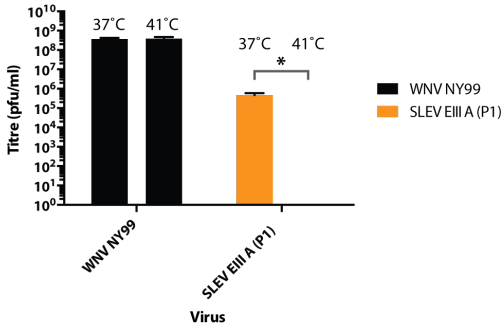

D) Temperature Sensitivity - Log Fold Change and Statistical Analysis

Virus	37˚C Titre	41˚C Titre	Log_{10} Diff.	P-Value
WNV NY99	$3.73x10^8$	$3.85x10^8$	-0.013	0.418
WNV IC SLEV EIII A (P1)	$4.67x10^5$	$<1.00x10^2$	>3.669	0.030

E) Location of Additional Mutations in SLEV A P1

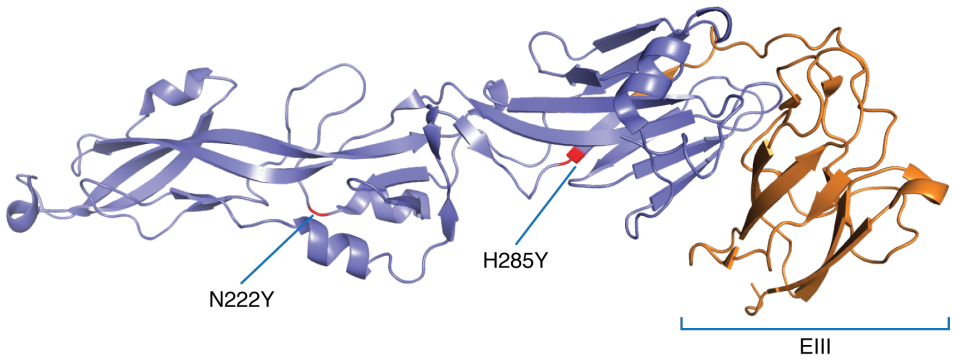

Figure 3.9: Characterization of SLEV A Passage 1. *A*: Plaque morphology of recovered and passaged SLEV A showing gain of plaquing ability. *B*: Growth of SLEV A P1 in Vero cells compared to WNV NY99 and SLEV A P0. *C*: Plaque counts following incubation at 37°C and 41°C. Columns show mean of triplicate values with standard error. (* $p<0.05$) *D*: Comparison of titers at 37°C and 41°C with log_{10} fold-change and statistical analysis. *E*. Location of additional mutations in E (Figure is based on PDB 2I69).

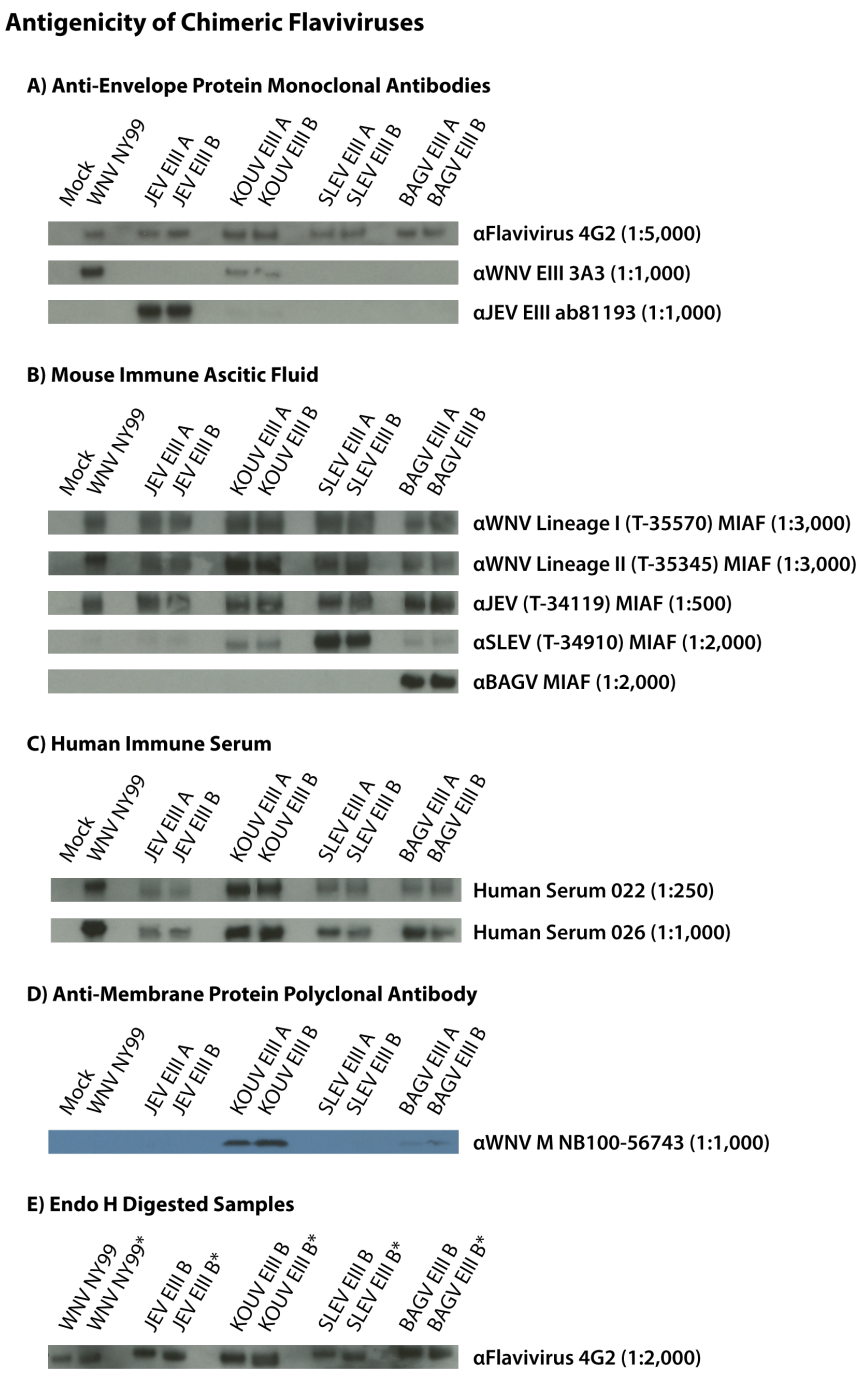

Figure 3.10: Antigenicity of Chimeric Viruses. *A*: Reactivity of chimeric E proteins with monoclonal antibodies against flavivirus EII (4G2), WNV EIII (3A3), and JEV EIII (ab81193). *B*: Reactivity of chimeric E proteins with various MIAFs. *C*: Reactivity of chimeric E proteins with human sera samples. *D*: Reactivity of whole cell lysates with anti-WNV M polyclonal antibody (NB100-56743). *E*: Endo H digestion of chimera B-forms. Asterisk indicates digested sample. Concentrations of each antibody provided in brackets.

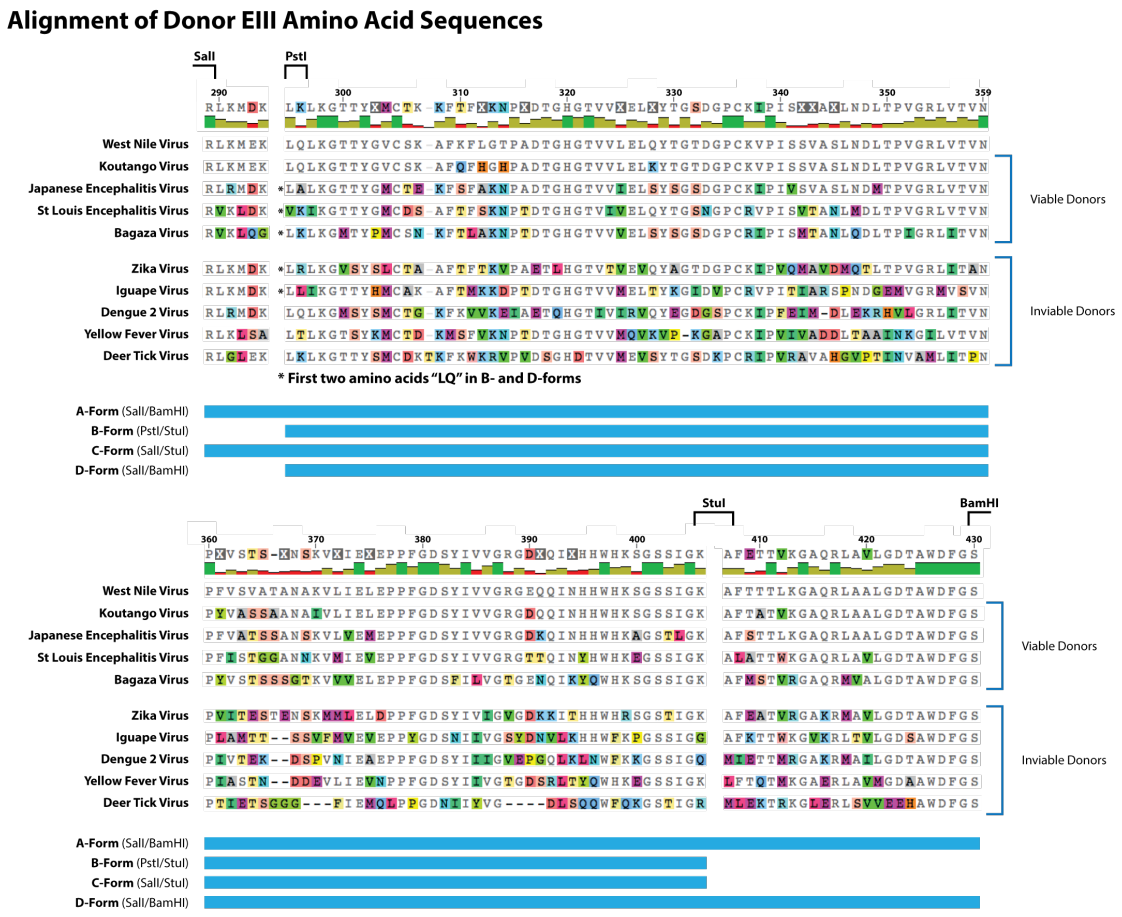

Figure 3.11: Alignment of Donor EIII Amino Acid Sequences. The EIIIs for the donor viruses are listed in increasing divergence from WNV NY99, with the viable and inviable sequences grouped accordingly.

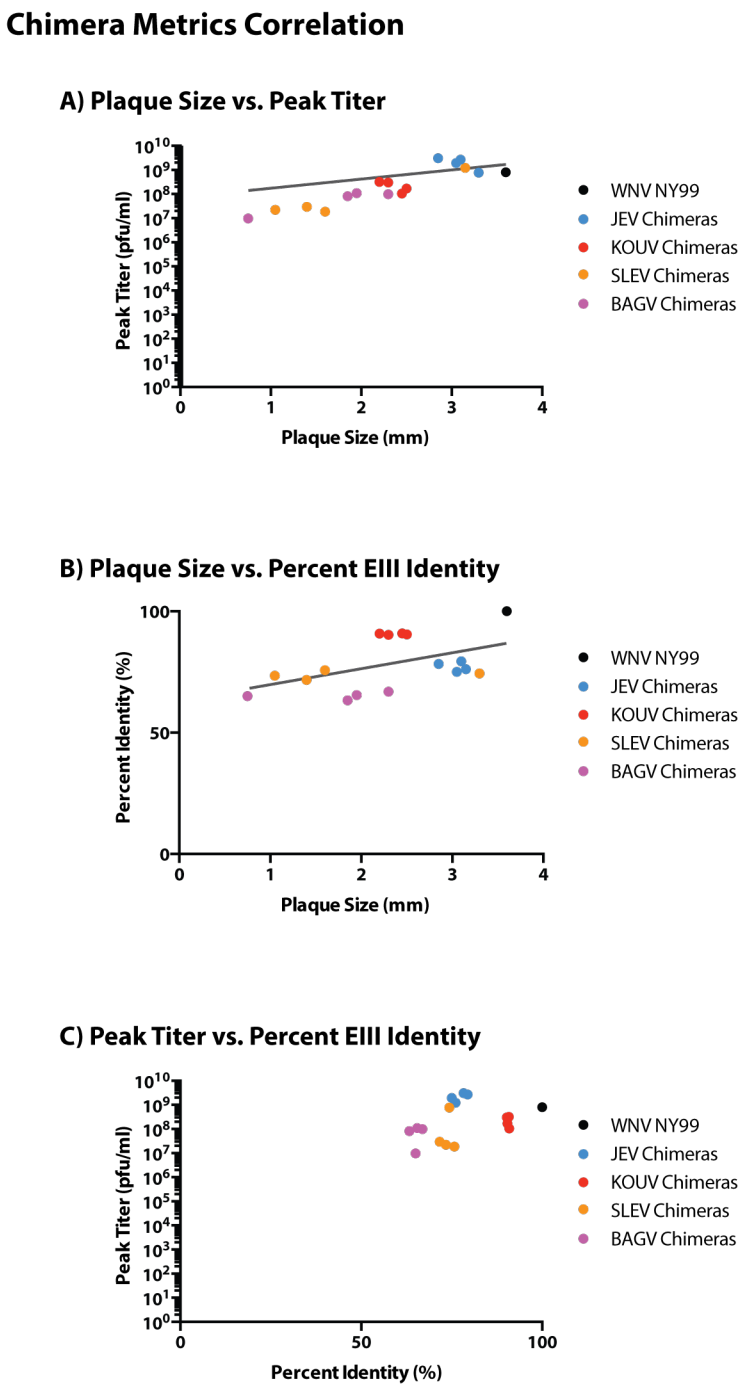

Figure 3.12: Correlation Between Chimera Metrics. *A*: Strong and significant correlation between peak titer in Vero cells and plaque size ($p<0.001$; $R^2=0.8047$). *B*: Significant correlation between plaque size and percent identity of substituted EIII compared to WNV NY99 ($p<0.0154$; $R^2=0.3150$). Clustering of data points show minimal effect of additional sequence for JEV and KOUV EIII chimeras. *C*: No significant correlation between peak titer in Vero cells and percent identity within EIII ($p<0.6870$; $R^2=0.0111$).

Mutations in Chimera Plasmids Compared to Published Sequences

		A-Form (SalI/BamHI)		**B-Form** (PstI/StuI)		**C-Form** (SalI/StuI)		**D-Form** (PstI/BamHI)	
Donor Virus	**Accession Number**	Mutation	Amino Acid	Mutation	Amino Acid	Mutation	Amino Acid	Mutation	Amino Acid
Koutango Virus (KOUV)	EU082200	None		None		None		None	
Japanese Encephalitis Virus (JEV)	EF571853	**T2049C**	***(Silent)***	**T2049C**	***(Silent)***	**T2049C**	***(Silent)***	**T2049C**	***(Silent)***
		C2222T	**A419V**					**C2222T**	**A419V**
St Louis Encephalitis Virus (SLEV)	EF158070	None		**A1936G**	**I324V**	None		None	
Bagaza Virus (BAGV)	NC_012534	None		None		None		None	
Zika Virus (ZIKV)	NC_012532	None		None		None		None	
Iguape Virus (IGUV)	AY632538	**T1916C**	**I332T**	**T1916C**	**I332T**	**T1916C**	**I332T**	**T1916C**	**I332T**
		C2007T	***(Silent)***	**C2007T**	***(Silent)***	**C2007T**	***(Silent)***	**C2007T**	***(Silent)***
		A2107T	**N381Y**	**A2107T**	**N381Y**	**A2107T**	**N381Y**	**A2107T**	**N381Y**
		A2126C	**Y387S**	**A2126C**	**Y387S**	**A2126C**	**Y387S**	**A2126C**	**Y387S**
		G2134A	**V390K**	**G2134A**	**V390K**	**G2134A**	**V390K**	**G2134A**	**V390K**
		T2135A	**V390K**	**T2135A**	**V390K**	**T2135A**	**V390K**	**T2135A**	**V390K**
		C2190A	***(Silent)***					**C2190A**	***(Silent)***
Dengue 2 Virus (DENV-2)	KM204118	**A2179T**	**I405F**			**A2118G**	***(Silent)***	**A2179T**	**I405L**
								T2181A	**I405L**
Yellow Fever Virus (YFV)	AY640589	**A1949G**	**K328R**						
		A1973G	**K336R**						
Deer Tick Virus (DTV)	AF357218	**A2213G**	**E416G**						

Table 3.1: Mutations in the Chimeric Plasmids Compared to Published Sequences. Chimeric plasmids were sequenced with output sequences aligned to those previously published for the donor viruses (accession numbers in Table 2.1).

Chimeras Generated and Recovered

Donor Virus	**A-Form** (SalI/BamHI)		**B-Form** (PstI/StuI)		**C-Form** (SalI/StuI)		**D-Form** (PstI/BamHI)	
	Generated	Recoverable	Generated	Recoverable	Generated	Recoverable	Generated	Recoverable
Koutango Virus (KOUV)	■	■	■	■	■	■	■	■
Japanese Encephalitis Virus (JEV)	■	■	■	■	■	■	■	■
St Louis Encephalitis Virus (SLEV)	■	■	■	■	■	■	■	■
Bagaza Virus (BAGV)	■	■	■	■	■	■	■	■
Iguape Virus (IGUV)	■	■	■	■	■	■	■	■
Zika Virus (ZIKV)	■	■	■	■	■	■	■	■
Dengue 2 Virus (DENV-2)	■	■	■	■	■	■	■	■
Yellow Fever Virus (YFV)	■	■	■	■	■	■	■	■
Deer Tick Virus (DTV)	■	■	■	■	■	■	■	■

Table 3.2: Chimeric Plasmids Generated and Viruses Recovered. Chimeric plasmids were generated incorporating EIII sequences from KOUV, JEV, SLEV, BAGV, IGUV, ZIKV, DENV-2, YFV, and DTV. Of these, only the chimeras containing EIIIs from KOUV, JEV, SLEV, and BAGV were recoverable.

A) Plaque Sizes and Standard Deviations

Virus	**A-Form** (SalI/BamHI)		**B-Form** (PstI/StuI)		**C-Form** (SalI/StuI)		**D-Form** (PstI/BamHI)	
	Plaque Size	Std Dev	Plaque Size	Std Dev	Plaque Size	Std Dev	Plaque Size	Std Dev
Koutango Virus (KOUV)	2.45mm	0.72mm	2.30mm	0.42mm	2.20mm	0.42mm	2.5mm	0.41mm
Japanese Encephalitis Virus (JEV)	2.85mm	0.34mm	3.15mm	0.47mm	3.05mm	0.50mm	3.10mm	0.57mm
St Louis Encephalitis Virus (SLEV)	No Plaques		3.30mm	0.71mm	1.40mm	0.32mm	1.60mm	0.39mm
Bagaza Virus (BAGV)	0.75mm	0.26mm	1.95mm	0.37mm	1.85mm	0.24mm	2.30mm	0.67mm
West Nile Virus (WNV)	3.6mm	0.52mm						

B) Statistical Analysis of Plaque Sizes

JEV Chimeras

Virus	WNV NY99	A-Form	B-Form	C-Form
WNV IC JEV EIII A	0.055			
WNV IC JEV EIII B	1.000	1.000		
WNV IC JEV EIII C	1.000	1.000	1.000	
WNC IC JEV EIII D	1.000	1.000	1.000	1.000

KOUV Chimeras

Virus	WNV NY99	A-Form	B-Form	C-Form
WNV IC KOUV EIII A	**0.000**			
WNV IC KOUV EIII B	**0.000**	1.000		
WNV IC KOUV EIII C	**0.000**	1.000	1.000	
WNC IC KOUV EIII D	**0.000**	1.000	1.000	1.000

SLEV Chimeras

Virus	WNV NY99	A-Form	B-Form	C-Form
WNV IC SLEV EIII A	**0.000**			
WNV IC SLEV EIII B	1.000	**0.000**		
WNV IC SLEV EIII C	**0.000**	1.000	**0.000**	
WNC IC SLEV EIII D	**0.000**	1.000	**0.000**	1.000

BAGV Chimeras

Virus	WNV NY99	A-Form	B-Form	C-Form
WNV IC BAGV EIII A	**0.000**			
WNV IC BAGV EIII B	**0.000**	**0.000**		
WNV IC BAGV EIII C	**0.000**	**0.000**	1.000	
WNC IC BAGV EIII D	**0.000**	**0.000**	1.000	1.000

Table 3.3: Mean Plaque Sizes and Statistical Comparison. *A*: Ten representative plaques were measured for each virus and mean plaque size and standard deviation was determined. *B*: Plaque sizes were compared by one-way ANOVA to determine significant differences between the four versions of each chimera and wild-type WNV NY99. Significant ($p<0.05$) values are in bold.

Statistical Analysis of Vero Cell Growth Kinetics

A) JEV Chimeras

	Virus	WNV NY99	A-Form	B-Form	C-Form
Day 1	WNV IC JEV EIII A	1.000			
	WNV IC JEV EIII B	0.271	0.199		
	WNV IC JEV EIII C	1.000	1.000	**0.025**	
	WNC IC JEV EIII D	0.189	0.257	**0.003**	1.000
Day 2	WNV IC JEV EIII A	**0.001**			
	WNV IC JEV EIII B	1.000	**0.001**		
	WNV IC JEV EIII C	0.079	0.162	0.087	
	WNC IC JEV EIII D	**0.004**	1.000	**0.004**	0.881
Day 3	WNV IC JEV EIII A	**0.003**			
	WNV IC JEV EIII B	1.000	**0.027**		
	WNV IC JEV EIII C	**0.047**	0.956	0.609	
	WNC IC JEV EIII D	**0.004**	1.000	**0.047**	1.000
Day 4	WNV IC JEV EIII A	**0.008**			
	WNV IC JEV EIII B	1.000	0.062		
	WNV IC JEV EIII C	**0.023**	1.000	0.186	
	WNC IC JEV EIII D	0.056	1.000	0.469	1.000
Day 5	WNV IC JEV EIII A	0.460			
	WNV IC JEV EIII B	0.969	1.000		
	WNV IC JEV EIII C	0.252	1.000	1.000	
	WNC IC JEV EIII D	0.670	1.000	1.000	1.000

B) KOUV Chimeras

	Virus	WNV NY99	A-Form	B-Form	C-Form
Day 1	WNV IC KOUV EIII A	0.051			
	WNV IC KOUV EIII B	**0.006**	1.000		
	WNV IC KOUV EIII C	**0.007**	1.000	1.000	
	WNC IC KOUV EIII D	**0.001**	0.379	1.000	1.000
Day 2	WNV IC KOUV EIII A	**0.000**			
	WNV IC KOUV EIII B	**0.004**	0.111		
	WNV IC KOUV EIII C	**0.006**	0.061	1.000	
	WNC IC KOUV EIII D	**0.000**	1.000	0.640	0.349
Day 3	WNV IC KOUV EIII A	**0.002**			
	WNV IC KOUV EIII B	**0.003**	1.000		
	WNV IC KOUV EIII C	**0.003**	1.000	1.000	
	WNC IC KOUV EIII D	**0.004**	1.000	1.000	1.000
Day 4	WNV IC KOUV EIII A	**0.003**			
	WNV IC KOUV EIII B	**0.002**	1.000		
	WNV IC KOUV EIII C	**0.002**	1.000	1.000	
	WNC IC KOUV EIII D	**0.001**	1.000	1.000	1.000
Day 5	WNV IC KOUV EIII A	**0.000**			
	WNV IC KOUV EIII B	**0.000**	0.556		
	WNV IC KOUV EIII C	**0.000**	1.000	1.000	
	WNC IC KOUV EIII D	**0.000**	1.000	1.000	1.000

Table 3.4: Statistical Comparison of Growth Kinetics in Vero Cells. Statistical analysis of JEV EIII (*A*) and KOUV EIII (*B*) chimeras compared to one another and WNV NY99 by one-way ANOVA. Significant ($p<0.05$) values are in bold.

Statistical Analysis of Vero Cell Growth Kinetics

C) SLEV Chimeras

	Virus	WNV NY99	A-Form	B-Form	C-Form
Day 1	WNV IC SLEV EIII A	**0.000**			
	WNV IC SLEV EIII B	**0.002**	1.000		
	WNV IC SLEV EIII C	**0.000**	1.000	1.000	
	WNC IC SLEV III D	**0.000**	1.000	1.000	1.000
Day 2	WNV IC SLEV EIII A	**0.000**			
	WNV IC SLEV EIII B	**0.000**	**0.000**		
	WNV IC SLEV EIII C	**0.000**	1.000	**0.000**	
	WNC IC SLEV EIII D	**0.000**	1.000	**0.000**	1.000
Day 3	WNV IC SLEV EIII A	**0.002**			
	WNV IC SLEV EIII B	1.000	**0.003**		
	WNV IC SLEV EIII C	**0.002**	1.000	**0.003**	
	WNC IC SLEV EIII D	**0.002**	1.000	**0.003**	1.000
Day 4	WNV IC SLEV EIII A	**0.006**			
	WNV IC SLEV EIII B	1.000	**0.001**		
	WNV IC SLEV EIII C	**0.006**	1.000	**0.001**	
	WNC IC SLEV EIII D	**0.006**	1.000	**0.001**	1.000
Day 5	WNV IC SLEV EIII A	**0.000**			
	WNV IC SLEV EIII B	**0.000**	**0.000**		
	WNV IC SLEV EIII C	**0.000**	1.000	**0.000**	
	WNC IC SLEV EIII D	**0.000**	1.000	**0.000**	1.000

D) BAGV Chimeras

	Virus	WNV NY99	A-Form	B-Form	C-Form
Day 1	WNV IC BAGV EIII A	**0.000**			
	WNV IC BAGV EIII B	**0.000**	1.000		
	WNV IC BAGV EIII C	**0.001**	1.000	1.000	
	WNC IC BAGV EIII D	**0.000**	1.000	1.000	1.000
Day 2	WNV IC BAGV EIII A	**0.000**			
	WNV IC BAGV EIII B	**0.000**	0.099		
	WNV IC BAGV EIII C	**0.000**	1.000	1.000	
	WNC IC BAGV EIII D	**0.000**	0.171	1.000	1.000
Day 3	WNV IC BAGV EIII A	**0.001**			
	WNV IC BAGV EIII B	**0.001**	1.000		
	WNV IC BAGV EIII C	**0.001**	1.000	1.000	
	WNC IC BAGV EIII D	**0.001**	1.000	1.000	1.000
Day 4	WNV IC BAGV EIII A	**0.001**			
	WNV IC BAGV EIII B	**0.001**	1.000		
	WNV IC BAGV EIII C	**0.001**	1.000	1.000	
	WNC IC BAGV EIII D	**0.001**	1.000	1.000	1.000
Day 5	WNV IC BAGV EIII A	**0.000**			
	WNV IC BAGV EIII B	**0.000**	1.000		
	WNV IC BAGV EIII C	**0.000**	1.000	1.000	
	WNC IC BAGV EIII D	**0.000**	1.000	1.000	1.000

Table 3.4: (Continued) Statistical Comparison of Growth Kinetics in Vero Cells. Statistical analysis of SLEV EIII (*C*) and BAGV EIII (*D*) chimeras compared between versions and WNV NY99 by one-way ANOVA. Significant ($p<0.05$) values are in bold.

Statistical Analysis of C6/36 Cell Growth Kinetics

A) JEV Chimeras

	Virus	WNV NY99	A-Form
Day 1	WNV IC JEV EIII A	1.000	
	WNV IC JEV EIII B	0.948	1.000
Day 2	WNV IC JEV EIII A	1.000	
	WNV IC JEV EIII B	1.000	1.000
Day 3	WNV IC JEV EIII A	0.192	
	WNV IC JEV EIII B	0.500	1.000
Day 4	WNV IC JEV EIII A	0.411	
	WNV IC JEV EIII B	0.385	1.000
Day 5	WNV IC JEV EIII A	0.147	
	WNV IC JEV EIII B	0.109	1.000

B) KOUV Chimeras

	Virus	WNV NY99	A-Form
Day 1	WNV IC KOUV EIII A	1.000	
	WNV IC KOUV EIII B	0.277	0.140
Day 2	WNV IC KOUV EIII A	1.000	
	WNV IC KOUV EIII B	1.000	1.000
Day 3	WNV IC KOUV EIII A	**0.002**	
	WNV IC KOUV EIII B	**0.001**	1.000
Day 4	WNV IC KOUV EIII A	0.229	
	WNV IC KOUV EIII B	0.181	1.000
Day 5	WNV IC KOUV EIII A	**0.049**	
	WNV IC KOUV EIII B	0.050	1.000

C) SLEV Chimeras

	Virus	WNV NY99	A-Form
Day 1	WNV IC SLEV EIII A	1.000	
	WNV IC SLEV EIII B	0.076	**0.021**
Day 2	WNV IC SLEV EIII A	0.307	
	WNV IC SLEV EIII B	**0.001**	**0.000**
Day 3	WNV IC SLEV EIII A	0.060	
	WNV IC SLEV EIII B	**0.021**	**0.001**
Day 4	WNV IC SLEV EIII A	0.139	
	WNV IC SLEV EIII B	0.897	**0.033**
Day 5	WNV IC SLEV EIII A	0.051	
	WNV IC SLEV EIII B	0.290	0.713

D) BAGV Chimeras

	Virus	WNV NY99	A-Form
Day 1	WNV IC BAGV EIII A	1.000	
	WNV IC BAGV EIII B	0.409	0.112
Day 2	WNV IC BAGV EIII A	1.000	
	WNV IC BAGV EIII B	0.266	1.000
Day 3	WNV IC BAGV EIII A	**0.000**	
	WNV IC BAGV EIII B	**0.000**	1.000
Day 4	WNV IC BAGV EIII A	0.112	
	WNV IC BAGV EIII B	0.114	1.000
Day 5	WNV IC BAGV EIII A	**0.045**	
	WNV IC BAGV EIII B	**0.048**	1.000

Table 3.5: Statistical Comparison of Growth Kinetics in C6/36 Cells. Statistical analysis of JEV EIII (*A*), KOUV EIII (*B*), SLEV EIII (*C*), and BAGV EIII (*D*) chimeras compared between versions and WNV NY99 by one-way ANOVA. Significant ($p<0.05$) values are in bold.

Mutations in Passage 0 (Recovered Virus) Samples

A) JEV Chimeras

A-Form (SalI/BamHI)			**B-Form** (PstI/StuI)			**C-Form** (SalI/StuI)			**D-Form** (PstI/BamHI)		
Mutation	Amino Acid	Frequency	Mutation	Amino Acid	Frequency	Mutation	Amino Acid	Frequency	Mutation	Amino Acid	Frequency
T2049	E *(Silent)*	100%	T2049C	E *(Silent)*	100%	T2049C	E *(Silent)*	100%	T2049C	E *(Silent)*	100%
T2222C*	**E A419V**	**100%**	T10888A	3′ UTR	1.60%	G5166A	NS3 *(Silent)*	1.14%	**T2222C***	**E A419V**	**100%**
G5166A	NS3 *(Silent)*	1.10%				T10888A	3′ UTR	1.81%	G5166A	NS3 *(Silent)*	1.00%
T10888A	3′ UTR	1.16%							T10888A	3′ UTR	1.46%

B) KOUV Chimeras

A-Form (SalI/BamHI)			**B-Form** (PstI/StuI)			**C-Form** (SalI/StuI)			**D-Form** (PstI/BamHI)		
Mutation	Amino Acid	Frequency	Mutation	Amino Acid	Frequency	Mutation	Amino Acid	Frequency	Mutation	Amino Acid	Frequency
C1939G	**E L325V**	**17.70%**	**A382C**	**C N96H**	**1.85%**	C1939T	E *(Silent)*	8.98%	A2277T	E *(Silent)*	37.63%
A1941G	E *(Silent)*	5.10%	**T592C**	**prM Y43G**	**6.20%**	**A4171G**	**NS2a M216V**	**9.48%**	T4248C	NS2b *(Silent)*	4.39%
A4014T	NS2a *(Silent)*	15.59%	A1243C	E *(Silent)*	1.51%	G5166A	NS3 *(Silent)*	1.08%	G5166A	NS3 *(Silent)*	1.16%
A5070T	NS3 *(Silent)*	12.63%	**A1798T**	**E T278S**	**1.81%**	A6912C	2K *(Silent)*	9.24%	T10888A	3′ UTR	1.81%
G5166A	NS3 *(Silent)*	1.08%	**A2135G**	**E D390G**	**12.79%**	A7191C	NS4b *(Silent)*	1.79%			
A6079T	**NS3 T490S**	**6.62%**	A5070T	NS3 *(Silent)*	2.71%	T10888A	3′ UTR	1.21%			
A7794G	NS5 *(Silent)*	2.98%	**A5074T**	**NS3 I155L**	**2.35%**						
A8025C	NS5 *(Silent)*	3.19%	G5166A	NS3 *(Silent)*	1.17%						
A10873G	3′ UTR	8.53%	**A5881G**	**NS3 I424L**	**7.78%**						
T10888A	3′ UTR	1.00%	**A7408T**	**NS4b T165S**	**11.16%**						
			A7648C	**NS4b I245L**	**2.75%**						
			A8679C	NS5 *(Silent)*	20.10%						
			A9170G	**NS5 D497G**	**2.40%**						
			A9882G	NS5 *(Silent)*	1.80%						
			A10664C	3′ UTR	1.12%						
			T10888A	3′ UTR	1.34%						

Table 3.6: Mutations in Passage 0 Viruses. SNPs with frequency >1% were determined by Next-Generation Sequencing for the JEV EIII (*A*) and KOUV EIII (*B*) chimeras. Non-synonymous mutations are in bold, with mutations with >5% prevalence in red.

Mutations in Passage 0 (Recovered Virus) Samples

C) SLEV Chimeras

A-Form (SalI/BamHI)			**B-Form** (PstI/StuI)			**C-Form** (SalI/StuI)			**D-Form** (PstI/BamHI)		
Mutation	Amino Acid	Frequency	Mutation	Amino Acid	Frequency	Mutation	Amino Acid	Frequency	Mutation	Amino Acid	Frequency
T10888A	3′ UTR	1.43%	**G597C**	**prM M44I**	**0.92%**	**T232C**	**C F46L**	**1.97%**	**A1031C**	**E D22A**	**1.53%**
			A1369C	**E I135L**	**2.31%**	G363A	C *(Silent)*	1.47%	**A1630T**	**E N222Y**	**69.21%**
			A1512C	**E E182D**	**1.13%**	**A1630T**	**E N222Y**	**98.24%**	**G1842C**	**E M292I**	**5.29%**
			A1630T	**E N222Y**	**11.29%**	G5166A	NS3 *(Silent)*	1.61%	**A2409G**	**E I481M**	**25.80%**
			A1785T	**E E273D**	**2.54%**	A5172 +A	NS3	0.94%	**C2440G**	**E L492V**	**7.45%**
			A1795T	**E N277Y**	**1.93%**	**T5587C**	**NS3 F326L**	**2.35%**	**A3019G**	**NS1 I184V**	**7.62%**
			A1853G	**E Q296R**	**1.32%**	T6790C	NS4a *(Silent)*	12.17%	G5166A	NS3 *(Silent)*	1.17%
			A1855C	**E I297L**	**1.60%**	A10651G	3′ UTR	3.10%	**A6094C**	**NS3 M495L**	**3.02%**
			A2194T	**E T410S**	**1.17%**	T10888A	3′ UTR	2.61%	**A6509C**	**NS4a E14G**	**4.31%**
			A2285T	**E Y440M**	**1.05%**				**G8855C**	**NS5 R392P**	**5.81%**
			C2484G	NS1 *(Silent)*	1.08%				A9655C	NS5 *(Silent)*	4.82%
			A3205C	**NS1 T246P**	**3.33%**						
			A3966C	NS2a *(Silent)*	1.31%						
			G5166A	NS3 *(Silent)*	1.13%						
			A7077T	NS4b *(Silent)*	3.06%						
			A8470T	**NS5 T264S**	**1.31%**						
			A10452C	3′ UTR	1.17%						
			A10746C	3′ UTR	0.91%						
			T10888A	3′ UTR	1.21%						

Table 3.6: (Continued) Mutations in Passage 0 Viruses. SNPs with frequency >1% were determined by Next-Generation Sequencing for the SLEV EIII (*C*) chimeras. Non-synonymous mutations are in bold, with mutations with >5% prevalence in red.

Mutations in Passage 0 (Recovered Virus) Samples

D) BAGV Chimeras

A-Form (SalI/BamHI)			**B-Form** (PstI/StuI)			**C-Form** (SalI/StuI)			**D-Form** (PstI/BamHI)		
Mutation	Amino Acid	Frequency	Mutation	Amino Acid	Frequency	Mutation	Amino Acid	Frequency	Mutation	Amino Acid	Frequency
G5166A	NS3 *(Silent)*	0.92%	**A364G**	**C T90A**	**2.88%**	**A1630T**	**E N222Y**	**95.25%**	**A1630T**	**E N222Y**	**1.90%**
			A1497C	E *(Silent)*	4.60%	A1746C	E *(Silent)*	25.79%	G5166A	NS3 *(Silent)*	0.92%
			A1630T	**E N222Y**	**80.71%**	**A2234C**	**E D423A**	**0.93%**	T10888A	3′ UTR	0.99%
			A1853G	**E Q296R**	**1.65%**	G5166A	NS3 *(Silent)*	1.42%			
			A1971A	E *(Silent)*	59.97%	A5487C	NS3 *(Silent)*	11.39%			
			A2234C	**E D423A**	**5.16%**	A6732G	NS4a *(Silent)*	12.41%			
			A2256G	E *(Silent)*	6.57%	**G7180T**	**NS4b V89F**	**2.29%**			
			C2321T	**E S451L**	**4.79%**	**C9722T**	**NS5 T681I**	**1.22%**			
			A3426G	NS1 *(Silent)*	1.37%	A10881G	3′ UTR	2.35%			
			A3726G	NS2a *(Silent)*	3.04%	T10888A	3′ UTR	1.11%			
			A4425G	NS2b *(Silent)*	2.22%						
			A5016G	NS3 *(Silent)*	1.84%						
			G5166A	NS3 *(Silent)*	0.97%						
			A5392C	**NS3 M261L**	**7.69%**						
			A5571C	NS3 *(Silent)*	1.23%						
			A5575T	**NS3 T322S**	**4.20%**						
			A5964T	NS3 *(Silent)*	4.47%						
			A6169C	**NS3 M520L**	**1.63%**						
			A7184C	**NS4b D90A**	**1.53%**						
			C8194T	NS5 *(Silent)*	1.23%						
			A8370G	NS5 *(Silent)*	1.22%						
			A8409G	NS5 *(Silent)*	13.24%						
			T10106A	**NS5 M809Y**	**1.12%**						

Table 3.6: (Continued) Mutations in Passage 0 Viruses. SNPs with prevalence >1% were determined by Next-Generation Sequencing for the BAGV EIII (*D*) chimeras. Non-synonymous mutations are in bold, with mutations with >5% prevalence in red.

Mutations in Passage 1 Samples

A) SLEV Chimeras

A-Form (SalI/BamHI)		
Mutation	Amino Acid	Frequency
T896C	**prM M144T**	**26.35%**
A1630T	**E N222Y**	**96.14%**
C1819T	**E H285Y**	**63.22%**
T2345C	**E I460T**	**1.43%**
A4033G	**NS2a N170D**	**3.28%**
A5958T	NS3 *(Silent)*	98.39%
A6374G	**NS3 E588G**	**1.82%**

B) BAGV Chimeras

A-Form (SalI/BamHI)		
Mutation	Amino Acid	Frequency
A332G	**C K79R**	**1.22%**
C849T	prM *(Silent)*	1.29%
T1062C	E *(Silent)*	1.34%
A1063C	**E I33L**	**0.99%**
C1154T	**E A63V**	**1.01%**
T1410C	E *(Silent)*	0.90%
A1630T	**E N222Y**	**23.87%**
A2032G	**E I356V**	**2.27%**
T2481C	NS1 *(Silent)*	1.06%
A2491C	**NS1 I8L**	**2.21%**
A3239C	**NS1 E274A**	**1.42%**
A3630T	NS2a *(Silent)*	1.59%
A3966C	NS2a *(Silent)*	1.42%
A4071C	NS2a *(Silent)*	4.21%
C5040T	NS3 *(Silent)*	1.31%
G5166A	NS3 *(Silent)*	1.12%
A5174T	**NS3 Q188L**	**2.37%**
A6144G	NS3 *(Silent)*	1.70%
T6742C	**NS4a F92L**	**1.80%**
C8517T	NS5 *(Silent)*	1.33%
C10772T	3′UTR	1.40%
T10888A	3′UTR	1.22%

Table 3.7: Mutations in Passage 1 Viruses. SNPs with frequency >1% were determined by Next-Generation Sequencing for the SLEV A EIII (*A*) and BAGV A EIII (*B*) chimeras. Non-synonymous mutations are in bold, with mutations with >5% prevalence in red.

Neutralization Titers of WNV-Specific Antibodies

Virus	αWNV EIII Rabbit pAb	Lineage I MIAF (T-35570)	Lineage II MIAF (T-35345)	αWNV Human Serum 022	αWNV Human Serum 026
West Nile Virus NY99	1280	5120	1280	1280	10240
WNV IC KOUV EIII B	2560	2560	2560	1280	10240
WNV IC JEV EIII B	80	640	80	1280	1280
WNV IC SLEV EIII B	<40	640	80	1280	5120
WNV IC BAGV EIII B	<40	2560	640	1280	5120

Table 3.8: Neutralization of B-Form Chimeras with WNV-Specific Immune Sera and MIAF. B-form chimeras were incubated with different concentrations of immune sera and MIAF to determine $TCID_{50}$ neutralization titers. A 4-fold difference is considered significant.

Chapter 4: *in vivo* Characterization of Chimeric Viruses

INTRODUCTION

Few studies have been conducted to date to determine the effect of flavivirus chimerization on disease presentation and progression in animal models, aside from attaining basic mortality data. Bray & Lai demonstrated that chimeras of DENV-4 containing prM-E from DENV-2 possessed increased neurovirulence in suckling mice compared to the DENV-4 control virus when administered intracranially (i.c.) (Bray and Lai, 1991a). Similar studies by Pletnev *et al*. showed that a TBEV prM-E-expressing DENV-4 chimera gained neurovirulence in suckling and 6-week-old mice following i.c. inoculation, but that the chimerization did not lead to mortality following i.p. or i.d. administration (Pletnev et al., 1992). Many of the chimeric viruses that have been subsequently generated were deliberately produced using attenuated virus strains, such as YFV 17D, with the specific goals of exploiting the attenuated properties of the backbone virus and with the resulting chimeras unsurprisingly also attenuated. Consequently, the role of EIII in virulence, disease presentation, and tissue tropism are poorly understood.

The Swiss Webster mouse model of WNV infection is well established, having been used for decades due to the high susceptibility of young adult mice to inoculation with wild-type virus by a number of routes (Reagan et al., 1952b). Typically, following i.p. inoculation with WNV NY99, the infection progresses for the first week without any overt clinical signs. Internally, after inoculation, the virus replicates and causes a viremia that peaks on Day 3 post infection. With the generation of an adaptive immune response, this viremia is usually cleared by Day 5. At the same time, peripheral infection of lung,

spleen, and kidney is reaching its peak, with neuroinvasion leading to low, but detectable, virus in the brain. Mortality is usually observed between Days 8 and 11, with death at the earlier timepoints rarely preceded by clinical signs. Between Days 9 and 11, clinical signs of infection may be observed, including ruffled fur, hunched posture, and hypoactivity. Towards the end of the mortality window, neurological signs may be seen including tremors and hind-limb paralysis. While reasonably well studied, significant gaps still remain in the understanding of WNV-induced disease pathogenesis, including the exact mechanism by which the virus crosses the blood-brain barrier to infect the central nervous system. Three potential mechanisms of neuroinvasion have been proposed: axonal translocation, permeabilization of the blood-brain barrier, and entry within infected immune cells (Neal, 2014).

The aim of this study was to determine whether differences occurred in virulence and disease presentation following infection with the EIII chimeras compared to the wild-type WNV NY99. This would allow for potential determination of both the effect of EIII chimerization on viral virulence, compared to *in vitro* growth, and the role that EIII plays in pathogenesis as well as potential differences in tissue tropism resulting from EIII substitution.

CHIMERIC VIRUS VIRULENCE STUDIES – SINGLE DOSE (100PFU) I.P.

In order to determine whether chimerization had affected virulence of the chimeric viruses, 100pfu doses were administered i.p. with each of the 16 chimeras, as well as the wild-type WNV NY99 and the 4 site backbone virus. The 4-site virus showed significantly different mortality compared to WNV NY99 as determined by Mantel-Cox comparison of the survival curves, with an average survival time of 10.3±1.2 days, compared to the 8.8±1.0 days observed for NY99 (Figure 4.1).

All four of the JEV chimeras maintained substantial virulence following i.p. inoculation, with only JEV A having a significantly different survival curve compared to WNV NY99 ($p<0.0459$; Figure 4.2A), with an average survival time of 10.1±1.5 days compared to 8.8±1.0 days for WNV NY99.

The KOUV chimeras caused significantly less mortality than WNV NY99, based on the survival curves, with mortality rates under 50% for all of the viruses (Figure 4.2B). The A- and C-forms had the longest average survival time (12.5±0.7 days, and 13.5±1.7 days, respectively), with the B- and C-forms having values closer to WNV NY99 (10.0±2.8 days, and 9.0±1.0 days, respectively).

The SLEV and BAGV chimeras appeared to be strongly attenuated following administration via the intraperitoneal route (Figure 4.2C&D). None of the SLEV chimeras killed any of the infected mice, and only the BAGV B- and C- forms caused any mortality (10% and 20%, respectively), with substantially protracted average survival times of 10.0±0.0 days and 19.0±2.83 days, respectively. The SLEV A Passage 1 virus, discussed in the previous chapter, also failed to cause any mortality or signs of illness.

NEUROVIRULENCE STUDIES WITH CHIMERA B-FORMS

Given that significant variations in the incidence of neuroinvasive disease were observed for some of the EIII chimeras compared to NY99, the neurovirulence of the B-form chimeras was assessed via intracranial inoculation of 3-4-week-old Swiss Webster mice with 10 and 100pfu of virus (Figure 4.3). With both dose levels, WNV NY99 caused 100% mortality with average survival times of 6.1±0.6 days and 6.7±1.5 days for the 100pfu and the 10pfu doses, respectively. The JEV B chimera also caused 100% mortality with 100pfu, and 80% mortality with 10pfu, with average survival times of

7.2±0.5 days and 8.8±1.7 days, respectively. Compared to WNV NY99, the mortality curve for the 100pfu dose were significantly different ($p<0.0061$), but that of the 10pfu dose was not.

The KOUV B chimera showed a less apparent dose response than the other chimeras, with 60% mortality with 100pfu, and 40% mortality with 10pfu. The average survival time for 100pfu was 7.3±0.8 days, while the survival time for 10pfu was 9.3±2.9 days, both of which were significantly different to WNV NY99. The SLEV B chimera displayed 100% mortality with 100pfu (AST 6.8±0.9 days), but only 30% mortality with 10pfu (AST 7.7±1.2 days), with both survival curves significantly different to the wild-type control. The BAGV B chimera showed 78% mortality with 100pfu (AST 6.6±0.5 days), but only 10% mortality with 10pfu (AST 7.0 days).

SERIAL SACRIFICE STUDIES WITH CHIMERA B-FORMS

The single-dose studies with all of the chimeric viruses suggested that the constructs display a range of virulence phenotypes in mice following i.p. inoculation. In order to better characterize the particulars of the infection, a serial sacrifice study was carried out using the B-forms of the chimeras. The B-forms were chosen as they all grew similarly to the parental virus in Vero cells, minimizing any potential confounding effects of inhibited viral replication. For each B-variant chimera and the wild-type parent, five mice were microchipped, and their temperatures and weights were recorded daily throughout the course of the experiment until Day 21. Fifteen mice were used for each group for sample harvesting on days 1, 3, 5, 7, and 9 post infection. The mice were dosed with 100pfu of virus, with inoculating doses confirmed by back titration.

Survival

The survival data obtained in this experiment (Figure 4.4A) were generally consistent with the findings from the initial virulence screening described above. Both WNV NY99 and the JEV B chimera caused 100% mortality, while the other three chimeras had substantially lower mortality rates. KOUV B caused 40% mortality with an average survival time of 12.5±2.1 days, while SLEV B was completely attenuated following i.p. inoculation. The BAGV B chimera caused 20% mortality, with the one mouse that died doing so on Day 8. ELISAs run on sera from the survivors confirmed seroconversion, indicating that the mice had indeed been infected.

Temperatures & Weights

Temperatures measured during the first seven days post-infection did not differ significantly from baseline measurements for all groups (Figure 4.4B). For the WNV NY99- and JEV B-infected mice, the temperatures declined rapidly from Day 8 until death by Day 10. For the mice infected with the KOUV B chimera, temperature drops were seen in the mice that proceeded to a fatal outcome, with these drops also occurring from Day 8. Interestingly, the rate of decrease was a lot lower than with the WNV NY99 and JEV B chimera: with the more virulent viruses, the temperature dropped up to 5°C in 24hrs; while with the KOUV B-infected mice, daily temperature drops rarely exceeded 1°C. The one lethal BAGV infection had no preceding temperature drop, but this may just be due to this mouse dying on Day 8, the first day of observable temperature drops with any of the viruses.

Comparison of the weight changes across the different groups infected with the four chimeras or the wild-type virus identified three different profiles (Figure 4.4C, D, E). As was observed with the temperature data, mice infected with WNV NY99 or the

JEV B chimera lost weight rapidly until death (Figure 4.4C). Compared to the temperature drop, the weight loss started a day earlier on Day 7 post infection, prior to the observation of any overt clinical signs of disease. The second weight profile, shared by the KOUV B- and SLEV B-infected mice, was one of a gradual decrease in weight from Day 7 to around Day 13, suggesting that some illness associated with infection occurred in the animals despite the absence of other clinical signs (Figure 4.4D). This period of weight loss was followed by an increase in weight of more than 5% between Days 13 and 15. From Day 15 onward, the weight continued to increase steadily, almost paralleling the mock-infected animals. The third weight change profile, that of the BAGV B chimera-infected mice, showed a brief, reasonably gentle, two-day weight drop on Days 8 and 9, followed by a steady increase in weight such that from Day 18 onward the mean weight was identical to that of the mock-infected mice (Figure 4.4E).

Viremia and Virus Loads in Organs

All of the viruses caused detectable viremia with a peak on Day 3 post infection (Figure 4.5). Only one of the three WNV NY99-infected mice had detectable viremia on Day 1, but by Day 3 all three mice were viremic (Figure 4.5A). On Day 5 and subsequent timepoints, there was no detectable circulating virus in the NY99-infected mice, indicating that it had been effectively cleared. The JEV B chimera appeared to have a slightly different viremia profile to that of the control virus. Virus was detectable in at least two of the three mice sacrified on each of Days 1, 3, and 5, although the peak viremia on Day 3 was 7-fold lower than for WNV NY99 ($1.3x10^4$ pfu/ml (SD $7.4x10^3$) vs. $7.1x10^4$ pfu/ml (SD $5.4x10^4$); $p>0.05$). Despite the protracted viremia, which persisted two days longer than the NY99 viremia, plasma titers were below the limit of detection on Days 7 and 9. Notwithstanding the attenuated phenotype of the KOUV B chimera, the viremia caused by this virus appeared most similar to that of WNV NY99, although the

Day 1 titers were the highest of any of the viruses tested. By Day 3 the peak viremia titers were similar to that of the control virus, $9.9x10^4$ pfu/ml (SD $9.6x10^4$). Similar to WNV NY99, the KOUV B chimera was mostly cleared by Day 5, and was not detected in any samples collected on Days 7 or 9. The SLEV B and BAGV B chimera-infected mice had no detectable viremia on Day 1, and the peak viremia on Day 3 was over 100-fold lower than for NY99 (SLEV B: $6.2x10^2$ pfu/ml (SD $9.8x10^2$); BAGV B: $5.5x10^2$ pfu/ml (SD $6.9x10^2$)). With the exception of one BAGV B-infected mouse, the viruses were cleared from circulation by Day 5.

Within the brains there was no detectable virus with any of the agents until Day 5 (Figure 4.5B). With WNV NY99, there was one virus-positive mouse on Day 5, and by Day 7 and Day 9, all of the mice were positive, with average titers between 10^6 and 10^7 pfu/100mg tissue. Neuroinvasion in JEV B-infected mice was more variable, with two of the three having detectable virus on Day 3, but only one of the three having detectable virus on Day 7. By Day 9, still only two of the three mice had virus in the brain. The mean titer of 10^6 pfu/100mg tissue at Day 9 neither substantially nor significantly different from that of the WNV NY99-infected mice. For the other three chimeras, detection of virus in the brain was infrequent, and in those animals with detectable virus the titers were low, often barely above the limit of detection. Only one KOUV B-infected mouse had any quantifiable virus, on Day 7. The SLEV B-infected mice had one virus-positive mouse on Day 3, and two on Day 5, but these titers were only around 10^2 pfu/100mg tissue. None of the BAGV B-infected mice had detectable virus in the brain over the course of the infection.

Similar to other WNV serial sacrifice studies, no detectable virus was present in the liver with any of the viruses at any time (Figure 4.5C). Titers of WNV NY99 and the JEV B chimera within the spleen were similar to one another (Figure 4.5D). On Day 3,

all of the mice infected with these viruses had detectable virus with mean titers slightly higher than 10^3 pfu/100mg tissue. By Day 5 this had increased to $4.8x10^4$ pfu/100mg (SD $5.7x10^3$) for NY99 with detectable virus in two of the three mice, and $1.2x10^4$ pfu/100mg (SD $1x10^4$) for JEV B, with all three mice with detectable virus. Unlike WNV NY99 and JEV B, the other chimeras appeared to be delayed in their infection of the spleen. KOUV B had a mean titer of $3.4x10^2$ pfu/100mg (SD $4.6x10^2$) on Day 5, but only two of the three mice had detectable virus. SLEV B had a mean titer of 49 pfu/100mg, with only one mouse with detectable virus, while BAGV B had a mean titer of $1.7x10^2$ pfu/100mg (SD $1.5x10^2$) with a two-thirds infection rate.

Virus titers in lung tissue varied greatly amongst the wild-type and chimeras (Figure 4.5). None of the mice had detectable virus on Day 1, but all of the WNV NY99- and JEV B-infected mice were positive on Day 3, with WNV NY99 having a mean titer of $1.1x10^3$ pfu/100mg (SD $1x10^3$), and JEV B having a mean titer of $4.2x10^2$ pfu/100mg (SD $4.9x10^2$). At Day 5, only WNV NY99 had detectable virus, with a mean titer of $3.5x10^4$ pfu/100mg (SD $1.2x10^4$). None of the KOUV B-, SLEV B-, or BAGV B-infected mice had detectable virus in the lung at any of the timepoints.

Within the kidney, none of the mice had any detectable virus on Day 1 (Figure 4.5E). With WNV NY99, all of the infected mice had detectable virus on Days 3 and 5, with mean titers of $5.0x10^3$ pfu/100mg (SD $4.4x10^3$) and $5.3x10^4$ pfu/100mg (SD $8.3x10^4$), respectively. Samples from two of the three mice infected with JEV B chimera and harvested on Day 3 had detectable virus, as did all of the samples from Day 5. Mean titers in the kidneys were $2.1x10^2$ pfu/100mg (SD $3.2x10^2$) and $5.0x10^3$ pfu/100mg (SD $3.8x10^3$), respectively, for those groups, both of which were at least 10-fold lower than mean WNV NY99 titers on each day (Figure 4.5F). Interestingly, unlike what was observed for most of the virus load comparisons in other organs, the KOUV B chimera

demonstrated similar titers to WNV NY99 and JEV B in the kidney, in that on Day 3, all of the mice had detectable virus, with a mean titer of $6.9x10^2$ pfu/100mg (SD $3.4x10^2$), and on Day 5, two of the three mice had detectable virus, with a mean titer of $1.4x10^4$ pfu/100mg (SD $1.6x10^4$). Only one of the three SLEV B-infected mice had detectable levels of virus on Days 3 or 5, and the titers were very low, <120pfu/100mg. None of the BAGV B-infected mice yielded detectable virus in the kidney on any of the study days.

Hematology

There were no significant differences in whole white blood cell count during the course of the experiment, likely due to the degree of variability within the mock-infected group (Figure 4.6A). There was however, a trend towards leukocytopenia on Days 1, 3, and 5, with Day 3 having particularly low values for almost all of the infected mice. By Day 7, the WNV NY99-infected mice had particularly low WBC counts, with an average count of just 2.8 K/µl (SD 0.32) compared to an average of 9.7 K/µl (SD 4.9) for the mock-infected mice. In the mice infected with the other viruses the values ad Day 7 had started to increase to approach those of the mock-infected mice. By Day 9, even the WNV NY99-infected mouse WBC counts were starting to increase, and the values for the KOUV B-, SLEV B-, and BAGV B-infected mice were almost indistinguishable from the mock. The JEV B-infected mice showed high variability in their WBC counts.

Comparison of individual immune cell counts and proportions revealed some statistically significant differences, particularly with the WNV NY99-infected mice (Figure 4.6B). The greatest difference was seen with the lymphocytes. Absolute counts were significantly lower in the WNV NY99-infected mice on Days 3 and 7 ($p<0.033$ and $p<0.024$, respectively), but not for the other viruses, although the mean counts were less than half that of the mock-infected mice on Days 1 and 3 post infection. This apparent

lymphocytopenia resulted in lower lymphocyte proportions, particularly on Day 3 for all of the viruses, and Days 7 and 9 for the WNV NY99- and JEV B-infected mice. Statistical significance was observed for the WNV NY99-infected mice on Days 3, 7, and 9 ($p<0.001$, $p<0.000$, and $p<0.003$, respectively) compared to the mock, but no significance was shown for the other viruses. Between the infected mice, the lymphocyte values for the NY99 mice were significantly lower than those of the SLEV B and BAGV B-infected mice on Days 7 and 9, with Day 9 additionally showing significant differences between NY99 and KOUV B.

The reduced proportion of lymphocytes led to an overrepresentation of neutrophils, particularly in the WNV NY99- and SLEV B-infected mice, which, although not having significantly higher counts, showed significant increases in proportions on Day 3 ($p<0.001$ for SLEV B, and $p<0.035$ for NY99), with additional significance on Days 7 and 9 ($p<0.001$ for both) for WNV NY99. Monocyte proportions were significantly increased on Day 1 for WNV NY99 and SLEV B ($p<0.034$ and $p<0.002$, respectively, but not at any other time. Eosinophil levels and proportions remained reasonably unaffected, with only a slightly increased proportion on Day 9 with JEV B ($p<0.023$). No significant differences were observed in basophil counts or proportions throughout the experiment.

With regards to red blood cells and their associated metrics, few alterations of note were observed (Figure 4.7). For red blood cell count, hemoglobin levels, and hematocrit, the only significant differences compared to the mock were seen on Day 9 in samples collected from the JEV B-infected mice. The only other significant differences were seen with mean corpuscular volume, which was slightly, but significantly, decreased in the WNV NY99-infected mice on Day 3, and the BAGV B-infected mice on Day 7.

Cytokines and Chemokines

Plasma cytokine and chemokine levels were determined for the WNV NY99-, JEV B- KOUV B-, and SLEV B-infected mice on Days 1, 3, and 5 of the infection (n=3 per group per day), as well as for three mock-infected mice using the Milliplex MAP Mouse Cytokine/Chemokine 25-plex assay on a Bio-Rad Bioplex 200 instrument (Figure 4.8). These timepoints were chosen as peak viremia tends to be around Day 3, and the peak titers in peripheral organs are usually about Day 5. The majority of the differences in the data between the different chimeras occurred on Day 3, which tallies with the peak viremia.

IL-10 showed most variability early in the infection, with a decrease compared to the mock in the WNV NY99-, KOUV B-, and SLEV B-infected mice. By contrast, the JEV B-infected mice had a very slight increase in IL-10 concentration on Day 1. KOUV B had a greater than two-fold decrease in IL-10 levels, significantly different from both the mock and the JEV B-infected mouse samples. By Day 3, the WNV NY99-, KOUV B- and SLEV B-infected mouse levels had increased to become more similar to the mock, while the JEV B-induced concentrations had dropped to nearly half that of the mock. By Day 5 the samples were somewhat leveling out to mock-like concentrations.

IL-2 also showed significant chimera-specific differences, particularly with the SLEV B-infected mice. On Day 1, most of the samples were similar to the mock, with the exception of the KOUV B-infected mice, which, although not significant, had almost a 2-fold reduction in IL-2 levels. By Day 3, slightly raised IL-2 levels were observed in the WNV NY99- and KOUV B-infected mice. By contrast, the levels in the JEV B-infected mice were slightly lower than for the mock. Significantly higher levels (almost 2.5-fold higher than the mock) were observed in the SLEV B-infected mice compared to the

mock, WNV NY99, and the JEV B chimera. By Day 5 the cytokine levels in the infected mice were similar to the mock, although the KOUV B- and SLEV B-infected mouse levels were slightly higher.

The results for IFNγ were quite similar to those for IL-2, with little in the way of differences on Day 1 or Day 5, but a significant increase with the SLEV B-infected viruses on Day 3, compared to the mock, the WNV NY99-, and the JEV B-infected mice, with concentrations nearly 4-fold higher than for the mock-infected mice.

Small differences in the levels of IL-1α were observed, particularly with the SLEV B-infected mice on Days 1 and 3, but these differences were not statistically significance. Interestingly, on Day 3, all of the chimeric virus-infected mice showed a slight increase, but the values for the WNV NY99-infected mice remained similar to the mock mice throughout the assessed period.

IL-1β levels were for the most part similar to those of the mock mice on Day 1, although the values for the KOUV B-infected mice were slightly, but not significantly, lower. Day 3 showed an increase in levels for the WNV NY99-, KOUV B-, and SLEV B-infected mice, but not with the JEV B-infected mice. Differences between the JEV B-infected mice and the KOUV B and SLEV B samples were statistically significant. By Day 5 the levels were elevated with all of the viruses when compared to the mock.

IL-7 and IL-12 (p70) behaved very similarly to IL-1β, with SLEV B inducing an almost 2-fold increase over the mock on Day 3. KOUV B- and WNV NY99-infected mice also had increased IL-7 on Day 3, while JEV B maintained an almost mock-like level. By Day 5 the levels were greater than those of the mock for all of the viruses,

particularly the KOUV B-infected mice, who had a significant 2-fold higher concentration.

IL-4 showed no significant differences, but had a trend towards slightly raised levels on Days 3 and 5, particularly with the KOUV B and SLEV B chimeras. Similar results were seen for IL-6, IL-12 (p40), IL-13, and IL-15. In each of these cases, the levels in the JEV B-infected mice tended to be lower than the others on Day 3.

IL-5 responses appeared to be rather minimal on Day 1 and 3, but by Day 5 the levels in the WNV NY99- and KOUV B-infected samples had increased by 50-100% over the mock. Interestingly, the JEV B-infected samples were similar to, or slightly lower, than the mock at all three of the timepoints, and only a minor increase was seen on Day 5 with the SLEV chimera.

TNFα also showed little variability on Day 1, however by Day 3 the levels had increased with WNV NY99, KOUV B, and SLEV B, the latter having a significant 2-fold difference compared to the mock mice. The JEV B-infected mice did not see such an increase on Day 3, but by Day 5 all of the infected mice had 2-fold higher TNFα levels compared to the mock.

Some of the chemokines showed similar concentration profiles to some of the cytokines (Figure 4.8). MCP-1 showed some slight variation on Day 1, with a significantly lower concentration with the KOUV B-infected mice compared to WNV NY99. By Day 3, the levels in the WNV NY99-, KOUV B-, and SLEV B-infected mice were slightly raised compared to the mock and the JEV B mice. Day 5 saw increased concentrations across the board, particularly in the KOUV B-infected mice, but no significance. The MIP-1α concentrations told a similar story, except this time the

concentrations on Day 5 for the JEV B- and KOUV B-infected mice were significantly higher than the mock, although the elevated levels were similar to the WNV NY99- and SLEV B-infected mice.

MIP-1β and MIP-2 were only minimally altered during infection, with MIP-1β a little raised on Day 3 with the SLEV B chimera. RANTES showed little variability on Day 1, but was increased on Day 3, particularly in the SLEV B-infected mice, which showed a significant 2-fold increase over the mock. On Day 5 the levels were still increased for all of the viruses, with a significantly higher concentration in the JEV B-infected mice compared to the mock.

IP-10 showed the most change following infection. Day 1 saw increased levels for all of the viruses, particularly SLEV B. By Day 3, all of the viruses had significantly higher concentrations than the mock, with almost a 10-fold increase. These high concentrations persisted to Day 5 for the WNV NY99-infected mice, but had started to drop for the other chimeras, particularly the SLEV B-infected mice, whose increase over the mock was no longer significant.

G-CSF was interesting as the highest levels were with WNV NY99, rather than any of the chimeras as has generally been the case with the other factors studied. Although not significant, WNV NY99 induced a 2.5-fold increase on Day 3, and an almost 3.5-fold increase on Day 5. The chimeric viruses had levels similar to one another, but lower than WNV NY99 on Days 3 and 5.

Finally, GM-CSF showed an increase during the course of infection with all of the viruses, although for the JEV B-infected mice, this increase was delayed until Day 5, whereas the others saw increases two days earlier on Day 3.

Hierarchical clustering of the cytokine and chemokine data revealed that a number of the factors showed similar profiles to one another, particularly the T_H1 and T_H2-associated factors, including IL-2, IL-4, IL-5, IL-6, IFNγ, and TNFα (Figure 4.8). On Day 3 of the infection, most of these factors were slightly upregulated to similar degrees with WNV NY99 and the KOUV B chimera, barely affected with JEV B, and further upregulated with SLEV B. Other factors had slightly different profiles, with the monocyte/macrophage-associated chemokines MCP-1, GM-CSF, and MIP-1α clustering together separate from the main group of cytokines.

SERIAL SACRIFICE COMPARISON OF JEV A- AND JEV B-FORMS

In order to determine whether the subtle differences in mortality between the JEV A- and JEV B-infected mice following i.p. inoculation was associated with any differences in the course of infection, a serial sacrifice study was run to compare the temperatures and weights of the infected mice, as well as virus titers in harvested organs, over the during infection. Ten 3-4 week-old female Swiss Webster mice were microchipped to allow for weights and temperatures to be recorded during infection, five mice per virus. A further fifteen mice were used for organ sample acquisition on days 1, 3, 5, 7, and 9 post infection. The mice were infected with 100pfu virus administered i.p., with the virus titer in the doses confirmed by back titration.

The survival data clearly showed that the average survival time with the JEV A chimera is slightly longer than that of the JEV B chimera (10.1±1.5 days vs. 9.2±1.2 days), and that unlike with the JEV B chimera, there was one survivor (Figure 4.9A). Seroconversion, as determined by ELISA, confirmed that this mouse had indeed been infected. The temperature data showed the same trend as for the previous serial sacrifice study with the different B-forms (the JEV B data is the same as for that study), namely

that the virulent viruses cause a sharp drop in temperature over the days immediately prior to death (Figure 4.9B). Interestingly, the decrease is not quite as steep for the JEV A chimera compared to the JEV B one. The JEV A-infected mouse that survived showed no comparable temperature drop.

Both of the JEV chimeras induced weight loss from Day 7 onward in the mice that succumbed to the viruses (Figure 4.9C). As seen with the temperatures, the weight loss with the JEV A chimera was not as rapid as for the JEV B-infected mice. Unlike the other chimera-infected mice, weight loss was not observed in the survivor mouse, with the apparent drop between Day 6 and Day 8 also present in the mock-infected mouse data (not shown).

Comparison of virus titers in multiple organs showed some minor differences between the JEV A- and JEV B-forms, but nothing that was statistically significant (Figure 4.10). Infection with both viruses led to a viremia that peaked on Day 3, and persisted until Day 5 (Figure 4.10A). Although the JEV A chimera was detected earlier in the brain than JEV B, the titers for JEV A on Day 3 were at the limit of detection for the assay, and by Day 5 the JEV B virus had reached a 10-fold higher mean titer than the A-form. On Days 7 and 9 the brain titers were somewhat variable, but it appears that the titers of the B-form tend to be higher than those of the A-form by the end of the experiment (Figure 4.10B).

As is usual for WNV, no detectable virus was present in the liver, and the data for the spleen showed similar titers for both viruses at each timepoint (Figure 4.10C,D). The lung data showed some differences between the two viruses, particularly on Day 3, where all three of the JEV B-infected mice, but only one of the JEV A-infected mice, had detectable virus (Figure 4.10E). The A-form-infected mice appeared to have virus present

for longer than the B-form, but at each timepoint, only a proportion of the mice were positive for infection. The kidney data showed a little variability between the two viruses, with average titers being almost 10-fold higher on Day 5 for the B-form, but by Days 7 and 9 the titers, and prevalence of infection, was starting to wain (Figure 4.10F). Hematological analysis was run on the blood from each mouse, but no significant differences were observed with any parameter (Data not shown).

DISCUSSION

The animal data shows that the effects of EIII substitution on virulence and pathogenesis within the animal model can be quite variable. Even viruses that grow similarly to WNV NY99 *in vitro*, such as SLEV B, can have drastically different behavior when introduced to a whole organism.

Within the animal model, WNV NY99 is highly pathogenic, whether administered via the i.p. or i.c. route. This was clear from the virulence studies, which showed 100% mortality with 100pfu i.p. and with both 100 and 10pfu i.c. By contrast, the backbone virus containing the four restriction sites was slightly, but statistically significantly, attenuated following i.p. inoculation. This virus only differed from NY99 by a conservative V290L mutation in the EI, at the location of the SalI site, but caused a significantly different survival curve with an average survival time of 10.25±1.2 days, compared to 8.8±1.0 days for NY99, with this extended survival time associated with an increase in observed gastrointestinal swelling, previously described for WNV (Nagata et al., 2015). This mutation has been observed in a naturally-occurring WNV isolate without additional mutations nearby, and is present in a significant proportion of JEV isolates, suggesting that it does not preclude virus survival in nature, but to minimize any

confounding effects on the chimeras, the B-versions were used for the majority of the comparisons as they lack this substitution (Ergunay et al., 2015).

The serial sacrifice study data for WNV NY99 is in keeping with previously published studies, as well as other studies carried out in our laboratory (see Chapter 5) (Peña et al., 2014). Few clinical signs of infection were observable for the first seven days post inoculation, with the mice apparently lacking the febrile phase usually seen in WNV infection of humans and non-human primates (Weiss et al., 2001, Melnick et al., 1951). However, it is possible that the fever was transient, and was not detected by daily temperature measurement. Continuous monitoring of temperature would be necessary to rule out such an occurrence.

Following seven days of subclinical infection, weights and temperatures started to decrease rapidly from Day 7 and Day 8, respectively, until death. At this point, other clinical signs of infection started to develop, including ruffling of the fur, tremors, and occasional hind-limb paralysis, particularly in the mice that survived until Day 9. Weight loss has been previously associated with anorexia in infection, for which a number of cytokines have been implicated, including IL-1, IL-2, IL-6, IL-8, TNFα, and IFNγ (Langhans, 2000). A number of these, particularly IL-1β, IL-6, and TNFα, are upregulated in the plasma of mice infected with all of the viruses on Day 5, with a number of the other cytokines differentially upregulated on Day 3, but returning to near-normal levels by Day 5.

Similar to previous descriptions, WNV NY99 was shown to be capable of infecting a range of organs within the host, with the exception of the liver. Strong viremia was observed, with a peak around 10^5 pfu/ml on Day 3, although this was effectively cleared such that, from Day 5 onward, virus was no longer detectable in the plasma of

any of the WNV NY99-infected mice. Virus titers in peripheral organs, including the spleen, kidney, and lung, were below the limit of detection on Day 1 post infection, but increased thenceforth such that by Day 5, mean titers in all three organs were between 10^4 and 10^5 pfu/100mg tissue. Other studies (see Chapter 5) have shown a peak peripheral organ titer on Day 5, with titers waning thereafter, so later timepoints were not characterized. Within the brain, neuroinvasion with WNV NY99 was associated with high virus titers on Days 7 and 9, consistent with the encephalitic nature of WNV infection.

The JEV chimeras behaved very similar to WNV NY99 *in vivo*. Following i.p. inoculation, only JEV A had a significantly different survival curve compared to NY99, although only the B-form had NY99-like 100% mortality. Similarly, mortality rates following i.c. inoculation with JEV B were very high (80% with 10pfu, 100% with 100pfu) indicating that the substitution of JEV EIII had minimal attenuating effect on the neurovirulence of the chimera.

Direct comparison of the slightly attenuated JEV A with JEV B showed some differences between the infection profiles that may be partially attributable to the additional sequences up- and downstream of EIII in the A-form. Although the survival curves for the two viruses were not statistically significantly different from one another, mice infected with JEV A had a slightly increased average survival time (10.1±1.5 days for JEV A compared to 9.2±1.2 days for JEV B), which was associated with a less rapid decrease in temperature and weight compared to the JEV B-infected mice, suggesting that disease progression may be slightly slower. This fits with an observation of increased levels of intestinal swelling in the JEV A-infected mice, similar to those infected with the four restriction site backbone virus.

Comparison of organ titers showed no statistically significant differences, but qualitative differences were observed for some of the tissues. In general, titers were higher with JEV B, although JEV A appeared to persist slightly longer in the lung. Neuroinvasion was first seen on Day 3 with JEV A compared to Day 5 for JEV B, but from Day 5 onward the JEV B titers were often substantially higher than JEV A, although slightly more variable. Peak peripheral organ titers for both viruses were on Day 5, with the majority of titers either remaining similar or dwindling on Days 7 and 9. The lack of clear differences between JEV A and B with respect to tissue titers is not particularly unexpected. The additional upstream JEV sequence present in the A-form contains four amino acid differences compare to the WNV sequence present in the B-form: V290L (a substitution present in the original JEV sequence, rather than a SalI-induced change), a conservative K291R, a similarly conservative E293D, and a less conservative Q296A. In the downstream region there is only one amino acid difference between the A- and B-forms: a conservative T409S. Of these differences, the Q296A appears to be the most significant difference, although this does not mean that it is solely, or even partly, responsible for the subtle differences in the infection profiles of JEV A and JEV B.

The infection profile of JEV B was rather similar to that of WNV NY99. In addition to a lack of significant differences between their survival curves, weight loss and temperature changes following infection were almost identical. The organ titers for JEV B were reasonably similar to those for WNV NY99, but were often slightly lower. This is apparent with the plasma titers, which showed a 10-fold lower peak viremia on Day 3 with JEV B compared to NY99. Wild-type JEV tends to grow poorly in mice, with lower viremia titers, so the observed lower peak viremia of the chimera compared to the parental strain, despite preserved mortality, is interesting (Rokutanda, 1969). The fact that a strong viremia is still present on Day 5 for the JEV B chimera, when virus is no longer detectable for WNV NY99, further suggests a shift in the profile of the chimeric

virus compared to the parent. Neuroinvasion with JEV B appears more variable than with WNV NY99, with less than 100% neuroinvasion at each timepoint with JEV B. Similarly, compared to WNV NY99, which showed increasing virus titers in the lung on Day 3 and Day 5, JEV B has titers similar to WNV NY99 on Day 3, but complete absence on Day 5.

Substitution of EIII from KOUV into WNV resulted in a virus with peculiar behavior *in vivo*. Despite having an EIII sequence 90% identical to WNV NY99 at the amino acid level, it was significantly attenuated by both the i.p. and i.c. routes. Intraperitoneal challenge with 100pfu doses of each of the KOUV constructs caused no more than 40% mortality, while i.c. inoculation with KOUV B resulted in a less dose-responsive result compared to the other viruses, with 60% mortality following 100pfu dose, and 40% following a 10pfu dose, suggesting that the attenuation of the KOUV B may be variable.

When the infection following i.p. inoculation with KOUV B was studied in more detail in the serial sacrifice study, the results were rather surprising. Similar to WNV NY99 and JEV B, the KOUV B-infected mice had a weight loss from Day 7 onward, but unlike the loss with the highly-virulent viruses, this loss was less severe, but more protracted, with values either decreasing or remaining steady for a further seven days before increasing in a manner similar to the mock-infected mice. Temperature drops were observed in the KOUV B-infected mice that succumbed to infection, but these decreases are obscured in the graph by the surviving mice, in which no temperature losses were measured.

Organ titrations revealed that the tissue distribution of KOUV B following infection was considerably restricted compared to WNV NY99, suggesting a significant

tropism change for the virus. Indeed, although the virus generated a viremia very similar to that of WNV NY99, consistent spread to other organs was only observed for the kidney, in which the titers were similar to NY99, and higher than for JEV B. The exact reasons behind the tropism change and variable attenuation of the KOUV B chimera is uncertain. Surprisingly, despite a 40% mortality rate, neuroinvasion was rarely observed, with only one mouse with detectable virus in the brain (Day 7). This may be presented as a loss of neurotropism, but the definition is a rather complicated affair, requiring a balance between neuroinvasion and neurovirulence. Most flaviviruses maintain a degree of neurovirulence when administered directly into the brain. Even DENV, which few would view as neurotropic, can cause mortality after i.c. administration in suckling mice (Gualano et al., 1998). By this definition, KOUV B could be said to have lost its neurotropic phenotype, quite a significant feat for a virus that is predominantly WNV. Wild-type KOUV has been demonstrated to be highly pathogenic in mice, with an affinity for the spleen (Prow et al., 2014). By comparison, the KOUV chimera is less pathogenic, with splenic titers substantially lower than for WNV NY99, suggesting that the observed behavior of the virus is different to both the backbone and donor viruses. It is possible that the attenuation results from the apparently increased adhesiveness of the virus, and the difference in Endo H sensitivity, as suggested by the data in the previous chapter. Whatever the cause(s) of its attenuation, the restriction of the virus compared to NY99 appears to be limited to particular cell types, with the virus demonstrating NY99-like titers in both the blood and the kidney.

An additional significant attenuation was observed with the SLEV chimeras, which, throughout the course of the studies, failed to cause lethal infection following i.p. inoculation with any of the four versions. Even the i.c. dosing showed signs of attenuation of neurovirulence, with significantly lower mortality following a 10pfu dose (30%) compared to the WNV NY99-infected mice (100%).

Surprisingly, despite the complete attenuation of SLEV B when administered peripherally, weight loss during infection was almost identical to that observed for KOUV B, suggesting that clinical, but non-lethal, disease is occurring. Peak viremia is substantially lower than for the more virulent viruses, and consistent spread to other organs following the viremia was not observed for the tissues characterized. Previous studies with pathogenic and attenuated SLEV strains in suckling mice have shown that even lethal infections are often associated with relatively low peak viremia titers (around $4x10^3$ pfu/ml), while attenuated strains usually cause viremias that are less than 10^2 pfu/ml (Monath et al., 1983). The peak viremia for the SLEV B chimera, $6.2x10^2$ pfu/ml, would put it somewhere in between, however the use of suckling mice for the WT SLEV experiment may give higher titers than would be seen in young adult mice, such as those used for these studies, and thus affect the comparison. Nevertheless, it appears that the low viremia of SLEV B may be attributable to the SLEV EIII, potentially affecting the rate of infection of early target cells, such as dendritic cells.

In spite of a more diverse EIII sequence, and apparently reduced particle stability, compared to SLEV B (see Chapter 3), BAGV B had greater associated mortality following i.p. inoculation (20%), although lower neurovirulence following i.c. administration (80% mortality with 100pfu, 20% mortality with 10pfu). Weight loss, as measured during the serial sacrifice study, was minimal, with an average decrease of 0.5g/day on Days 8 and 9, in stark contrast to even the avirulent SLEV B virus. Similar to the other non-lethal infections, no temperature decreases were seen during the infections. Although a viremia similar in magnitude to that of SLEV B was observed, virus spread to other tissues was minimal, with only the spleen showing detectable levels of virus in two of the three mice on Day 5, with titers barely higher than the limit of detection. Nevertheless, the 20% mortality rate indicated that lethal infection with the chimera was possible, although the cause of death is uncertain.

Hematological data from infected mice showed an apparent general leukocytopenia on Days 1 and 3 for all of the viruses. While the values for the KOUV B-, SLEV B-, and BAGV B-infected mice started to recover from Day 5 onward, the values for the WNV NY99-infected mice remained low, particularly on Day 7. The values for the JEV B-infected mice were rather variable. Lymphocyte counts and proportions were particularly affected during the course of infection, with percentages around 65% for almost all of the viruses on Day 3, compared to 80% for the mock mice, dropping to levels below 50% for WNV NY99 on Day 7. Other hematological parameters, including those concerned with red blood cells, such as RBC count and hematocrit, remained essentially normal. These observations are similar to those made with human patients during the outbreak in New York in 1999 (Nash et al., 2001). During that outbreak, patients had little in the way of hematological abnormalities, with WBC counts within normal range, but with a mean lymphocyte percentage of 14.1% compared to the normal range of >25% (Nash et al., 2001).

The cytokine and chemokine data reveal quite a bit about the early immune responses to the chimeras, and potentially help to explain some of the differences observed in neuroinvasion and virulence. The greatest variability between the different viruses is on Day 3, which corresponds to the peak viremia. Compared to some of the chimeras, WNV NY99 appears to be quite efficient at minimizing immune responses early in the course of infection. Many of the pro-inflammatory cytokines, such as IL-1α, IL-1β, IL-2, and IFNγ, are only minimally affected over the first 5 days of infection, while some others, such as Il-6, IL-12, and TNFα are upregulated on Days 3 and 5, but less so than with some of the other viruses. IL-10 levels were slightly lower than the mock for each timepoint, suggesting a mild inhibition of anti-inflammatory responses. With the chemokines, WNV NY99 fails to induce significant expression during the first five days of infection, with the exception of IP-10 (CXCL10). Levels of this chemokine

are significantly and substantially increased on Days 3 and 5, but this increase is not unique to NY99. The role of CXCL10 in WNV infection is not well understood. Some studies have shown that secretion of IP-10 by neuronal cells leads to the recruitment of $CD8^+$ T-cells, with inhibition of IP-10 leading to increased viral titers in the brain and enhanced morbidity and mortality (Klein et al., 2005). The role of circulating IP-10 during WNV infection is unknown. Interestingly, levels of circulating G-CSF were highest in WNV NY99-infected mice. This factor is involved in neutrophil survival and proliferation, as well as granulocyte production; its role in WNV infection is unknown.

The JEV B chimera also appears to be efficient at minimizing, or failing to stimulate, immune responses, particularly on Day 3, where cytokine levels were often lower than that of WNV NY99, in spite of a similar-magnitude viremia. Compared to WNV NY99, some of the largest differences occur with IL-5 and IL-10. Unlike any of the other viruses, IL-10 levels on Day 1 were the same as the mock, with a drop on Day 3 before rising again on Day 5. IL-5 levels remained the same over the course of the five days, in contrast to WNV NY99 and KOUV B, which saw an increase on Day 5. Both IFNγ and TNFα levels were least affected in the JEV B mice on Day 3, but by Day 5 the levels had increased to those of the other viruses. The low IFNγ level may help to explain the prolonged viremia and apparently earlier neuroinvasion of the JEV B chimera compared to WNV NY99. Studies by Shrestha *et al*. demonstrated that WNV infection of mice lacking IFNγ saw higher viremia titers on Day 5, and earlier neuroinvasion compared to wild-type control mice (Shrestha et al., 2006). Some minor differences in chemokine levels were seen with the JEV B chimera compared to the mock and the other viruses. MIP-1α was significantly higher than the mock on Day 5, but minimally higher than with the other viruses. RANTES was also significantly higher than the mock on Day 5, and slightly higher than the other viruses.

In general, the KOUV B chimera failed to silence the immune response as efficiently as WNV NY99 and the JEV B chimera. For most of the pro- and anti-inflammatory cytokines, as well as the chemokines, the values for the KOUV B-infected mice on Day 3 are second highest of all the viruses, with the other viruses catching up on Day 5. Interestingly, on Day 1, IL-10 levels in the KOUV B-infected mice are the lowest of any of the viruses, less than half those of the mock-infected mice. Studies looking at the role of IL-10 during WNV infection have shown that inhibition of IL-10 signaling leads to improved control of infection through the upregulation of type I interferon and Th1 responses, including IFNγ (Bai et al., 2009). Although IFNγ levels with the KOUV B chimera are slightly elevated compared to the mock and WNV NY99 values, they are certainly not as high as those seen for SLEV B. Nevertheless, the slightly stronger IFNγ response may help to explain the lower virulence of KOUV B compared to WNV NY99.

The SLEV B chimera-infected mice consistently had the highest levels of circulating cytokines on Day 3, particularly the T_H1 immune factors IL-2 and IFNγ, shown to be important in protection against WNV, which were significantly different to all but the KOUV B-infected mice (Bai et al., 2009, Shrestha et al., 2006). This suggests a strong pro-inflammatory response early in the course of infection. Both of these cytokines are expressed by dendritic cells and T-cells, suggesting a potential role for these cell types early in infection. Indeed, previous studies have suggested that dendritic cells may be early targets during WNV infection, supporting the idea that these cells may be the source of these cytokines (Suthar et al., 2013b, Johnston et al., 2000). One of the chemokines significantly upregulated during SLEV B infection, RANTES (CCL5), has been shown to be upregulated in mouse brain endothelial cells infected with the attenuated WNV MAD78 strain compared to NY99 (Hussmann and Fredericksen, 2014). Whether it has a protective effect, and whether circulating RANTES induces the same effects are unclear, however studies by Terao *et al*. suggest that RANTES may play a role

in increasing blood-brain barrier permeability, which one might expect to lead to increased neuroinvasion (Terao et al., 2008).

Increased cytokine levels may contribute to the reduced neuroinvasion and peripheral organ infection seen during KOUV B and SLEV B infection by accelerating virus clearance by the immune system. Since the exact mechanism of neuroinvasion by WNV is unclear, it is hard to hypothesize the effect the increased cytokine levels may have. IL-1β, IFNγ, and TNFα have all been implicated as cytokines that can permeabilize the blood-brain barrier, however, since these cytokines are highest in the KOUV B- and SLEV B-infected mice, the two viruses that show the least neuroinvasion, the question of BBB permeability as a major route for neuroinvasion remains unanswered (Wong et al., 2004, Argaw et al., 2006, Lv et al., 2010). Since these cytokines are not particularly elevated in the WNV NY99- and JEV B-infected mice during the days prior to neuroinvasion, it suggests that BBB permeability may not be the main route of entry for WNV into the brain. Indeed, a number of studies have suggested that infection of the brain starts with the olfactory bulb (Suen et al., 2014). Studies by Lazear *et al*. have suggested a role for IFNλ in decreasing blood-brain barrier permeability during WNV infection, reducing neuroinvasion (Lazear et al., 2015). Altered levels of this cytokine may explain the differences observed in neuroinvasion, but as it was not part of the panel screened, this is just a speculation.

The *in vivo* studies clearly show that EIII chimerization has a significant effect on virulence within the mouse model, an effect that often does not correspond to growth *in vitro* or the EIII sequence diversity compared to WNV NY99. Indeed, for KOUV B it appears that, contrary to the findings of Suthar *et al*. immune responses alone cannot explain the tropism differences between it and WNV NY99, as most of the plasma cytokine and chemokine levels are similar in the mice infected with each virus (Suthar et

al., 2013a). The failure to effectively spread to the brain and peripheral tissues other than the kidney following a viremia of similar magnitude to WNV NY99 suggests that the change in tropism may be directly attributable to the substituted EIII. Whether the attenuation of SLEV B is dependent upon host immune responses or differences in receptor usage arising from the EIII substitution is uncertain. Clearly, significant differences in innate immune responses are occurring, including the increase of IL-2 and IFNγ levels in the plasma on Day 3, the latter of which has been shown to contribute significantly to early antiviral responses against WNV (Shrestha et al., 2006). These observations do not preclude the possibility of alternative receptor usage. Indeed, the differences in immune response induction are suggestive of differential signaling pathway activation following receptor binding, with the most likely cause of this being differences in the receptors utilized.

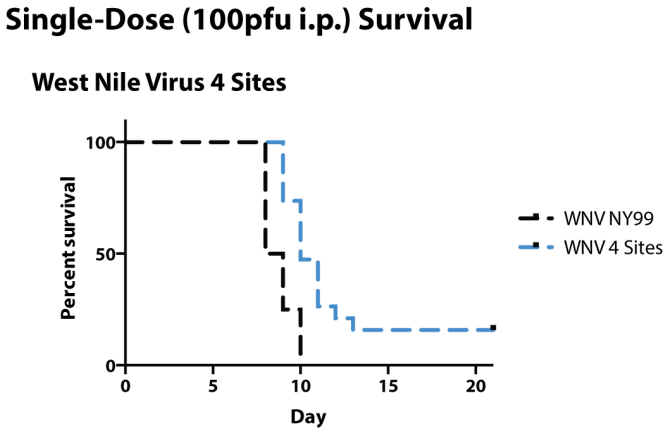

Virus	AST (Days)	Std Dev
WNV NY99	8.75	0.96
WNV 4 Sites	10.25	1.18

Figure 4.1: Virulence of WNV 4 Sites Following i.p. Inoculation. *Top*: 3-4 week-old female Swiss Webster mice were infected with 100pfu of WNV NY99 (n=4) or WNV 4 Sites (n=19). Statistical significance ($p<0.0048$) was demonstrated by Log-rank (Mantel-Cox) test. *Bottom*: Average survival times (AST) with standard deviations were calculated for the mice that succumbed to infection.

Single-Dose (100pfu i.p.) Survival

A) JEV Chimeras

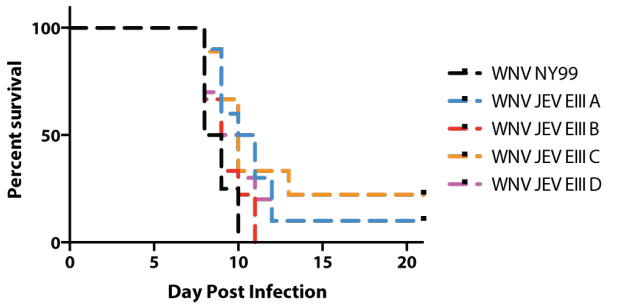

Donor Virus	AST (Days)	Std Dev
WNV IC JEV EIII A	10.10	1.45
WNV IC JEV EIII B	9.22	1.20
WNV IC JEV EIII C	9.86	1.57
WNC IC JEV EIII D	9.44	1.42

B) KOUV Chimeras

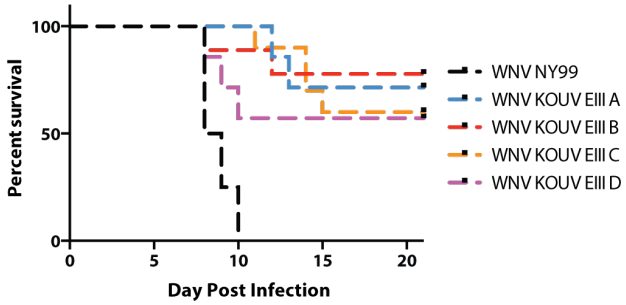

Donor Virus	AST (Days)	Std Dev
WNV IC KOUV EIII A	12.50	0.71
WNV IC KOUV EIII B	10.00	2.83
WNV IC KOUV EIII C	13.50	1.73
WNC IC KOUV EIII D	9.00	1.00

C) SLEV Chimeras

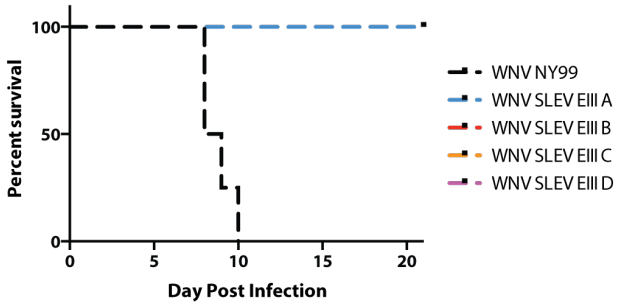

Donor Virus	AST (Days)	Std Dev
WNV IC SLEV EIII A	N/A	
WNV IC SLEV EIII B	N/A	
WNV IC SLEV EIII C	N/A	
WNC IC SLEV EIII D	N/A	

D) BAGV Chimeras

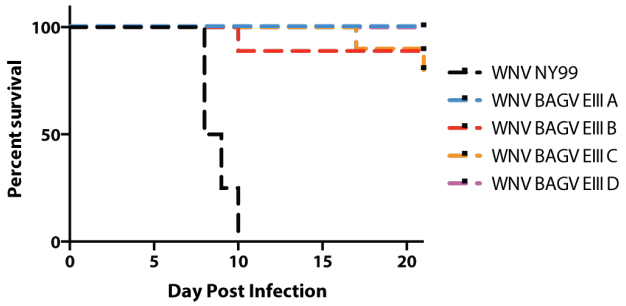

Donor Virus	AST (Days)	Std Dev
WNV IC BAGV EIII A	N/A	
WNV IC BAGV EIII B	10.00	0.00
WNV IC BAGV EIII C	19.00	2.83
WNC IC BAGV EIII D	N/A	

Figure 4.2: Virulence of Chimeric Viruses Following i.p. Inoculation. Swiss Webster mice were infected with 100pfu virus i.p. (n=5 or 10). For the mice that succumbed to infection, average survival times with standard deviations were calculated.

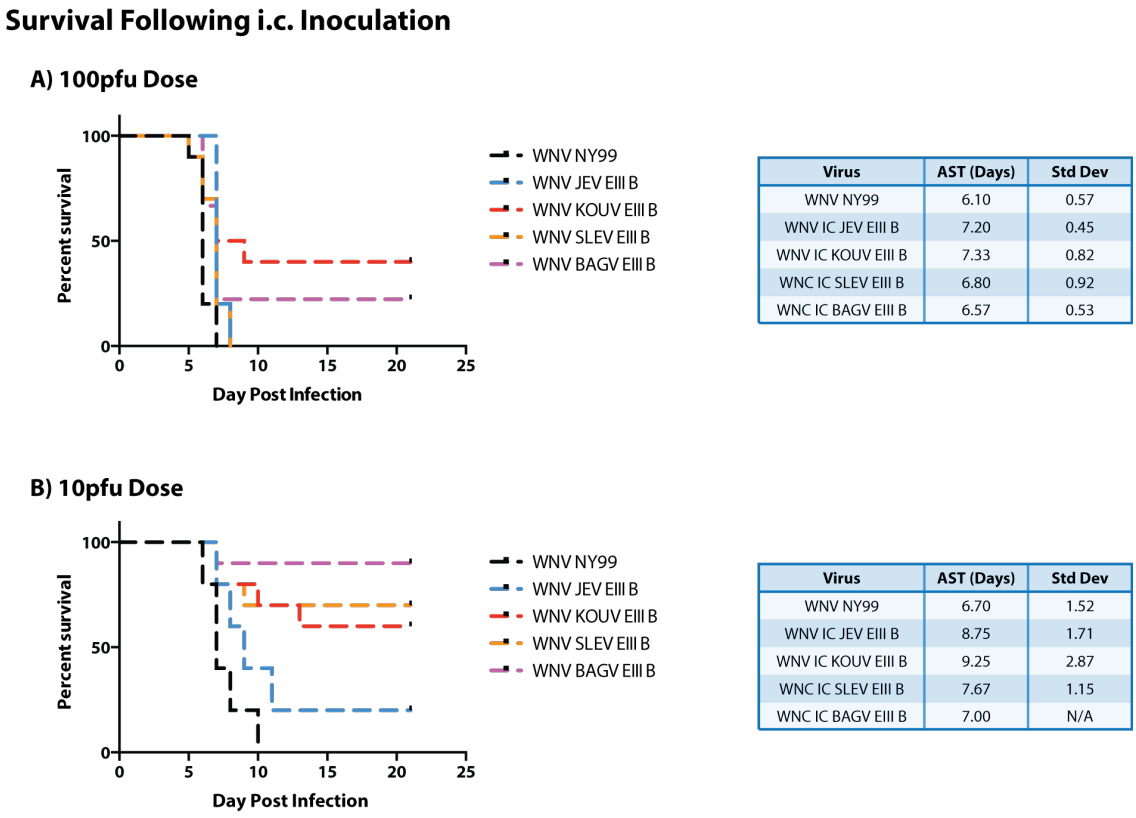

Virus	AST (Days)	Std Dev
WNV NY99	6.10	0.57
WNV IC JEV EIII B	7.20	0.45
WNV IC KOUV EIII B	7.33	0.82
WNC IC SLEV EIII B	6.80	0.92
WNC IC BAGV EIII B	6.57	0.53

Virus	AST (Days)	Std Dev
WNV NY99	6.70	1.52
WNV IC JEV EIII B	8.75	1.71
WNV IC KOUV EIII B	9.25	2.87
WNC IC SLEV EIII B	7.67	1.15
WNC IC BAGV EIII B	7.00	N/A

Figure 4.3: Virulence of Chimera B-Forms Following i.c. Inoculation. 3-4 week-old female Swiss Webster mice were inoculated with 10 or 100pfu of WNV NY99 (n=5 each), JEV B (n=5 each), KOUV B (n=10 each), SLEV B (n=10 each), or BAGV B (n=10 each) via the i.c. route. Average survival times with standard deviations were calculated for all of the viruses.

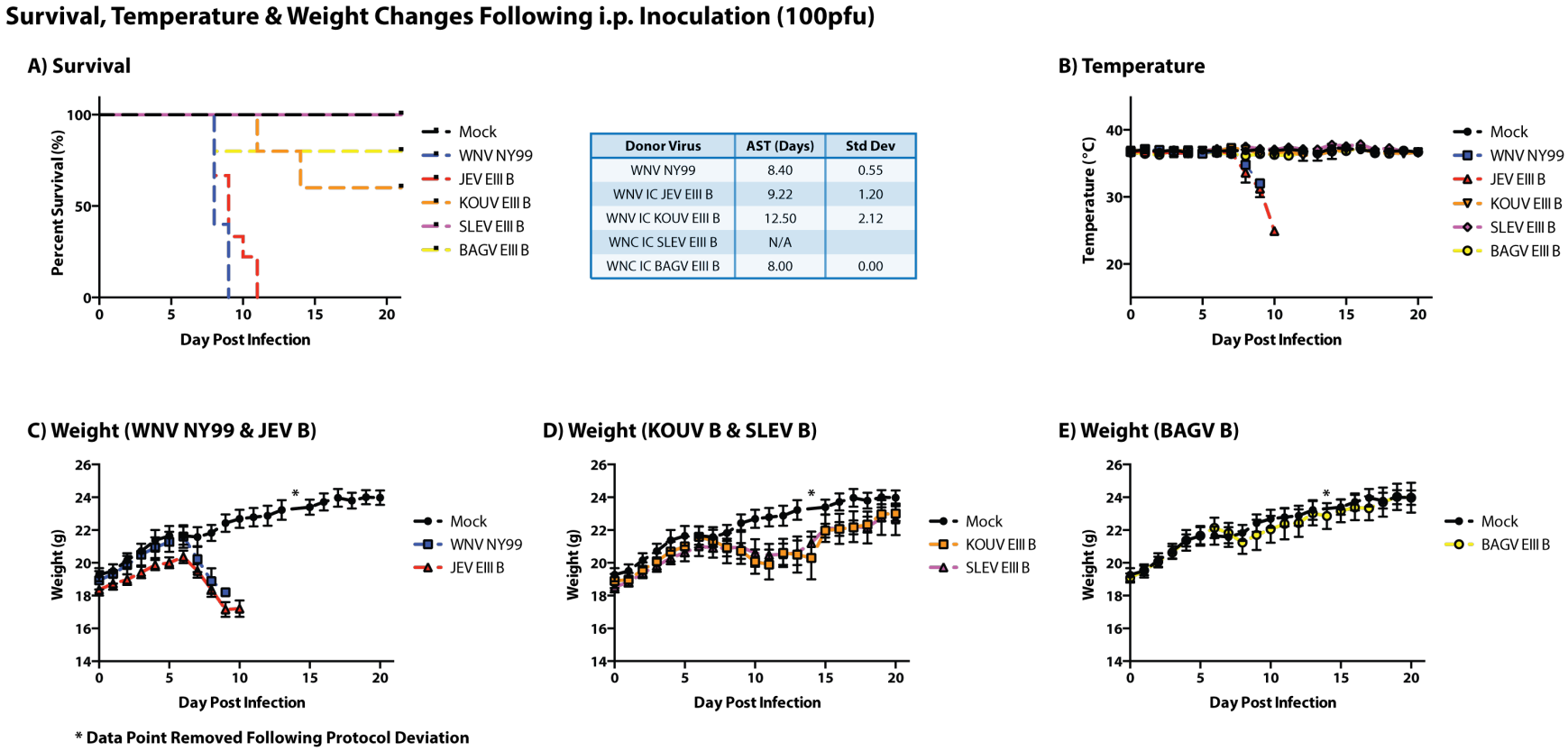

Donor Virus	AST (Days)	Std Dev
WNV NY99	8.40	0.55
WNV IC JEV EIII B	9.22	1.20
WNV IC KOUV EIII B	12.50	2.12
WNC IC SLEV EIII B	N/A	
WNC IC BAGV EIII B	8.00	0.00

Figure 4.4: Survival, Temperature, and Weight Changes Following i.p. Inoculation with B-Form Chimeras. Groups of five 3-4 week-old female Swiss Webster mice were infected with 100pfu of WNV NY99 or a B-form chimera via the i.p. route. (*A*) Average survival times with standard deviations were calculated for mice infected with each virus. Temperatures (*B*) and weights (*C*, *D*, *E*) were measured daily for 21days following infection. Three different weight profiles emerged, one for the WNV NY99- and JEV B-infected mice (*C*), one for the KOUV B- and SLEV B-infected mice (*D*), and a third for the BAGV B-infected mice (*E*).

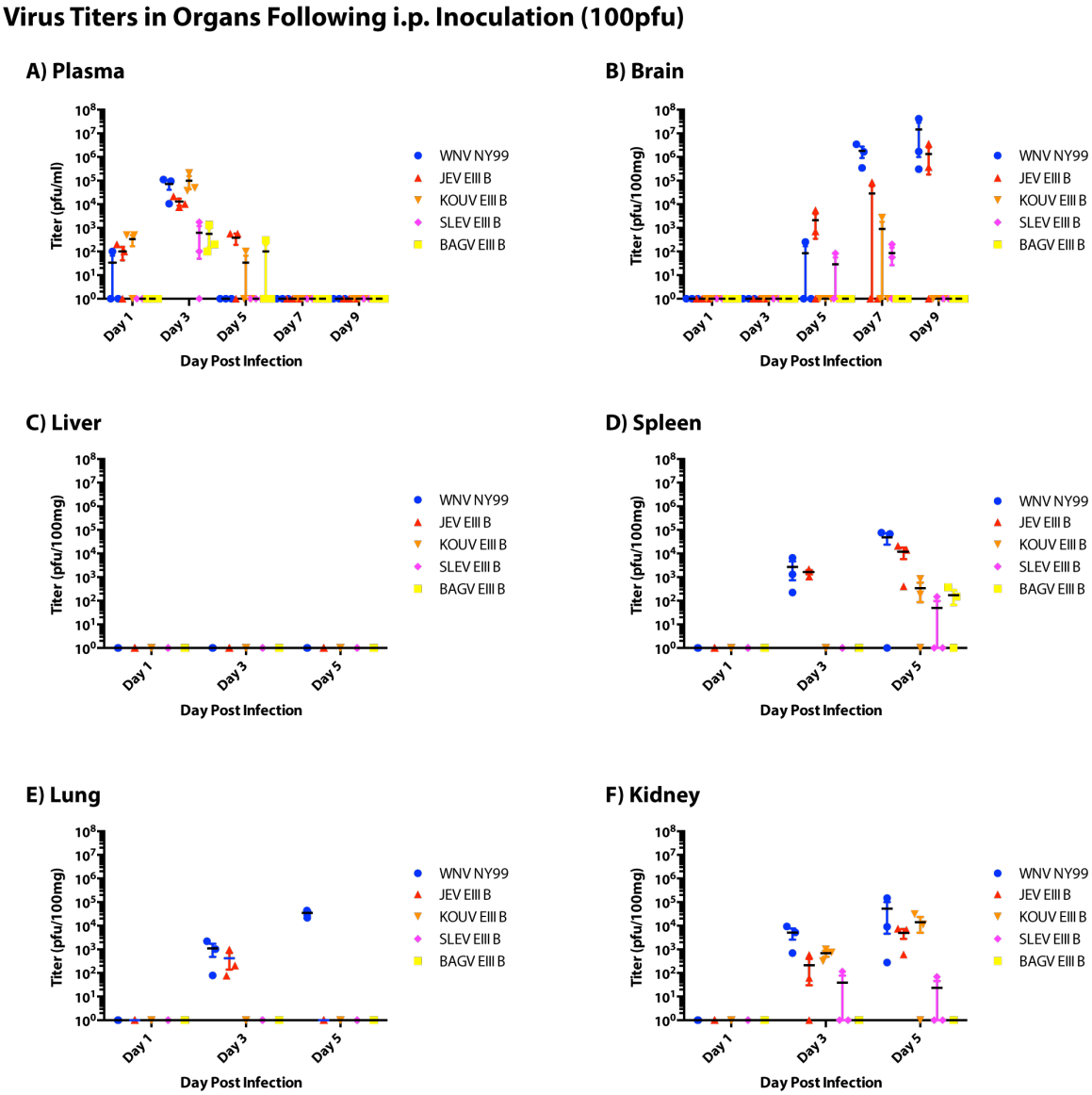

Figure 4.5: Organ Titers Following i.p. Inoculation. 3-4 week-old female Swiss Webster mice were inoculated with either WNV NY99 or one of the B-form chimeras with 100pfu i.p. Three mice per group were euthanized on Days 1, 3, 5, 7, and 9, with blood and organs removed for titration. Plasma (*A*) and brain (*B*) titers were determined for all of the timepoints, while liver (*C*), spleen (*D*), lung (*E*), and kidney (*F*) titers were determined for Days 1, 3, and 5. Graphs show individual values with mean and standard error.

Hematological Data

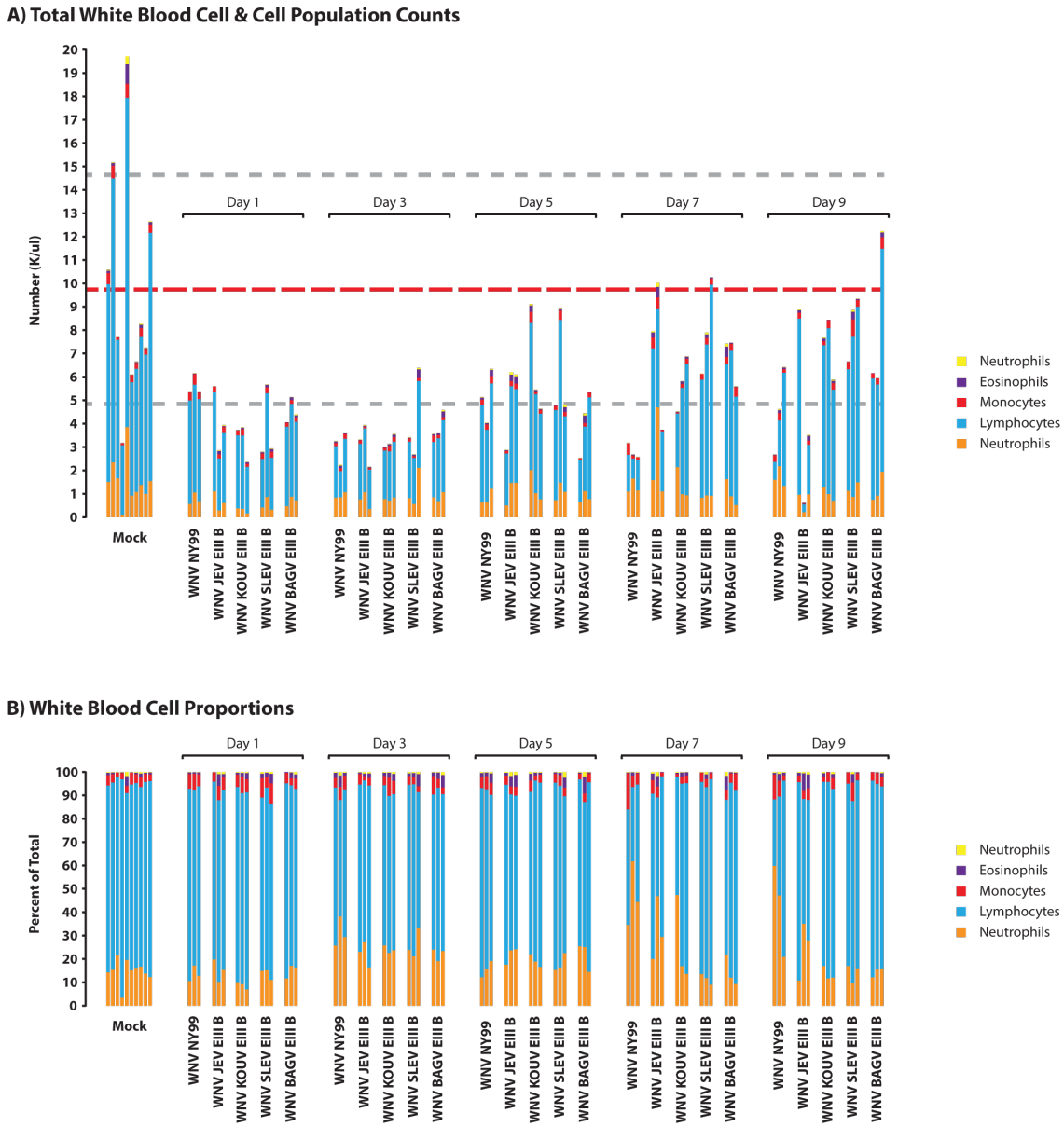

Figure 4.6: White Blood Cell Counts and Proportions Following i.p. Inoculation. Blood taken from the mice euthanized as part of the serial sacrifice study was analyzed to determine hematological parameters. *A*: Counts for total white blood cells and cell populations were determined. The mean value for the mock-infected mice is represented by the red dashed line, with the grey lines representing mean ± 1SD. *B*: Proportions for white blood cell populations.

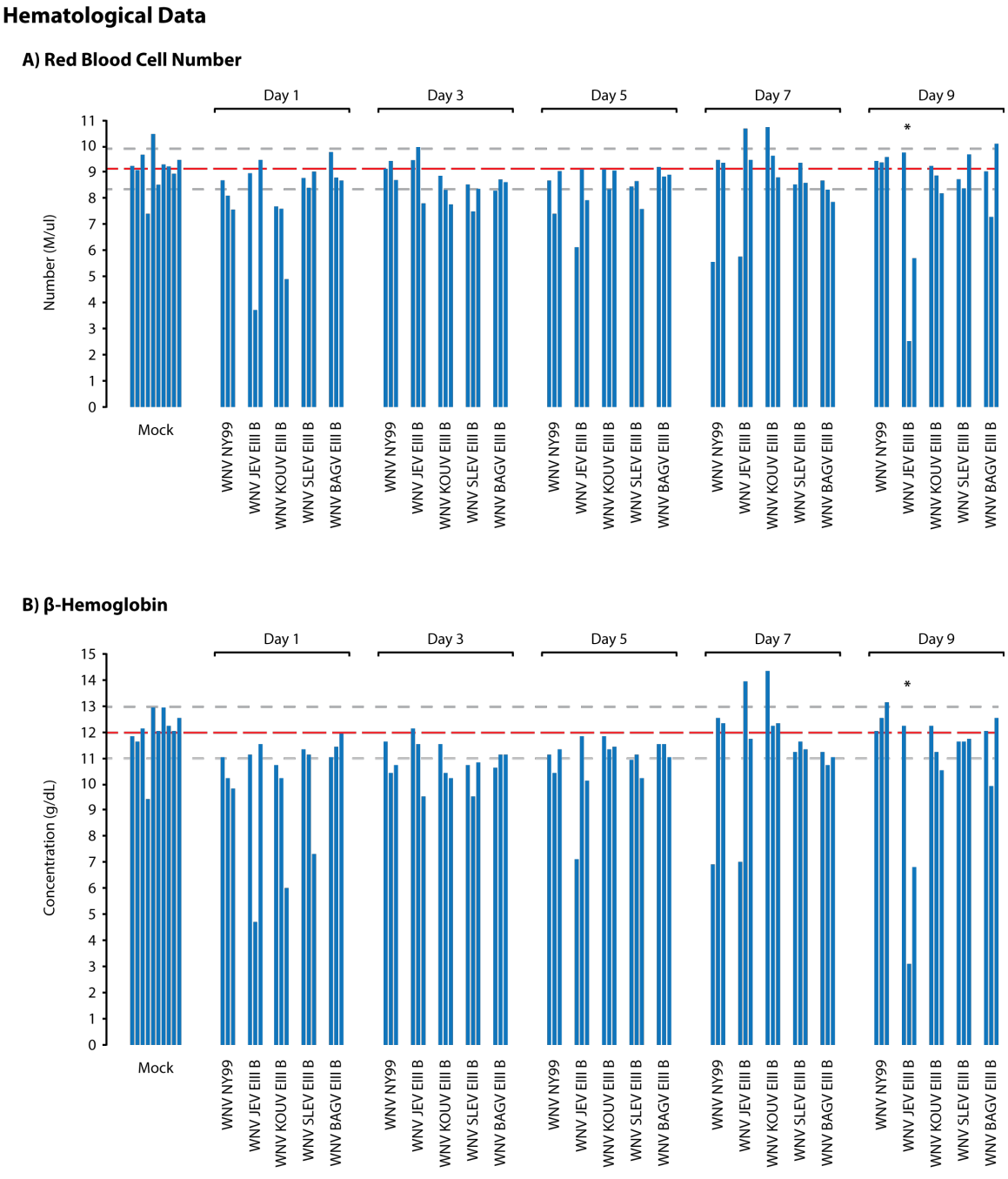

Figure 4.7: Hematological Values Following i.p. Inoculation. Blood taken from the mice euthanized as part of the serial sacrifice study was analyzed to determine hematological parameters. *A*: Red blood cell counts. *B*: β-hemoglobin levels. The mean value for the mock-infected mice is represented by the red dashed line, with the grey lines representing mean ± 1SD.

Hematological Data

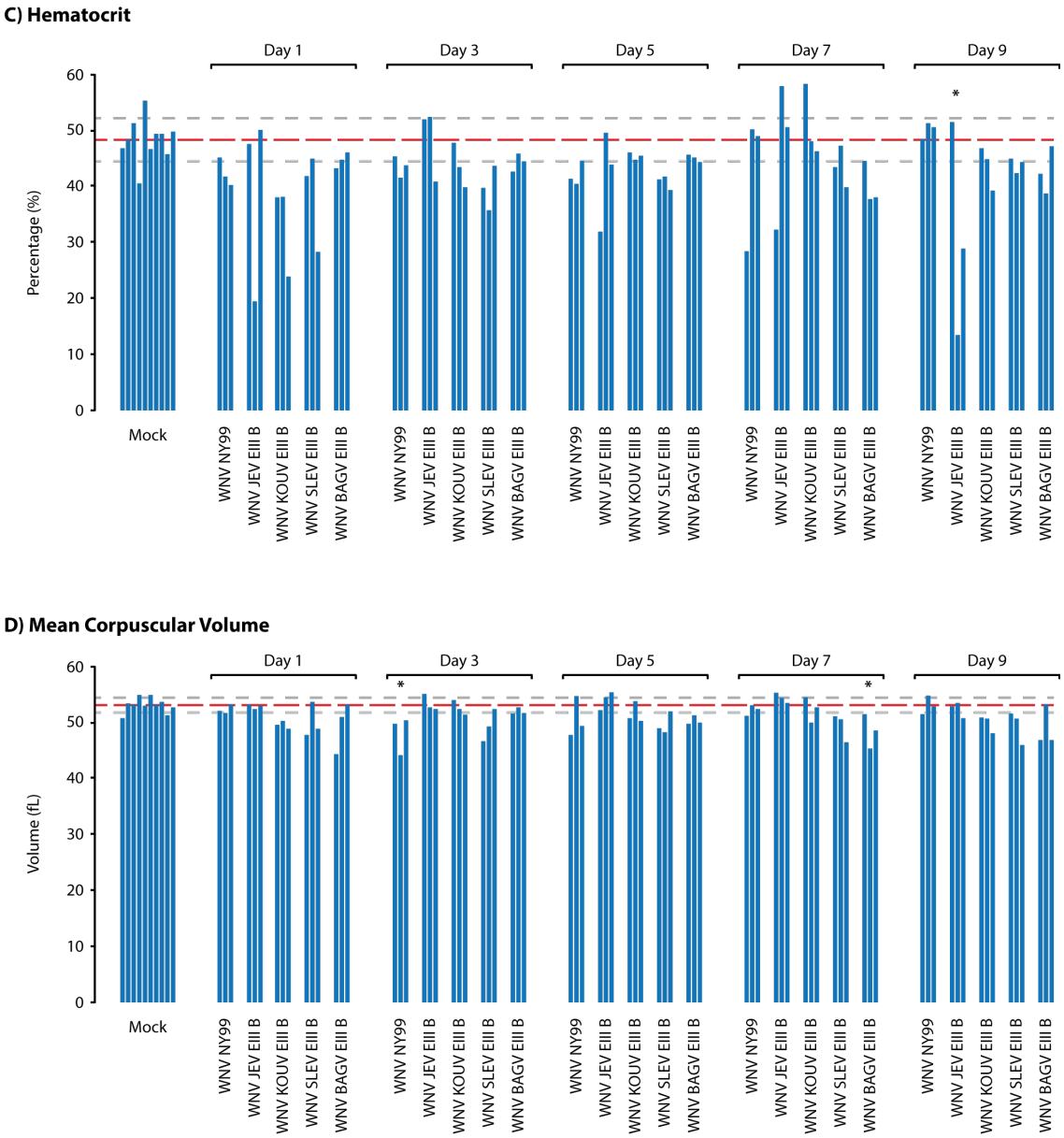

Figure 4.7: (Continued) Hematological Values Following i.p. Inoculation. Blood taken from the mice euthanized as part of the serial sacrifice study was analyzed to determine hematological parameters. *C*: Hematocrit levels. *D*: Mean corpuscular volumes. The mean value for the mock-infected mice is represented by the red dashed line, with the grey lines representing mean ± 1SD.

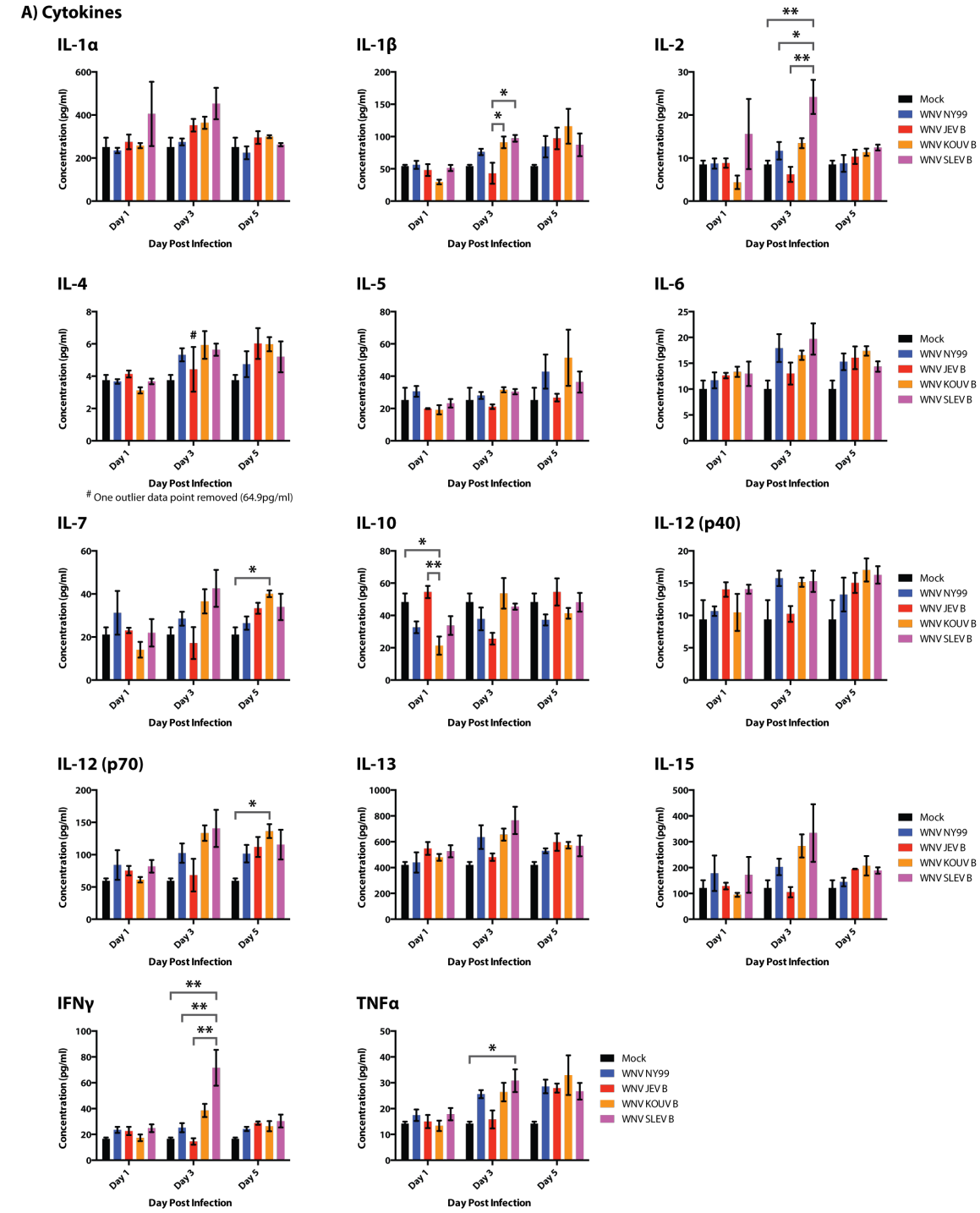

Figure 4.8: Plasma Cytokine and Chemokine Concentrations Following i.p. Inoculation. *A*: Plasma samples from Days 1, 3, and 5 of the serial sacrifice study were analyzed to determine cytokine levels. Three mock-infected controls were analyzed to give base values. Statistical analysis was performed by ANOVA (* $p<0.05$; ** $p<0.01$). Graphs show mean values with standard error.

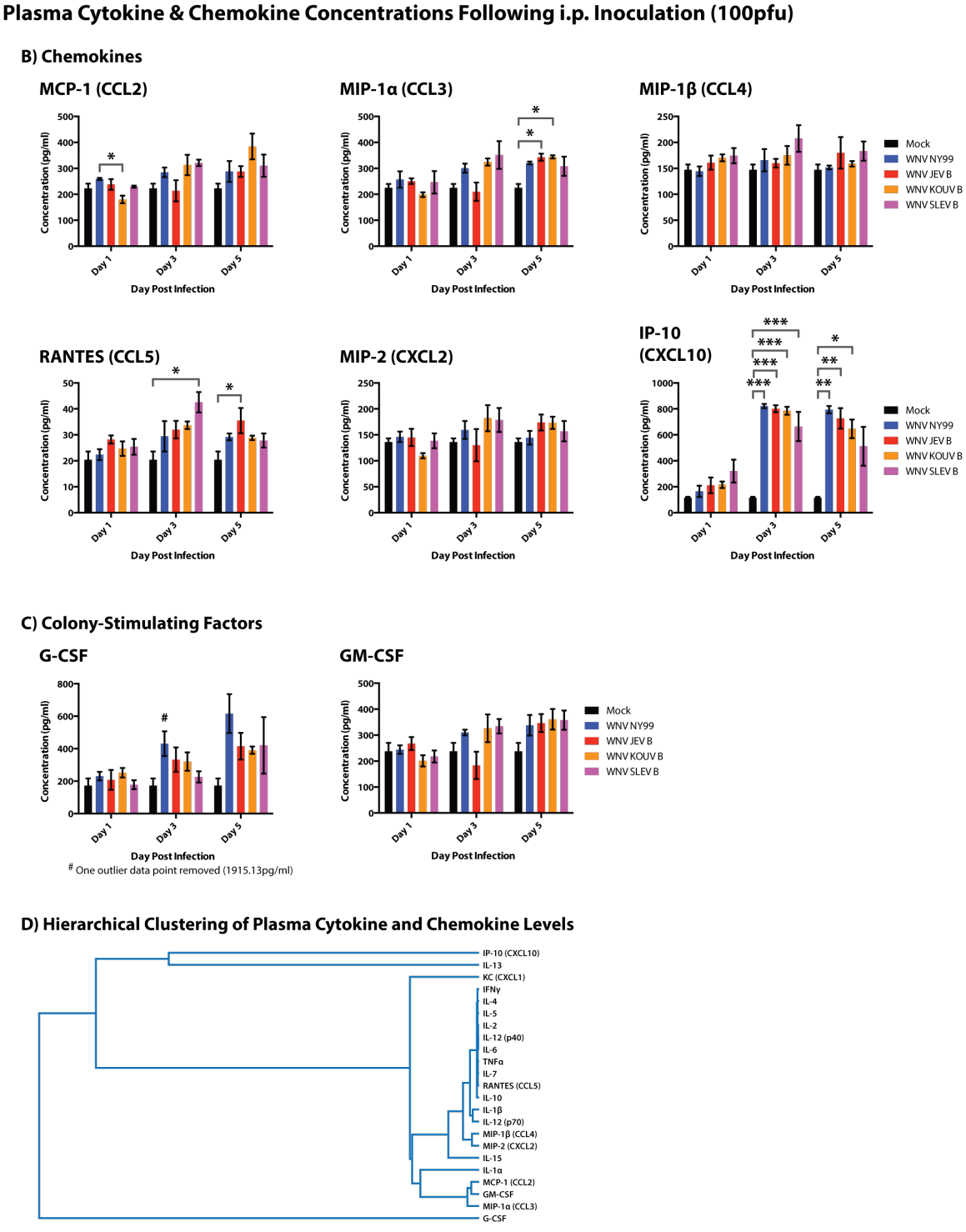

Figure 4.8: (Continued) Plasma Cytokine and Chemokine Concentrations Following i.p. Inoculation. Plasma samples from Days 1, 3, and 5 of the serial sacrifice study were analyzed to determine chemokine (*B*) and colony-stimulating factor (*C*) levels, with three mock-infected control mice. Statistical analysis was performed by ANOVA (* $p<0.05$; ** $p<0.01$). Graphs show mean values with standard error. *D*: Hierarchical clustering of the concentration values was carried out to determine clusters in the cytokine and chemokine profiles.

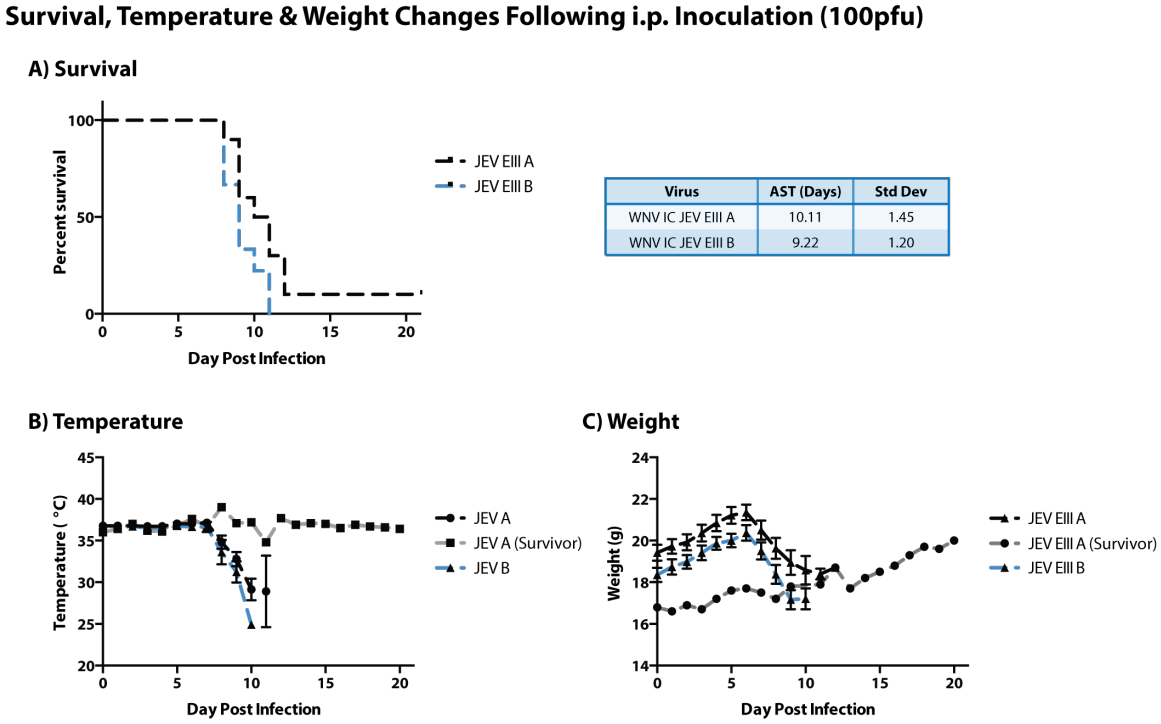

Figure 4.9: Survival, Temperature, and Weight Changes Following i.p. Inoculation with JEV A and JEV B. 3-4 week-old female Swiss Webster mice were infected with 100pfu of JEV A (n=10) or JEV B (n=9) by the i.p. route. *A*: Survival of mice following infection. Average survival times with standard deviations were calculated for the mice that succumbed to infection. *B*: Temperature changes during infection. *C*: Weight changes during infection. Graphs show mean values with standard error.

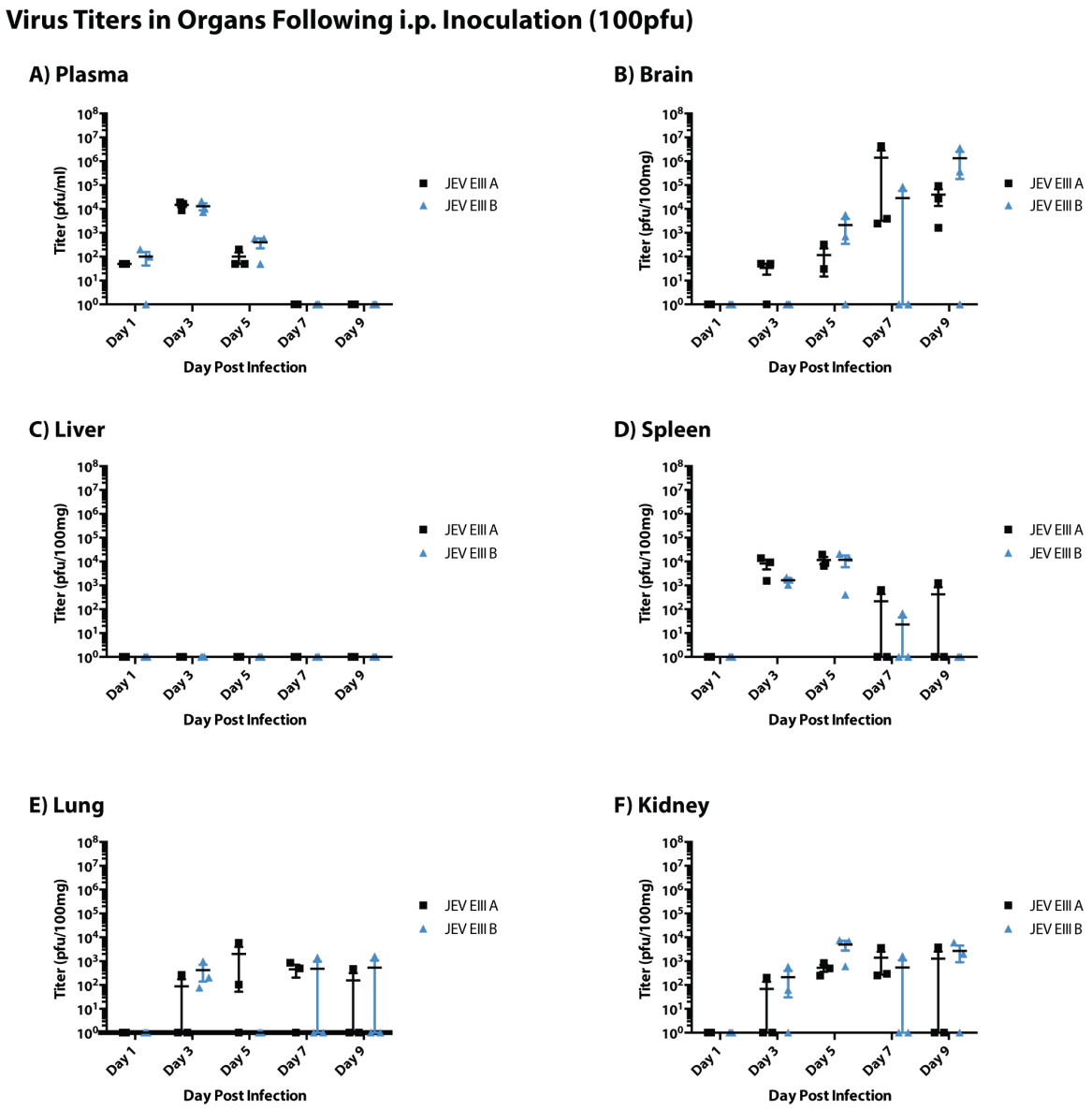

Figure 4.10: Organ Titers Following i.p. Inoculation with JEV A and JEV B. 3-4 week-old female Swiss Webster mice were infected with JEV A or JEV B (n=15 each). Three mice for each group were euthanized on Days 1, 3, 5, 7, and 9, and plasma (*A*), brain (*B*), liver (*C*), spleen (*D*), lung (*E*), and kidney (*F*) samples were harvested for titration. Graphs show individual data points with mean and standard error.

Chapter 5: *in vivo* Characterization of WNV EIII Single-Site G331A Mutation

INTRODUCTION

As has been outlined previously, the structural domain III (EIII) of the flavivirus envelope glycoprotein is important for initial interactions between the virus and target host cells. Studies to identify WNV neutralization escape mutants with reduced neutralization by EIII-targeting antibodies, both *in vitro* and *in vivo*, have shown that such mutations are often localized to four amino acids within EIII: K307; T330 and T332 within the BC loop; and A367 within the DE loop (Figure 5.1) (Zhang et al., 2010, Beasley and Barrett, 2002, Choi et al., 2007, Zhang et al., 2009). While mutation of these particular residues had minimal effects on virulence following i.p. inoculation, they suggested a potential role for these regions in receptor-binding: if antibodies targeting these regions are potently neutralizing, perhaps these areas govern receptor interaction.

Studies by Zhang *et al*. to determine the effect of mutation of residues in the WNV BC loop (amino acids 329-333 of E) demonstrated that, while many of the mutations had significant effects on antigenicity, only two, G331A and D333N, significantly affected *in vivo* virulence via the i.p. route (Zhang et al., 2010). While the specific amino acid encoded at residues equivalent to WNV 333 varies between different flaviviruses, G331 is highly conserved amongst most flaviviruses. Although the G331A mutant was significantly attenuated *in vivo*, it still grew reasonably well in Vero cells, with a peak virus titer of around $1x10^7$ pfu/ml, about 50-fold lower than WNV NY99, albeit with a small plaque morphology.

The aim of this study was to further characterize the attenuation of the G331A mutant *in vivo*, to compare the distribution of the virus post-infection within the outbred Swiss Webster mouse model compared to WNV NY99, and to determine the virulence of this highly-attenuated virus in an immunodeficient IFNα/β receptor knock-out mouse model to determine whether the virus is intrinsically less virulent *in vivo*: unable to cause lethal disease even in the absence of an effective antiviral immune response. To aid in the determination, a WNV L107F mutant, with an attenuating substitution in the EII fusion loop, was used for comparison. This virus is strongly attenuated via the i.p. route, but maintains its neurovirulence when administered i.c. (Zhang et al., 2006). It is believed that this mutation attenuates the virus by slowing its entry into target cells, allowing an effective immune response to be generated before the virus has a chance to replicate effectively. The working hypothesis was that the G331A mutation attenuates WNV by affecting the receptor-binding activity of EIII, reducing the repertoire of receptors that can be used by the virus, meaning that even in the absence of an effective antiviral immune response, the virus would still be attenuated.

VIRULENCE IN SWISS WEBSTER MICE FOLLOWING I.P. AND I.C. INOCULATION

In order to confirm the loss of virulence following i.p. inoculation, and the effect of the G331A mutation on neurovirulence following i.c. inoculation, groups of five 3-4 week-old female Swiss Webster mice were inoculated with 100pfu of virus by one or other route (Figure 5.2). As seen previously, peripheral inoculation resulted in no mortality with WNV G331A, whereas WNV NY99 killed 100% of the mice with an average survival time of 8.4±0.6 days (Figure 5.2A). Interestingly, intracranial inoculation with WNV G331A resulted in only 40% mortality suggesting a very strong attenuation of neurovirulence for this mutant compared to other attenuated WNV strains,

with an AST of 11.5±2.1 days, substantially different to the 100% mortality with WNV NY99 (AST 5.8±0.5 days) (Figure 5.2B).

SERIAL SACRIFICE STUDY WITH WNA G331A FOLLOWING I.P. INOCULATION (100PFU)

Since the G331A-containing virus is clearly attenuated for both neuroinvasiveness and neurovirulence *in vivo*, a serial sacrifice study was carried out to characterize the course of infection with respect to temperature and weight changes, and virus titers in organs. Ten mice were microchipped to allow for daily weight and temperature measurements over the course of two weeks. Five of the chipped mice were infected with WNV NY99, while the other five were infected with WNV G331A. Twenty-four unchipped mice per group were infected with either WNV NY99 or WNV G331A, with three from each group euthanised each day from Days 1 to 8 post infection. Serum, brain, liver, spleen, lung, and kidney samples were taken from each mouse for homogenization and virus titration.

The survival data for the chipped mice show a similar result to the first experiment, with WNV NY99 infection resulting in 100% mortality with an average survival time of 9.0±0.7 days (Figure 5.3A). This time there was one WNV G331A mouse that died on Day 11. Daily temperature measurements indicated that the mice had no febrile phase, with the WNV G331A survivor mice maintaining a normal temperature throughout the experiment (Figure 5.3B). The WNV NY99-infected mice showed a sharp drop in temperature from Day 8 until death of approximately 2-3°C per day. Similarly, the one WNV G331A-infected mouse that succumbed to infection had a temperature drop, but this was delayed by a day, although the drop itself was of a similar magnitude to that of WNV NY99, with an average loss of 3°C per day. Similar to previous observations, the WNV NY99-infected mice had a rapid weight loss from Day 7 until

death, while weight loss in the lethal WNV G331A mouse was delayed by a day, similar to the temperature observations (Figure 5.3C). Interestingly, the rate of weight loss with this mouse was almost identical to that of the WNV NY99-infected mice. The WNV G331A survivor mice showed a subtle, transient weight loss on Day 9, but by Day 10 the weight had started to increase again.

The organ titration data showed that, despite generating a measureable viremia, WNV G331A was not readily detectable in any of the peripheral organs or the brain. The viremia caused by G331A was somewhat different to that of WNV NY99 in that it was of lower magnitude and longer duration (Figure 5.4). Similar to previous observations, WNV NY99 generated a strong viremia that peaked at Day 3 post-infection and was effectively cleared by Day 5. By contrast, peak viremia for WNV G331A occurred on Day 4, and was 10-fold lower than for WNV NY99. In addition, two of the three WNV G331A-infected mice still showed detectable levels of virus on Day 5 post infection, in contrast to WNV NY99.

VIRULENCE IN IFNA/B RECEPTOR KNOCK-OUT MICE

Given the apparent attenuation of neuroinvasive and neurovirulent properties of WNV G331A, peripheral (i.p.) infection of highly-susceptible, immunodeficient AG129 IFNα/β receptor knock-out mice was carried out using 100pfu of G331A virus. 100pfu doses of WNV NY99 and WNV L107F were also used as control viruses (Figure 5.5). WNV L107F contains an attenuating mutation in the hydrophobic region of the EII fusion loop, which, while not affecting receptor binding, slows infection by reducing the efficiency of viral fusion. This mutant is significantly attenuated within the Swiss Webster animal model.

Within these immunosuppressed mice, WNV NY99 is particularly virulent, with 100% mortality and an average survival time of 3.0±0.0 days. WNV L107F, despite being highly attenuated in outbred mice, demonstrated similar virulence to WNV NY99, with a mortality rate of 92% (although the survivor failed to seroconvert, suggesting it was not infected) and an average survival time of 3.5±0.8 days. By contrast, WNV G331A caused only 70% mortality (with 100% seroconversion), with a significantly prolonged AST of 8.3±1.0 days.

Brains were removed from five of the seven fatal WNV G331A-infected mice for virus isolation and sequencing (Table 5.1). Of these, only one maintained the G331A mutation without any sequence changes in or around the EIII domain. One of the viruses had a reversion to a wild-type sequence at position 331 (A331G), while the other three had one additional nucleotide mutation each, resulting in amino acid changes H395Y (G331A mb1), Q391H (G331A mb3), or N394S (G331A mb4). Brains recovered from the lethal WNV L107F-infected mice showed no changes in the sequence of E, indicating that reversion and adaptive changes were not necessary for virulence in this model.

VIRULENCE OF WNV G331A ADAPTIVE MUTANTS IN SWISS WEBSTER AND IFNA/B KNOCK-OUT MICE

In order to determine whether the additional mutations identified from two of the brains of deceased WNV G331A-infected IFNα/β receptor knock-out mice were adaptive changes that resulted in increased virulence of the virus in both immunocompetent and immunosuppressed mice, groups of Swiss Webster and knock-out mice were challenged with 100pfu of G331A mb1 or mb4 viruses administered via the i.p. route (Figure 5.6). In the knock-out mice, WNV NY99 once again had high virulence, with 100% mortality

and an average survival time of just 3.0±0.0 days. In contrast to the parental WNV G331A, both mouse-brain isolates showed increased virulence, with WNV G331A mb1 (containing the H395Y mutation) causing 87.5% mortality with an AST of 4.3±0.5 days, and WNV G331A mb3 (containing the Q391H mutation) causing 100% mortality with an AST of 5.1±0.4 days (Figure 5.6A).

This increased mortality extended to the outbred Swiss Webster mice in which WNV NY99 displayed 100% mortality with an average survival time of 9.2±1.6 days (Figure 5.6B). In this mouse model, both WNV G331A mb1 and mb3 displayed 87.5% mortality, with an AST of 9.0±1.6 days and 11.4±4.9 days, respectively.

DISCUSSION

Previous studies have shown that mutation of residue 331 within the BC loop of WNV EIII has a significant attenuating effect on the virus, with a G331A substitution resulting in a virus that, while capable of growing *in vitro*, has very low associated mortality *in vivo*, with an LD_{50} >1,000pfu following i.p. inoculation (Zhang et al., 2010). The fact that the BC loop appears to be a particularly important target for neutralizing antibodies, containing two of the four residues shown to allow for effective escape mutants, supports an important role for EIII in receptor-binding (Zhang et al., 2010). This, combined with its high conservation between different flaviviruses, suggests that G331 may potentially play a key role in the interaction between EIII and cell surface receptors. This study aimed to determine how the G331A mutation affects the pathogenesis of WNV *in vivo* using both immunocompetent Swiss Webster and immunocompromised IFNα/β receptor knock-out mice.

Within the immunocompetent Swiss Webster mouse model, WNV NY99 is highly virulent with low LD_{50} values around 1pfu following inoculation by both the i.p. and i.c. routes (Zhang et al., 2006). By contrast, G331A appears highly attenuated following inoculation by both routes, with the only mortality observed via the peripheral route potentially due to a revertant virus, and less than 50% mortality following i.c. inoculation with a significantly extended average survival time. These observations run contrary to those made with other attenuated WNV mutants, such as L107F, which although attenuated following peripheral inoculation (LD_{50} >1,000pfu) often maintain substantial neurovirulence following direct intracranial inoculation (LD_{50} 1.3pfu) (Zhang et al., 2006). The fact that the residues adjacent to 331 (330 and 332) may be mutated reasonably freely, with even a T332P mutation being tolerated, suggests that G331A may be having more of an effect on the virus than just reduced protein/virion stability, potentially through disruption of virus-host interactions. Indeed, the serial sacrifice study demonstrated that the G331A mutant is still capable of generating a detectable viremia in outbred mice, albeit with a lower peak titer to WNV NY99, suggesting that early infection is still occurring, but that spread to other organs following this viremia is significantly inhibited.

The similarity of the temperature and weight loss of the single fatal WNV G331A-infected mouse during the serial sacrifice study suggests that this mouse may have died from a revertant virus, or a virus containing a compensating mutation. Sequencing of virus isolated from this mouse would be necessary to be certain. Such alterations to the virus were observed in the majority of isolates from IFNα/β receptor knock-out mice that succumbed to WNV G331A infection. These mice were used to determine the virulence of the mutant G331A virus in a susceptible animal model lacking an effective antiviral innate immune response. Within these mice, both WNV NY99 and the L107F mutant had high mortality and short average survival times, with viruses

isolated from brains of animals that succumbed to infection lacking any additional mutations within E. By contrast, the G331A mutant had significantly extended AST, and lower mortality. This, combined with the presence of revertive or additional mutations within the E of viruses that led to a fatal outcome, suggests that even in the absence of an effective innate immune response, the virus containing the G331A substitution alone is highly attenuated.

This observation suggests significantly different mechanisms of attenuation for the L107F and G331A mutant viruses. Since the L107F is located within the fusion loop of E, a region thought not to be involved in receptor binding, its mechanism of attenuation likely lies in less efficient fusion between the virus envelope and endosomal membranes. This would result in a slowing of replication, allowing for viral clearance by the immune system in immunocompetent mice, but permitting lethal infection in mice lacking effective antiviral responses. By contrast, the G331A mutant is incapable of causing lethal infection, even in immunodeficient mice, without either reversion or the acquisition of adaptive mutations. This would suggest that the G331A mutation fundamentally affects the ability of the virus to effectively interact with target cells, likely by altering the range of receptors it is capable of binding to. This could significantly affect tissue tropism, as seen in the serial sacrifice study, by restricting the range of cell types the virus can infect.

A curious and somewhat surprising feature of the adaptive mutations identified is their distance from residue 331 in E (Figure 5.7). All three of the mutations lie on a region of EIII quite distinct from the BC loop, and are capable of permitting viruses containing the G331A to increase their virulence in both immunodeficient and immunocompetent animal models. Such “long-range communication” has been described before for EIII: Maillard *et al*. demonstrated that mutations at 330 and 332 can affect the

surface electrostatics and structural dynamics around W397 (Maillard et al., 2008). Whether these mutations are having a similar effect with the G331A virus is uncertain, but his region has also been demonstrated to include the RGD/E integrin-binding motif present in many JE complex flaviviruses, suggesting that they may be compensating for the G331A mutation by improving integrin-binding activity (Lobigs et al., 1990). Further studies would be needed to determine the exact role these adaptive mutations are playing in increasing the virulence of the G331A mutant viruses. Some of these mutations are present in other flaviviruses, for instance the H395Y substitution is found in the EIII of SLEV and BAGV, while the N394S mutation has a similar N394T in ZIKV. Q391 is a rather variable residue between flaviviruses, but the change to a positive charge as seen in Q391H is seen in JEV, which possesses a Q391K substitution. It is possible that this region is the true flavivirus receptor-binding domain, or at the very least responsible for interactions with cell receptors, and that these adaptive mutations are resulting in the virus using alternative factors on the cell surface to gain entry.

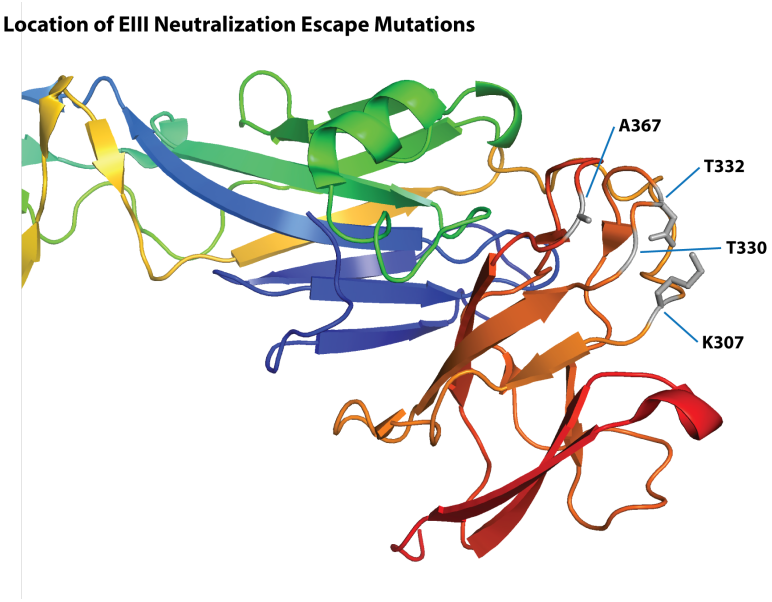

Figure 5.1: Location of EIII Neutralization Escape Mutants. Previous studies to characterize the location of mutants permitting escape from EIII-targeted monoclonal antibodies identified four residues, K307, T330, T332, A367, two of which were located in the BC loop or EIII (T330 and T332).

A) Survival Following i.p. Inoculation (100pfu)

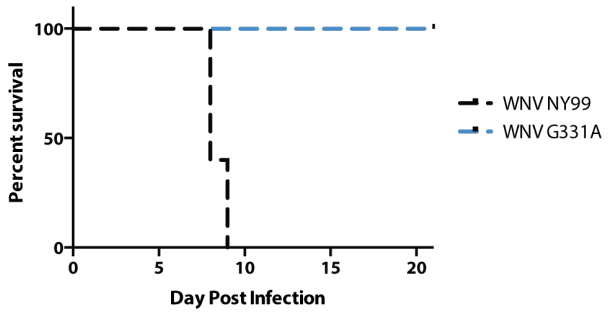

Virus	AST (Days)	Std Dev
WNV NY99	8.40	0.55
WNV G331A	N/A	N/A

B) Survival Following i.c. Inoculation (100pfu)

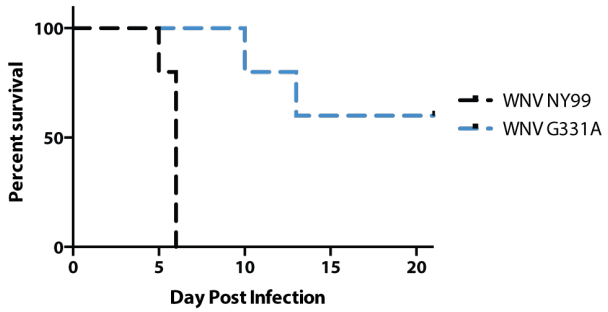

Virus	AST (Days)	Std Dev
WNV NY99	5.80	0.45
WNV G331A	11.50	2.12

Figure 5.2: Survival Following i.p. and i.c. Inoculation with WNV NY99 and WNV G331A. 3-4 week-old female Swiss Webster mice (n=5 per group) were inoculated with WNV NY99 or WNV G331A via the i.p. (*A*) or i.c. (*B*) route. Average survival times with standard deviations were calculated for the mice that succumbed to infection.

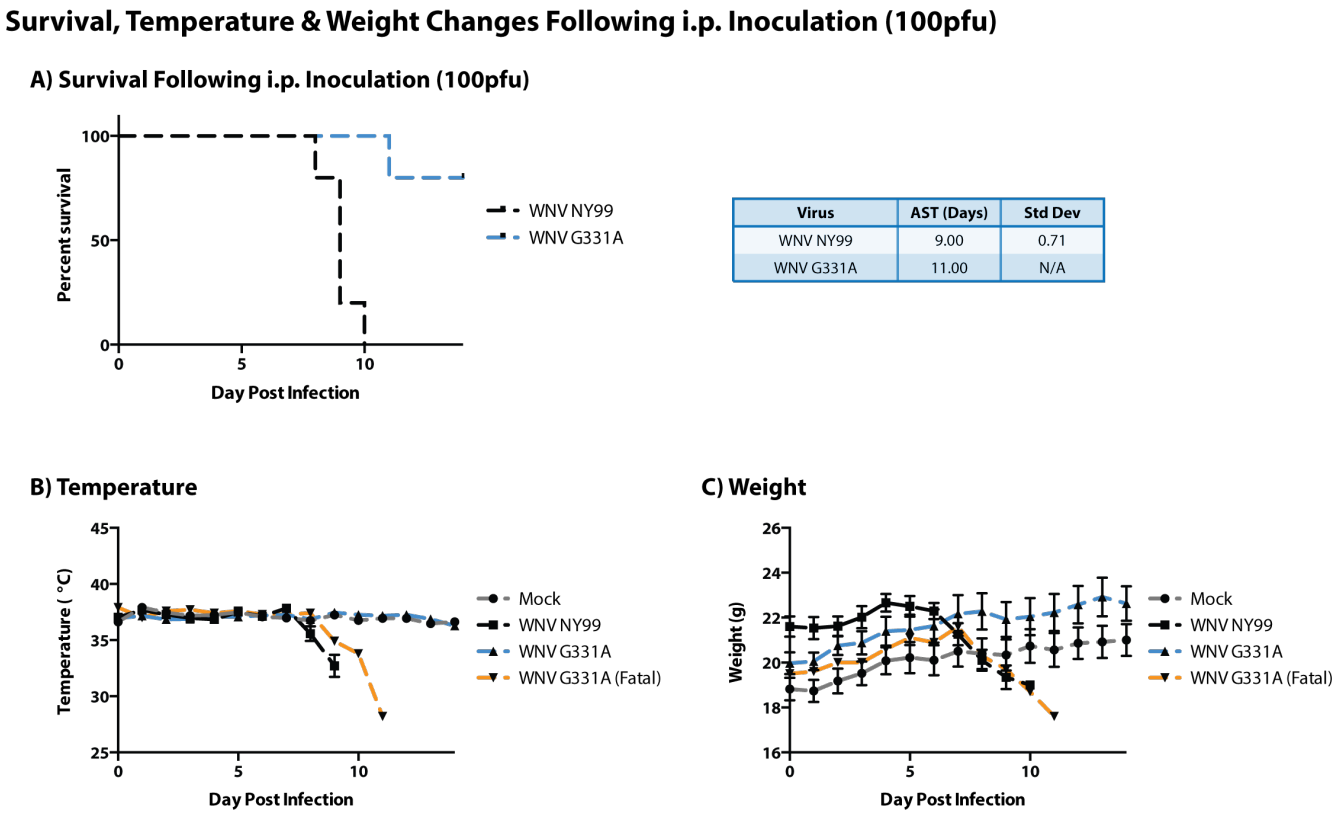

Figure 5.3: Survival, Temperature, and Weight Changes Following i.p. Inoculation. 3-4 week-old female Swiss Webster mice (n=5 per group) were infected with WNV NY99 or WNV G331A, and monitored for 21days. *A*: Survival following infection with average survival times. *B*: Temperature changes during infection. *C*: Weight changes during infection. Graphs show mean values with standard error.

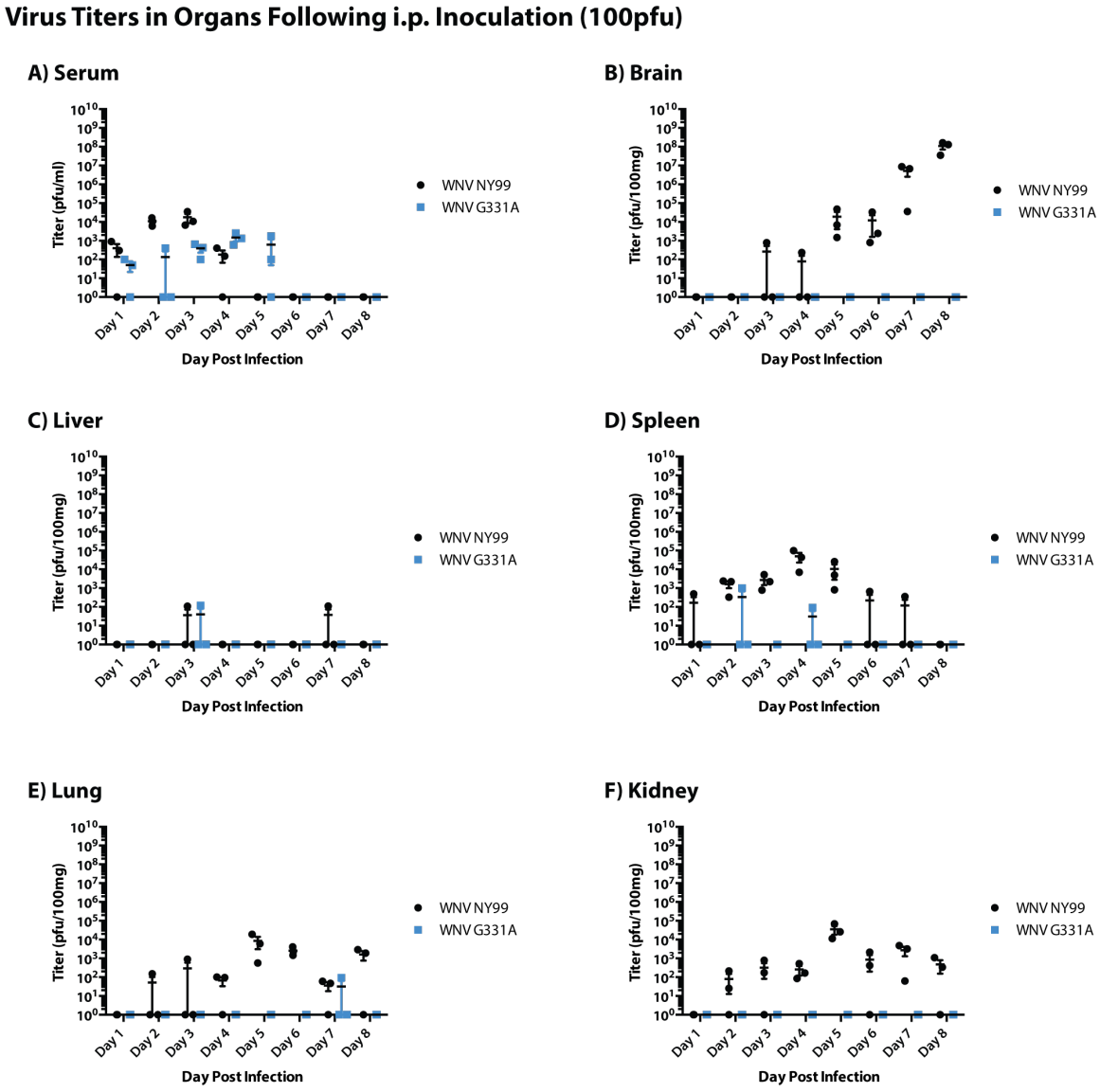

Figure 5.4: Organ Titers Following i.p. Inoculation with WNV NY99 and WNV G331A. 3-4 week-old Swiss Webster mice were inoculated with 100pfu i.p. of WNV NY99 or WNV G331A (n=24 per group). Three mice were euthanized daily from Day 1 to Day 8, and serum (*A*), brain (*B*), liver (*C*), spleen (*D*), lung (*E*), and kidney (*F*) samples were harvested for titration. Graphs show individual data points with mean and standard error.

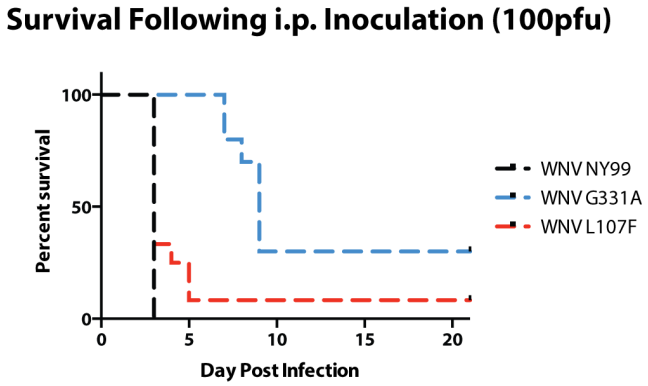

Virus	AST (Days)	Std Dev
WNV NY99	3.00	0.00
WNV G331A	8.28	0.95
WNV L107F	3.45	0.82

Figure 5.5: Survival Following i.p. Inoculation with WNV NY99, WNV L107F, and WNV G331A in IFNα/β Receptor Knock-Out Mice. Adult male and female IFNα/β knock-out mice were infected with 100pfu WNV NY99 (n=10), WNV L107F (n=12), or WNV G331A (n=10) via the i.p. route. Average survival times with standard deviations were calculated for the mice that succumbed to infection.

A) IFNα/β Receptor Knock-Out Mice (100pfu i.p.)

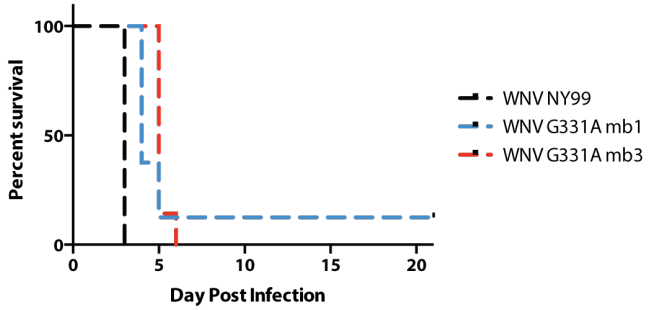

Virus	AST (Days)	Std Dev
WNV NY99	3.00	0.00
WNV G331A mb1	4.29	0.49
WNV G331A mb3	5.14	0.38

B) Swiss Webster Mice (100pfu i.p.)

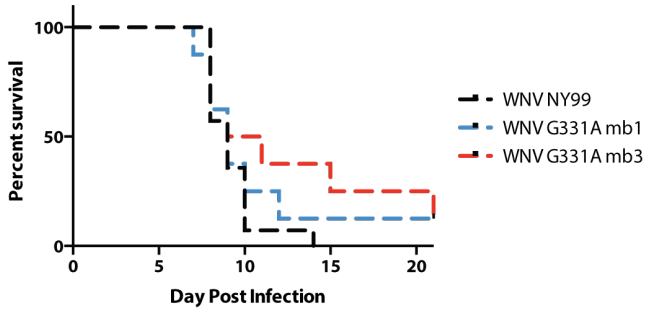

Virus	AST (Days)	Std Dev
WNV NY99	9.21	1.63
WNV G331A mb1	9.00	1.63
WNV G331A mb3	11.43	4.93

Figure 5.6: Survival Following i.p. Inoculation of Swiss Webster and IFNα/β Receptor Knock-Out Mice with WNV NY99 and WNV G331A Adaptive Mutants. *A*: 3-4 week-old female Swiss Webster (n=5 per group) were inoculated with 100pfu of WNV NY99 or WNV G331A containing an H395Y or Q391H adaptive mutation via the i.p. route. *B*: Adult male and female IFNα/β receptor knock-out mice were infected with WNV NY99 (n=14), WNV G331A mb1 (with H395Y; n=8), or WNV G331A mb3 (with Q391H; n=8) via the i.p. route. Average survival times with standard deviations were calculated for the mice that succumbed to infection.

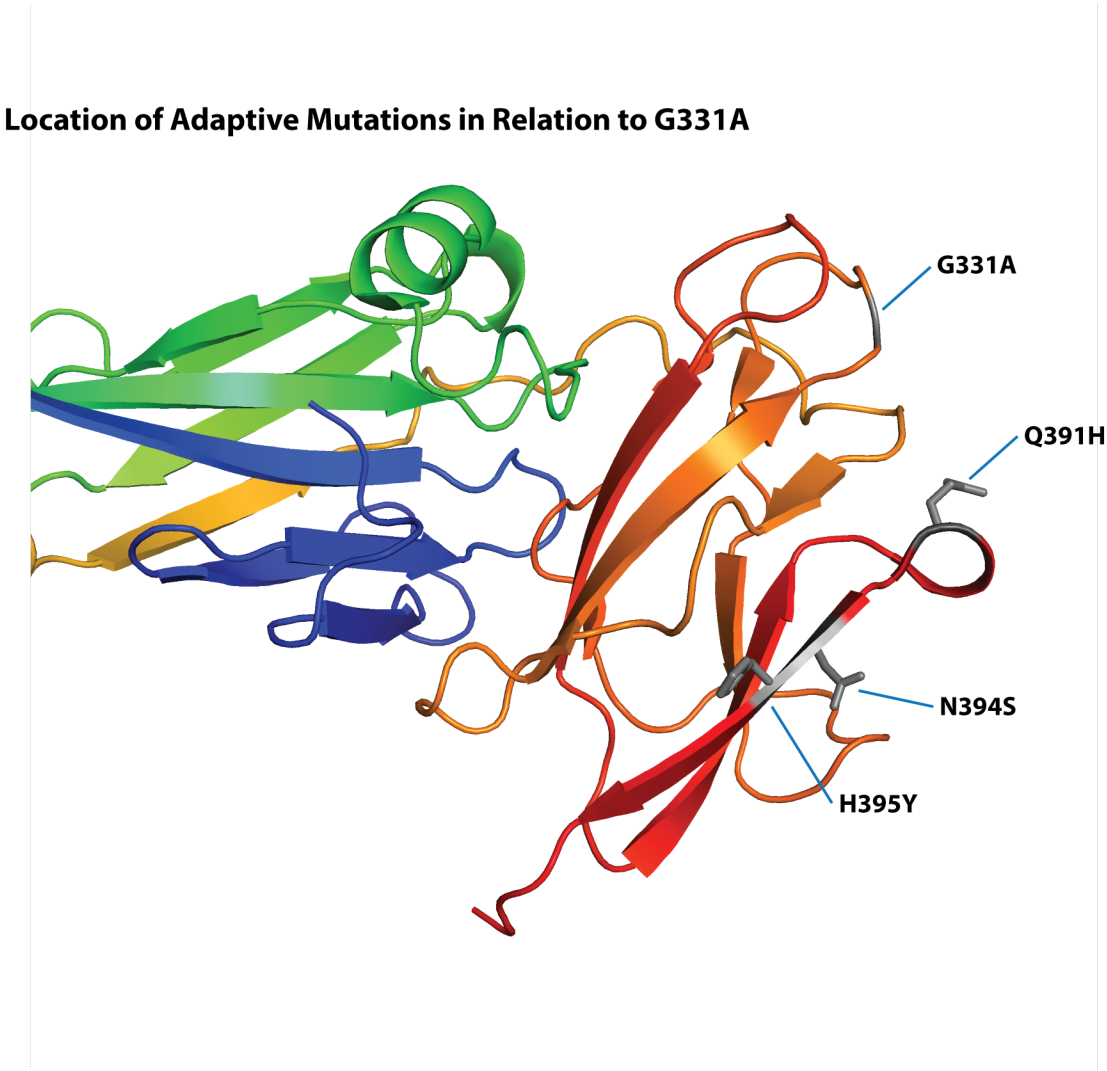

Figure 5.7: Location of Adaptive Mutations in Relation to G331A. The G331A mutation is located in the BC loop of EIII, quite distinct from the locations of the adaptive mutations identified from the mouse brain samples.

Adaptive Mutations in Viruses from Brains

Mouse	Nucleotide Mutation	Codon Mutation	Adaptive Mutation
WNV G331A mb1	nt2149 C → U	CAC → UAC	**E H395Y**
WNV G331A mb2	None in EIII	None in EIII	None in EIII
WNV G331A mb3	nt2139 A → C	CAA → CAC	**E Q391H**
WNV G331A mb4	nt2147 A → G	AAU → AGU	**E N394S**
WNV G331A mb5	nt195C A → G	GCC → GGC	**E A331G** (Reversion)

Table 5.1: Adaptive Mutations Present in WNV G331A Isolated from Mouse Brains. Brains were collected from IFNα/β receptor knock-out mice that succumbed to WNV G331A infection. Viruses were isolated from these brains and sequenced within and around EIII to identify potential adaptive mutations. Three of the five showed adaptive mutations in the region of EIII between residues 391 and 395, while one virus was an A331G revertant. Only one of the five mouse brains contained no additional mutations in the region sequenced.

Chapter 6: Final Discussion, Summary, and Future Direction

DISCUSSION

The flaviviruses, such as WNV, are responsible for significant morbidity and mortality worldwide, causing diseases in humans and animals ranging from encephalitis to hemorrhagic fever. Even flaviviruses that are genetically very similar, such as OHFV and TBEV, which share 80% nucleotide and 90% amino acid identity, can cause substantially different diseases within the mammalian host. The exact mechanisms governing the differences in disease presentation are unknown, but are thought to involve a combination of differences in host responses to infection and differences in tissue tropism for the viruses. Indeed, studies comparing OHFV and TBEV in the mouse model show differences in tropism, with OHFV growing to detectable levels in the liver, in contrast to TBEV, which, as is the case with many encephalitic flaviviruses, is absent from this organ (Tigabu et al., 2009). Similarly, immune responses against the two viruses differ quite significantly throughout the course of infection (Tigabu et al., 2010).

The envelope glycoprotein is the predominant feature on the surface of flavivirus virions, and is responsible for most aspects of the attachment and entry of the virus to host cells. One of its main roles is in mediating the interaction between the virus and cell surface receptors. Receptor attachment is believed to involve structural domain III, EIII, a somewhat distinct unit of the protein connected upstream to EI by a single amino acid chain linker region (Cruz-Oliveira et al., 2015, Crill and Roehrig, 2001, Hung et al., 2004, Chen et al., 1996, Nybakken et al., 2005, Volk et al., 2004). Accordingly, EIII is thought to be a major viral determinant of tissue tropism by determining which cell types

are readily infectable, although it is likely that other E domains also interact with cell surface ligands.

The original aims of this study were twofold: firstly, to determine whether viable chimeric viruses could be generated following EIII substitutions. Secondly, to determine whether the substitution of EIII from one flavivirus to another would affect disease presentation - that is, if an EIII from a hemorrhagic fever virus were inserted into an encephalitic virus, would we see a more hemorrhagic fever-like, viscerotropic disease associated with the chimera? As can be seen from Table 3.2, the first aim is answerable in the affirmative, whilst the second aim is less so, owing to the inviability of WNV chimeras containing EIIIs from DENV-2 or YFV. Notwithstanding the issue of inviability of some of the constructs, the viable chimeric viruses presented some interesting data.

The delineation of a limit of tolerance for heterologous EIII sequences for WNV has been determined during this study. Three of the four donor viruses (KOUV, JEV, and SLEV) for which viable chimeras could be recovered are members of the JE complex, with SLEV being the most diverse of the three, sharing 73.4% amino acid identity with WNV within EIII. The fourth donor virus permitting a viable chimera was BAGV, which shares 65% amino acid identity with WNV within EIII, and is a member of the Ntaya virus complex. EIIIs from ZIKV and IGUV, members of the two complexes adjacent to the JE and Ntaya complexes, were incapable of generating recoverable viruses. These sequences share 60.8% and 57.3% amino acid identity in EIII compared to WNV, respectively.

With the engineering of four restriction sites into the infectious clone plasmid, allowing for the generation of four different versions of the chimeras, it was hoped that some differences might be observed between the different chimera forms that may be attributable to the additional donor sequences up- and downstream of EIII. For the most part this was not the case, with the additional sequences appearing to have more of a destabilizing effect on the chimeric viruses, further indicating that EIII substitution is tolerated better when the region is substituted alone, without additional flanking sequences. For the JEV, KOUV, and BAGV chimeras, the B-, C-, and D-forms behaved very similarly to one another, indeed for the JEV and KOUV chimeras, even the presence of both additional sequences in the A-form had but a minimal effect on mammalian and mosquito cell growth kinetics, as well as plaque morphology. The BAGV A-form appeared to grow less well than the other three versions but, at least compared to BAGV B, this may be explained by the temperature sensitivity data suggesting a significantly lower stability, resulting in a nearly 100-fold decrease in titer when grown at the higher temperature. The SLEV chimeras showed the most significant differences between the different versions, with SLEV B growing comparable to WNV NY99 in both mammalian and mosquito cell cultures. The C- and D-forms grew a little less well, with peak titers in Vero cells around 10-fold lower than either the B-form or WNV NY99. SLEV A was particularly strongly affected by the chimerization, growing to barely-detectable levels immediately following recovery and failing to plaque, requiring immunostaining to determine titer following recovery. Passaging of SLEV A in Vero cells allowed for a presumably more stable mutant to emerge, with a consensus-level N222Y mutation, as well as a histidine to tyrosine mutation at either residue 285 or 398 in the envelope glycoprotein, however, despite the increased ability to grow in mammalian cells and generate plaques, the adapted virus was still significantly impaired, with its titer dropping at least 2,500-fold, below the limit of detection, when grown at 41°C.

When compared to WNV NY99, the substitution of EIIIs from donor viruses appears to have but a minimal effect on growth in mammalian cells. If the B-forms of the chimeras are compared, all four chimeras grew very similarly to WNV NY99 over the first two days, with titers on Day 2 within 10-fold of one another (Figure 6.1). For JEV B and SLEV B, this similarity to WNV NY99 extends through the remainder of the days. For KOUV B and BAGV B, the titers drop almost in parallel to one another on Day 3 and 4, with a slight divergence on Day 5. This is particularly curious as these two chimeras represent the most and least similar EIII sequences compared to WNV, respectively. Whether the reasons for these drops in titer are similar for both is uncertain. As demonstrated using an anti-membrane protein antibody on western blot samples of whole cell lysates, both of these chimeras have detectable mature M bands (Figure 3.10), suggesting either a failure to release mature virions into the supernatant, or a tendency for the mature particles to associate with cells more strongly than any of the other viruses. The latter possibility would explain the drop in titer on the later days: virions being drawn out of suspension faster than they can be produced from exhausted cells. However the discrepancy between the band intensities with the KOUV and BAGV chimeras suggests that, for BAGV B, this may not fully explain the decreasing titers.

In mosquito cells the identity of the EIII donor virus appears to have a more significant impact on growth than the size of the insert, even for BAGV A. This differs from growth in Vero cells, where the most stable chimeras (the B-forms) grew very similarly to one another and WNV NY99. Indeed, in C6/36 cells, the rate of B-form chimera virus production appeared to be affected quite substantially, with statistically significant differences in titer compared to WNV NY99 on Day 2 onwards, with the order of Day 5 titers being WNV>SLEV B>JEV B>KOUV B>BAGV B, although even by Day 5 the differences in titers was less than 100-fold. The similarity of growth between the A- and B-forms in C6/36 cells may be due to increased stability at the lower

temperature (29°C) used to culture the cells, but the differences in growth kinetics of the chimeras compared to WNV NY99 appears to arise as a result of differences in the interaction between EIII and receptors on the cell surface.

The difference in antigenicity between BAGV EIII and the other donor viruses, resulting in its placement outside the JE complex, is readily demonstrated by the western blot data, which shows that MIAF raised against BAGV reacts solely with the BAGV chimeras. The neutralization of the BAGV B chimera is slightly different to its recognition by MIAF and sera by western blot. Samples with an apparently large EIII-reactive antibody component, as evidenced by substantial differences in neutralization titers for other chimeric viruses, often failed to neutralize BAGV B as strongly as those with a stronger EI-EII antibody response, as indicated by similar reactivity with each of the other viruses. The data suggests the possibility that the neutralization of the BAGV B chimera follows a different mechanism than for the other JE complex chimeras, potentially indicating that BAGV EIII may be less important for virus entry than it is for WNV and more closely-related viruses. An alternative explanation is that the apparent lower stability of the BAGV B chimeric protein, as suggested by the reduced plaque size following incubation at 41°C compared to 37°C, may result in a virus that is more sensitive to antibody binding: a more dynamically-structured protein may be forced into a less optimal form following binding by an antibody that would not normally be neutralizing. A related phenomenon has been observed with some DENV isolates, whose surfaces appear more dynamic than others, resulting in the rendering available of epitopes that would not normally be exposed (Kuhn et al., 2015).

Despite the apparently minimal effects of EIII substitution on growth in mammalian cells *in vitro*, at least for the B-forms, differences in growth and virulence *in vivo* were considerable. Single-dose screening with 100pfu of virus administered i.p.

showed that the JEV chimeras maintained high virulence, with mortality rates between 80 and 100%. The KOUV chimeras were significantly attenuated, with mortality rates lower than 50% for all four versions. Most surprising were the SLEV chimeras, especially SLEV B, for which there was no associated mortality. Indeed, throughout the course of the study, none of the mice died following i.p infection with an SLEV chimera. The BAGV chimeras showed some minimal mortality, with rates between 0 and 20%. Interestingly, the different forms of the chimeras appeared to have greater differences *in vivo* than they did *in vitro*, particularly with respect to average survival times. For both the JEV and KOUV A- and C-form chimeras, inclusion of the additional upstream donor sequences resulted in prolonged average survival times compared to WNV NY99 and the B-forms, but did not significantly affect mortality rates compared to the B-form chimeras. For the BAGV chimeras, only those without the downstream stem helix region from the donor virus had any associated mortality, although as seen with BAGV A in the temperature sensitivity assays, this may be more of an effect of particle stability.

Intracranial inoculation with 10 or 100pfu of virus demonstrated that many of the B-forms had lost a degree of neurovirulence, with increased survival following infection with 10pfu of the KOUV, SLEV, and BAGV chimeras compared to WNV NY99, as well as lower mortality rates with 100pfu doses with the KOUV and BAGV chimeras. Even JEV B, which behaved similar to WNV NY99 when administered i.p., showed a statistically different survival curve following i.c. inoculation with 10pfu, with an average survival time two days longer than for WNV NY99.

The serial sacrifice study revealed some interesting differences between the chimeras, and suggested some explanation for the differences in mortality observed. It additionally allowed for further characterization of the Swiss Webster animal model for use with WNV. The temperature drops with WNV NY99 and JEV B were rapid and

pronounced, starting on Day 8 post infection, and continuing until death. Similar temperature loss, and the lack of a febrile phase of infection, has been seen in OHFV- and TBEV-infected mice, although in these studies, which use different mouse strains, the decrease in body temperature occurred later in the course of infection (Tigabu et al., 2009). When compared to human infection, the apparent lack of a febrile phase is interesting. Studies into the cytokine-mediated development of fever in mice has suggested that Il-6 is the main pyrogenic factor, with TNFα playing an antagonistic role (Leon, 2002). Since plasma concentrations of these cytokines appear to parallel one another over the first five days of infection, they may be counteracting one another, resulting in the lack of detectable fever. More interesting than the temperatures are the weight changes during infection. The two highly-virulent viruses, WNV NY99 and JEV B, showed a rapid weight loss from Day 7 until death, while KOUV B and SLEV B, two viruses with significantly different mortality rates, showed a less rapid but more prolonged weight loss. BAGV B, which had a higher mortality rate than SLEV B, had only a minor two-day weight loss on Days 7 and 8, with a move towards a healthy weight gain thereafter. The differences in the weight profiles are rather curious, not least that of SLEV B, which shows a clear and protracted loss without any overt signs of infection. Studies into the effects of cytokines on anorexia have shown roles for IL-1, IL-2, IL-6, IL-8, TNFα, and IFNγ, however, in these studies, the levels of these factors in the plasma of the infected mice were rather variable, appearing not to correlate with the weight profiles for each virus (Langhans, 2000). The almost clockwork onset of the weight loss, seemingly independent of disease severity, is also very interesting and, at the moment, defies explanation.

The organ titrations show that substituting EIII can have a significant effect on the tissues targeted during infection. As might be expected, owing to the similarities in mortality rates, distribution of WNV NY99 and JEV B was similar, although differences

did occur. Both viruses were strongly neuroinvasive, and grew to similar levels in the spleen and kidney, although the titers of JEV B tended to be marginally lower. Within the blood JEV B appeared to generate lower titers, but a more prolonged viremia, with virus still detectable at Day 5. This would suggest that it is not as readily cleared as WNV NY99, potentially due to the apparent delay in immune responses seen with the cytokine data: whereas levels often increased on Day 3 with WNV NY99, with JEV B such increases were delayed until Day 5.

KOUV B is a curious virus. The virus generated a strong, WNV-like viremia, and infected the kidney similarly well. However, it failed to infect other organs quite as readily as WNV NY99. This suggests a significant shift in the tissue tropism of the virus towards a profile that is significantly restricted compared to its WNV parent. Whether this is due to an intrinsic feature of the KOUV EIII, or due to the apparent increased adhesiveness of the virus, potentially arising from differences in the nature of glycosylation, is uncertain. The former seems less likely, as studies with wild-type KOUV suggest it may be more virulent in mice than WNV, with observed persistence in the spleen, an organ in which KOUV B titers were very low, indicating that KOUV EIII should permit binding to these cell types (Prow et al., 2014). The apparently increased adhesiveness of KOUV B, as seen *in vitro*, may suggest that non-specific interactions may be affecting the entry efficacy of the virus. If these interactions are predominant for particular cell type, and result in reduced viral entry, it may help to explain the tropism shift and the attenuation of the virus.

Despite its strong growth *in vitro*, SLEV B failed to cause a similarly strong infection *in vivo*. This appears to be due to the very low viremia produced early in infection, indicative of a poor infection of early targets such as dendritic cells. This, combined with strong antiviral responses, likely resulted in significant virus clearance

quite early, although low but detectable quantities of virus were be found in a number of organs, including the brain, on Day 5 and Day 7 post infection. Curiously, despite this apparently rapid viral clearance, weight loss still occurred in a manner similar to KOUV B, raising the possibility that the virus infected and remained in an organ that was not titrated. Alternatively, the observed weight loss may be a consequence of immune responses raised against the virus. BAGV B had a similar organ distribution profile to SLEV B, with a low viremia and little peripheral organ infection. It had a significantly different weight loss profile, however, and none of the mice had detectable virus in the brain at any of the timepoints following infection. This is interesting in the light of the fact that this virus is capable of causing low levels of mortality (between 10 and 20%) following peripheral inoculation. This would suggest that either death is not dependent on neuroinvasion, or that neuroinvasion is rare such that the number of mice per group and the timing of sample collection during the serial sacrifice study was insufficient to observe it.

Hematologically, mice appeared to behave similarly to humans following WNV infection, with an apparent leuko- and lymphocytopenia, but few alterations in red blood cell-associated parameters. Whether the drop in immune cell numbers was due to direct viral infection or immunological effects is unclear. The cytokine and chemokine data suggest that WNV NY99 was quite effective at minimizing immune response induction early in infection, with the only significant increase being IP-10 on Days 3 and 5. JEV B is similar, if not more effective, at minimizing immune responses, with levels on Day 3 often lower than those for WNV NY99. For some of the studied factors, the levels on Day 3 were marginally higher for KOUV B than for WNV NY99, however the differences do not appear to be substantial enough to account for the lower virulence of KOUV B. SLEV B strongly induced cytokines associated with antiviral T_H1 responses, including IL-2 and IFNγ. The fact that by Day 5, levels of most of the cytokines and

chemokines were similar with all of the viruses, suggests that the early immune responses may have a significant and substantial effect on the outcome of infection. Indeed, previous studies by Shrestha *et al*. have suggested that early IFNγ responses may play a significant role in determining the outcome to WNV infection (Shrestha et al., 2006). The data also suggest that these early immune responses may be EIII-dependent, presumably via signaling pathways activated as a result of virus binding to the cell surface, whereas on Day 5 the non-structural proteins that are common to all of the chimeras, are taking over to modulate the response to favor the virus (e.g. inhibition of interferon signaling). Since the plasma cytokines are indicative of broad, systemic immune responses, rather than local organ-specific responses, the rapid drop in levels between Day 3 and Day 5 for some of the factors is interesting. Since NS1 is a viral factor that is secreted from infected cells, and is found in the blood during infection, it is possible that it plays a role in remote modulation of host immune responses in uninfected cells, and may thus contribute to the normalization of cytokine levels observed on Day 5. Indeed, Crook *et al*. demonstrated that secreted WNV NS1 can interfere with signal transduction from TLR3, affecting cytokine production in macrophages and dendritic cells (Crook et al., 2014). Similarly, antibodies against DENV NS1 have been shown to decrease the severity of clinical signs, reduce viral titer, and reduce macrophage infiltration, despite its absence from viral particles (Wan et al., 2014).

The results of this study demonstrate that it is possible to generate structural domain chimeras for flavivirus EIII, but that viability of these chimeras is highly dependent upon the amino acid similarity of the donor sequence compared to that of the backbone virus. What is less clear are the particular regions and features of EIII and of other parts of the virus that determine the sequences that may be tolerated: after ten passages the amino acid sequences of the majority of the chimeras remained the same, suggesting that, for the most part, adaptive mutations are unnecessary or impossible. The

exception is with SLEV A, which showed increased viability following a passage in Vero cells. This increased viability was associated with a consensus-level N222Y substitution, and a prevalent H298Y alteration. Interestingly, the N222Y substitution was observed in most of the SLEV and BAGV chimeras at Passage 1, and all of them by Passage 10, suggesting a favorable role for this mutation in the chimeras, however the location of this mutation, in a region distinct from EIII in both the monomeric and dimeric forms of E, leaves a mechanistic explanation wanting. The data suggest that EIII itself has minimal effects on virus growth in Vero cells, although slightly more of an effect in C6/36 mosquito cells, fitting with the hypotheses that the primary role of EIII is in initial receptor-binding, and that replication is more of a non-structural protein-related process. Since all of the EIII donor viruses grow efficiently in Vero cells, it suggests that this cell type expresses receptors that may be efficiently utilized by each of these viruses and, by extension, the chimeras containing their EIIIs. The differences in tropism observed during the *in vivo* studies suggests that, if other cell types were used that express a different complement of receptors on their surface, more significant differences in virus growth may be observed between the chimeras. In addition, since the *in vivo* cytokine data suggest that some of the chimeras may induce stronger antiviral responses than others, performing growth kinetics in IFN-competent cells such as A549 cells, rather than the IFN-deficient Vero cells, may show greater differences in growth between the viruses *in vitro*. The fact that the chimeras are stimulating such differences in immune responses suggests that there may be differences in cell signaling occurring following binding of the virus to the cell surface, which would further suggest differences in receptor usage.

The *in vivo* data suggests that EIII sequences do contribute to differences in organ/cell tropism in the mouse model. SLEV B, which shows no apparent attenuation *in vitro*, is significantly attenuated *in vivo*, with no associated mortality following i.p. inoculation observed throughout the investigation. The cytokine data suggest that this

chimera is inducing a strong antiviral immune response early in infection that may account for the low viremia and lack of spread of the virus to other organs. Cytokine responses alone, however, fail to explain the modified tissue tropism seen for the KOUV B chimera, whose plasma cytokine levels were often very similar to those of WNV NY99.

The WNV G331A data strongly suggest that this residue, which is conserved in most flaviviruses, may play an important role in receptor-binding, although it is still not entirely clear whether this is due to direct effects of residue 331 in receptor binding or possibly due to indirect effects at an alternative binding site in EIII. As evidenced by the chimeric viruses, EIIIs from viruses that can readily infect mammalian cells can be substituted into WNV without substantially affecting growth kinetics, suggesting that virus replication is predominantly a non-structural protein-driven affair. The observation that substituting G331A in WNV EIII without altering any other residues has such a significant effect on the virus both *in vitro* and *in vivo* suggests that this alteration affects receptor-binding, protein stability, or both. The fact that the flanking amino acids may be altered more substantially than 331, with less significant effects on virus growth and virulence, suggests that the observed effects of the G331A substitution are not a result of protein stability issues. An effect of the G331A mutation on receptor binding is further suggested by the *in vivo* data. Administration of the virus by both the i.p. and i.c. routes shows significant attenuation, with LD_{50}s more than 100-fold higher than for the wild-type virus.

The serial sacrifice study showed that the G331A mutant still causes a viremia, but that it is lower and more protracted than for the wild-type virus, suggesting that the mutant cannot infect early targets of infection as readily. The fact that in spite of the viremia the virus failed to be readily detected in other organs suggests that the mutation

was affecting either viral entry or, similar to SLEV B, the immune responses being generated early in infection. If the latter were occurring, one would expect that removing antiviral immune responses would restore a wild-type WNV-like disease progression. The administration of WNV G331A to IFNα/β receptor knock-out mice showed that this was not the case. Indeed, although increased mortality was observed compared to similar infection in Swiss Webster mice, four of the five viruses isolated from the brains of fatal infections showed either reversion or adaptive mutations. This suggests that, even without the pressure of a strong antiviral immune response, WNV containing the G331A substitution alone was all but incapable of causing lethal neuroinvasive disease following i.p. inoculation.

The fact that the three adaptive mutations identified in viruses recovered from brains of G331A-infected IFNα/β receptor knock-out mice lie within four amino acids of each other (residues 391, 394, and 395) suggests that this may also be an important region for receptor binding (Figure 5.7). When two of the adapted viruses were administered to Swiss Webster and IFNα/β receptor knock-out mice, the viruses showed significantly increased mortality, suggesting that the adaptations had overcome the impediment caused by the G331A substitution. Interestingly, some of the adaptive mutations were to amino acids present, or similar to, those found in other related flaviviruses such as SLEV and JEV. Whether these mutations result in a receptor usage more similar to these other viruses is unknown, but it appears that such mutations either shift the focus of receptor binding away from residue 331, or compensate for it by targeting the virus to other, presumably similar, receptors.

SUMMARY AND CONCLUSION

In conclusion, substitution of EIII from different donor flaviviruses into WNV is possible, but appears to result in viruses with properties *in vivo* that cannot be readily predicted based upon the sequence identity of the donor EIII with that of NY99, or the growth of the chimeric virus *in vitro*. EIII appears to play a significant role in early immune responses, presumably through the differential activation of cell signaling pathways following receptor-binding, as well as determining the particular cell types infected. These immune responses significantly affect the progression of, and the outcome to, infection. Notwithstanding the argument of Suthar *et al*., that tissue tropism of WNV is governed by host immune responses, the organ distribution of the KOUV B chimera suggests that EIII may play a significant role. The data for the WNV G331A mutant strongly suggests that this residue plays a significant role in infection, other than just slowing the rate of entry. This is evidenced by the fact that for the most part, even in mice lacking effective antiviral immune responses, a lethal infection required either a reversion to a wild-type sequence, or an adaptive mutation in the 391-395 region. The fact that such adaptive mutations increased virulence of the G331A mutant even in outbred Swiss Webster mice suggests that these complementary mutations are overcoming whatever impediment was induced by the G331A substitution. These observations, combined with the less efficient growth in Vero cells, suggests that residue 331 in EIII may contribute significantly to receptor-binding, but that its role may be compensated for by other parts of EIII.

FUTURE DIRECTIONS

For the chimera studies, a number of future studies could be carried out to tease out the mechanisms of differences in virulence, tissue distribution, and cytokine/chemokine responses observed between the viruses *in vivo*. Since the Vero cell

growth kinetics for many of the chimeras were similar, it would suggest that innate immune response differences may be playing significant roles in determining the outcome of infection. One way to test this *in vitro* would be to determine growth kinetics in IFN-competent cells, such as A549 cells, to determine whether antiviral innate immune responses are differentially affected by the different chimeras. Since A549 cells are derived from lung tissue, a direct comparison with Vero cell growth kinetics would not be possible, so an interferon knock-down control would need to be included. The KOUV B data suggests that, for some of the chimeras, tropism differences may be directly attributable to receptor binding through EIII, rather than immune responses. This would suggest a change in receptor usage by the viruses affecting the range of cells that may be infected. To determine whether this is the case, characterization of growth kinetics in a range of cell types would be useful, as well as studying in greater detail differences in the attachment and entry mechanisms for the chimeras compared to WNV NY99. Similar studies have been carried out for DENV and some alphaviruses, and would allow for an in-depth analysis of the early stages of infection likely causing the differences observed *in vivo* (Ayala-Nuñez et al., 2011, van Duijl-Richter et al., 2015, van der Schaar et al., 2008).

Since the non-structural proteins of the chimeras are identical to those of WNV NY99, differences in immune responses must be due to the presence of heterologous EIII sequences. This would suggest that receptor-binding mediated by the donor EIII sequences is resulting in differences in cell signaling pathway activation, leading to altered gene expression within infected cells. If this were the case, it would suggest that different complements of receptors are in use for different chimeras. Studies to look at signaling pathway activation and gene expression following infection would be useful for determining the reasons for the differences in virulence within the mouse model. Similarly, the chimeric viruses would be helpful for investigating receptor usage in

different cell types, thus allowing for a better understanding of the differences observed between the viruses *in vivo*.

Studies by Suthar *et al*. have suggested that tissue tropism for WNV is determined by immune responses generated during infection (Suthar et al., 2013a). If this were the case, one would expect that infection of IFNα/β receptor knock-out mice with the different chimeras might result in similar mortality and virus tissue distribution to WNV NY99. If differences were still seen in these mice, it would suggest that the EIII sequences are playing more of a role in tissue tropism than just differentially modulating immune responses.

The KOUV B chimera has a behavior *in vivo* that is not readily explained by immune response differences compared to WNV NY99. The observation that it appears to have a different glycosylation profile than WNV NY99 and the other chimeras with regards to Endo H sensitivity may go some way to explain its variable attenuation and altered tissue tropism. Glycan analysis of purified virions would allow for a greater understanding of the nature of the differences in glycosylation, and may lend an explanation for the apparently increased adhesiveness of the KOUV chimeras.

The suggestion from the neutralization data that BAGV B may be using an alternative mode of attachment is quite interesting. Serum samples that appear to show significant lower EIII binding compared to WNV NY99 remain potently neutralizing. To determine whether the BAGV B chimera has lower EIII-dependency for binding, competition assays could be run. This would involve the pre-treatment of cells with recombinant WNV EIII, BAGV EIII, and WNV 80% E followed by infection with the BAGV B chimera. If binding is EIII-dependent, and the receptor usage is different for BAGV B compared to WNV, one would expect little inhibition following pre-treatment

with WNV EIII or 80% E, but significant inhibition with BAGV EIII. If binding is EIII-dependent, and the virus uses similar receptors to WNV NY99, these two competitors should inhibit infection. If infection is EIII-independent, WNV 80% E should inhibit infection but the two recombinant EIIIs should not.

For the WNV G331A study, a potential future direction would be to perform a serial sacrifice study using the adaptive mutant viruses, comparing tissue titers and distribution to wild-type WNV NY99. This would help to determine whether the adaptive mutations are causing a difference in organ distribution resulting from differences in receptor usage. A further test to determine differences in receptor binding could involve running competition assays as described above. If the adapted viruses were less readily inhibited by recombinant WNV EIII, it would suggest that a shift in receptor usage may be occurring.

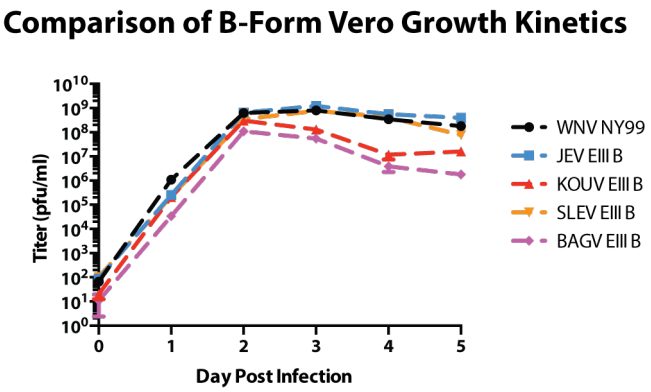

Figure 6.1: Comparison of Chimera B-Form Growth Kinetics in Vero Cells. Growth of the chimera B-forms are very similar to one another and WNV NY99, suggesting that the substitution of EIII has little effect on growth within Vero cells.

APPENDICES

Appendix A: Primer List

Mutagenesis Primers

pWN-AB Restriction Site Primers

pWN-AB SalI Mutagenesis Forward:
5'-CCTTCAGCTGCAATTTTTCCATCTTCAGTCGACACTTCAAATGACCC-3' 66.8°C

pWN-AB SalI Mutagenesis Reverse:
5'-GGGTCATTTGAAGTGTCGACTGAAGATGGAAAAATTGCAGCTGAAGG-3' 66.8°C

pWN-AB BamHI Mutagenesis Forward:
5'- TGAACACCCCTCCAACGGATCCAAAGTCCCAAG -3' 72.2°C

pWN-AB BamHI Mutagenesis Reverse:
5'- CTTGGGACTTTGGATCCGTTGGAGGGGTGTTCA -3' 72.2°C

JEV EIII Amplification Primers

JEV EIII SalI Forward:
5'-ATGCGTCGACTGAGAATGGACAAACTGGCTCTGAA-3' 71.8°C

JEV EIII PstI Forward:
5'-ATGCCTGCAGCTGAAAGGCACAACCTATGGCATGT-3' 74.1°C

JEV EIII StuI Reverse:
5'-ATCGAGGCCTTGCCCAGCGTGCTTCCAGCCTTGTG-3' 78.1°C

JEV EIII BamHI Reverse:
5'-ATCGGGATCCAAAGTCCCAGGCTGTGTCGCCCAAC-3' 76.2°C

KOUV EIII Amplification Primers

KOUV EIII SalI Forward:
5'-ATCGGTCGACTCAAAATGGAAAAGCTCCAACTTAA-3' 68.1°C

KOUV EIII PstI Forward:
5’-ATCGCTGCAGCTTAAGGGGACCACTTACGGAGTGT-3’ 74.1°C

KOUV EIII StuI Reverse:
5’-ATGCAGGCCTTCCCAATACTGCTTCCTGACTTGTG-3’ 72.3°C

KOUV EIII BamHI Reverse:
5’-ATGCGGATCCAAAGTCCCAAGCTGTGTCTCCTAGC-3’ 73.2°C

SLEV EIII Amplification Primers

SLEV EIII XhoI Forward:
5’-ATCGCTCGAGTGAAGCTTGACAAGGTCAAAATCAA-3’ 69.2°C

SLEV EIII PstI Forward:
5’-ATCGCTGCAGATCAAGGGAACGACATATGGTATGT-3’ 70.1°C

SLEV EIII StuI Reverse:
5’-ATGCAGGCCTTCCCAATGCTGCTTCCCTCTTTGTG-3’ 74.3°C

SLEV EIII BamHI Reverse:
5’-ATGCGGATCCAAAGTCCCACGCAGTGTCCCCTAAG-3’ 74.6°C

BAGV EIII Amplification Primers

BAGV EIII XhoI Forward:
5’-ATCGCTCGAGTGAAATTACAAGGACTGAAATTGAA-3’ 66.7°C

BAGV EIII PstI Forward:
5’-ATCGCTGCAGTTGAAAGGAATGACTTACCCCATGT-3’ 70.7°C

BAGV EIII StuI Reverse:
5’-ATGCAGGCCTTACCGATGGAGCTTCCACTCTTGTG-3’ 73.4°C

BAGV EIII BamHI Reverse:
5’-ATGCGGATCCAAAGTCCCATGCGGTGTCTCCAAGT-3’ 74.6°C

ZIKV EIII Amplification Primers

ZIKV EIII SalI Forward:
5’-ATGCGTCGACTAAAAATGGACAAGCTTAGATTGA-3’ 66.8°C

ZIKV EIII PstI Forward:

5’-ATGCCTGCAGTTGAAGGGCGTGTCATATTCCTTG-3’	71.5°C
ZIKV EIII StuI Reverse:	
5’-ATCGAGGCCTTTCCGATGGTGCTACCACTCCTAT-3’	72.3°C
ZIKV EIII BamHI Reverse:	
5’-ATCGGGATCCGAAGTCCCAGGCTGTATCCCCCAG-3’	75.2°C

IGUV EIII Amplification Primers

IGUV EIII SalI Forward:	
5’-ATCGGTCGACTGAAGATGGACAAGTTACTGATCAA-3’	68.4°C
IGUV EIII PstI Forward:	
5’-ATCGCTGCAGATCAAGGGCACCACGTATCACATGT-3’	73.3°C
IGUV EIII StuI Reverse:	
5’-ATGCAGGCCTCTCCGATGGAACTTCCAGGCTTGAA-3’	74.4°C
IGUV EIII BamHI Reverse:	
5’-ATGCGGATCCGAAGTCCCAAGCAGAATCTCCTAGA-3’	72.1°C

DENV-2 EIII Amplification Primers

DENV-2 EIII SalI Forward:	
5’-ATGCGTCGACTGAGGATGGACAAACTACAGCTCAA-3’	71.5°C
DENV-2 EIII PstI Forward:	
5’-ATGCCTGCAGCTCAAAGGAATGTCATACTCTATGT-3’	68.1°C
DENV-2 EIII StuI Reverse:	
5’-ATCGAGGCCTGGCCGATAGAACTTCCTTTCTTAAAC-3’	70.3°C
DENV-2 EIII BamHI Reverse:	
5’-ATCGGGATCCAAAATCCCAAGCTGTGTCACCTAAAA-3’	70.5°C

YFV EIII Amplification Primers

YFV EIII SalI Forward:	
5’-GTCGACTGAAATTGTCAGCTTTGACAC-3’	63.2°C
YFV EIII BamHI Reverse:	
5’-GGATCCGAAATCCCAGGCGGCGTCTC-3’	70.8°C

DTV EIII Amplification Primers

DTV EIII SalI Forward:
5’-GTCGACTGGGACTGGAAAAGCTGAAA-3’ 65.2°C

DTV EIII BamHI Reverse:
5’-GGATCCAAAGTCCCATGCATGTTCTTC-3’ 64.3°C

Sequencing Primers

401 Sequencing Primer:
5’-AAAAGAAAAGAGGAGGAAAG-3’ 50.8°C

1101 Sequencing Primer:
5’-GATGAATATGGAGGCGGTCA-3’ 57.2°C

1751 Sequencing Primer:
5’-TGCATCAAGCTTTGGCTGGA-3’ 60.5°C

1219c Sequencing Primer:
5’-GTTTGTCATTGTGAGCTTCT-3’ 51.4°C

1816a Sequencing Primer:
5’-CCGACGTCAACTTGACAGTG-3’ 59.1°C

2504a Sequencing Primer:
5’-TCTTGCCGGCTGATGTCTAT-3’ 58.1°C

Appendix B: Antibody List

Mono- and Polyclonal Antibodies

4G2: Anti-Flavivirus Group Antigen Antibody
EMD Millipore MAB10216

3A3: Anti-WNV EIII Monoclonal Antibody
Bioreliance Corp. 80-524-WNV3A3

ab81193: Anti-JEV EIII Monoclonal Antibody ab81193
Abcam ab81193

NB100-56743: Anti-WNV M Polyclonal Antibody
Novus Biologicals NB100-56743

Mouse Immune Ascitic Fluid

T-35570: Anti-WNV Lineage I MIAF
World Reference Center for Emerging Viruses and Arboviruses T-35570

T-35345: Anti-WNV Lineage II MIAF
World Reference Center for Emerging Viruses and Arboviruses T-35345

T-34119: Anti-JEV MIAF
World Reference Center for Emerging Viruses and Arboviruses T-34119

T-34910: Anti-SLEV MIAF
World Reference Center for Emerging Viruses and Arboviruses T-34910

Anti-BAGV MIAF
World Reference Center for Emerging Viruses and Arboviruses (No Ref #)

References

ABDELWAHAB, K. S., ALMEIDA, J. D., DOANE, F. W. & MCLEAN, D. M. 1964. Powassan Virus: Morphology and Cytopathology. *Can Med Assoc J,* 90**,** 1068-1072.

ACKERMANN, M. & PADMANABHAN, R. 2001. De novo synthesis of RNA by the dengue virus RNA-dependent RNA polymerase exhibits temperature dependence at the initiation but not elongation phase. *J Biol Chem,* 276**,** 39926-39937.

ADA, G. L. & ANDERSON, S. G. 1959a. The Infectivity of Preparations made by the Action of Phenol on Dengue I, Dengue II, GD VII and Herpes Simplex Viruses. *Austral J Sci,* 21**,** 259-260.

ADA, G. L. & ANDERSON, S. G. 1959b. Yield of Infective "Ribonucleic Acid" from Impure Murray Valley Encephalitis Virus after Different Treatments. *Nature,* 183**,** 799-800.

ADAMS, S. C., BROOM, A. K., SAMMELS, L. M., HARTNETT, A. C., HOWARD, M. J., COELEN, R. J., MACKENZIE, J. S. & HALL, R. A. 1995. Glycosylation and antigenic variation among Kunjin virus isolates. *Virology,* 206**,** 49-56.

AKEY, D. L., BROWN, W. C., DUTTA, S., KONWERSKI, J., JOSE, J., JURKIW, T. J., DELPROPOSTO, J., OGATA, C. M., SKINIOTIS, G., KUHN, R. J. & SMITH, J. L. 2014. Flavivirus NS1 structures reveal surfaces for associations with membranes and the immune system. *Science,* 343**,** 881-885.

AKEY, D. L., BROWN, W. C., JOSE, J., KUHN, R. J. & SMITH, J. L. 2015. Structure-guided insights on the role of NS1 in flavivirus infection. *Bioessays,* 37**,** 489-494.

ALEN, M. M. F., DALLMEIER, K., BALZARINI, J., NEYTS, J. & SCHOLS, D. 2012. Crucial role of the N-glycans on the viral E-envelope glycoprotein in DC-SIGN-mediated dengue virus infection. *Antiviral Res,* 96**,** 280-287.

ALESHIN, A. E., SHIRYAEV, S. A., STRONGIN, A. Y. & LIDDINGTON, R. C. 2007. Structural evidence for regulation and specificity of flaviviral proteases and evolution of the Flaviviridae fold. *Protein Sci.,* 16**,** 795-806.

ALLISON, S. L., SCHALICH, J., STIASNY, K., MANDL, C. W. & HEINZ, F. X. 2001. Mutational evidence for an internal fusion peptide in flavivirus envelope protein E. *J Virol,* 75**,** 4268-4275.

ALLISON, S. L., SCHALICH, J., STIASNY, K., MANDL, C. W., KUNZ, C. & HEINZ, F. X. 1995. Oligomeric rearrangement of tick-borne encephalitis virus envelope proteins induced by an acidic pH. *J Virol,* 69**,** 695-700.

ALLISON, S. L., STIASNY, K., STADLER, K., MANDL, C. W. & HEINZ, F. X. 1999. Mapping of functional elements in the stem-anchor region of tick-borne encephalitis virus envelope protein E. *J Virol,* 73**,** 5605-5612.

ALLISON, S. L., TAO, Y. J., O'RIORDAIN, G., MANDL, C. W., HARRISON, S. C. & HEINZ, F. X. 2003. Two distinct size classes of immature and mature subviral particles from tick-borne encephalitis virus. *J Virol,* 77**,** 11357-11366.

ALVAREZ, D. E., DE LELLA EZCURRA, A. L., FUCITO, S. & GAMARNIK, A. V. 2005a. Role of RNA structures present at the 3'UTR of dengue virus on translation, RNA synthesis, and viral replication. *Virology,* 339**,** 200-212.

ALVAREZ, D. E., FILOMATORI, C. V. & GAMARNIK, A. V. 2008. Functional analysis of dengue virus cyclization sequences located at the 5' and 3' UTRs. *Virology,* 375**,** 223-235.

ALVAREZ, D. E., LODEIRO, M. F., LUDUEÑA, S. J., PIETRASANTA, L. I. & GAMARNIK, A. V. 2005b. Long-range RNA-RNA interactions circularize the dengue virus genome. *J Virol,* 79**,** 6631-6643.

AMBROSE, R. L. & MACKENZIE, J. M. 2011. West Nile virus differentially modulates the unfolded protein response to facilitate replication and immune evasion. *J Virol,* 85**,** 2723-2732.

ANDERSON, S. G. & ADA, G. L. 1959. Murray Valley Encephalitis Virus: Preparation of an Infective “Ribonucleic Acid” Fraction. *Aust J Exp Biol Med,* 37**,** 353-364.

ANON 1900. Yellow Fever and Mosquitoes. *Science,* 12**,** 692-693.

AOKI, C., HIDARI, K. I. P. J., ITONORI, S., YAMADA, A., TAKAHASHI, N., KASAMA, T., HASEBE, F., ISLAM, M. A., HATANO, K., MATSUOKA, K., TAKI, T., GUO, C.-T., TAKAHASHI, T., SAKANO, Y., SUZUKI, T., MIYAMOTO, D., SUGITA, M., TERUNUMA, D., MORITA, K. & SUZUKI, Y. 2006. Identification and characterization of carbohydrate molecules in mammalian cells recognized by dengue virus type 2. *J Biochem,* 139**,** 607-614.

APT, D., RAVIPRAKASH, K., BRINKMAN, A., SEMYONOV, A., YANG, S., SKINNER, C., DIEHL, L., LYONS, R., PORTER, K. & PUNNONEN, J. 2006. Tetravalent neutralizing antibody response against four dengue serotypes by a single chimeric dengue envelope antigen. *Vaccine,* 24**,** 335-344.

ARGAW, A. T., ZHANG, Y., SNYDER, B. J., ZHAO, M.-L., KOPP, N., LEE, S. C., RAINE, C. S., BROSNAN, C. F. & JOHN, G. R. 2006. IL-1beta regulates blood-brain barrier permeability via reactivation of the hypoxia-angiogenesis program. *J Immunol,* 177**,** 5574-5584.

ARIAS, C. F., PREUGSCHAT, F. & STRAUSS, J. H. 1993. Dengue 2 virus NS2B and NS3 form a stable complex that can cleave NS3 within the helicase domain. *Virology,* 193**,** 888-899.

ARMSTRONG, P. M., VOSSBRINCK, C. R., ANDREADIS, T. G., ANDERSON, J. F., PESKO, K. N., NEWMAN, R. M., LENNON, N. J., BIRREN, B. W., EBEL, G. D. & HENN, M. R. 2011. Molecular evolution of West Nile virus in a northern temperate region: Connecticut, USA 1999-2008. *Virology,* 417**,** 203-210.

ASHBURN, P. M. & CRAIG, C. F. 1907. Experimental Investigations Regarding the Etiology of Dengue Fever. *JID,* 4**,** 440-475.

ASHOUR, J., LAURENT-ROLLE, M., SHI, P.-Y. & GARCÍA-SASTRE, A. 2009. NS5 of dengue virus mediates STAT2 binding and degradation. *J Virol,* 83**,** 5408-5418.

ASNIS, D. S., CONETTA, R., TEIXEIRA, A. A., WALDMAN, G. & SAMPSON, B. A. 2000. The West Nile Virus outbreak of 1999 in New York: the Flushing Hospital experience. *Clin Infect Dis,* 30**,** 413-418.

AUDSLEY, M., EDMONDS, J., LIU, W., MOKHONOV, V., MOKHONOVA, E., MELIAN, E. B., PROW, N., HALL, R. A. & KHROMYKH, A. A. 2011. Virulence determinants between New York 99 and Kunjin strains of West Nile virus. *Virology,* 414**,** 63-73.

AVIRUTNAN, P., FUCHS, A., HAUHART, R. E., SOMNUKE, P., YOUN, S., DIAMOND, M. S. & ATKINSON, J. P. 2010. Antagonism of the complement component C4 by flavivirus nonstructural protein NS1. *J Exp Med,* 207**,** 793-806.

AVIRUTNAN, P., HAUHART, R. E., SOMNUKE, P., BLOM, A. M., DIAMOND, M. S. & ATKINSON, J. P. 2011. Binding of flavivirus nonstructural protein NS1 to C4b binding protein modulates complement activation. *J Immunol,* 187**,** 424-433.

AYALA-NUÑEZ, N. V., WILSCHUT, J. & SMIT, J. M. 2011. Monitoring virus entry into living cells using DiD-labeled dengue virus particles. *Methods,* 55**,** 137-143.

BAI, F., TOWN, T., QIAN, F., WANG, P., KAMANAKA, M., CONNOLLY, T. M., GATE, D., MONTGOMERY, R. R., FLAVELL, R. A. & FIKRIG, E. 2009. IL-10 signaling blockade controls murine West Nile virus infection. *PLoS Pathog,* 5**,** e1000610.

BALTIMORE, D. 1971. Expression of Animal Virus Genomes. *Bacteriol Rev,* 35**,** 235-241.

BANCROFT, T. L. 1906. On the Etiology of Dengue Fever. *Australasian Med Gazette,* 25**,** 17-18.

BARONTI, C., SIRE, J., DE LAMBALLERIE, X. & QUÉRAT, G. 2010. Nonstructural NS1 proteins of several mosquito-borne Flavivirus do not inhibit TLR3 signaling. *Virology,* 404**,** 319-330.

BARTELMA, G. & PADMANABHAN, R. 2002. Expression, purification, and characterization of the RNA 5'-triphosphatase activity of dengue virus type 2 nonstructural protein 3. *Virology,* 299**,** 122-132.

BASHKIROV, P. V., AKIMOV, S. A., EVSEEV, A. I., SCHMID, S. L., ZIMMERBERG, J. & FROLOV, V. A. 2008. GTPase cycle of dynamin is coupled to membrane squeeze and release, leading to spontaneous fission. *Cell,* 135**,** 1276-1286.

BASU, M. & BRINTON, M. A. 2011. West Nile virus (WNV) genome RNAs with up to three adjacent mutations that disrupt long distance 5'-3' cyclization sequence basepairs are viable. *Virology,* 412**,** 220-232.

BAWDEN, F. C. & PIRIE, N. W. 1937. The Isolation and some Properties of Liquid Crystalline Substances from Solanaceous Plants infected with Three Strains of Tobacco Mosaic Virus. *Proc R Soc B,* 123**,** 274-320.

BAZAN, J. F. & FLETTERICK, R. J. 1989. Detection of a trypsin-like serine protease domain in flaviviruses and pestiviruses. *Virology,* 171**,** 637-639.

BEASLEY, D. W. C. & BARRETT, A. D. T. 2002. Identification of neutralizing epitopes within structural domain III of the West Nile virus envelope protein. *J Virol,* 76**,** 13097-13100.

BEASLEY, D. W. C., DAVIS, C. T., ESTRADA-FRANCO, J., NAVARRO-LOPEZ, R., CAMPOMANES-CORTES, A., TESH, R. B., WEAVER, S. C. & BARRETT, A. D. T. 2004a. Genome sequence and attenuating mutations in West Nile virus isolate from Mexico. *Emerging Infect. Dis.,* 10**,** 2221-2224.

BEASLEY, D. W. C., HOLBROOK, M. R., TRAVASSOS DA ROSA, A. P. A., COFFEY, L., CARRARA, A.-S., PHILLIPPI-FALKENSTEIN, K., BOHM, R. P., RATTERREE, M. S., LILLIBRIDGE, K. M., LUDWIG, G. V., ESTRADA-FRANCO, J., WEAVER, S. C., TESH, R. B., SHOPE, R. E. & BARRETT, A. D. T. 2004b. Use of a recombinant envelope protein subunit antigen for specific serological diagnosis of West Nile virus infection. *J Clin Microbiol,* 42**,** 2759-2765.

BEASLEY, D. W. C., LI, L., SUDERMAN, M. T. & BARRETT, A. D. T. 2002. Mouse neuroinvasive phenotype of West Nile virus strains varies depending upon virus genotype. *Virology,* 296**,** 17-23.

BEASLEY, D. W. C., WHITEMAN, M. C., ZHANG, S., HUANG, C. Y. H., SCHNEIDER, B. S., SMITH, D. R., GROMOWSKI, G. D., HIGGS, S., KINNEY, R. M. & BARRETT, A. D. T. 2005. Envelope protein glycosylation status influences mouse neuroinvasion phenotype of genetic lineage 1 West Nile virus strains. *J Virol,* 79**,** 8339-8347.

BEIJERINCK, M. W. 1898. Ueber ein Contagium vivum fluidum als Ursache der Fleckenkrankheit der Tabaksblätter. *Verhand Kon Akad Wetensch Amsterdam,* 6**,** 1-21.

BEIJERINCK, M. W. 1942. Concerning a Contagium Vivum Fluidum as a Cause of the Spot Disease of Tobacco Leaves. *Phytopathol Classics,* 7**,** 33-52.

BELL, J. R., KINNEY, R. M., TRENT, D. W., LENCHES, E. M., DALGARNO, L. & STRAUSS, J. H. 1985. Amino-Terminal Amino Acid Sequences of Structural Proteins of Three Flaviviruses. *Virology,* 143**,** 224-229.

BENARROCH, D., SELISKO, B., LOCATELLI, G. A., MAGA, G., ROMETTE, J.-L. & CANARD, B. 2004. The RNA helicase, nucleotide 5'-triphosphatase, and RNA 5'-triphosphatase activities of Dengue virus protein NS3 are Mg2+-dependent and require a functional Walker B motif in the helicase catalytic core. *Virology,* 328**,** 208-218.

BERGE, T. O. (ed.) 1975. *International Catalogue of Arboviruses,* Washington, DC: Public Health Service.

BERNKOPF, H., LEVINE, S. & NERSON, R. 1953. Isolation of West Nile virus in Israel. *JID,* 93**,** 207-218.

BERTHET, F. X., ZELLER, H. G., DROUET, M. T., RAUZIER, J., DIGOUTTE, J. P. & DEUBEL, V. 1997. Extensive nucleotide changes and deletions within the envelope glycoprotein gene of Euro-African West Nile viruses. *J Gen Virol,* 78**,** 2293-2297.

BEST, S. M., MORRIS, K. L., SHANNON, J. G., ROBERTSON, S. J., MITZEL, D. N., PARK, G. S., BOER, E., WOLFINBARGER, J. B. & BLOOM, M. E. 2005. Inhibition of interferon-stimulated JAK-STAT signaling by a tick-borne flavivirus and identification of NS5 as an interferon antagonist. *J Virol,* 79**,** 12828-12839.

BHATT, S., GETHING, P. W., BRADY, O. J., MESSINA, J. P., FARLOW, A. W., MOYES, C. L., DRAKE, J. M., BROWNSTEIN, J. S., HOEN, A. G., SANKOH, O., MYERS, M. F., GEORGE, D. B., JAENISCH, T., WINT, G. R. W., SIMMONS, C. P., SCOTT, T. W., FARRAR, J. J. & HAY, S. I. 2013. The global distribution and burden of dengue. *Nature,* 496**,** 504-507.

BHUVANAKANTHAM, R., CHEONG, Y. K. & NG, M.-L. 2010a. West Nile virus capsid protein interaction with importin and HDM2 protein is regulated by protein kinase C-mediated phosphorylation. *Microbes Infect,* 12**,** 615-625.

BHUVANAKANTHAM, R., LI, J., TAN, T. T. T. & NG, M.-L. 2010b. Human Sec3 protein is a novel transcriptional and translational repressor of flavivirus. *Cell. Microbiol.,* 12**,** 453-472.

BHUVANAKANTHAM, R. & NG, M.-L. 2013. West Nile virus and dengue virus capsid protein negates the antiviral activity of human Sec3 protein through the proteasome pathway. *Cell. Microbiol.,* 15**,** 1688-1706.

BIDET, K. & GARCIA-BLANCO, M. A. 2014. Flaviviral RNAs: Weapons and Targets in the War Between Virus and Host. *Biochem J,* 462**,** 215-230.

BIELEFELDT-OHMANN, H., BEASLEY, D. W., FITZPATRICK, D. R. & AASKOV, J. G. 1997. Analysis of a recombinant dengue-2 virus-dengue-3 virus hybrid envelope protein expressed in a secretory baculovirus system. *J Gen Virol,* 78 (Pt 11)**,** 2723-2733.

BLACKWELL, J. L. & BRINTON, M. A. 1995. BHK cell proteins that bind to the 3' stem-loop structure of the West Nile virus genome RNA. *J Virol,* 69**,** 5650-5658.

BLACKWELL, J. L. & BRINTON, M. A. 1997. Translation Elongation Factor-1 Alpha Interacts with the 3' Stem-Loop Region of West Nile Virus Genomic RNA. *J Virol,* 71**,** 6433-6444.

BLANEY, J. E., HANSON, C. T., FIRESTONE, C.-Y., HANLEY, K. A., MURPHY, B. R. & WHITEHEAD, S. S. 2004. Genetically modified, live attenuated dengue virus type 3 vaccine candidates. *Am J Trop Med Hyg,* 71**,** 811-821.

BLANEY, J. E., SATHE, N. S., HANSON, C. T., FIRESTONE, C.-Y., MURPHY, B. R. & WHITEHEAD, S. S. 2007. Vaccine candidates for dengue virus type 1 (DEN1) generated by replacement of the structural genes of rDEN4 and rDEN4Delta30 with those of DEN1. *Virol J,* 4**,** 23.

BLANEY, J. E. J., SPEICHER, J., HANSON, C. T., SATHE, N. S., WHITEHEAD, S. S., MURPHY, B. R. & PLETNEV, A. G. 2008. Evaluation of St. Louis encephalitis virus/dengue virus type 4 antigenic chimeric viruses in mice and rhesus monkeys. *Vaccine,* 26**,** 4150-4159.

BLÁZQUEZ, A.-B., MARTÍN-ACEBES, M. A. & SAIZ, J.-C. 2014. Amino acid substitutions in the non-structural proteins 4A or 4B modulate the induction of

autophagy in West Nile virus infected cells independently of the activation of the unfolded protein response. *Front Microbiol,* 5**,** 797.

BLETCHLY, C. 2002. *Antigenic and Structural Analysis of the NS1 Glycoprotein of Dengue Virus.* PhD, University of Queensland.

BLITVICH, B. J., MACKENZIE, J. S., COELEN, R. J., HOWARD, M. J. & HALL, R. A. 1995. A novel complex formed between the flavivirus E and NS1 proteins: analysis of its structure and function. *Arch Virol,* 140**,** 145-156.

BLITVICH, B. J., SCANLON, D., SHIELL, B. J., MACKENZIE, J. S. & HALL, R. A. 1999. Identification and analysis of truncated and elongated species of the flavivirus NS1 protein. *Virus Res,* 60**,** 67-79.

BOEGE, U., HEINZ, F. X., WENGLER, G. & KUNZ, C. 1983. Amino acid compositions and amino-terminal sequences of the structural proteins of a flavivirus, European Tick-Borne Encephalitis virus. *Virology,* 126**,** 651-657.

BORK, P., HOLM, L. & SANDER, C. 1994. The immunoglobulin fold. Structural classification, sequence patterns and common core. *J. Mol. Biol.,* 242**,** 309-320.

BOULTON, P. S. & WEBB, H. E. 1971. An electron microscopic study of Langat virus encephalitis in mice. *Brain,* 94**,** 411-418.

BOULTON, P. S., WEBB, H. E., FAIRBAIRN, G. E. & ILLAVIA, S. J. 1971. An electron microscope study of Langat virus in tissue culture of the non-neuronal cells of mouse brain. *Brain,* 94**,** 403-410.

BOULTON, R. W. & WESTAWAY, E. G. 1972. Comparisons of togaviruses: Sindbis virus (group A) and Kunjin virus (group B). *Virology,* 49**,** 283-289.

BRABANT, M., BAUX, L., CASIMIR, R., BRIAND, J. P., CHALOIN, O., PORCEDDU, M., BURON, N., CHAUVIER, D., LASSALLE, M., LECOEUR, H., LANGONNÉ, A., DUPONT, S., DÉAS, O., BRENNER, C., REBOUILLAT, D., MULLER, S., BORGNE-SANCHEZ, A. & JACOTOT, E. 2009. A flavivirus protein M-derived peptide directly permeabilizes mitochondrial membranes, triggers cell death and reduces human tumor growth in nude mice. *Apoptosis,* 14**,** 1190-1203.

BRADY, O. J., GETHING, P. W., BHATT, S., MESSINA, J. P., BROWNSTEIN, J. S., HOEN, A. G., MOYES, C. L., FARLOW, A. W., SCOTT, T. W. & HAY, S. I. 2012. Refining the global spatial limits of dengue virus transmission by evidence-based consensus. *PLoS Negl Trop Dis,* 6**,** e1760.

BRANDT, W. E., CARDIFF, R. D. & RUSSELL, P. K. 1970. Dengue virions and antigens in brain and serum of infected mice. *J Virol,* 6**,** 500-506.

BRATHWAITE DICK, O., SAN MARTÍN, J. L., MONTOYA, R. H., DEL DIEGO, J., ZAMBRANO, B. & DAYAN, G. H. 2012. The history of dengue outbreaks in the Americas. *Am J Trop Med Hyg,* 87**,** 584-593.

BRAY, M. & LAI, C.-J. 1991a. Construction of intertypic chimeric dengue viruses by substitution of structural protein genes. *PNAS,* 88**,** 10342-10346.

BRAY, M. & LAI, C.-J. 1991b. Dengue virus premembrane and membrane proteins elicit a protective immune response. *Virology,* 185**,** 505-508.

BRAY, M., MEN, R. & LAI, C. J. 1996. Monkeys immunized with intertypic chimeric dengue viruses are protected against wild-type virus challenge. *J Virol,* 70**,** 4162-4166.

BRAY, M., MEN, R., TOKIMATSU, I. & LAI, C.-J. 1998. Genetic determinants responsible for acquisition of dengue type 2 virus mouse neurovirulence. *J Virol,* 72**,** 1647-1651.

BRIESE, T., JIA, X.-Y., HUANG, C., GRADY, L. J. & LIPKIN, W. I. 1999. Identification of a Kunjin/West Nile-like flavivirus in brains of patients with New York encephalitis. *Lancet,* 354**,** 1261-1262.

BRINTON, M. A. 2009. Molecular Biology of West Nile Virus. *In:* DIAMOND, M. S. (ed.) *West Nile Encephalitis Virus Infection.* 1st Edition ed. New York.

BRINTON, M. A. 2014. Replication cycle and molecular biology of the West Nile virus. *Viruses,* 6**,** 13-53.

BRINTON, M. A. & BASU, M. 2015. Functions of the 3' and 5' genome RNA regions of members of the genus Flavivirus. *Virus Res*.

BRINTON, M. A. & DISPOTO, J. H. 1988. Sequence and Secondary Structure Analysis of the 5'-Terminal Region of Flavivirus Genome RNA. *Virology,* 162**,** 290-299.

BRINTON, M. A., FERNANDEZ, A. V. & DISPOTO, J. H. 1986. The 3'-nucleotides of flavivirus genomic RNA form a conserved secondary structure. *Virology,* 153**,** 113-121.

BROOKS, A. J., JOHANSSON, M., JOHN, A. V., XU, Y., JANS, D. A. & VASUDEVAN, S. G. 2002. The interdomain region of dengue NS5 protein that binds to the viral helicase NS3 contains independently functional importin beta 1 and importin alpha/beta-recognized nuclear localization signals. *J Biol Chem,* 277**,** 36399-36407.

BRYANT, J. E., CALVERT, A. E., MESESAN, K., CRABTREE, M. B., VOLPE, K. E., SILENGO, S., KINNEY, R. M., HUANG, C. Y. H., MILLER, B. R. & ROEHRIG, J. T. 2007. Glycosylation of the dengue 2 virus E protein at N67 is critical for virus growth in vitro but not for growth in intrathoracically inoculated Aedes aegypti mosquitoes. *Virology,* 366**,** 415-423.

BULICH, R. & AASKOV, J. G. 1992. Nuclear localization of dengue 2 virus core protein detected with monoclonal antibodies. *J Gen Virol,* 73**,** 2999-3003.

BUTRAPET, S., KIMURA-KURODA, J., ZHOU, D. S. & YASUI, K. 1998. Neutralizing mechanism of a monoclonal antibody against Japanese encephalitis virus glycoprotein E. *Am J Trop Med Hyg,* 58**,** 389-398.

BYLON, D. 1780. Korte Aanteekening, wegens eene Algemeene Ziekte, doorgaans genaamd de Knokkel-Koorts. *Verhandel Batav Genootsch Kunsten Wetensch,* 2**,** 17-30.

CABRERA-HERNANDEZ, A., THEPPARIT, C., SUKSANPAISAN, L. & SMITH, D. R. 2007. Dengue virus entry into liver (HepG2) cells is independent of hsp90 and hsp70. *J Med Virol,* 79**,** 386-392.

CAHOUR, A., PLETNEV, A. G., VAZIELLE-FALCOZ, M., ROSEN, L. & LAI, C.-J. 1995. Growth-restricted dengue virus mutants containing deletions in the 5' noncoding region of the RNA genome. *Virology,* 207**,** 68-76.

CAMPBELL, C. L., SMITH, D. R., SANCHEZ-VARGAS, I., ZHANG, B., SHI, P.-Y. & EBEL, G. D. 2014. A positively selected mutation in the WNV 2K peptide

confers resistance to superinfection exclusion in vivo. *Virology,* 464-465**,** 228-232.

CARDIFF, R. D., BRANDT, W. E., MCCLOUD, T. G., SHAPIRO, D. & RUSSELL, P. K. 1971. Immunological and biophysical separation of dengue-2 antigens. *J Virol,* 7**,** 15-23.

CARVALHO, F. A., CARNEIRO, F. A., MARTINS, I. C., ASSUNÇÃO-MIRANDA, I., FAUSTINO, A. F., PEREIRA, R. M., BOZZA, P. T., CASTANHO, M. A. R. B., MOHANA-BORGES, R., DA POIAN, A. T. & SANTOS, N. C. 2012. Dengue virus capsid protein binding to hepatic lipid droplets (LD) is potassium ion dependent and is mediated by LD surface proteins. *J Virol,* 86**,** 2096-2108.

CASALS, J. 1944. Immunological Relationships Among Central Nervous System Viruses. *J Exp Med,* 79**,** 341-359.

CASALS, J. 1957. Viruses: the versatile parasites; the arthropod-borne group of animal viruses. *Trans N Y Acad Sci,* 19**,** 219-235.

CASALS, J. & BROWN, L. V. 1954. Hemagglutination with arthropod-borne viruses. *J Exp Med,* 99**,** 429-449.

CASTLE, E., LEIDNER, U., NOWAK, T., WENGLER, G. & WENGLER, G. 1986. Primary structure of the West Nile flavivirus genome region coding for all nonstructural proteins. *Virology,* 149**,** 10-26.

CASTLE, E., NOWAK, T., LEIDNER, U., WENGLER, G. & WENGLER, G. 1985. Sequence analysis of the viral core protein and the membrane-associated proteins V1 and NV2 of the flavivirus west nile virus and of the genome sequence for these proteins. *Virology,* 145**,** 227-236.

CASTLE, E. & WENGLER, G. 1987. Nucleotide sequence of the 5'-terminal untranslated part of the genome of the flavivirus West Nile virus. *Arch Virol,* 92**,** 309-313.

CATTEAU, A., KALININA, O., WAGNER, M.-C., DEUBEL, V., COURAGEOT, M.-P. & DESPRES, P. 2003a. Dengue virus M protein contains a proapoptotic sequence referred to as ApoptoM. *J Gen Virol,* 84**,** 2781-2793.

CATTEAU, A., ROUÉ, G., YUSTE, V. J., SUSIN, S. A. & DESPRES, P. 2003b. Expression of dengue ApoptoM sequence results in disruption of mitochondrial potential and caspase activation. *Biochimie,* 85**,** 789-793.

CAUFOUR, P. S., MOTTA, M. C., YAMAMURA, A. M., VAZQUEZ, S., FERREIRA, I. I., JABOR, A. V., BONALDO, M. C., FREIRE, M. S. & GALLER, R. 2001. Construction, characterization and immunogenicity of recombinant yellow fever 17D-dengue type 2 viruses. *Virus Res,* 79**,** 1-14.

CDC. 2015. *West Nile Virus: Statistics and Maps* [Online]. Centers for Disease Control and Prevention. Available: http://www.cdc.gov/westnile/statsmaps/ [Accessed 20 Jul 2015 2015].

CEAUŞU, E., ERŞCOIU, S., CALISTRU, P., ISPAS, D., DOROBĂŢ, O., HOMOŞ, M., BĂRBULESCU, C., COJOCARU, I., SIMION, C. V., CRISTEA, C., OPREA, C., DUMITRESCU, C., DUICULESCU, D., MARCU, I., MOCIORNIŢĂ, C., STOICEV, T., ZOLOTUŞCA, I., CALOMFIRESCU, C., RUSU, R., HODREA, R., GEAMAI, S. & PĂUN, L. 1997. Clinical manifestations in the West Nile virus outbreak. *Rom J Virol,* 48**,** 3-11.

CHAMBERS, T. J., HAHN, C. S., GALLER, R. & RICE, C. M. 1990a. Flavivirus Genome Organization, Expression, and Replication. *Annu Rev Microbiol.,* 44**,** 649-688.

CHAMBERS, T. J., MCCOURT, D. W. & RICE, C. M. 1990b. Production of yellow fever virus proteins in infected cells: identification of discrete polyprotein species and analysis of cleavage kinetics using region-specific polyclonal antisera. *Virology,* 177**,** 159-174.

CHAMBERS, T. J., NESTOROWICZ, A., MASON, P. W. & RICE, C. M. 1999. Yellow fever/Japanese encephalitis chimeric viruses: construction and biological properties. *J Virol,* 73**,** 3095-3101.

CHAMBERS, T. J., WEIR, R. C., GRAKOUI, A., MCCOURT, D. W., BAZAN, J. F., FLETTERICK, R. J. & RICE, C. M. 1990c. Evidence that the N-terminal domain of nonstructural protein NS3 from yellow fever virus is a serine protease responsible for site-specific cleavages in the viral polyprotein. *PNAS,* 87**,** 8898-8902.

CHAN, A. H. Y., TAN, H. C., CHOW, A. Y., LIM, A. P. C., LOK, S.-M., MORELAND, N. J., VASUDEVAN, S. G., MACARY, P. A., OOI, E. E. & HANSON, B. J.

2012. A human PrM antibody that recognizes a novel cryptic epitope on dengue E glycoprotein. *PLoS One,* 7**,** e33451.

CHANG, R.-Y., HSU, T.-W., CHEN, Y.-L., LIU, S.-F., TSAI, Y.-J., LIN, Y.-T., CHEN, Y.-S. & FAN, Y.-H. 2013. Japanese encephalitis virus non-coding RNA inhibits activation of interferon by blocking nuclear translocation of interferon regulatory factor 3. *Vet. Microbiol.,* 166**,** 11-21.

CHANOCK, R. M. & SABIN, A. B. 1953a. The Hemagglutinin of St. Louis Encephalitis Virus: I. Recovery of Stable Hemagglutinin from the Brains of Infected Mice. *J Immunol,* 70**,** 271-285.

CHANOCK, R. M. & SABIN, A. B. 1953b. The Hemagglutinin of St. Louis Encephalitis Virus: II. Physico-Chemical Properties and Nature of its Reaction with Erythrocytes. *J Immunol,* 70**,** 286-301.

CHANOCK, R. M. & SABIN, A. B. 1953c. The Hemagglutinin of St. Louis Encephalitis Virus: III. Properties of Normal Inhibitors and Specific Antibody; use of Hemagglutination-Inhibition for Diagnosis of Infection. *J Immunol,* 70**,** 302-316.

CHANOCK, R. M. & SABIN, A. B. 1954. The Hemagglutinin of West Nile Virus: Recovery, Properties, and Antigenic Relationships. *J Immunol,* 73**,** 352-362.

CHAO, L. H., KLEIN, D. E., SCHMIDT, A. G., PEÑA, J. M. & HARRISON, S. C. 2014. Sequential conformational rearrangements in flavivirus membrane fusion. *Elife,* 3**,** e04389.

CHAPMAN, E. G., COSTANTINO, D. A., RABE, J. L., MOON, S. L., WILUSZ, J., NIX, J. C. & KIEFT, J. S. 2014a. The structural basis of pathogenic subgenomic flavivirus RNA (sfRNA) production. *Science,* 344**,** 307-310.

CHAPMAN, E. G., MOON, S. L., WILUSZ, J. & KIEFT, J. S. 2014b. RNA structures that resist degradation by Xrn1 produce a pathogenic Dengue virus RNA. *Elife,* 3**,** e01892.

CHAPPELL, K. J., NALL, T. A., STOERMER, M. J., FANG, N.-X., TYNDALL, J. D. A., FAIRLIE, D. P. & YOUNG, P. R. 2005. Site-directed mutagenesis and kinetic studies of the West Nile Virus NS3 protease identify key enzyme-substrate interactions. *J Biol Chem,* 280**,** 2896-2903.

CHARLIER, N., DAVIDSON, A. D., DALLMEIER, K., MOLENKAMP, R., DE CLERCQ, E. & NEYTS, J. 2010. Replication of not-known-vector flaviviruses in mosquito cells is restricted by intracellular host factors rather than by the viral envelope proteins. *J Gen Virol,* 91**,** 1693-1697.

CHARLIER, N., MOLENKAMP, R., LEYSSEN, P., PAESHUYSE, J., DROSTEN, C., PANNING, M., DE CLERCQ, E., BREDENBEEK, P. J. & NEYTS, J. 2004. Exchanging the yellow fever virus envelope proteins with Modoc virus prM and E proteins results in a chimeric virus that is neuroinvasive in SCID mice. *J Virol,* 78**,** 7418-7426.

CHASTEL, C., MAIN, A. J., GUIGUEN, C., LE LAY, G., QUILLIEN, M. C., MONNAT, J. Y. & BEAUCOURNU, J. C. 1985. The isolation of Meaban virus, a new Flavivirus from the seabird tick Ornithodoros (Alectorobius) maritimus in France. *Arch Virol,* 83**,** 129-140.

CHE, P., TANG, H. & LI, Q. 2013. The interaction between claudin-1 and dengue viral prM/M protein for its entry. *Virology,* 446**,** 303-313.

CHEN, C.-J., KUO, M.-D., CHIEN, L.-J., HSU, S.-L., WANG, Y.-M. M. & LIN, J.-H. 1997a. RNA-protein interactions: involvement of NS3, NS5, and 3' noncoding regions of Japanese encephalitis virus genomic RNA. *J Virol,* 71**,** 3466-3473.

CHEN, L.-C., YEH, T.-M., LIN, Y.-Y., WANG, Y.-F., SU, S.-J., CHEN, C.-Y., LIN, K.-H., CHOU, M.-C. & SHYU, H.-W. 2010. The envelope glycoprotein domain III of dengue virus type 2 induced the expression of anticoagulant molecules in endothelial cells. *Mol Cell Biochem,* 342**,** 215-221.

CHEN, S.-T., LIN, Y.-L., HUANG, M.-T., WU, M.-F., CHENG, S.-C., LEI, H.-Y., LEE, C.-K., CHIOU, T.-W., WONG, C.-H. & HSIEH, S.-L. 2008. CLEC5A is critical for dengue-virus-induced lethal disease. *Nature,* 453**,** 672-676.

CHEN, S.-T., LIU, R.-S., WU, M.-F., LIN, Y.-L., CHEN, S.-Y., TAN, D. T.-W., CHOU, T.-Y., TSAI, I.-S., LI, L. & HSIEH, S.-L. 2012. CLEC5A regulates Japanese encephalitis virus-induced neuroinflammation and lethality. *PLoS Pathog,* 8**,** e1002655.

CHEN, X., XIA, J., ZHAO, Q., WANG, Y., LIU, J., FENG, L., HE, J. & ZHANG, P. 2015. Eukaryotic initiation factor 4AI interacts with NS4A of Dengue virus and plays an antiviral role. *Biochem Biophys Res Commun,* 461**,** 148-153.

CHEN, Y., MAGUIRE, T., HILEMAN, R. E., FROMM, J. R., ESKO, J. D., LINHARDT, R. J. & MARKS, R. M. 1997b. Dengue virus infectivity depends on envelope protein binding to target cell heparan sulfate. *Nat Med,* 3**,** 866-871.

CHEN, Y., MAGUIRE, T. & MARKS, R. M. 1996. Demonstration of binding of dengue virus envelope protein to target cells. *J Virol,* 70**,** 8765-8772.

CHEN, Y.-C., WANG, S.-Y. & KING, C.-C. 1999. Bacterial lipopolysaccharide inhibits dengue virus infection of primary human monocytes/macrophages by blockade of virus entry via a CD14-dependent mechanism. *J Virol,* 73**,** 2650-2657.

CHENG, G., COX, J., WANG, P., KRISHNAN, M. N., DAI, J., QIAN, F., ANDERSON, J. F. & FIKRIG, E. 2010. A C-type lectin collaborates with a CD45 phosphatase homolog to facilitate West Nile virus infection of mosquitoes. *Cell,* 142**,** 714-725.

CHIANG, P. K., GORDON, R. K., TAL, J., ZENG, G. C., DOCTOR, B. P., PARDHASARADHI, K. & MCCANN, P. P. 1996. S-Adenosylmethionine and methylation. *FASEB J,* 10**,** 471-480.

CHIN, J. F. L., CHU, J. J. H. & NG, M.-L. 2007. The envelope glycoprotein domain III of dengue virus serotypes 1 and 2 inhibit virus entry. *Microbes Infect,* 9**,** 1-6.

CHIPPAUX-HYPPOLITE, C., CHOUX, R., OLMER, H. & TAMALET, J. 1970. Multiplication du virus West-Nile dans les cultures cellulaires d'embryon de poulet, observé en microscopie électronique. *C R Hebd Séances Acad Sci, Ser D, Sci Nat,* 270**,** 3162-3165.

CHIU, M.-W., SHIH, H.-M., YANG, T.-H. & YANG, Y.-L. 2007. The type 2 dengue virus envelope protein interacts with small ubiquitin-like modifier-1 (SUMO-1) conjugating enzyme 9 (Ubc9). *J. Biomed. Sci.,* 14**,** 429-444.

CHOI, K.-S., NAH, J.-J., KO, Y.-J., KIM, Y.-J. & JOO, Y.-S. 2007. The DE loop of the domain III of the envelope protein appears to be associated with West Nile virus neutralization. *Virus Res,* 123**,** 216-218.

CHOWERS, M. Y., LANG, R., NASSAR, F., BEN-DAVID, D., GILADI, M., RUBINSHTEIN, E., ITZHAKI, A., MISHAL, J., SIEGMAN-IGRA, Y., KITZES, R., PICK, N., LANDAU, Z., WOLF, D., BIN, H., MENDELSON, E.,

PITLIK, S. D. & WEINBERGER, M. 2001. Clinical characteristics of the West Nile fever outbreak, Israel, 2000. *Emerging Infect Dis,* 7**,** 675-678.

CHU, J. J.-H., LEONG, P. W. H. & NG, M.-L. 2006. Analysis of the endocytic pathway mediating the infectious entry of mosquito-borne flavivirus West Nile into Aedes albopictus mosquito (C6/36) cells. *Virology,* 349**,** 463-475.

CHU, J. J.-H. & NG, M.-L. 2003. Characterization of a 105-kDa plasma membrane associated glycoprotein that is involved in West Nile virus binding and infection. *Virology,* 312**,** 458-469.

CHU, J. J.-H. & NG, M.-L. 2004a. Infectious entry of West Nile virus occurs through a clathrin-mediated endocytic pathway. *J Virol,* 78**,** 10543-10555.

CHU, J. J.-H. & NG, M.-L. 2004b. Interaction of West Nile virus with alpha v beta 3 integrin mediates virus entry into cells. *J Biol Chem,* 279**,** 54533-54541.

CHU, J. J.-H., RAJAMANONMANI, R., LI, J., BHUVANAKANTHAM, R., LESCAR, J. & NG, M.-L. 2005. Inhibition of West Nile virus entry by using a recombinant domain III from the envelope glycoprotein. *J Gen Virol,* 86**,** 405-412.

CHU, P. W. & WESTAWAY, E. G. 1987. Characterization of Kunjin virus RNA-Dependent RNA Polymerase: Reinitiation of Synthesis in Vitro. *Virology,* 157**,** 330-337.

CHU, P. W. G. & WESTAWAY, E. G. 1985. Replication strategy of Kunjin Virus: Evidence for recycling role of replicative form RNA as template in semiconservative and asymmetric replication. *Virology,* 140**,** 68-79.

CHUA, J. J.-E., BHUVANAKANTHAM, R., CHOW, V. T.-K. & NG, M.-L. 2005. Recombinant non-structural 1 (NS1) protein of dengue-2 virus interacts with human STAT3beta protein. *Virus Res,* 112**,** 85-94.

CHUANG, Y.-C., LIN, Y.-S., LIU, H.-S. & YEH, T.-M. 2014. Molecular mimicry between dengue virus and coagulation factors induces antibodies to inhibit thrombin activity and enhance fibrinolysis. *J Virol,* 88**,** 13759-13768.

CHUMAKOV, M. P. & GLADKIKH, S. G. 1939. On the Role of Ixodes Ticks in the Transmission of the Spring-Summer Encephalitis. *Bull Biol Méd Exp URSS,* 7-8**,** 221.

CHUMAKOV, M. P. & SEITLENOK, N. A. 1940. Tick-Borne Human Encephalitis in the European Part of USSR and Siberia. *Science,* 92**,** 263-264.

CHUNG, K. M., LISZEWSKI, M. K., NYBAKKEN, G., DAVIS, A. E., TOWNSEND, R. R., FREMONT, D. H., ATKINSON, J. P. & DIAMOND, M. S. 2006. West Nile virus nonstructural protein NS1 inhibits complement activation by binding the regulatory protein factor H. *PNAS,* 103**,** 19111-19116.

CLARKE, B. D., ROBY, J. A., SLONCHAK, A. & KHROMYKH, A. A. 2015. Functional non-coding RNAs derived from the flavivirus 3' untranslated region. *Virus Res*.

CLEAVES, G. R. & DUBIN, D. T. 1979. Methylation status of intracellular dengue type 2 40 S RNA. *Virology,* 96**,** 159-165.

CLEAVES, G. R., RYAN, T. E. & SCHLESINGER, R. W. 1981. Identification and characterization of type 2 dengue virus replicative intermediate and replicative form RNAs. *Virology,* 111**,** 73-83.

CLEAVES, G. R. & SCHLESINGER, R. W. 1977. Characterization of Polysomal RNAs from Dengue Virus Infected KB Cells. *Abstr Am Soc Microbiol,* S-50**,** 287.

CLELAND, J. B. & BRADLEY, B. 1918. Dengue Fever in Australia: Its History and Clinical Course, its Experimental Transmission by Stegomyia fasciata, and the results of Inoculation and other Experiments. *J Hyg (Lond),* 16**,** 317-418.

CLUM, S., EBNER, K. E. & PADMANABHAN, R. 1997. Cotranslational membrane insertion of the serine proteinase precursor NS2B-NS3(Pro) of dengue virus type 2 is required for efficient in vitro processing and is mediated through the hydrophobic regions of NS2B. *J Biol Chem,* 272**,** 30715-30723.

CLYDE, K. & HARRIS, E. 2006. RNA secondary structure in the coding region of dengue virus type 2 directs translation start codon selection and is required for viral replication. *J Virol,* 80**,** 2170-2182.

COIA, G., PARKER, M. D., SPEIGHT, G., BYRNE, M. E. & WESTAWAY, E. G. 1988. Nucleotide and complete amino acid sequences of Kunjin virus: definitive gene order and characteristics of the virus-specified proteins. *J Gen Virol,* 69 (Pt 1)**,** 1-21.

COLPITTS, T. M., BARTHEL, S., WANG, P. & FIKRIG, E. 2011. Dengue Virus Capsid Protein Binds Core Histones and Inhibits Nucleosome Formation in Human Liver Cells. *PLoS One,* 6**,** e24365.

COLTER, J. S., BIRD, H. H., MOYER, A. W. & BROWN, R. A. 1957. Infectivity of Ribonucleic Acid Isolated from Virus-Infected Tissues. *Virology,* 4**,** 522-532.

CORVER, J., LENCHES, E., SMITH, K., ROBISON, R. A., SANDO, T., STRAUSS, E. G. & STRAUSS, J. H. 2003. Fine Mapping of a cis-Acting Sequence Element in Yellow Fever Virus RNA that is Required for RNA Replication and Cyclization. *J Virol,* 77**,** 2265-2270.

COZ, J., VALADE, M., CORNET, M. & ROBIN, Y. 1976. Transmission Transovarienne d'un Flavivirus, le virus Koutango Chez Aedes aegypti. *C R Hebd Séances Acad Sci, Ser D, Sci Nat,* 283**,** 109-110.

CREIGHTON, C. (ed.) 1883. *Handbook of Geographical and Historical Pathology*: The New Sydenham Society.

CRILL, W. D. & CHANG, G.-J. J. 2004. Localization and characterization of flavivirus envelope glycoprotein cross-reactive epitopes. *J Virol,* 78**,** 13975-13986.

CRILL, W. D. & ROEHRIG, J. T. 2001. Monoclonal antibodies that bind to domain III of dengue virus E glycoprotein are the most efficient blockers of virus adsorption to Vero cells. *J Virol,* 75**,** 7769-7773.

CROOK, K. R., MILLER-KITTRELL, M., MORRISON, C. R. & SCHOLLE, F. 2014. Modulation of innate immune signaling by the secreted form of the West Nile virus NS1 glycoprotein. *Virology,* 458-459**,** 172-182.

CRUZ-OLIVEIRA, C., FREIRE, J. M., CONCEIÇÃO, T. M., HIGA, L. M., CASTANHO, M. A. R. B. & DA POIAN, A. T. 2015. Receptors and routes of dengue virus entry into the host cells. *FEMS Microbiol Rev,* 39**,** 155-170.

CUI, T., SUGRUE, R. J., XU, Q., LEE, A. K., CHAN, Y.-C. & FU, J. 1998. Recombinant dengue virus type 1 NS3 protein exhibits specific viral RNA binding and NTPase activity regulated by the NS5 protein. *Virology,* 246**,** 409-417.

DALGARNO, L., TRENT, D. W., STRAUSS, J. H. & RICE, C. M. 1986. Partial nucleotide sequence of the Murray Valley encephalitis virus genome: Comparison of the encoded polypeptides with yellow fever virus structural and non-structural proteins. *Journal of Molecular Biology,* 187**,** 309-323.

DALRYMPLE, N. A., CIMICA, V. & MACKOW, E. R. 2015. Dengue Virus NS Proteins Inhibit RIG-I/MAVS Signaling by Blocking TBK1/IRF3 Phosphorylation: Dengue Virus Serotype 1 NS4A Is a Unique Interferon-Regulating Virulence Determinant. *MBio,* 6**,** e00553-15.

DAS, S., LAXMINARAYANA, S. V., CHANDRA, N., RAVI, V. & DESAI, A. 2009. Heat shock protein 70 on Neuro2a cells is a putative receptor for Japanese encephalitis virus. *Virology,* 385**,** 47-57.

DAVIES, D. R., PADLAN, E. A. & SHERIFF, S. 1990. Antibody-antigen complexes. *Annu Rev Biochem,* 59**,** 439-473.

DAVIS, C. W., MATTEI, L. M., NGUYEN, H.-Y., ANSARAH-SOBRINHO, C., DOMS, R. W. & PIERSON, T. C. 2006a. The location of asparagine-linked glycans on West Nile virions controls their interactions with CD209 (dendritic cell-specific ICAM-3 grabbing nonintegrin). *J Biol Chem,* 281**,** 37183-37194.

DAVIS, C. W., NGUYEN, H.-Y., HANNA, S. L., SÁNCHEZ, M. D., DOMS, R. W. & PIERSON, T. C. 2006b. West Nile virus discriminates between DC-SIGN and DC-SIGNR for cellular attachment and infection. *J Virol,* 80**,** 1290-1301.

DAVIS, W. G., BLACKWELL, J. L., SHI, P.-Y. & BRINTON, M. A. 2007. Interaction between the Cellular Protein eEF1A and the 3'-Terminal Stem-Loop of West Nile Virus Genomic RNA Facilitates Viral Minus-Strand RNA Synthesis. *J Virol,* 81**,** 10172-10187.

DE MADRID, A. T. & PORTERFIELD, J. S. 1974. The flaviviruses (group B arboviruses): a cross-neutralization study. *J Gen Virol,* 23**,** 91-96.

DE WISPELAERE, M. & YANG, P. L. 2012. Mutagenesis of the DI/DIII linker in dengue virus envelope protein impairs viral particle assembly. *J Virol,* 86**,** 7072-7083.

DEAS, T. S., BINDUGA-GAJEWSKA, I., TILGNER, M., REN, P., STEIN, D. A., MOULTON, H. M., IVERSEN, P. L., KAUFFMAN, E. B., KRAMER, L. D. & SHI, P.-Y. 2005. Inhibition of flavivirus infections by antisense oligomers specifically suppressing viral translation and RNA replication. *J Virol,* 79**,** 4599-4609.

DEJNIRATTISAI, W., JUMNAINSONG, A., ONSIRISAKUL, N., FITTON, P., VASANAWATHANA, S., LIMPITIKUL, W., PUTTIKHUNT, C., EDWARDS, C., DUANGCHINDA, T., SUPASA, S., CHAWANSUNTATI, K., MALASIT, P., MONGKOLSAPAYA, J. & SCREATON, G. 2010. Cross-reacting antibodies enhance dengue virus infection in humans. *Science,* 328**,** 745-748.

DEJNIRATTISAI, W., WEBB, A. I., CHAN, V., JUMNAINSONG, A., DAVIDSON, A. D., MONGKOLSAPAYA, J. & SCREATON, G. 2011. Lectin switching during dengue virus infection. *J Infect Dis,* 203**,** 1775-1783.

DEUBEL, V., CROUSET, J., BÉNICHOU, D., DIGOUTTE, J. P., BOULOY, M. & GIRARD, M. 1983. Preliminary Characterisation of the Ribonucleic Acid of Yellow Fever Virus. *Ann Virol (Inst Pasteur),* 134**,** 581-588.

DEUBEL, V., KINNEY, R. M. & TRENT, D. W. 1988. Nucleotide sequence and deduced amino acid sequence of the nonstructural proteins of dengue type 2 virus, Jamaica genotype: Comparative analysis of the full-length genome. *Virology,* 165**,** 234-244.

DONG, H., ZHANG, B. & SHI, P.-Y. 2008. Terminal structures of West Nile virus genomic RNA and their interactions with viral NS5 protein. *Virology,* 381**,** 123-135.

DOWD, K. A. & PIERSON, T. C. 2011. Antibody-mediated neutralization of flaviviruses: a reductionist view. *Virology,* 411**,** 306-315.

DUAN, X., LU, X., LI, J. & LIU, Y. 2008. Novel binding between pre-membrane protein and vacuolar ATPase is required for efficient dengue virus secretion. *Biochem Biophys Res Commun,* 373**,** 319-324.

DURBIN, A. P., KARRON, R. A., SUN, W., VAUGHN, D. W., REYNOLDS, M. J., PERREAULT, J. R., THUMAR, B., MEN, R., LAI, C.-J., ELKINS, W. R., CHANOCK, R. M., MURPHY, B. R. & WHITEHEAD, S. S. 2001. Attenuation and immunogenicity in humans of a live dengue virus type-4 vaccine candidate with a 30 nucleotide deletion in its 3'-untranslated region. *Am J Trop Med Hyg,* 65**,** 405-413.

DURBIN, A. P., WRIGHT, P. F., COX, A., KAGUCIA, W., ELWOOD, D., HENDERSON, S., WANIONEK, K., SPEICHER, J., WHITEHEAD, S. S. & PLETNEV, A. G. 2013. The live attenuated chimeric vaccine rWN/DEN4Δ30 is well-tolerated and immunogenic in healthy flavivirus-naïve adult volunteers. *Vaccine,* 31**,** 5772-5777.

ECKELS, K. H., HETRICK, F. M. & RUSSELL, P. K. 1975. Virion and Soluble Antigens of Japanese Encephalitis Virus. *Infect Immun,* 11**,** 1053-1060.

EDELING, M. A., DIAMOND, M. S. & FREMONT, D. H. 2014. Structural basis of Flavivirus NS1 assembly and antibody recognition. *PNAS,* 111**,** 4285-4290.

EGLOFF, M.-P., BENARROCH, D., SELISKO, B., ROMETTE, J.-L. & CANARD, B. 2002. An RNA cap (nucleoside-2'-O-)-methyltransferase in the flavivirus RNA polymerase NS5: crystal structure and functional characterization. *EMBO J,* 21**,** 2757-2768.

ELDADAH, A. H. & NATHANSON, N. 1967. Pathogenesis of West Nile Virus encepahlitis in mice and rats: II. Virus multiplication, evolution of immunofluorescence, and development of histological lesions in the brain. *Am J Epidemiol,* 86**,** 776-790.

ELDADAH, A. H., NATHANSON, N. & SARSITIS, R. 1967. Pathogenesis of West Nile Virus encephalitis in mice and rats: I. Influence of age and species on mortality and infection. *Am J Epidemiol,* 86**,** 765-775.

ELGHONEMY, S., DAVIS, W. G. & BRINTON, M. A. 2005. The majority of the nucleotides in the top loop of the genomic 3' terminal stem loop structure are cis-acting in a West Nile virus infectious clone. *Virology,* 331**,** 238-246.

ELSHUBER, S., ALLISON, S. L., HEINZ, F. X. & MANDL, C. W. 2003. Cleavage of protein prM is necessary for infection of BHK-21 cells by tick-borne encephalitis virus. *J Gen Virol,* 84**,** 183-191.

ELSHUBER, S. & MANDL, C. W. 2005. Resuscitating mutations in a furin cleavage-deficient mutant of the flavivirus tick-borne encephalitis virus. *J Virol,* 79**,** 11813-11823.

EMIG, M. & APPLE, D. J. 2004. Severe West Nile virus disease in healthy adults. *Clin Infect Dis,* 38**,** 289-292.

ENGEL, A. R., MITZEL, D. N., HANSON, C. T., WOLFINBARGER, J. B., BLOOM, M. E. & PLETNEV, A. G. 2011. Chimeric tick-borne encephalitis/dengue virus is attenuated in Ixodes scapularis ticks and Aedes aegypti mosquitoes. *Vector Borne Zoonotic Dis.,* 11**,** 665-674.

ERBEL, P., SCHIERING, N., D'ARCY, A., RENATUS, M., KROEMER, M., LIM, S. P., YIN, Z., KELLER, T. H., VASUDEVAN, S. G. & HOMMEL, U. 2006. Structural basis for the activation of flaviviral NS3 proteases from dengue and West Nile virus. *Nat Struct Mol Biol,* 13**,** 372-373.

ERGUNAY, K., BAKONYI, T., NOWOTNY, N. & OZKUL, A. 2015. Close relationship between West Nile virus from Turkey and lineage 1 strain from Central African Republic. *Emerging Infect Dis,* 21**,** 352-355.

ESTRADA-FRANCO, J. G., NAVARRO-LOPEZ, R., BEASLEY, D. W. C., COFFEY, L., CARRARA, A.-S., TRAVASSOS DA ROSA, A., CLEMENTS, T., WANG, E., LUDWIG, G. V., CORTES, A. C., RAMÍREZ, P. P., TESH, R. B., BARRETT, A. D. T. & WEAVER, S. C. 2003. West Nile virus in Mexico: evidence of widespread circulation since July 2002. *Emerging Infect. Dis.,* 9**,** 1604-1607.

FAGGIONI, G., CIAMMARUCONI, A., DE SANTIS, R., POMPONI, A., SCICLUNA, M. T., BARBARO, K., MASUELLI, L., AUTORINO, G., BEI, R. & LISTA, F. 2009. Evidence of a humoral response to a novel protein WARF4 embedded in the West Nile virus NS4B gene encoded by an alternative open reading frame. *Int J Mol Med,* 23**,** 509-512.

FAGGIONI, G., POMPONI, A., DE SANTIS, R., MASUELLI, L., CIAMMARUCONI, A., MONACO, F., DI GENNARO, A., MARZOCCHELLA, L., SAMBRI, V., LELLI, R., REZZA, G., BEI, R. & LISTA, F. 2012. West Nile alternative open reading frame (N-NS4B/WARF4) is produced in infected West Nile Virus (WNV) cells and induces humoral response in WNV infected individuals. *Virol J,* 9**,** 283.

FALCONAR, A. K. 1997. The dengue virus nonstructural-1 protein (NS1) generates antibodies to common epitopes on human blood clotting, integrin/adhesin proteins and binds to human endothelial cells: potential implications in haemorrhagic fever pathogenesis. *Arch Virol,* 142**,** 897-916.

FALCONAR, A. K. & YOUNG, P. R. 1991. Production of dimer-specific and dengue virus group cross-reactive mouse monoclonal antibodies to the dengue 2 virus non-structural glycoprotein NS1. *J Gen Virol,* 72**,** 961-965.

FALGOUT, B., CHANOCK, R. M. & LAI, C.-J. 1989. Proper processing of dengue virus nonstructural glycoprotein NS1 requires the N-terminal hydrophobic signal sequence and the downstream nonstructural protein NS2a. *J Virol,* 63**,** 1852-1860.

FALGOUT, B. & MARKOFF, L. 1995. Evidence that flavivirus NS1-NS2A cleavage is mediated by a membrane-bound host protease in the endoplasmic reticulum. *J Virol,* 69**,** 7232-7243.

FALGOUT, B., PETHEL, M., ZHANG, Y. M. & LAI, C. J. 1991. Both nonstructural proteins NS2B and NS3 are required for the proteolytic processing of dengue virus nonstructural proteins. *J Virol,* 65**,** 2467-2475.

FAN, Y.-H., NADAR, M., CHEN, C.-C., WENG, C.-C., LIN, Y.-T. & CHANG, R.-Y. 2011. Small noncoding RNA modulates Japanese encephalitis virus replication and translation in trans. *Virol J,* 8**,** 492.

FERGUSON, S. M., FERGUSON, S., RAIMONDI, A., PARADISE, S., SHEN, H., MESAKI, K., FERGUSON, A., DESTAING, O., KO, G., TAKASAKI, J., CREMONA, O., O'TOOLE, E. & DE CAMILLI, P. 2009. Coordinated actions of actin and BAR proteins upstream of dynamin at endocytic clathrin-coated pits. *Dev Cell,* 17**,** 811-822.

FIBRIANSAH, G., NG, T.-S., KOSTYUCHENKO, V. A., LEE, J., LEE, S., WANG, J. & LOK, S.-M. 2013. Structural changes in dengue virus when exposed to a temperature of 37°C. *J Virol,* 87**,** 7585-7592.

FILOMATORI, C. V., LODEIRO, M. F., ALVAREZ, D. E., SAMSA, M. M., PIETRASANTA, L. & GAMARNIK, A. V. 2006. A 5' RNA element promotes dengue virus RNA synthesis on a circular genome. *Genes Dev.,* 20**,** 2238-2249.

FINLAY, C. J. 1881. El Mosquito Hypotéticamente Considerado Como Agente de Transmisión de la Fiebre Amarilla. *Anal Real Acad Cien Méd Fís Nat Hab,* 18**,** 147-169.

FINLAY, C. J. 1899. Mosquitoes Considered as Transmitters of Yellow Fever and Malaria. *Med Record,* 55**,** 737-739.

FIRTH, A. E. & ATKINS, J. F. 2009. A conserved predicted pseudoknot in the NS2A-encoding sequence of West Nile and Japanese encephalitis flaviviruses suggests NS1' may derive from ribosomal frameshifting. *Virol J,* 6**,** 14.

FISCHL, W., ELSHUBER, S., SCHRAUF, S. & MANDL, C. W. 2008. Changing the protease specificity for activation of a flavivirus, tick-borne encephalitis virus. *J Virol,* 82**,** 8272-8282.

FLAMAND, M., MEGRET, F., MATHIEU, M., LEPAULT, J., REY, F. A. & DEUBEL, V. 1999. Dengue virus type 1 nonstructural glycoprotein NS1 is secreted from mammalian cells as a soluble hexamer in a glycosylation-dependent fashion. *J Virol,* 73**,** 6104-6110.

FRAENKEL-CONRAT, H. 1956. The Role of the Nucleic Acid in the Reconstitution of Active Tobacco Mosaic Virus. *J Am Chem Soc,* 78**,** 882-883.

FRAENKEL-CONRAT, H., SINGER, B. & WILLIAMS, R. C. 1957. Infectivity of Viral Nucleic Acid. *Biochim Biophys Acta,* 25**,** 87-96.

FRIEBE, P. & HARRIS, E. 2010. Interplay of RNA elements in the dengue virus 5' and 3' ends required for viral RNA replication. *J Virol,* 84**,** 6103-6118.

FRIEBE, P., SHI, P.-Y. & HARRIS, E. 2011. The 5' and 3' downstream AUG region elements are required for mosquito-borne flavivirus RNA replication. *J Virol,* 85**,** 1900-1905.

FRITZ, R., BLAZEVIC, J., TAUCHER, C., PANGERL, K., HEINZ, F. X. & STIASNY, K. 2011. The Unique Transmembrane Hairpin of Flavivirus Fusion Protein E is Essential for Membrane Fusion. *J Virol,* 85**,** 4377-4385.

FRITZ, R., STIASNY, K. & HEINZ, F. X. 2008. Identification of specific histidines as pH sensors in flavivirus membrane fusion. *J Cell Biol,* 183**,** 353-361.

FUNK, A., TRUONG, K., NAGASAKI, T., TORRES, S., FLODEN, N., BALMORI MELIAN, E., EDMONDS, J., DONG, H., SHI, P.-Y. & KHROMYKH, A. A. 2010. RNA Structures Required for Production of Subgenomic Flavivirus RNA. *J Virol,* 84**,** 11407-11417.

GADOTH, N., WEITZMAN, S. & LEHMANN, E. E. 1979. Acute anterior myelitis complicating West Nile fever. *Arch Neurol,* 36**,** 172-173.

GAO, F., DUAN, X., LU, X., LIU, Y., ZHENG, L., DING, Z. & LI, J. 2010. Novel binding between pre-membrane protein and claudin-1 is required for efficient dengue virus entry. *Biochem Biophys Res Commun,* 391**,** 952-957.

GARCÍA CORDERO, J., LEÓN JUÁREZ, M., GONZÁLEZ-Y-MERCHAND, J. A., CEDILLO BARRÓN, L. & GUTIÉRREZ CASTAÑEDA, B. 2014. Caveolin-1 in lipid rafts interacts with dengue virus NS3 during polyprotein processing and replication in HMEC-1 cells. *PLoS One,* 9**,** e90704.

GAUNT, M. W., SALL, A. A., DE LAMBALLERIE, X., FALCONAR, A. K., DZHIVANIAN, T. I. & GOULD, E. A. 2001. Phylogenetic relationships of flaviviruses correlate with their epidemiology, disease association and biogeography. *J Gen Virol,* 82**,** 1867-1876.

GERMI, R., CRANCE, J.-M., GARIN, D., GUIMET, J., LORTAT-JACOB, H., RUIGROK, R. W. H., ZARSKI, J.-P. & DROUET, E. 2002. Heparan sulfate-mediated binding of infectious dengue virus type 2 and yellow fever virus. *Virology,* 292**,** 162-168.

GIERER, A. & SCHRAMM, G. 1956a. Die Infektiosität der Nucleinsäure aus Tabakmosaikvirus. *Z Naturforschg,* 11b**,** 138-142.

GIERER, A. & SCHRAMM, G. 1956b. Infectivity of Ribonucleic Acid from Tobacco Mosaic Virus. *Nature,* 177**,** 702-703.

GOLLINS, S. W. & PORTERFIELD, J. S. 1984. Flavivirus infection enhancement in macrophages: radioactive and biological studies on the effect of antibody on viral fate. *J Gen Virol,* 65**,** 1261-1272.

GOLLINS, S. W. & PORTERFIELD, J. S. 1985. Flavivirus infection enhancement in macrophages: an electron microscopic study of viral cellular entry. *J Gen Virol,* 66**,** 1969-1982.

GOLLINS, S. W. & PORTERFIELD, J. S. 1986a. A new mechanism for the neutralization of enveloped viruses by antiviral antibody. *Nature,* 321**,** 244-246.

GOLLINS, S. W. & PORTERFIELD, J. S. 1986b. pH-dependent fusion between the flavivirus West Nile and liposomal model membranes. *J Gen Virol,* 67**,** 157-166.

GOLLINS, S. W. & PORTERFIELD, J. S. 1986c. The uncoating and infectivity of the flavivirus West Nile on interaction with cells: effects of pH and ammonium chloride. *J Gen Virol,* 67**,** 1941-1950.

GORBALENYA, A. E., DONCHENKO, A. P., KOONIN, E. V. & BLINOV, V. M. 1989. N-terminal domains of putative helicases of flavi- and pestiviruses may be serine proteases. *Nucleic Acids Res,* 17**,** 3889-3897.

GORGAS, W. C. 1901. The Results of Yellow Fever Sanitation in Havana, Cuba, for the Year 1901 up to September 1st, Carried on upon the Basis that the Stegomyia Mosquito is the Sole Means of its Transmission. *Public Health Pap Rep,* 27**,** 130-133.

GORGAS, W. C. 1915. *Sanitation in Panama*, D. Appleton and Company.

GOULD, E. A., BUCKLEY, A., BARRETT, A. D. T. & CAMMACK, N. 1986. Neutralizing (54K) and non-neutralizing (54K and 48K) monoclonal antibodies against structural and non-structural yellow fever virus proteins confer immunity in mice. *J Gen Virol,* 67**,** 591-595.

GRAHAM, H. 1902. Dengue: A Study of its Mode of Propagation and Pathology. *Med Record,* 61**,** 204-207.

GRAHAM, H. 1903. The Dengue: A Study of its Pathology and Mode of Propagation. *J Trop Med,* 61.

GRANGE, T., BOULOY, M. & GIRARD, M. 1985. Stable secondary structures at the 3'-end of the genome of yellow fever virus (17 D vaccine strain). *FEBS Letters,* 188**,** 159-163.

GREENER, T., ZHAO, X., NOJIMA, H., EISENBERG, E. & GREENE, L. E. 2000. Role of cyclin G-associated kinase in uncoating clathrin-coated vesicles from non-neuronal cells. *J Biol Chem,* 275**,** 1365-1370.

GRITSUN, T. S. & GOULD, E. A. 2007. Origin and evolution of flavivirus 5' UTRs and panhandles: trans-terminal duplications? *Virology,* 366**,** 8-15.

GROMOWSKI, G. D., FIRESTONE, C.-Y., HANSON, C. T. & WHITEHEAD, S. S. 2014. Japanese encephalitis virus vaccine candidates generated by chimerization with dengue virus type 4. *Vaccine,* 32**,** 3010-3018.

GROVE, J. & MARSH, M. 2011. The cell biology of receptor-mediated virus entry. *J Cell Biol,* 195**,** 1071-1082.

GRUN, J. B. & BRINTON, M. A. 1986. Characterization of West Nile virus RNA-dependent RNA polymerase and cellular terminal adenylyl and uridylyl transferases in cell-free extracts. *J Virol,* 60**,** 1113-1124.

GU, J. & TANIGUCHI, N. 2008. Potential of N-glycan in cell adhesion and migration as either a positive or negative regulator. *Cell Adh Migr,* 2**,** 243-245.

GUALANO, R. C., PRYOR, M. J., CAUCHI, M. R., WRIGHT, P. J. & DAVIDSON, A. D. 1998. Identification of a major determinant of mouse neurovirulence of dengue virus type 2 using stably cloned genomic-length cDNA. *J Gen Virol,* 79**,** 437-446.

GUBLER, D. J. 2002. The global emergence/resurgence of arboviral diseases as public health problems. *Arch Med Res,* 33**,** 330-342.

GUBLER, D. J. 2014. Dengue Viruses: Their Evolution, History and Emergence as a Global Public Health Problem. *In:* GUBLER, D. J., OOI, E. E., VASUDEVAN, S. G. & FARRAR, J. J. (eds.) 2nd ed. Wallingford, UK.

GUBLER, D. J., KUNO, G. & MARKOFF, L. 2007. Flaviviruses. *In:* KNIPE, D. M., HOWLEY, P. M., GRIFFIN, D. E., MARTIN, M. A., LAMB, R. A., ROIZMAN, B. & STRAUS, S. E. (eds.) 5th ed. Philadelphia: Lippincott Williams and Wilkins.

GUBLER, D. J. & ROSEN, L. 1977. Quantitative aspects of replication of dengue viruses in Aedes albopictus (Diptera: Culicidae) after oral and parenteral infection. *J Med Entomol,* 13**,** 469-472.

GUIRAKHOO, F., BOLIN, R. A. & ROEHRIG, J. T. 1992. The Murray Valley encephalitis virus prM protein confers acid resistance to virus particles and alters

the expression of epitopes within the R2 domain of E glycoprotein. *Virology,* 191**,** 921-931.

GUIRAKHOO, F., HEINZ, F. X. & KUNZ, C. 1989. Epitope model of tick-borne encephalitis virus envelope glycoprotein E: analysis of structural properties, role of carbohydrate side chain, and conformational changes occurring at acidic pH. *Virology,* 169**,** 90-99.

GUIRAKHOO, F., PUGACHEV, K., ARROYO, J., MILLER, C., ZHANG, Z. X., WELTZIN, R., GEORGAKOPOULOS, K., CATALAN, J., OCRAN, S., DRAPER, K. & MONATH, T. P. 2002. Viremia and immunogenicity in nonhuman primates of a tetravalent yellow fever-dengue chimeric vaccine: genetic reconstructions, dose adjustment, and antibody responses against wild-type dengue virus isolates. *Virology,* 298**,** 146-159.

GUYATT, K. J., WESTAWAY, E. G. & KHROMYKH, A. A. 2001. Expression and purification of enzymatically active recombinant RNA-dependent RNA polymerase (NS5) of the flavivirus Kunjin. *J Virol Methods,* 92**,** 37-44.

GUZMAN, M. G., ALVAREZ, M. & HALSTEAD, S. B. 2013. Secondary infection as a risk factor for dengue hemorrhagic fever/dengue shock syndrome: an historical perspective and role of antibody-dependent enhancement of infection. *Arch Virol,* 158**,** 1445-1459.

HAAHR, S. 1968. The occurrence of virus and interferon in the spleen, serum and brain in mice after experimental infection with West Nile virus. *Acta Pathol Microbiol Scand,* 74**,** 445-457.

HAHN, C. S., DALRYMPLE, J. M., STRAUSS, J. H. & RICE, C. M. 1987a. Comparison of the virulent Asibi strain of yellow fever virus with the 17D vaccine strain derived from it. *PNAS,* 84**,** 2019-2023.

HAHN, C. S., HAHN, Y. S., RICE, C. M., LEE, E., DALGARNO, L., STRAUSS, E. G. & STRAUSS, J. H. 1987b. Conserved elements in the 3' untranslated region of flavivirus RNAs and potential cyclization sequences. *J. Mol. Biol.,* 198**,** 33-41.

HAHN, Y. S., CALLER, R., HUNKAPILLER, T., DALRYMPLE, J. M., STRAUSS, J. H. & STRAUSS, E. G. 1988. Nucleotide sequence of dengue 2 RNA and comparison of the encoded proteins with those of other flaviviruses. *Virology,* 162**,** 167-180.

HALL, R. A., KAY, B. H., BURGESS, G. W., CLANCY, P. & FANNING, I. D. 1990. Epitope analysis of the envelope and non-structural glycoproteins of Murray Valley encephalitis virus. *J Gen Virol,* 71**,** 2923-2930.

HALLAUER, C. 1946. Über den Virusnachweis mit dem Hirst-Test. *Schweiz Z Pathol Bakteriol,* 9**,** 553-554.

HALSTEAD, S. B. 1970. Observations related to pathogensis of dengue hemorrhagic fever. VI. Hypotheses and discussion. *Yale J Biol Med,* 42**,** 350-362.

HALSTEAD, S. B. & O'ROURKE, E. J. 1977a. Antibody-enhanced dengue virus infection in primate leukocytes. *Nature,* 265**,** 739-741.

HALSTEAD, S. B. & O'ROURKE, E. J. 1977b. Dengue viruses and mononuclear phagocytes. I. Infection enhancement by non-neutralizing antibody. *J Exp Med,* 146**,** 201-217.

HALSTEAD, S. B., O'ROURKE, E. J. & ALLISON, A. C. 1977. Dengue viruses and mononuclear phagocytes. II. Identity of blood and tissue leukocytes supporting in vitro infection. *J Exp Med,* 146**,** 218-229.

HALSTEAD, S. B. & THOMAS, S. J. 2011. New Japanese encephalitis vaccines: alternatives to production in mouse brain. *Expert Rev Vaccines,* 10**,** 355-364.

HASHIMOTO, H., NOMOTO, A., WATANABE, K., MORI, T., TAKEZAWA, T., AIZAWA, C., TAKEGAMI, T. & HIRAMATSU, K. 1988. Molecular cloning and complete nucleotide sequence of the genome of Japanese encephalitis virus Beijing-1 strain. *Virus Genes,* 1**,** 305-317.

HAYES, E. B. & GUBLER, D. J. 2006. West Nile virus: epidemiology and clinical features of an emerging epidemic in the United States. *Annu. Rev. Med.,* 57**,** 181-194.

HAYES, E. B., SEJVAR, J. J., ZAKI, S. R., LANCIOTTI, R. S., BODE, A. V. & CAMPBELL, G. L. 2005. Virology, pathology, and clinical manifestations of West Nile virus disease. *Emerging Infect. Dis.,* 11**,** 1174-1179.

HEINZ, F. X., BERGER, R., MAJDIC, O., KNAPP, W. & KUNZ, C. 1982. Monoclonal antibodies to the structural glycoprotein of tick-borne encephalitis virus. *Infect Immun,* 37**,** 869-874.

HEINZ, F. X., BERGER, R., TUMA, W. & KUNZ, C. 1983a. Location of immunodominant antigenic determinants on fragments of the tick-borne encephalitis virus glycoprotein: evidence for two different mechanisms by which antibodies mediate neutralization and hemagglutination inhibition. *Virology,* 130**,** 485-501.

HEINZ, F. X., BERGER, R., TUMA, W. & KUNZ, C. 1983b. A topological and functional model of epitopes on the structural glycoprotein of tick-borne encephalitis virus defined by monoclonal antibodies. *Virology,* 126**,** 525-537.

HEINZ, F. X. & KUNZ, C. 1977. Characterization of tick-borne encephalitis virus and immunogenicity of its surface components in mice. *Acta Virol,* 21**,** 308-316.

HEINZ, F. X., STIASNY, K., PÜSCHNER-AUER, G., HOLZMANN, H., ALLISON, S. L., MANDL, C. W. & KUNZ, C. 1994. Structural changes and functional control of the tick-borne encephalitis virus glycoprotein E by the heterodimeric association with protein prM. *Virology,* 198**,** 109-117.

HEINZ, F. X., TUMA, W. & KUNZ, C. 1981. Antigenic and immunogenic properties of defined physical forms of tick-borne encephalitis virus structural proteins. *Infect Immun,* 33**,** 250-257.

HENCHAL, E. A., GENTRY, M. K., MCCOWN, J. M. & BRANDT, W. E. 1982. Dengue virus-specific and flavivirus group determinants identified with monoclonal antibodies by indirect immunofluorescence. *Am J Trop Med Hyg,* 31**,** 830-836.

HENCHAL, E. A., HENCHAL, L. S. & SCHLESINGER, J. J. 1988. Synergistic interactions of anti-NS1 monoclonal antibodies protect passively immunized mice from lethal challenge with dengue 2 virus. *J Gen Virol,* 69**,** 2101-2107.

HENCHAL, E. A., HENCHAL, L. S. & THAISOMBOONSUK, B. K. 1987. Topological mapping of unique epitopes on the dengue-2 virus NS1 protein using monoclonal antibodies. *J Gen Virol,* 68**,** 845-851.

HENNE, W. M., BOUCROT, E., MEINECKE, M., EVERGREN, E., VALLIS, Y., MITTAL, R. & MCMAHON, H. T. 2010. FCHo proteins are nucleators of clathrin-mediated endocytosis. *Science,* 328**,** 1281-1284.

HERSHEY, A. D. & CHASE, M. 1952. Independent Functions of Viral Protein and Nucleic Acid in Growth of Bacteriophage. *J Gen Physiol,* 36**,** 39-56.

HERSHKOVITZ, O., ROSENTAL, B., ROSENBERG, L. A., NAVARRO-SANCHEZ, M. E., JIVOV, S., ZILKA, A., GERSHONI-YAHALOM, O., BRIENT-LITZLER, E., BEDOUELLE, H., HO, J. W., CAMPBELL, K. S., RAGER-ZISMAN, B., DESPRES, P. & PORGADOR, A. 2009. NKp44 receptor mediates interaction of the envelope glycoproteins from the West Nile and dengue viruses with NK cells. *J Immunol,* 183**,** 2610-2621.

HILGARD, P. & STOCKERT, R. 2000. Heparan sulfate proteoglycans initiate dengue virus infection of hepatocytes. *Hepatology,* 32**,** 1069-1077.

HINSHAW, J. E. & SCHMID, S. L. 1995. Dynamin self-assembles into rings suggesting a mechanism for coated vesicle budding. *Nature,* 374**,** 190-192.

HIRST, G. K. 1941. The Agglutination of Red Cells by Allantoic Fluid of Chick Embryos Infected with Influenza Virus. *Science,* 94**,** 22-23.

HOLBROOK, M. R. & GOWEN, B. B. 2008. Animal models of highly pathogenic RNA viral infections: encephalitis viruses. *Antiviral Res,* 78**,** 69-78.

HOLBROOK, M. R., WANG, H. & BARRETT, A. D. T. 2001. Langat virus M protein is structurally homologous to prM. *J Virol,* 75**,** 3999-4001.

HOLDEN, K. L., STEIN, D. A., PIERSON, T. C., AHMED, A. A., CLYDE, K., IVERSEN, P. L. & HARRIS, E. 2006. Inhibition of dengue virus translation and RNA synthesis by a morpholino oligomer targeted to the top of the terminal 3' stem-loop structure. *Virology,* 344**,** 439-452.

HOLZMANN, H., UTTER, G., NORRBY, E., MANDL, C. W., KUNZ, C. & HEINZ, F. X. 1993. Assessment of the antigenic structure of tick-borne encephalitis virus by the use of synthetic peptides. *J Gen Virol,* 74**,** 2031-2035.

HÖNING, S., RICOTTA, D., KRAUSS, M., SPÄTE, K., SPOLAORE, B., MOTLEY, A., ROBINSON, M., ROBINSON, C., HAUCKE, V. & OWEN, D. J. 2005. Phosphatidylinositol-(4,5)-bisphosphate regulates sorting signal recognition by the clathrin-associated adaptor complex AP2. *Mol. Cell,* 18**,** 519-531.

HUNG, J.-J., HSIEH, M.-T., YOUNG, M.-J., KAO, C.-L., KING, C.-C. & CHANG, W. 2004. An external loop region of domain III of dengue virus type 2 envelope protein is involved in serotype-specific binding to mosquito but not mammalian cells. *J Virol,* 78**,** 378-388.

HUNT, T. A., URBANOWSKI, M. D., KAKANI, K., LAW, L.-M. J., BRINTON, M. A. & HOBMAN, T. C. 2007. Interactions between the West Nile virus capsid protein and the host cell-encoded phosphatase inhibitor, I2PP2A. *Cell Microbiol,* 9**,** 2756-2766.

HURLBUT, H. S., TAYLOR, R. M., WORK, T. H. & RIZK, F. 1956. A study of the ecology of West Nile virus in Egypt. *Am J Trop Med Hyg,* 5**,** 579-620.

HURRELBRINK, R. J. & MCMINN, P. C. 2001. Attenuation of Murray Valley encephalitis virus by site-directed mutagenesis of the hinge and putative receptor-binding regions of the envelope protein. *J Virol,* 75**,** 7692-7702.

HUSSAIN, M. & ASGARI, S. 2014. MicroRNA-like viral small RNA from Dengue virus 2 autoregulates its replication in mosquito cells. *PNAS,* 111**,** 2746-2751.

HUSSAIN, M., TORRES, S., SCHNETTLER, E., FUNK, A., GRUNDHOFF, A., PIJLMAN, G. P., KHROMYKH, A. A. & ASGARI, S. 2012. West Nile virus encodes a microRNA-like small RNA in the 3' untranslated region which up-regulates GATA4 mRNA and facilitates virus replication in mosquito cells. *Nucleic Acids Res,* 40**,** 2210-2223.

HUSSMANN, K. L. & FREDERICKSEN, B. L. 2014. Differential induction of CCL5 by pathogenic and non-pathogenic strains of West Nile virus in brain endothelial cells and astrocytes. *J Gen Virol,* 95**,** 862-867.

IACONO-CONNORS, L. C., SMITH, J. F., KSIAZEK, T. G., KELLEY, C. L. & SCHMALJOHN, C. S. 1996. Characterization of Langat virus antigenic determinants defined by monoclonal antibodies to E, NS1 and preM and identification of a protective, non-neutralizing preM-specific monoclonal antibody. *Virus Res,* 43**,** 125-136.

ICTV. 2014. *Virus Taxonomy: 2014 Release* [Online]. International Committee on Taxonomy of Viruses. Available: http://www.ictvonline.org/virusTaxonomy.asp [Accessed 25 Jul 2015].

IGARASHI, A., FUKUNAGA, T. & FUKAI, K. 1964. Sedimentation Characteristics of Japanese Encephalitis Virus Ribonucleic Acid. *Biken J,* 7**,** 111-119.

IGARASHI, A., KITANO, H. & FUKAI, K. 1963. An Infectious and Ribonuclease-Sensitive Fraction from Mouse Brain Infected with Japanese B Encephalitis. *Biken J,* 6**,** 21-23.

ISHAK, R., TOVEY, D. G. & HOWARD, C. R. 1988. Morphogenesis of yellow fever virus 17D in infected cell cultures. *J Gen Virol,* 69**,** 325-335.

ISSUR, M., GEISS, B. J., BOUGIE, I., PICARD-JEAN, F., DESPINS, S., MAYETTE, J., HOBDEY, S. E. & BISAILLON, M. 2009. The flavivirus NS5 protein is a true RNA guanylyltransferase that catalyzes a two-step reaction to form the RNA cap structure. *RNA,* 15**,** 2340-2350.

IVANOVSKY, D. 1892. Über die Mosaikkrankheit der Tabakspflanze. *Bull Scient Acad Imp Sci St Petersb,* 35**,** 67-70.

IVANOVSKY, D. 1942. Concerning the Mosaic Disease of the Tobacco Plant. *Phytopathol Classics,* 7**,** 27-30.

JACOBS, M. G., ROBINSON, P. J., BLETCHLY, C., MACKENZIE, J. M. & YOUNG, P. R. 2000. Dengue virus nonstructural protein 1 is expressed in a glycosyl-phosphatidylinositol-linked form that is capable of signal transduction. *FASEB J.,* 14**,** 1603-1610.

JEHA, L. E., SILA, C. A., LEDERMAN, R. J., PRAYSON, R. A., ISADA, C. M. & GORDON, S. M. 2003. West Nile virus infection: a new acute paralytic illness. *Neurology,* 61**,** 55-59.

JEMIELITY, S., WANG, J. J., CHAN, Y. K., AHMED, A. A., LI, W., MONAHAN, S., BU, X., FARZAN, M., FREEMAN, G. J., UMETSU, D. T., DEKRUYFF, R. H. & CHOE, H. 2013. TIM-family proteins promote infection of multiple enveloped viruses through virion-associated phosphatidylserine. *PLoS Pathog,* 9**,** e1003232.

JINDADAMRONGWECH, S., THEPPARIT, C. & SMITH, D. R. 2004. Identification of GRP 78 (BiP) as a liver cell expressed receptor element for dengue virus serotype 2. *Arch Virol,* 149**,** 915-927.

JOHANSSON, M., BROOKS, A. J., JANS, D. A. & VASUDEVAN, S. G. 2001. A small region of the dengue virus-encoded RNA-dependent RNA polymerase, NS5, confers interaction with both the nuclear transport receptor importin-beta and the viral helicase, NS3. *J Gen Virol,* 82**,** 735-745.

JOHNSTON, L. J., HALLIDAY, G. M. & KING, N. J. 2000. Langerhans cells migrate to local lymph nodes following cutaneous infection with an arbovirus. *J. Invest. Dermatol.,* 114**,** 560-568.

JONES, C. T., MA, L., BURGNER, J. W., GROESCH, T. D., POST, C. B. & KUHN, R. J. 2003. Flavivirus capsid is a dimeric alpha-helical protein. *J Virol,* 77**,** 7143-7149.

KAKUMANI, P. K., PONIA, S. S., S, R. K., SOOD, V., CHINNAPPAN, M., BANERJEA, A. C., MEDIGESHI, G. R., MALHOTRA, P., MUKHERJEE, S. K. & BHATNAGAR, R. K. 2013. Role of RNA interference (RNAi) in dengue virus replication and identification of NS4B as an RNAi suppressor. *J Virol,* 87**,** 8870-8883.

KANAI, R., KAR, K., ANTHONY, K., GOULD, L. H., LEDIZET, M., FIKRIG, E., MARASCO, W. A., KOSKI, R. A. & MODIS, Y. 2006. Crystal structure of west nile virus envelope glycoprotein reveals viral surface epitopes. *J Virol,* 80**,** 11000-11008.

KAPOOR, M., ZHANG, L., RAMACHANDRA, M., KUSUKAWA, J., EBNER, K. E. & PADMANABHAN, R. 1995. Association between NS3 and NS5 proteins of dengue virus type 2 in the putative RNA replicase is linked to differential phosphorylation of NS5. *J Biol Chem,* 270**,** 19100-19106.

KAWANO, H., ROSTAPSHOV, V., ROSEN, L. & LAI, C.-J. 1993. Genetic determinants of dengue type 4 virus neurovirulence for mice. *J Virol,* 67**,** 6567-6575.

KEATING, J. A., BHATTACHARYA, D., RUND, S. S. C., HOOVER, S., DASGUPTA, R., LEE, S. J., DUFFIELD, G. E. & STRIKER, R. 2013. Mosquito protein kinase G phosphorylates flavivirus NS5 and alters flight behavior in Aedes aegypti and Anopheles gambiae. *Vector Borne Zoonotic Dis.,* 13**,** 590-600.

KELLEY, J. F., KAUFUSI, P. H. & NERURKAR, V. R. 2012. Dengue hemorrhagic fever-associated immunomediators induced via maturation of dengue virus nonstructural 4B protein in monocytes modulate endothelial cell adhesion molecules and human microvascular endothelial cells permeability. *Virology,* 422**,** 326-337.

KELLEY, J. F., KAUFUSI, P. H., VOLPER, E. M. & NERURKAR, V. R. 2011. Maturation of dengue virus nonstructural protein 4B in monocytes enhances production of dengue hemorrhagic fever-associated chemokines and cytokines. *Virology,* 418**,** 27-39.

KHROMYKH, A. A., KONDRATIEVA, N., SGRO, J.-Y., PALMENBERG, A. & WESTAWAY, E. G. 2003. Significance in replication of the terminal nucleotides of the flavivirus genome. *J Virol,* 77**,** 10623-10629.

KHROMYKH, A. A., MEKA, H., GUYATT, K. J. & WESTAWAY, E. G. 2001. Essential Role of Cyclization Sequences in Flavivirus RNA Replication. *J Virol,* 75**,** 6719-6728.

KHUNCHAI, S., JUNKING, M., SUTTITHEPTUMRONG, A., KOOPTIWUT, S., HAEGEMAN, G., LIMJINDAPORN, T. & YENCHITSOMANUS, P.-T. 2015. NF-κB is required for dengue virus NS5-induced RANTES expression. *Virus Res,* 197**,** 92-100.

KIERMAYR, S., KOFLER, R. M., MANDL, C. W., MESSNER, P. & HEINZ, F. X. 2004. Isolation of Capsid Protein Dimers from the Tick-Borne Encephalitis Flavivirus and In Vitro Assembly of Capsid-Like Particles. *J Virol,* 78**,** 8078-8084.

KIM, J.-M., YUN, S.-I., SONG, B.-H., HAHN, Y.-S., LEE, C.-H., OH, H.-W. & LEE, Y.-M. 2008. A single N-linked glycosylation site in the Japanese encephalitis virus prM protein is critical for cell type-specific prM protein biogenesis, virus particle release, and pathogenicity in mice. *J Virol,* 82**,** 7846-7862.

KIMURA, T., SASAKI, M., OKUMURA, M., KIM, E. & SAWA, H. 2010. Flavivirus encephalitis: pathological aspects of mouse and other animal models. *Vet Pathol,* 47**,** 806-818.

KIMURA-KURODA, J. & YASUI, K. 1983. Topographical analysis of antigenic determinants on envelope glycoprotein V3 (E) of Japanese encephalitis virus, using monoclonal antibodies. *J Virol,* 45**,** 124-132.

KINNEY, R. M., HUANG, C. Y. H., ROSE, B. C., KROEKER, A. D., DREHER, T. W., IVERSEN, P. L. & STEIN, D. A. 2005. Inhibition of Dengue Virus Serotypes 1 to 4 in Vero Cell Cultures with Morpholino Oligomers. *J Virol,* 79**,** 5116-5128.

KITANO, T., SUZUKI, K. & YAMAGUCHI, T. 1974. Morphological, chemical, and biological characterization of Japanese encephalitis virus virion and its hemagglutinin. *J Virol,* 14**,** 631-639.

KITAOKA, M. 1950. Experimental transmission of the West Nile virus by the mosquito. *Jpn Med J (Natl Inst Health Jpn),* 3**,** 77-81.

KITAOKA, M., SHIMIZU, A., TUCHINDA, P. & KIM-ANAKE, C. 1971. Electron microscopic observations on dengue type 2 virus. *Biken J,* 14**,** 361-364.

KLAUSNER, R. D., DONALDSON, J. G. & LIPPINCOTT-SCHWARTZ, J. 1992. Brefeldin A: insights into the control of membrane traffic and organelle structure. *J Cell Biol,* 116**,** 1071-1080.

KLEIN, R. S., LIN, E., ZHANG, B., LUSTER, A. D., TOLLETT, J., SAMUEL, M. A., ENGLE, M. & DIAMOND, M. S. 2005. Neuronal CXCL10 directs CD8+ T-cell recruitment and control of West Nile virus encephalitis. *J Virol,* 79**,** 11457-11466.

KOFLER, R. M., HEINZ, F. X. & MANDL, C. W. 2002. Capsid protein C of tick-borne encephalitis virus tolerates large internal deletions and is a favorable target for attenuation of virulence. *J Virol,* 76**,** 3534-3543.

KOMAR, N. 2003. West Nile Virus: Epidemiology and Ecology in North America. *Adv Virus Res,* 61**,** 185-234.

KONISHI, E. & MASON, P. W. 1993. Proper maturation of the Japanese encephalitis virus envelope glycoprotein requires cosynthesis with the premembrane protein. *J Virol,* 67**,** 1672-1675.

KOONIN, E. V. 1993. Computer-assisted identification of a putative methyltransferase domain in NS5 protein of flaviviruses and lambda 2 protein of reovirus. *J Gen Virol,* 74**,** 733-740.

KOONIN, E. V. & DOLJA, V. V. 1993. Evolution and Taxonomy of Positive-Strand RNA Viruses: Implications of Comparative Analysis of Amino Acid Sequences. *Crit Rev Biochem Mol Biol,* 28**,** 375-430.

KROSCHEWSKI, H., ALLISON, S. L., HEINZ, F. X. & MANDL, C. W. 2003. Role of heparan sulfate for attachment and entry of tick-borne encephalitis virus. *Virology,* 308**,** 92-100.

KUADKITKAN, A., WIKAN, N., FONGSARAN, C. & SMITH, D. R. 2010. Identification and characterization of prohibitin as a receptor protein mediating DENV-2 entry into insect cells. *Virology,* 406**,** 149-161.

KUDO, M., URAGUCHI, K., MATSUDA, S. & HASHIMOTO, H. 1937. Experimental Studies on Encephalitis Virus of 1935 Epidemic in Tokyo with Special Reference to Its Serological Difference from the Virus of St. Louis Encephalitis. *J Immunol,* 32**,** 129-135.

KUHN, R. J., DOWD, K. A., BETH POST, C. & PIERSON, T. C. 2015. Shake, rattle, and roll: Impact of the dynamics of flavivirus particles on their interactions with the host. *Virology,* 479-480**,** 508-517.

KUHN, R. J., ZHANG, W., ROSSMANN, M. G., PLETNEV, S. V., CORVER, J., LENCHES, E., JONES, C. T., MUKHOPADHYAY, S., CHIPMAN, P. R., STRAUSS, E. G., BAKER, T. S. & STRAUSS, J. H. 2002. Structure of dengue virus: implications for flavivirus organization, maturation, and fusion. *Cell,* 108**,** 717-725.

KUMAR, A., BÜHLER, S., SELISKO, B., DAVIDSON, A. D., MULDER, K., CANARD, B., MILLER, S. & BARTENSCHLAGER, R. 2013. Nuclear localization of dengue virus nonstructural protein 5 does not strictly correlate with efficient viral RNA replication and inhibition of type I interferon signaling. *J Virol,* 87**,** 4545-4557.

KÜMMERER, B. M. 2006. The Molecular Biology of Yellow Fever Virus. *In:* KALITZKY, M. & BOROWSKI, P. (eds.) 1st ed. Wymondham.

KÜMMERER, B. M. & RICE, C. M. 2002. Mutations in the yellow fever virus nonstructural protein NS2A selectively block production of infectious particles. *J Virol,* 76**,** 4773-4784.

KURZ, M., STEFAN, N., ZHU, J. & SKERN, T. 2012. NS2B/3 proteolysis at the C-prM junction of the tick-borne encephalitis virus polyprotein is highly membrane dependent. *Virus Res,* 168**,** 48-55.

KUTTNER, A. G. & TS'UN, T. U. 1936. Encephalitis in North China. Results Obtained with Neutralization Tests. *J Clin Invest,* 15**,** 525-530.

LAHELLE, O. & HORSFALL, F. L. 1949. Hemagglutination with the GDVII strain of mouse encephalo myelitis virus. *Proc Soc Exp Biol Med,* 71**,** 713-718.

LANCIOTTI, R. S., ROEHRIG, J. T., DEUBEL, V., SMITH, J., PARKER, M., STEELE, K., CRISE, B., VOLPE, K. E., CRABTREE, M. B., SCHERRET, J. H., HALL, R. A., MACKENZIE, J. S., CROPP, C. B., PANIGRAHY, B., OSTLUND, E., SCHMITT, B., MALKINSON, M., BANET, C., WEISSMAN, J., KOMAR, N., SAVAGE, H. M., STONE, W., MCNAMARA, T. S. & GUBLER, D. J. 1999. Origin of the West Nile virus responsible for an outbreak of encephalitis in the northeastern United States. *Science,* 286**,** 2333-2337.

LANGEVIN, S. A., ARROYO, J., MONATH, T. P. & KOMAR, N. 2003. Host-range restriction of chimeric yellow fever-West Nile vaccine in fish crows (Corvus ossifragus). *Am J Trop Med Hyg,* 69**,** 78-80.

LANGHANS, W. 2000. Anorexia of infection: current prospects. *Nutrition,* 16**,** 996-1005.

LATCHMAN, D. S. 2005. *Gene Regulation,* Abingdon, Taylor and Francis.

LAURENT-ROLLE, M., BOER, E. F., LUBICK, K. J., WOLFINBARGER, J. B., CARMODY, A. B., ROCKX, B., LIU, W., ASHOUR, J., SHUPERT, W. L., HOLBROOK, M. R., BARRETT, A. D., MASON, P. W., BLOOM, M. E., GARCÍA-SASTRE, A., KHROMYKH, A. A. & BEST, S. M. 2010. The NS5 protein of the virulent West Nile virus NY99 strain is a potent antagonist of type I interferon-mediated JAK-STAT signaling. *J Virol,* 84**,** 3503-3515.

LAURENT-ROLLE, M., MORRISON, J., RAJSBAUM, R., MACLEOD, J. M. L., PISANELLI, G., PHAM, A., AYLLON, J., MIORIN, L., MARTÍNEZ-ROMERO, C., TENOEVER, B. R. & GARCÍA-SASTRE, A. 2014. The interferon signaling antagonist function of yellow fever virus NS5 protein is activated by type I interferon. *Cell Host Microbe,* 16**,** 314-327.

LAVILLAUREIX, J., VERMEIL, C. & PETROVIC, A. 1958. Pouvoir pathogène expérimental du virus West Nile pour la gerbille et pour la souris blanche. *C R Seances Soc Biol Fil,* 152**,** 1007-1009.

LAZEAR, H. M., DANIELS, B. P., PINTO, A. K., HUANG, A. C., VICK, S. C., DOYLE, S. E., GALE, M., KLEIN, R. S. & DIAMOND, M. S. 2015. Interferon-λ restricts West Nile virus neuroinvasion by tightening the blood-brain barrier. *Sci Transl Med,* 7**,** 284ra59-284ra59.

LEARY, K. & BLAIR, C. D. 1980. Sequential Events in the Morphogenesis of Japanese Encephalitis Virus. *J Ultrastruct Res,* 72**,** 123-129.

LEE, C. M., XIE, X., ZOU, J., LI, S.-H., LEE, M. Y. Q., DONG, H., QIN, C.-F., KANG, C. & SHI, P.-Y. 2015. Determinants of Dengue Virus NS4A Protein Oligomerization. *J Virol,* 89**,** 6171-6183.

LEE, E., FERNON, C., SIMPSON, R., WEIR, R. C., RICE, C. M. & DALGARNO, L. 1990. Sequence of the 3' half of the Murray Valley encephalitis virus genome and mapping of the nonstructural proteins NS1, NS3, and NS5. *Virus Genes,* 4**,** 197-213.

LEE, E., HALL, R. A. & LOBIGS, M. 2004. Common E protein determinants for attenuation of glycosaminoglycan-binding variants of Japanese encephalitis and West Nile viruses. *J Virol,* 78**,** 8271-8280.

LEE, E., LEANG, S. K., DAVIDSON, A. & LOBIGS, M. 2010. Both E protein glycans adversely affect dengue virus infectivity but are beneficial for virion release. *J Virol,* 84**,** 5171-5180.

LEE, E. & LOBIGS, M. 2000. Substitutions at the putative receptor-binding site of an encephalitic flavivirus alter virulence and host cell tropism and reveal a role for glycosaminoglycans in entry. *J Virol,* 74**,** 8867-8875.

LEE, E., PAVY, M., YOUNG, N., FREEMAN, C. & LOBIGS, M. 2006. Antiviral effect of the heparan sulfate mimetic, PI-88, against dengue and encephalitic flaviviruses. *Antiviral Res,* 69**,** 31-38.

LEE, E., STOCKS, C. E., AMBERG, S. M., RICE, C. M. & LOBIGS, M. 2000. Mutagenesis of the signal sequence of yellow fever virus prM protein:

enhancement of signalase cleavage In vitro is lethal for virus production. *J Virol,* 74**,** 24-32.

LENNETTE, E. H. & KOPROWSKI, H. 1946. Antigenic Relationships of the West Nile, Japanese B Encephalitis, and St. Louis Encephalitis Viruses. *J Immunol,* 52**,** 235-246.

LEON, L. R. 2002. Invited review: cytokine regulation of fever: studies using gene knockout mice. *J. Appl. Physiol.,* 92**,** 2648-2655.

LEUNG, J. Y., PIJLMAN, G. P., KONDRATIEVA, N., HYDE, J., MACKENZIE, J. M. & KHROMYKH, A. A. 2008. Role of nonstructural protein NS2A in flavivirus assembly. *J Virol,* 82**,** 4731-4741.

LI, H., CLUM, S., YOU, S., EBNER, K. E. & PADMANABHAN, R. 1999. The serine protease and RNA-stimulated nucleoside triphosphatase and RNA helicase functional domains of dengue virus type 2 NS3 converge within a region of 20 amino acids. *J Virol,* 73**,** 3108-3116.

LI, L., LOK, S.-M., YU, I.-M., ZHANG, Y., KUHN, R. J., CHEN, J. & ROSSMANN, M. G. 2008. The flavivirus precursor membrane-envelope protein complex: structure and maturation. *Science,* 319**,** 1830-1834.

LI, W., LI, Y., KEDERSHA, N., ANDERSON, P., EMARA, M., SWIDEREK, K. M., MORENO, G. T. & BRINTON, M. A. 2002. Cell Proteins TIA-1 and TIAR Interact ith the 3' Stem-Loop of the West Nile Virus Complementary Minus-Strand RNA and Facilitate Virus Replication. *J Virol,* 76**,** 11989-12000.

LI, X.-D., YE, H.-Q., DENG, C.-L., LIU, S.-Q., ZHANG, H.-L., SHANG, B.-D., SHI, P.-Y., YUAN, Z.-M. & ZHANG, B. 2015. Genetic interaction between NS4A and NS4B for replication of Japanese encephalitis virus. *J Gen Virol*.

LI, Y., KAKINAMI, C., LI, Q., YANG, B. & LI, H. 2013. Human apolipoprotein A-I is associated with dengue virus and enhances virus infection through SR-BI. *PLoS One,* 8**,** e70390.

LIBRATY, D. H., YOUNG, P. R., PICKERING, D., ENDY, T. P., KALAYANAROOJ, S., GREEN, S., VAUGHN, D. W., NISALAK, A., ENNIS, F. A. & ROTHMAN, A. L. 2002. High circulating levels of the dengue virus nonstructural protein NS1

early in dengue illness correlate with the development of dengue hemorrhagic fever. *JID,* 186**,** 1165-1168.

LIN, C., AMBERG, S. M., CHAMBERS, T. J. & RICE, C. M. 1993. Cleavage at a novel site in the NS4A region by the yellow fever virus NS2B-3 proteinase is a prerequisite for processing at the downstream 4A/4B signalase site. *J Virol,* 67**,** 2327-2335.

LIN, C.-F., CHIU, S.-C., HSIAO, Y.-L., WAN, S.-W., LEI, H.-Y., SHIAU, A.-L., LIU, H.-S., YEH, T.-M., CHEN, S.-H., LIU, C.-C. & LIN, Y.-S. 2005. Expression of cytokine, chemokine, and adhesion molecules during endothelial cell activation induced by antibodies against dengue virus nonstructural protein 1. *J Immunol,* 174**,** 395-403.

LIN, C.-F., LEI, H.-Y., SHIAU, A.-L., LIU, H.-S., YEH, T.-M., CHEN, S.-H., LIU, C.-C., CHIU, S.-C. & LIN, Y.-S. 2002. Endothelial cell apoptosis induced by antibodies against dengue virus nonstructural protein 1 via production of nitric oxide. *J Immunol,* 169**,** 657-664.

LIN, C.-W., CHENG, C.-W., YANG, T.-C., LI, S.-W., CHENG, M.-H., WAN, L., LIN, Y.-J., LAI, C.-H., LIN, W.-Y. & KAO, M.-C. 2008. Interferon antagonist function of Japanese encephalitis virus NS4A and its interaction with DEAD-box RNA helicase DDX42. *Virus Res,* 137**,** 49-55.

LIN, J.-C., LIN, S.-C., CHEN, W.-Y., YEN, Y.-T., LAI, C.-W., TAO, M.-H., LIN, Y.-L., MIAW, S.-C. & WU-HSIEH, B. A. 2014. Dengue viral protease interaction with NF-κB inhibitor α/β results in endothelial cell apoptosis and hemorrhage development. *J Immunol,* 193**,** 1258-1267.

LIN, R.-J., CHANG, B.-L., YU, H.-P., LIAO, C.-L. & LIN, Y.-L. 2006. Blocking of interferon-induced Jak-Stat signaling by Japanese encephalitis virus NS5 through a protein tyrosine phosphatase-mediated mechanism. *J Virol,* 80**,** 5908-5918.

LIN, S.-R., ZOU, G., HSIEH, S.-C., QING, M., TSAI, W.-Y., SHI, P.-Y. & WANG, W.-K. 2011. The helical domains of the stem region of dengue virus envelope protein are involved in both virus assembly and entry. *J Virol,* 85**,** 5159-5171.

LIN, T.-Y., DOWD, K. A., MANHART, C. J., NELSON, S., WHITEHEAD, S. S. & PIERSON, T. C. 2012. A Novel Approach for the Rapid Mutagenesis and Directed Evolution of the Structural Genes of West Nile Virus. *J Virol,* 86**,** 3501-3512.

LINDENBACH, B. D. & RICE, C. M. 1997. trans-Complementation of yellow fever virus NS1 reveals a role in early RNA replication. *J Virol,* 71**,** 9608-9617.

LINDENBACH, B. D. & RICE, C. M. 1999. Genetic interaction of flavivirus nonstructural proteins NS1 and NS4A as a determinant of replicase function. *J Virol,* 73**,** 4611-4621.

LINDENBACH, B. D., THIEL, H.-J. & RICE, C. M. 2007. Flaviviridae: The Viruses and Their Replication. *In:* KNIPE, D. M., HOWLEY, P. M., GRIFFIN, D. E., MARTIN, M. A., LAMB, R. A., ROIZMAN, B. & STRAUS, S. E. (eds.) *Fields Virology.* 5th ed. Philadelphia.

LISOVA, O., HARDY, F., PETIT, V. & BEDOUELLE, H. 2007. Mapping to completeness and transplantation of a group-specific, discontinuous, neutralizing epitope in the envelope protein of dengue virus. *J Gen Virol,* 88**,** 2387-2397.

LIU, W. J., CHEN, H. B. & KHROMYKH, A. A. 2003. Molecular and functional analyses of Kunjin virus infectious cDNA clones demonstrate the essential roles for NS2A in virus assembly and for a nonconservative residue in NS3 in RNA replication. *J Virol,* 77**,** 7804-7813.

LIU, W. J., CHEN, H. B., WANG, X. J., HUANG, H. & KHROMYKH, A. A. 2004. Analysis of adaptive mutations in Kunjin virus replicon RNA reveals a novel role for the flavivirus nonstructural protein NS2A in inhibition of beta interferon promoter-driven transcription. *J Virol,* 78**,** 12225-12235.

LIU, W. J., WANG, X. J., CLARK, D. C., LOBIGS, M., HALL, R. A. & KHROMYKH, A. A. 2006. A single amino acid substitution in the West Nile virus nonstructural protein NS2A disables its ability to inhibit alpha/beta interferon induction and attenuates virus virulence in mice. *J Virol,* 80**,** 2396-2404.

LIU, W. J., WANG, X. J., MOKHONOV, V. V., SHI, P.-Y., RANDALL, R. & KHROMYKH, A. A. 2005. Inhibition of interferon signaling by the New York 99 strain and Kunjin subtype of West Nile virus involves blockage of STAT1 and STAT2 activation by nonstructural proteins. *J Virol,* 79**,** 1934-1942.

LIU, Y., LIU, H., ZOU, J., ZHANG, B. & YUAN, Z. 2014. Dengue virus subgenomic RNA induces apoptosis through the Bcl-2-mediated PI3k/Akt signaling pathway. *Virology,* 448**,** 15-25.

LO, M. K., TILGNER, M., BERNARD, K. A. & SHI, P.-Y. 2003. Functional Analysis of Mosquito-Borne Flavivirus Conserved Sequence Elements Within 3' Untranslated Region of West Nile Virus by use of a Reporting Replicon that Differentiates Between Viral Translation and RNA Replication. *J Virol,* 77**,** 10004-10014.

LOBIGS, M. 1993. Flavivirus premembrane protein cleavage and spike heterodimer secretion require the function of the viral proteinase NS3. *PNAS,* 90**,** 6218-6222.

LOBIGS, M. & LEE, E. 2004. Inefficient signalase cleavage promotes efficient nucleocapsid incorporation into budding flavivirus membranes. *J Virol,* 78**,** 178-186.

LOBIGS, M., LEE, E., NG, M.-L., PAVY, M. & LOBIGS, P. 2010. A Flavivirus Signal Peptide Balances the Catalytic Activity of Two Proteases and Thereby Facilitates Virus Morphogenesis. *Virology,* 401**,** 80-89.

LOBIGS, M., USHA, R., NESTOROWICZ, A., MARSHALL, I. D., WEIR, R. C. & DALGARNO, L. 1990. Host cell selection of Murray Valley encephalitis virus variants altered at an RGD sequence in the envelope protein and in mouse virulence. *Virology,* 176**,** 587-595.

LODEIRO, M. F., FILOMATORI, C. V. & GAMARNIK, A. V. 2009. Structural and functional studies of the promoter element for dengue virus RNA replication. *J Virol,* 83**,** 993-1008.

LOENEN, W. A. M. 2006. S-adenosylmethionine: jack of all trades and master of everything? *Biochem Soc Trans,* 34**,** 330-333.

LOK, S.-M., KOSTYUCHENKO, V., NYBAKKEN, G. E., HOLDAWAY, H. A., BATTISTI, A. J., SUKUPOLVI-PETTY, S., SEDLAK, D., FREMONT, D. H., CHIPMAN, P. R., ROEHRIG, J. T., DIAMOND, M. S., KUHN, R. J. & ROSSMANN, M. G. 2008. Binding of a neutralizing antibody to dengue virus alters the arrangement of surface glycoproteins. *Nat Struct Mol Biol,* 15**,** 312-317.

LORENZ, I. C., ALLISON, S. L., HEINZ, F. X. & HELENIUS, A. 2002. Folding and dimerization of tick-borne encephalitis virus envelope proteins prM and E in the endoplasmic reticulum. *J Virol,* 76**,** 5480-5491.

LORENZ, I. C., KARTENBECK, J., MEZZACASA, A., ALLISON, S. L., HEINZ, F. X. & HELENIUS, A. 2003. Intracellular assembly and secretion of recombinant subviral particles from tick-borne encephalitis virus. *J Virol,* 77**,** 4370-4382.

LUBINIECKI, A. S. & HENRY, C. J. 1974. Autoradiographic localization of RNA synthesis directed by arboviruses in the cytoplasm of infected BHK-21 cells. *Proc Soc Exp Biol Med,* 145**,** 1165-1169.

LUO, Y., GUO, X., YAN, H., FANG, D., ZENG, G., ZHOU, J. & JIANG, L. 2015. Comprehensive mapping infection-enhancing epitopes of dengue pr protein using polyclonal antibody against prM. *Appl Microbiol Biotechnol*.

LV, S., SONG, H.-L., ZHOU, Y., LI, L.-X., CUI, W., WANG, W. & LIU, P. 2010. Tumour necrosis factor-alpha affects blood-brain barrier permeability and tight junction-associated occludin in acute liver failure. *Liver Int,* 30**,** 1198-1210.

MA, L., JONES, C. T., GROESCH, T. D., KUHN, R. J. & POST, C. B. 2004. Solution Structure of Dengue Virus Capsid Protein Reveals Another Fold. *PNAS,* 101**,** 3414-3419.

MACDONALD, F. 1952. Haemagglutination with the virus of Murray Valley encephalitis. *Brit J Exp Path,* 33**,** 537-542.

MACKENZIE, J. M., JONES, M. K. & WESTAWAY, E. G. 1999. Markers for trans-Golgi membranes and the intermediate compartment localize to induced membranes with distinct replication functions in flavivirus-infected cells. *J Virol,* 73**,** 9555-9567.

MACKENZIE, J. M., JONES, M. K. & YOUNG, P. R. 1996. Immunolocalization of the dengue virus nonstructural glycoprotein NS1 suggests a role in viral RNA replication. *Virology,* 220**,** 232-240.

MACKENZIE, J. M., KHROMYKH, A. A., JONES, M. K. & WESTAWAY, E. G. 1998. Subcellular localization and some biochemical properties of the flavivirus Kunjin nonstructural proteins NS2A and NS4A. *Virology,* 245**,** 203-215.

MACKENZIE, J. M. & WESTAWAY, E. G. 2001. Assembly and maturation of the flavivirus Kunjin virus appear to occur in the rough endoplasmic reticulum and along the secretory pathway, respectively. *J Virol,* 75**,** 10787-10799.

MACKERRAS, I. M. 1946. Transmission of dengue fever by Aedes (Stegomyia) scutellaris Walk. in New Guinea. *Trans R Soc Trop Med Hyg,* 40**,** 295-312.

MACKOW, E., MAKINO, Y., ZHAO, B., ZHANG, Y.-M., MARKOFF, L., BUCKLER-WHITE, A., GUILER, M., CHANOCK, R. & LAI, C.-J. 1987. The nucleotide sequence of dengue type 4 virus: Analysis of genes coding for nonstructural proteins. *Virology,* 159**,** 217-228.

MACLEOD, J. & GORDON, W. S. 1932. Studies in Louping-Ill (An Encephalomyelitis of Sheep): II—Transmission by the Sheep Tick, Ixodes Ricinus L. *J Comp Path Therap,* 45**,** 240-252.

MAHARAJ, P. D., ANISHCHENKO, M., LANGEVIN, S. A., FANG, Y., REISEN, W. K. & BRAULT, A. C. 2012. Structural gene (prME) chimeras of St Louis encephalitis virus and West Nile virus exhibit altered in vitro cytopathic and growth phenotypes. *J Gen Virol,* 93**,** 39-49.

MAILLARD, R. A., JORDAN, M., BEASLEY, D. W. C., BARRETT, A. D. T. & LEE, J. C. 2008. Long Range Communication in the Envelope Protein Domain III and Its Effect on the Resistance of West Nile Virus to Antibody-Mediated Neutralization. *J Biol Chem,* 283**,** 613-622.

MANDL, C. W., HEINZ, F. X., STÖCKL, E. & KUNZ, C. 1989. Genome sequence of tick-borne encephalitis virus (Western subtype) and comparative analysis of nonstructural proteins with other flaviviruses. *Virology,* 173**,** 291-301.

MANUELIDIS, E. E. 1956. Neuropathology of experimental West Nile virus infection in monkeys. *J Neuropathol Exp Neurol,* 15**,** 448-460.

MANZANO, M., REICHERT, E. D., POLO, S., FALGOUT, B., KASPRZAK, W., SHAPIRO, B. A. & PADMANABHAN, R. 2011. Identification of Cis-Acting Elements in the 3'-Untranslated Region of the Dengue Virus Type 2 RNA that Modulate Translation and Replication. *J Biol Chem,* 286**,** 22521-22534.

MARKOFF, L. 1989. In Vitro Processing of Dengue Virus Structural Proteins: Cleavage of the Pre-Membrane Protein. *J Virol,* 63**,** 3345-3352.

MARKOFF, L. 2003. 5′- and 3′-Noncoding Regions in Flavivirus RNA. *Adv Virus Res,* 59**,** 177-228.

MARKOFF, L., FALGOUT, B. & CHANG, A. 1997. A Conserved Internal Hydrophobic Domain Mediates the Stable Membrane Integration of the Dengue Virus Capsid Protein. *Virology,* 233**,** 105-117.

MARTÍN-ACEBES, M. A., MERINO-RAMOS, T., BLÁZQUEZ, A.-B., CASAS, J., ESCRIBANO-ROMERO, E., SOBRINO, F. & SAIZ, J.-C. 2014. The Composition of West Nile Virus Lipid Envelope Unveils a Role of Sphingolipid Metabolism in Flavivirus Biogenesis. *J Virol,* 88**,** 12041-12054.

MARTÍNEZ-BARRAGÁN, J. D. J. & DEL ANGEL, R. M. 2001. Identification of a putative coreceptor on Vero cells that participates in dengue 4 virus infection. *J Virol,* 75**,** 7818-7827.

MARTINS, I. C., GOMES-NETO, F., FAUSTINO, A. F., CARVALHO, F. A., CARNEIRO, F. A., BOZZA, P. T., MOHANA-BORGES, R., CASTANHO, M. A. R. B., ALMEIDA, F. C. L., SANTOS, N. C. & DA POIAN, A. T. 2012. The disordered N-terminal region of dengue virus capsid protein contains a lipid-droplet-binding motif. *Biochem J,* 444**,** 405-415.

MASON, P. W., MCADA, P. C., DALRYMPLE, J. M., FOURNIER, M. J. & MASON, T. L. 1987. Expression of Japanese encephalitis virus antigens in Escherichia coli. *Virology,* 158**,** 361-372.

MATSUMURA, T. & HOTTA, S. 1971. Electron microscopic observations on the purified dengue virus (Type I). *Kobe J Med Sci,* 17**,** 85-95.

MATSUMURA, T., STOLLAR, V. & SCHLESINGER, R. W. 1971. Studies on the nature of dengue viruses: V. Structure and development of dengue virus in vero cells. *Virology,* 46**,** 344-355.

MATUSAN, A. E., PRYOR, M. J., DAVIDSON, A. D. & WRIGHT, P. J. 2001. Mutagenesis of the Dengue virus type 2 NS3 protein within and outside helicase motifs: effects on enzyme activity and virus replication. *J Virol,* 75**,** 9633-9643.

MAY, F. J., LOBIGS, M., LEE, E., GENDLE, D. J., MACKENZIE, J. S., BROOM, A. K., CONLAN, J. V. & HALL, R. A. 2006. Biological, antigenic and phylogenetic characterization of the flavivirus Alfuy. *J Gen Virol,* 87**,** 329-337.

MAZZON, M., JONES, M., DAVIDSON, A. D., CHAIN, B. & JACOBS, M. 2009. Dengue virus NS5 inhibits interferon-alpha signaling by blocking signal

transducer and activator of transcription 2 phosphorylation. *J Infect Dis,* 200**,** 1261-1270.

MCLEAN, J. E., WUDZINSKA, A., DATAN, E., QUAGLINO, D. & ZAKERI, Z. 2011. Flavivirus NS4A-induced autophagy protects cells against death and enhances virus replication. *J Biol Chem,* 286**,** 22147-22159.

MCMAHON, H. T. & BOUCROT, E. 2011. Molecular mechanism and physiological functions of clathrin-mediated endocytosis. *Nat Rev Mol Cell Biol,* 12**,** 517-533.

MEDIN, C. L., FITZGERALD, K. A. & ROTHMAN, A. L. 2005. Dengue virus nonstructural protein NS5 induces interleukin-8 transcription and secretion. *J Virol,* 79**,** 11053-11061.

MEERTENS, L., CARNEC, X., LECOIN, M. P., RAMDASI, R., GUIVEL-BENHASSINE, F., LEW, E., LEMKE, G., SCHWARTZ, O. & AMARA, A. 2012. The TIM and TAM families of phosphatidylserine receptors mediate dengue virus entry. *Cell Host Microbe,* 12**,** 544-557.

MELIAN, E. B., HINZMAN, E., NAGASAKI, T., FIRTH, A. E., WILLS, N. M., NOUWENS, A. S., BLITVICH, B. J., LEUNG, J., FUNK, A., ATKINS, J. F., HALL, R. & KHROMYKH, A. A. 2010. NS1' of flaviviruses in the Japanese encephalitis virus serogroup is a product of ribosomal frameshifting and plays a role in viral neuroinvasiveness. *J Virol,* 84**,** 1641-1647.

MELNICK, J. L., PAUL, J. R., RIORDAN, J. T., BARNETT, V. H., GOLDBLUM, N. & ZABIN, E. 1951. Isolation from human sera in Egypt of a virus apparently identical to West Nile virus. *Proc Soc Exp Biol Med,* 77**,** 661-665.

MEN, R., BRAY, M., CLARK, D., CHANOCK, R. M. & LAI, C.-J. 1996. Dengue type 4 virus mutants containing deletions in the 3' noncoding region of the RNA genome: analysis of growth restriction in cell culture and altered viremia pattern and immunogenicity in rhesus monkeys. *J Virol,* 70**,** 3930-3937.

MERTENS, E., KAJASTE-RUDNITSKI, A., TORRES, S., FUNK, A., FRENKIEL, M.-P., ITEMAN, I., KHROMYKH, A. A. & DESPRES, P. 2010. Viral determinants in the NS3 helicase and 2K peptide that promote West Nile virus resistance to antiviral action of 2',5'-oligoadenylate synthetase 1b. *Virology,* 399**,** 176-185.

MILLER, J. L., DE WET, B. J. M., DEWET, B. J. M., MARTINEZ-POMARES, L., RADCLIFFE, C. M., DWEK, R. A., RUDD, P. M. & GORDON, S. 2008. The mannose receptor mediates dengue virus infection of macrophages. *PLoS Pathog,* 4**,** e17.

MILLER, S., KASTNER, S., KRIJNSE-LOCKER, J., BÜHLER, S. & BARTENSCHLAGER, R. 2007. The non-structural protein 4A of dengue virus is an integral membrane protein inducing membrane alterations in a 2K-regulated manner. *J Biol Chem,* 282**,** 8873-8882.

MILLER, S., SPARACIO, S. & BARTENSCHLAGER, R. 2006. Subcellular localization and membrane topology of the Dengue virus type 2 Non-structural protein 4B. *J Biol Chem,* 281**,** 8854-8863.

MODIS, Y., OGATA, S., CLEMENTS, D. & HARRISON, S. C. 2004. Structure of the dengue virus envelope protein after membrane fusion. *Nature,* 427**,** 313-319.

MONATH, T. P., CROPP, C. B. & HARRISON, A. K. 1983. Mode of entry of a neurotropic arbovirus into the central nervous system. Reinvestigation of an old controversy. *Lab Invest,* 48**,** 399-410.

MONATH, T. P., SOIKE, K., LEVENBOOK, I., ZHANG, Z. X., ARROYO, J., DELAGRAVE, S., MYERS, G., BARRETT, A. D., SHOPE, R. E., RATTERREE, M., CHAMBERS, T. J. & GUIRAKHOO, F. 1999. Recombinant, chimaeric live, attenuated vaccine (ChimeriVax) incorporating the envelope genes of Japanese encephalitis (SA14-14-2) virus and the capsid and nonstructural genes of yellow fever (17D) virus is safe, immunogenic and protective in non-human primates. *Vaccine,* 17**,** 1869-1882.

MONCKTON, R. P. & WESTAWAY, E. G. 1982. Restricted translation of the genome of the flavivirus Kunjin in vitro. *J Gen Virol,* 63 (Pt 1)**,** 227-232.

MONDOTTE, J. A., LOZACH, P.-Y., AMARA, A. & GAMARNIK, A. V. 2007. Essential role of dengue virus envelope protein N glycosylation at asparagine-67 during viral propagation. *J Virol,* 81**,** 7136-7148.

MOON, S. L., ANDERSON, J. R., KUMAGAI, Y., WILUSZ, C. J., AKIRA, S., KHROMYKH, A. A. & WILUSZ, J. 2012. A noncoding RNA produced by arthropod-borne flaviviruses inhibits the cellular exoribonuclease XRN1 and alters host mRNA stability. *RNA,* 18**,** 2029-2040.

MORRISON, C. R. & SCHOLLE, F. 2014. Abrogation of TLR3 inhibition by discrete amino acid changes in the C-terminal half of the West Nile virus NS1 protein. *Virology,* 456-457**,** 96-107.

MUÑOZ-JORDAN, J. L., LAURENT-ROLLE, M., ASHOUR, J., MARTÍNEZ-SOBRIDO, L., ASHOK, M., LIPKIN, W. I. & GARCÍA-SASTRE, A. 2005. Inhibition of alpha/beta interferon signaling by the NS4B protein of flaviviruses. *J Virol,* 79**,** 8004-8013.

MUÑOZ-JORDAN, J. L., SÁNCHEZ-BURGOS, G. G., LAURENT-ROLLE, M. & GARCÍA-SASTRE, A. 2003. Inhibition of interferon signaling by dengue virus. *PNAS,* 100**,** 14333-14338.

MURGUE, B., ZELLER, H. & DEUBEL, V. 2002. The ecology and epidemiology of West Nile virus in Africa, Europe and Asia. *Curr Top Microbiol Immunol,* 267**,** 195-221.

MUYLAERT, I. R., CHAMBERS, T. J., GALLER, R. & RICE, C. M. 1996. Mutagenesis of the N-linked glycosylation sites of the yellow fever virus NS1 protein: effects on virus replication and mouse neurovirulence. *Virology,* 222**,** 159-168.

NAEVE, C. W. & TRENT, D. W. 1978. Identification of Saint Louis encephalitis virus mRNA. *J Virol,* 25**,** 535-545.

NAGATA, N., IWATA-YOSHIKAWA, N., HAYASAKA, D., SATO, Y., KOJIMA, A., KARIWA, H., TAKASHIMA, I., TAKASAKI, T., KURANE, I., SATA, T. & HASEGAWA, H. 2015. The Pathogenesis of 3 Neurotropic Flaviviruses in a Mouse Model Depends on the Route of Neuroinvasion After Viremia. *J Neuropathol Exp Neurol,* 74**,** 250-260.

NAIK, N. G. & WU, H.-N. 2015. Mutation of Putative N-Glycosylation Sites on Dengue Virus NS4B Decreases RNA Replication. *J Virol,* 89**,** 6746-6760.

NAKAMURA, M. 1961. Infectious Ribonucleic Acids derived from Mouse Brains infected with Two Kinds of Arbor Virus Group B. *Nature,* 191**,** 624-624.

NALCA, A., FELLOWS, P. F. & WHITEHOUSE, C. A. 2003. Vaccines and animal models for arboviral encephalitides. *Antiviral Res,* 60**,** 153-174.

NASH, D., MOSTASHARI, F., FINE, A., MILLER, J., O&APOS;LEARY, D., MURRAY, K., HUANG, A., ROSENBERG, A., GREENBERG, A., SHERMAN, M., WONG, S. & LAYTON, M. 2001. The outbreak of West Nile virus infection in the New York City area in 1999. *N Engl J Med,* 344**,** 1807-1814.

NAVARRO-SANCHEZ, E., ALTMEYER, R., AMARA, A., SCHWARTZ, O., FIESCHI, F., VIRELIZIER, J.-L., ARENZANA-SEISDEDOS, F. & DESPRES, P. 2003. Dendritic-cell-specific ICAM3-grabbing non-integrin is essential for the productive infection of human dendritic cells by mosquito-cell-derived dengue viruses. *EMBO Rep,* 4**,** 723-728.

NAWA, M. 1997. Japanese encephalitis virus infection in Vero cells: the involvement of intracellular acidic vesicles in the early phase of viral infection was observed with the treatment of a specific vacuolar type H+-ATPase inhibitor, bafilomycin A1. *Microbiol Immunol,* 41**,** 537-543.

NAWA, M. 1998. Effects of bafilomycin A1 on Japanese encephalitis virus in C6/36 mosquito cells. *Arch Virol,* 143**,** 1555-1568.

NEAL, J. W. 2014. Flaviviruses are neurotropic, but how do they invade the CNS? *J. Infect.,* 69**,** 203-215.

NELSON, S., JOST, C. A., XU, Q., ESS, J., MARTIN, J. E., OLIPHANT, T., WHITEHEAD, S. S., DURBIN, A. P., GRAHAM, B. S., DIAMOND, M. S. & PIERSON, T. C. 2008. Maturation of West Nile virus modulates sensitivity to antibody-mediated neutralization. *PLoS Pathog,* 4**,** e1000060.

NEMÉSIO, H. & VILLALAÍN, J. 2014. Membrane interacting regions of Dengue virus NS2A protein. *J Phys Chem B,* 118**,** 10142-10155.

NESTOROWICZ, A., CHAMBERS, T. J. & RICE, C. M. 1994. Mutagenesis of the yellow fever virus NS2A/2B cleavage site: effects on proteolytic processing, viral replication, and evidence for alternative processing of the NS2A protein. *Virology,* 199**,** 114-123.

NETSAWANG, J., NOISAKRAN, S., PUTTIKHUNT, C., KASINRERK, W., WONGWIWAT, W., MALASIT, P., YENCHITSOMANUS, P.-T. & LIMJINDAPORN, T. 2010. Nuclear localization of dengue virus capsid protein is required for DAXX interaction and apoptosis. *Virus Res,* 147**,** 275-283.

NEWMAN, W. & SOUTHAM, C. M. 1954. Virus treatment in advanced cancer: A pathological study of fifty-seven cases. *Cancer,* 7**,** 106-118.

NG, M.-L. & HONG, S.-S. 1989. Flavivirus infection: essential ultrastructural changes and association of Kunjin virus NS3 protein with microtubules. *Arch Virol,* 106**,** 103-120.

NG, M.-L. & LAU, L. C. 1988. Possible involvement of receptors in the entry of Kunjin virus into Vero cells. *Arch Virol,* 100**,** 199-211.

NIELSEN, G. & MARQUARDT, J. 1962. Eine infektiöse Untereinheit von Ribonuleinsäurecharakter aus Gehirnen Gelbfiebervirus-infizierter Mäuse. *Arch Virol,* 12**,** 335-345.

NISHIMURA, C., NOMURA, M. & KITAOKA, M. 1968. Comparative studies on the structure and properties of two selected strains of Japanese encephalitis virus. *Jpn J Med Sci Biol,* 21**,** 1-10.

NISHIMURA, C. & TSUKEDA, H. 1971. Replication and Synthesis of Japanese Encephalitis Virus Ribonucleic Acids in Vero Cells. *Jpn J Microbiol,* 15**,** 309-316.

NOMAGUCHI, M., ACKERMANN, M., YON, C., YOU, S. & PADMANABHAN, R. 2003. De Novo Synthesis of Negative-Strand RNA by Dengue Virus RNA-Dependent RNA Polymerase In Vitro: Nucleotide, Primer, and Template Parameters. *J Virol,* 77**,** 8831-8842.

NOWAK, T., FÄRBER, P. M., WENGLER, G. & WENGLER, G. 1989. Analyses of the terminal sequences of West Nile virus structural proteins and of the in vitro translation of these proteins allow the proposal of a complete scheme of the proteolytic cleavages involved in their synthesis. *Virology,* 169**,** 365-376.

NOWAK, T. & WENGLER, G. 1987. Analysis of disulfides present in the membrane proteins of the West Nile flavivirus. *Virology,* 156**,** 127-137.

NUTTALL, P. A., JONES, L. D., LABUDA, M. & KAUFMAN, W. R. 1994. Adaptations of arboviruses to ticks. *J Med Entomol,* 31**,** 1-9.

NUTTALL, P. A. & LABUDA, M. 2003. Dynamics of infection in tick vectors and at the tick-host interface. *Adv Virus Res,* 60**,** 233-272.

NYBAKKEN, G. E., NELSON, C. A., CHEN, B. R., DIAMOND, M. S. & FREMONT, D. H. 2006. Crystal structure of the West Nile virus envelope glycoprotein. *J Virol,* 80**,** 11467-11474.

NYBAKKEN, G. E., OLIPHANT, T., JOHNSON, S., BURKE, S., DIAMOND, M. S. & FREMONT, D. H. 2005. Structural basis of West Nile virus neutralization by a therapeutic antibody. *Nature,* 437**,** 764-769.

OH, W.-K. & SONG, J. 2006. Hsp70 functions as a negative regulator of West Nile virus capsid protein through direct interaction. *Biochem. Biophys. Res. Commun.,* 347**,** 994-1000.

OHNO, H., STEWART, J., FOURNIER, M. C., BOSSHART, H., RHEE, I., MIYATAKE, S., SAITO, T., GALLUSSER, A., KIRCHHAUSEN, T. & BONIFACINO, J. S. 1995. Interaction of tyrosine-based sorting signals with clathrin-associated proteins. *Science,* 269**,** 1872-1875.

OKAMOTO, K., KINOSHITA, H., PARQUET, M. D. C., RAEKIANSYAH, M., KIMURA, D., YUI, K., ISLAM, M. A., HASEBE, F. & MORITA, K. 2012. Dengue virus strain DEN2 16681 utilizes a specific glycochain of syndecan-2 proteoglycan as a receptor. *J Gen Virol,* 93**,** 761-770.

OLIPHANT, T., NYBAKKEN, G. E., ENGLE, M., XU, Q., NELSON, C. A., SUKUPOLVI-PETTY, S., MARRI, A., LACHMI, B.-E., OLSHEVSKY, U., FREMONT, D. H., PIERSON, T. C. & DIAMOND, M. S. 2006. Antibody recognition and neutralization determinants on domains I and II of West Nile Virus envelope protein. *J Virol,* 80**,** 12149-12159.

OLITSKY, P. K. & YAGER, R. H. 1949. Hemagglutination by Columbia SK, Columbia MM, mengo encephalomyelitis and encephalomyocarditis viruses; experiments with other viruses. *Proc Soc Exp Biol Med,* 71**,** 719-724.

OSATOMI, K. & SUMIYOSHI, H. 1990. Complete nucleotide sequence of dengue type 3 virus genome RNA. *Virology,* 176**,** 643-647.

PARK, G. S., MORRIS, K. L., HALLETT, R. G., BLOOM, M. E. & BEST, S. M. 2007. Identification of residues critical for the interferon antagonist function of Langat

virus NS5 reveals a role for the RNA-dependent RNA polymerase domain. *J Virol,* 81**,** 6936-6946.

PEIRIS, J. S. & PORTERFIELD, J. S. 1979. Antibody-mediated enhancement of Flavivirus replication in macrophage-like cell lines. *Nature,* 282**,** 509-511.

PEÑA, J., PLANTE, J. A., CARILLO, A. C., ROBERTS, K. K., SMITH, J. K., JUELICH, T. L., BEASLEY, D. W. C., FREIBERG, A. N., LABUTE, M. X. & NARAGHI-ARANI, P. 2014. Multiplexed Digital mRNA Profiling of the Inflammatory Response in the West Nile Swiss Webster Mouse Model. *PLoS Negl Trop Dis,* 8**,** e3216.

PEPPERELL, C., RAU, N., KRAJDEN, S., KERN, R., HUMAR, A., MEDERSKI, B., SIMOR, A., LOW, D. E., MCGEER, A., MAZZULLI, T., BURTON, J., JAIGOBIN, C., FEARON, M., ARTSOB, H., DREBOT, M. A., HALLIDAY, W. & BRUNTON, J. 2003. West Nile virus infection in 2002: morbidity and mortality among patients admitted to hospital in southcentral Ontario. *CMAJ,* 168**,** 1399-1405.

PÉREZ-RAMÍREZ, E., LLORENTE, F. & JIMÉNEZ-CLAVERO, M. Á. 2014. Experimental infections of wild birds with West Nile virus. *Viruses,* 6**,** 752-781.

PESKO, K. N., FITZPATRICK, K. A., RYAN, E. M., SHI, P.-Y., ZHANG, B., LENNON, N. J., NEWMAN, R. M., HENN, M. R. & EBEL, G. D. 2012. Internally deleted WNV genomes isolated from exotic birds in New Mexico: function in cells, mosquitoes, and mice. *Virology,* 427**,** 10-17.

PHAC. 2015. *Surveillance of West Nile Virus* [Online]. Ottawa, CA: Government of Canada. Available: http://healthycanadians.gc.ca/diseases-conditions-maladies-affections/disease-maladie/west-nile-nil-occidental/surveillance-eng.php [Accessed 20 Jul 2015 2015].

PHILIP, C. B. & SMADEL, J. E. 1943. Transmission of West Nile Virus by Aedes albopictus. *Proc Soc Exp Biol Med,* 53**,** 49-49.

PIERSON, T. C., XU, Q., NELSON, S., OLIPHANT, T., NYBAKKEN, G. E., FREMONT, D. H. & DIAMOND, M. S. 2007. The stoichiometry of antibody-mediated neutralization and enhancement of West Nile virus infection. *Cell Host Microbe,* 1**,** 135-145.

PIJLMAN, G. P., FUNK, A., KONDRATIEVA, N., LEUNG, J., TORRES, S., VAN DER AA, L., LIU, W. J., PALMENBERG, A. C., SHI, P.-Y., HALL, R. A. & KHROMYKH, A. A. 2008. A Highly Structured, Nuclease-Resistant, Noncoding RNA Produced by Flaviviruses is Required for Pathogenicity. *Cell Host Microbe,* 4**,** 579-591.

PLETNEV, A. G., BRAY, M., HANLEY, K. A., SPEICHER, J. M. & ELKINS, R. 2001. Tick-borne Langat/mosquito-borne dengue flavivirus chimera, a candidate live attenuated vaccine for protection against disease caused by members of the tick-borne encephalitis virus complex: evaluation in rhesus monkeys and in mosquitoes. *J Virol,* 75**,** 8259-8267.

PLETNEV, A. G., BRAY, M., HUGGINS, J. & LAI, C.-J. 1992. Construction and characterization of chimeric tick-borne encephalitis/dengue type 4 viruses. *PNAS,* 89**,** 10532-10536.

PLETNEV, A. G., CLAIRE, M. S., ELKINS, R., SPEICHER, J., MURPHY, B. R. & CHANOCK, R. M. 2003. Molecularly engineered live-attenuated chimeric West Nile/dengue virus vaccines protect rhesus monkeys from West Nile virus. *Virology,* 314**,** 190-195.

PLETNEV, A. G. & MEN, R. 1998. Attenuation of the Langat tick-borne flavivirus by chimerization with mosquito-borne flavivirus dengue type 4. *PNAS,* 95**,** 1746-1751.

PLETNEV, A. G., PUTNAK, R., SPEICHER, J., WAGAR, E. J. & VAUGHN, D. W. 2002. West Nile virus/dengue type 4 virus chimeras that are reduced in neurovirulence and peripheral virulence without loss of immunogenicity or protective efficacy. *PNAS,* 99**,** 3036-3041.

PLETNEV, A. G., YAMSHCHIKOV, V. F. & BLINOV, V. M. 1990. Nucleotide sequence of the genome and complete amino acid sequence of the polyprotein of tick-borne encephalitis virus. *Virology,* 174**,** 250-263.

PLEVKA, P., BATTISTI, A. J., JUNJHON, J., WINKLER, D. C., HOLDAWAY, H. A., KEELAPANG, P., SITTISOMBUT, N., KUHN, R. J., STEVEN, A. C. & ROSSMANN, M. G. 2011. Maturation of flaviviruses starts from one or more icosahedrally independent nucleation centres. *EMBO Rep,* 12**,** 602-606.

POLACEK, C., FOLEY, J. E. & HARRIS, E. 2009. Conformational Changes in the Solution Structure of the Dengue Virus 5' End in the Presence and Absence of the 3' Untranslated Region. *J Virol,* 83**,** 1161-1166.

POOL, W. A., BROWNLEE, A. & WILSON, D. R. 1930. The Etiology of "Louping-Ill". *J Comp Path Therap,* 43**,** 253-290.

POST, P. R., SANTOS, C. N., CARVALHO, R., CRUZ, A. C., RICE, C. M. & GALLER, R. 1992. Heterogeneity in envelope protein sequence and N-linked glycosylation among yellow fever virus vaccine strains. *Virology,* 188**,** 160-167.

PRIKHOD'KO, G. G., PRIKHOD'KO, E. A., PLETNEV, A. G. & COHEN, J. I. 2002. Langat flavivirus protease NS3 binds caspase-8 and induces apoptosis. *J Virol,* 76**,** 5701-5710.

PROW, N. A., SETOH, Y. X., BIRON, R. M., SESTER, D. P., KIM, K. S., HOBSON-PETERS, J., HALL, R. A. & BIELEFELDT-OHMANN, H. 2014. The West Nile virus-like flavivirus Koutango is highly virulent in mice due to delayed viral clearance and the induction of a poor neutralizing antibody response. *J Virol,* 88**,** 9947-9962.

PUGACHEV, K. V., GUIRAKHOO, F., MITCHELL, F., OCRAN, S. W., PARSONS, M., JOHNSON, B. W., KOSOY, O. L., LANCIOTTI, R. S., ROEHRIG, J. T., TRENT, D. W. & MONATH, T. P. 2004. Construction of yellow fever/St. Louis encephalitis chimeric virus and the use of chimeras as a diagnostic tool. *Am J Trop Med Hyg,* 71**,** 639-645.

PUGACHEV, K. V., NOMOKONOVA, N. Y., DOBRIKOVA, E. Y. & WOLF, Y. I. 1993. Site-directed mutagenesis of the tick-borne encephalitis virus NS3 gene reveals the putative serine protease domain of the NS3 protein. *FEBS Letters,* 328**,** 115-118.

PUGACHEV, K. V., NOMOKONOVA, N. Y., MOROZOVA, O. V. & PLETNEV, A. G. 1992. A short form of the tick-borne encephalitis virus NS3 protein. *FEBS Letters,* 297**,** 67-69.

RAJAMANONMANI, R., NKENFOU, C., CLANCY, P., YAU, Y. H., SHOCHAT, S. G., SUKUPOLVI-PETTY, S., SCHUL, W., DIAMOND, M. S., VASUDEVAN, S. G. & LESCAR, J. 2009. On a mouse monoclonal antibody that neutralizes all four dengue virus serotypes. *J Gen Virol,* 90**,** 799-809.

RAMANATHAN, M. P., CHAMBERS, J. A., PANKHONG, P., CHATTERGOON, M., ATTATIPPAHOLKUN, W., DANG, K., SHAH, N. & WEINER, D. B. 2006. Host cell killing by the West Nile Virus NS2B-NS3 proteolytic complex: NS3 alone is sufficient to recruit caspase-8-based apoptotic pathway. *Virology,* 345**,** 56-72.

RAMOS-CASTAÑEDA, J., IMBERT, J. L., BARRÓN, B. L. & RAMOS, C. 1997. A 65-kDa trypsin-sensible membrane cell protein as a possible receptor for dengue virus in cultured neuroblastoma cells. *J Neurovirol,* 3**,** 435-440.

REAGAN, R. L., DAY, W. C., HARMON, M. P. & BRUECKNER, A. L. 1952a. Response of the baby chick to West Nile virus. *Proc Soc Exp Biol Med,* 80**,** 210-212.

REAGAN, R. L., ORLOWSKI, M. & BRUECKNER, A. L. 1953. Response of young dogs to West Nile virus. *Proc Soc Exp Biol Med,* 82**,** 261-262.

REAGAN, R. L., SCHENCK, D. M., HARMON, M. P. & BRUECKNER, A. L. 1952b. Effect of West Nile virus in the Swiss albino mouse and the cave bat. *J Bacteriol,* 64**,** 79-81.

REED, W. 1902. Recent Researches concerning the Etiology, Propagation, and Prevention of Yellow Fever, by the United States Army Commission. *J Hyg (Lond),* 2**,** 101-119.

REED, W. & CARROLL, J. 1902. The Etiology of Yellow Fever (A Supplemental Note). *American Medicine,* 3**,** 301-305.

REED, W., CARROLL, J., AGRAMONTE, A. & LAZEAR, J. W. 1900. The Etiology of Yellow Fever - A Preliminary Note. *Philadelphia Med J,* 6**,** 790-796.

REIDER, A., BARKER, S. L., MISHRA, S. K., IM, Y. J., MALDONADO-BÁEZ, L., HURLEY, J. H., TRAUB, L. M. & WENDLAND, B. 2009. Syp1 is a conserved endocytic adaptor that contains domains involved in cargo selection and membrane tubulation. *EMBO J,* 28**,** 3103-3116.

REY, F. A., HEINZ, F. X., MANDL, C. W., KUNZ, C. & HARRISON, S. C. 1995. The envelope glycoprotein from tick-borne encephalitis virus at 2 Å resolution. *Nature,* 375**,** 291-298.

REYES-DEL VALLE, J., CHÁVEZ-SALINAS, S., MEDINA, F. & DEL ANGEL, R. M. 2005. Heat shock protein 90 and heat shock protein 70 are components of dengue virus receptor complex in human cells. *J Virol,* 79**,** 4557-4567.

RICE, C. M., AEBERSOLD, R., TEPLOW, D. B., PATA, J., BELL, J. R., VORNDAM, A. V., TRENT, D. W., BRANDRISS, M. W., SCHLESINGER, J. J. & STRAUSS, J. H. 1986a. Partial N-terminal amino acid sequences of three nonstructural proteins of two flaviviruses. *Virology,* 151**,** 1-9.

RICE, C. M., LENCHES, E. M., EDDY, S. R., SHIN, S. J., SHEETS, R. L. & STRAUSS, J. H. 1985. Nucleotide Sequence of Yellow Fever Virus: Implications for Flavivirus Gene Expression and Evolution. *Science,* 229**,** 726-733.

RICE, C. M., STRAUSS, E. G. & STRAUSS, J. H. 1986b. Structure of the Flavivirus Genome. *In:* SCHLESINGER, S. & SCHLESINGER, M. J. (eds.) *The Togaviridae and Flaviviridae.* 1st ed. New York.

RINI, J. M., ESKO, J. D. & VARKI, A. 2009. Cellular Organisation of Glycosylation. *In:* VARKI, A., CUMMINGS, R. D., ESKO, J. D., FREEZE, H. H., STANLEY, P., BERTOZZI, C. R., HART, G. W. & ETZLER, M. E. (eds.) 2nd ed. Cold Spring Harbor.

ROBY, J. A., PIJLMAN, G. P., WILUSZ, J. & KHROMYKH, A. A. 2014. Noncoding Subgenomic Flavivirus RNA: Multiple Functions in West Nile Virus Pathogenesis and Modulation of Host Responses. *Viruses,* 6**,** 404-427.

RODENHUIS-ZYBERT, I. A., VAN DER SCHAAR, H. M., DA SILVA VOORHAM, J. M., VAN DER ENDE-METSELAAR, H., LEI, H.-Y., WILSCHUT, J. & SMIT, J. M. 2010. Immature dengue virus: a veiled pathogen? *PLoS Pathog,* 6**,** e1000718.

ROEDERER, M., BOWSER, R. & MURPHY, R. F. 1987. Kinetics and temperature dependence of exposure of endocytosed material to proteolytic enzymes and low pH: evidence for a maturation model for the formation of lysosomes. *J Cell Physiol,* 131**,** 200-209.

ROEHRIG, J. T. 2003. Antigenic Structure of Flavivirus Proteins. *In:* CHAMBERS, T. J. & MONATH, T. P. (eds.) *The Flaviviruses: Structure, Replication and Evolution.* San Diego, CA.

ROEHRIG, J. T. 2013. West Nile Virus in the United States - a Historical Perspective. *Viruses,* 5**,** 3088-3108.

ROEHRIG, J. T., BOLIN, R. A. & KELLY, R. G. 1998. Monoclonal antibody mapping of the envelope glycoprotein of the dengue 2 virus, Jamaica. *Virology,* 246**,** 317-328.

ROEHRIG, J. T., HUNT, A. R., JOHNSON, A. J. & HAWKES, R. A. 1989. Synthetic peptides derived from the deduced amino acid sequence of the E-glycoprotein of Murray Valley encephalitis virus elicit antiviral antibody. *Virology,* 171**,** 49-60.

ROEHRIG, J. T., MATHEWS, J. H. & TRENT, D. W. 1983. Identification of epitopes on the E glycoprotein of Saint Louis encephalitis virus using monoclonal antibodies. *Virology,* 128**,** 118-126.

ROKUTANDA, H. K. 1969. Relationship between viremia and interferon production of Japanese encephalitis virus. *J Immunol,* 102**,** 662-670.

ROOSENDAAL, J., WESTAWAY, E. G., KHROMYKH, A. & MACKENZIE, J. M. 2006. Regulated cleavages at the West Nile virus NS4A-2K-NS4B junctions play a major role in rearranging cytoplasmic membranes and Golgi trafficking of the NS4A protein. *J Virol,* 80**,** 4623-4632.

ROSEN, L., ROSEBOOM, L. E., GUBLER, D. J., LIEN, J. C. & CHANIOTIS, B. N. 1985. Comparative susceptibility of mosquito species and strains to oral and parenteral infection with dengue and Japanese encephalitis viruses. *Am J Trop Med Hyg,* 34**,** 603-615.

ROSEN, L., ROZEBOOM, L. E., SWEET, B. H. & SABIN, A. B. 1954. The transmission of dengue by *Aedes polynesiensis* Marks. *Am J Trop Med Hyg,* 3**,** 878-882.

ROUX, A., UYHAZI, K., FROST, A. & DE CAMILLI, P. 2006. GTP-dependent twisting of dynamin implicates constriction and tension in membrane fission. *Nature,* 441**,** 528-531.

RUOSLAHTI, E. & PIERSCHBACHER, M. D. 1987. New perspectives in cell adhesion: RGD and integrins. *Science,* 238**,** 491-497.

RUSH, B. 1789. An Account of the Bilious Remitting Fever as it Appeared in Philadelphia, in the Summer and Autumn of the Year 1780. Phildelphia: Prichard & Hall.

RUSSELL, P. K., BRANDT, W. E. & DALRYMPLE, J. M. 1980. Chemical and Antigenic Structure of Flaviviruses. *The Togaviruses.* New York: Academic Press.

SÁ E SILVA, M., ELLIS, A., KARACA, K., MINKE, J., NORDGREN, R., WU, S. & SWAYNE, D. E. 2013. Domestic goose as a model for West Nile virus vaccine efficacy. *Vaccine,* 31**,** 1045-1050.

SABIN, A. B. 1950. The dengue group of viruses and its family relationships. *Bacteriol Rev,* 14**,** 225-232.

SABIN, A. B. 1951. Hemagglutination by viruses affecting the human nervous system. *Fed. Proc.,* 10**,** 573-578.

SABIN, A. B. & BUESCHER, E. L. 1950. Unique physico-chemical properties of Japanese B encephalitis virus hemagglutinin. *Proc Soc Exp Biol Med,* 74**,** 222-230.

SAEEDI, B. J. & GEISS, B. J. 2013. Regulation of flavivirus RNA synthesis and capping. *Wiley Interdiscip Rev RNA,* 4**,** 723-735.

SAFFARIAN, S., COCUCCI, E. & KIRCHHAUSEN, T. 2009. Distinct dynamics of endocytic clathrin-coated pits and coated plaques. *PLoS Biol,* 7**,** e1000191.

SAKOONWATANYOO, P., BOONSANAY, V. & SMITH, D. R. 2006. Growth and production of the dengue virus in C6/36 cells and identification of a laminin-binding protein as a candidate serotype 3 and 4 receptor protein. *Intervirology,* 49**,** 161-172.

SALAS-BENITO, J., REYES-DEL VALLE, J., SALAS-BENITO, M., CEBALLOS-OLVERA, I., MOSSO, C. & DEL ANGEL, R. M. 2007. Evidence that the 45-kD glycoprotein, part of a putative dengue virus receptor complex in the mosquito cell line C6/36, is a heat-shock related protein. *Am J Trop Med Hyg,* 77**,** 283-290.

SALUZZO, J. F., HERVÉ, J. P., SALAUN, J. J., GERMAIN, M., CORNET, J. P., CAMICAS, J. L., HEME, G. & ROBIN, Y. 1980. Caractéristiques des souches du virus de la fiévre jaune isolées des ceufs et des larves d'une tique Amblyomma variegatum, récoltée sur le bétail à Bangui (Centrafrique). *Ann Virol (Inst Pasteur),* 131**,** 155-165.

SAMPATH, A., XU, T., CHAO, A., LUO, D., LESCAR, J. & VASUDEVAN, S. G. 2006. Structure-based mutational analysis of the NS3 helicase from dengue virus. *J Virol,* 80**,** 6686-6690.

SAMSA, M. M., MONDOTTE, J. A., IGLESIAS, N. G., ASSUNÇÃO-MIRANDA, I., BARBOSA-LIMA, G., DA POIAN, A. T., BOZZA, P. T. & GAMARNIK, A. V. 2009. Dengue virus capsid protein usurps lipid droplets for viral particle formation. *PLoS Pathog,* 5**,** e1000632.

SANGIAMBUT, S., KEELAPANG, P., AASKOV, J., PUTTIKHUNT, C., KASINRERK, W., MALASIT, P. & SITTISOMBUT, N. 2008. Multiple regions in dengue virus capsid protein contribute to nuclear localization during virus infection. *J Gen Virol,* 89**,** 1254-1264.

SAYAO, A.-L., SUCHOWERSKY, O., AL-KHATHAAMI, A., KLASSEN, B., KATZ, N. R., SEVICK, R., TILLEY, P., FOX, J. & PATRY, D. 2004. Calgary experience with West Nile virus neurological syndrome during the late summer of 2003. *Can J Neurol Sci,* 31**,** 194-203.

SCHALICH, J., ALLISON, S. L., STIASNY, K., MANDL, C. W., KUNZ, C. & HEINZ, F. X. 1996. Recombinant subviral particles from tick-borne encephalitis virus are fusogenic and provide a model system for studying flavivirus envelope glycoprotein functions. *J Virol,* 70**,** 4549-4557.

SCHLESINGER, J. J. & BRANDRISS, M. W. 1981. Antibody-mediated infection of macrophages and macrophage-like cell lines with 17D-yellow fever virus. *J Med Virol,* 8**,** 103-117.

SCHLESINGER, J. J. & BRANDRISS, M. W. 1983. 17D yellow fever virus infection of P388D1 cells mediated by monoclonal antibodies: properties of the macrophage Fc receptor. *J Gen Virol,* 64**,** 1255-1262.

SCHLESINGER, J. J., BRANDRISS, M. W., CROPP, C. B. & MONATH, T. P. 1986. Protection against yellow fever in monkeys by immunization with yellow fever virus nonstructural protein NS1. *J Virol,* 60**,** 1153-1155.

SCHLESINGER, J. J., BRANDRISS, M. W. & MONATH, T. P. 1983. Monoclonal antibodies distinguish between wild and vaccine strains of yellow fever virus by neutralization, hemagglutination inhibition, and immune precipitation of the virus envelope protein. *Virology,* 125**,** 8-17.

SCHLESINGER, J. J., BRANDRISS, M. W. & WALSH, E. E. 1985. Protection against 17D yellow fever encephalitis in mice by passive transfer of monoclonal antibodies to the nonstructural glycoprotein gp48 and by active immunization with gp48. *J Immunol,* 135**,** 2805-2809.

SCHLESINGER, J. J., BRANDRISS, M. W. & WALSH, E. E. 1987. Protection of mice against dengue 2 virus encephalitis by immunization with the dengue 2 virus non-structural glycoprotein NS1. *J Gen Virol,* 68**,** 853-857.

SCHLESINGER, M. 1933. Reindarstellung eines Bakteriophagen in mit freiem Auge sichtbaren Mengen. *Biochem Z,* 264**,** 6-12.

SCHLESINGER, M. 1934. Zur Frage der chemischen Zusammensetzung des Bacteriophagen. *Biochem Z,* 273**,** 306-311.

SCHLESINGER, M. 1936. The Feulgen Reaction of the Bacteriophage Substance. *Nature,* 138**,** 508-509.

SCHLOSSMAN, D. M., SCHMID, S. L., BRAELL, W. A. & ROTHMAN, J. E. 1984. An enzyme that removes clathrin coats: purification of an uncoating ATPase. *J Cell Biol,* 99**,** 723-733.

SCHMIDT, J. R. & ELMANSOURY, H. K. 1963. Natural and Experimental Infection of Egyptian Equines with West Nile Virus. *Ann Trop Med Parasitol,* 57**,** 415-427.

SCHNEIDER, H. 1931. Über Epidemische Akute "Meningitis Serosa". *Wien Klin Wochenschr,* 44**,** 350-352.

SCHNETTLER, E., STERKEN, M. G., LEUNG, J. Y., METZ, S. W., GEERTSEMA, C., GOLDBACH, R. W., VLAK, J. M., KOHL, A., KHROMYKH, A. A. & PIJLMAN, G. P. 2012. Noncoding Flavivirus RNA Displays RNA Interference Suppressor Activity in Insect and Mammalian Cells. *J Virol,* 86**,** 13486-13500.

SCHNETTLER, E., TYKALOVÁ, H., WATSON, M., SHARMA, M., STERKEN, M. G., OBBARD, D. J., LEWIS, S. H., MCFARLANE, M., BELL-SAKYI, L., BARRY, G., WEISHEIT, S., BEST, S. M., KUHN, R. J., PIJLMAN, G. P., CHASE-TOPPING, M. E., GOULD, E. A., GRUBHOFFER, L., FAZAKERLEY, J. K. & KOHL, A. 2014. Induction and suppression of tick cell antiviral RNAi responses by tick-borne flaviviruses. *Nucleic Acids Res,* 42**,** 9436-9446.

SCHUESSLER, A., FUNK, A., LAZEAR, H. M., COOPER, D. A., TORRES, S., DAFFIS, S., JHA, B. K., KUMAGAI, Y., TAKEUCHI, O., HERTZOG, P., SILVERMAN, R., AKIRA, S., BARTON, D. J., DIAMOND, M. S. & KHROMYKH, A. A. 2012. West Nile Virus Noncoding Subgenomic RNA Contributes to Viral Evasion of the Type I Interferon-Mediated Antiviral Response. *J Virol,* 86**,** 5708-5718.

SCHUSTER, H., SCHRAMM, G. & ZILLIG, W. 1956. Die Struktur der Ribonucleinsäure aus Tabakmosaikvirus. *Z Naturforschg,* 11b**,** 339-345.

SEJVAR, J. J., HADDAD, M. B., TIERNEY, B. C., CAMPBELL, G. L., MARFIN, A. A., VAN GERPEN, J. A., FLEISCHAUER, A., LEIS, A. A., STOKIC, D. S. & PETERSEN, L. R. 2003a. Neurologic manifestations and outcome of West Nile virus infection. *JAMA,* 290**,** 511-515.

SEJVAR, J. J., LEIS, A. A., STOKIC, D. S., VAN GERPEN, J. A., MARFIN, A. A., WEBB, R., HADDAD, M. B., TIERNEY, B. C., SLAVINSKI, S. A., POLK, J. L., DOSTROW, V., WINKELMANN, M. & PETERSEN, L. R. 2003b. Acute flaccid paralysis and West Nile virus infection. *Emerging Infect Dis,* 9**,** 788-793.

SHAFEE, N. & ABUBAKAR, S. 2003. Dengue virus type 2 NS3 protease and NS2B-NS3 protease precursor induce apoptosis. *J Gen Virol,* 84**,** 2191-2195.

SHAPIRO, D., BRANDT, W. E., CARDIFF, R. D. & RUSSELL, P. K. 1971. The Proteins of Japanese Encephalitis Virus. *Virology,* 44**,** 108-124.

SHAPIRO, D., BRANDT, W. E. & RUSSELL, P. K. 1972a. Change Involving a Viral Membrane Glycoprotein During Morphogenesis of Group B Arboviruses. *Virology,* 50**,** 906-911.

SHAPIRO, D., KOS, K. A. & RUSSELL, P. K. 1973a. Japanese Encephalitis Virus Glycoproteins. *Virology,* 56**,** 88-94.

SHAPIRO, D., KOS, K. A. & RUSSELL, P. K. 1973b. Protein Synthesis in Japanese Encephalitis Virus-Infected Cells. *Virology,* 56**,** 95-109.

SHAPIRO, D., TRENT, D. W., BRANDT, W. E. & RUSSELL, P. K. 1972b. Comparison of the virion polypeptides of group B arboviruses. *Infect Immun,* 6**,** 206-209.

SHATKIN, A. J. 1976. Capping of eucaryotic mRNAs. *Cell,* 9**,** 645-653.

SHETH, U. & PARKER, R. 2003. Decapping and Decay of Messenger RNA Occur in Cytoplasmic Processing Bodies. *Science,* 300**,** 805-808.

SHI, P.-Y., LI, W. & BRINTON, M. A. 1996. Cell Proteins Bind Specifically to West Nile Virus Minus-Strand 3' Stem-Loop RNA. *J Virol,* 70**,** 6278-6287.

SHIRATO, K., KIMURA, T., MIZUTANI, T., KARIWA, H. & TAKASHIMA, I. 2004a. Different chemokine expression in lethal and non-lethal murine West Nile virus infection. *J Med Virol,* 74**,** 507-513.

SHIRATO, K., MIYOSHI, H., GOTO, A., AKO, Y., UEKI, T., KARIWA, H. & TAKASHIMA, I. 2004b. Viral envelope protein glycosylation is a molecular determinant of the neuroinvasiveness of the New York strain of West Nile virus. *J Gen Virol,* 85**,** 3637-3645.

SHIRYAEV, S. A., CHERNOV, A. V., ALESHIN, A. E., SHIRYAEVA, T. N. & STRONGIN, A. Y. 2009. NS4A regulates the ATPase activity of the NS3 helicase: a novel cofactor role of the non-structural protein NS4A from West Nile virus. *J Gen Virol,* 90**,** 2081-2085.

SHRESTHA, B., WANG, T., SAMUEL, M. A., WHITBY, K., CRAFT, J., FIKRIG, E. & DIAMOND, M. S. 2006. Gamma interferon plays a crucial early antiviral role in protection against West Nile virus infection. *J Virol,* 80**,** 5338-5348.

SHUBLADSE, A. K. & SERDIUKOVA, G. V. 1939. The Tick Ixodes persulcatus as a Vector of the Spring-Summer Encephalitis [In Russian]. *Arkhiv Biol Nauk,* 56**,** 121-131.

SHYU, H.-W., LIN, Y.-Y., CHEN, L.-C., WANG, Y.-F., YEH, T.-M., SU, S.-J., CHENG, W.-C., CHEN, C.-Y., LIN, K.-H. & CHOU, M.-C. 2010. The dengue

virus envelope protein induced PAI-1 gene expression via MEK/ERK pathways. *Thromb. Haemost.,* 104**,** 1219-1227.

SILBER, L. A. 1939. The Spring-Summer Tick-Borne Endemic Encephalitis [In Russian]. *Arkhiv Biol Nauk,* 56**,** 255-261.

SILER, J. F., HALL, M. W. & HITCHENS, A. P. 1925. Results Obtained in the Transmission of Dengue Fever. *JAMA,* 84**,** 1163-1172.

SILVA, P. A. G. C., MOLENKAMP, R., DALEBOUT, T. J., CHARLIER, N., NEYTS, J. H., SPAAN, W. J. M. & BREDENBEEK, P. J. 2007. Conservation of the pentanucleotide motif at the top of the yellow fever virus 17D 3' stem-loop structure is not required for replication. *J Gen Virol,* 88**,** 1738-1747.

SILVA, P. A. G. C., PEREIRA, C. F., DALEBOUT, T. J., SPAAN, W. J. M. & BREDENBEEK, P. J. 2010. An RNA Pseudoknot is Required for Production of Yellow Fever Virus Subgenomic RNA by the Host Nuclease XRN1. *J Virol,* 84**,** 11395-11406.

SIMMONS, J. S., ST JOHN, J. H. & REYNOLDS, F. H. K. 1931. Experimental Studies of Dengue. *Philippine J Sci,* 44**,** 1-251.

SJATHA, F., KUWAHARA, M., SUDIRO, T. M., KAMEOKA, M. & KONISHI, E. 2014. Evaluation of chimeric DNA vaccines consisting of premembrane and envelope genes of Japanese encephalitis and dengue viruses as a strategy for reducing induction of dengue virus infection-enhancing antibody response. *Microbiol Immunol,* 58**,** 126-134.

SLÁVIK, I., MAYER, V. & MRENA, E. 1967. Morphology of purified tick-borne encephalitis virus. *Acta Virol,* 11**,** 66.

SLÁVIK, I., MRENA, E. & MAYER, V. 1970. Studies on Tick-borne encephalitis virus. II. Virus morphology and some data on virus structure. *Acta Virol,* 14**,** 8-16.

SMITH, T. J., BRANDT, W. E., SWANSON, J. L., MCCOWN, J. M. & BUESCHER, E. L. 1970. Physical and biological properties of dengue-2 virus and associated antigens. *J Virol,* 5**,** 524-532.

SMITHBURN, K. C. 1942. Differentiation of the West Nile Virus from the Viruses of St. Louis and Japanese B Encephalitis. *J Immunol,* 44**,** 25-31.

SMITHBURN, K. C., HUGHES, T. P., BURKE, A. W. & PAUL, J. H. 1940. A Neurotropic Virus Isolated from the Blood of a Native of Uganda. *Am J Trop Med Hyg,* s1-20**,** 471-492.

SMITHBURN, K. C. & JACOBS, H. R. 1942. Neutralization-Tests against Neurotropic Viruses with Sera Collected in Central Africa. *J Immunol,* 44**,** 9-23.

SMITHBURN, K. C., KERR, J. A. & GATNE, P. B. 1954. Neutralizing antibodies against certain viruses in the sera of residents of India. *J Immunol,* 72**,** 248-257.

SMORODINTSEFF, A. A. 1940. The spring-summer tick-borne encephalitis. *Arch Gesamte Virusforsch,* 1**,** 468-480.

SNIJDERS, E. P., DINGER, E. J. & SCHÜFFNER, W. A. P. 1931. On the Transmission of Dengue in Sumatra. *Am J Trop Med Hyg,* s1-11**,** 171-197.

SOKOL, F., LIBÍKOVÁ, H. & ŽEMLA, J. 1959. Infectious Ribonucleic Acid from Mouse Brains Infected with Tick-borne Encephalitis Virus. *Nature,* 184**,** 1581.

SOUTHAM, C. M. & MOORE, A. E. 1951. West Nile, Ilheus, and Bunyamwera Virus Infections in Man. *Am J Trop Med Hyg,* s1-31**,** 724-741.

SOUTHAM, C. M. & MOORE, A. E. 1952. Clinical studies of viruses as antineoplastic agents, with particular reference to egypt 101 virus. *Cancer,* 5**,** 1025-1034.

SOUTHAM, C. M. & MOORE, A. E. 1954a. Anti-virus antibody studies following induced infection of man with West Nile, Ilhéus, and other viruses. *J Immunol,* 72**,** 446-462.

SOUTHAM, C. M. & MOORE, A. E. 1954b. Induced virus infections in man by the Egypt isolates of West Nile virus. *Am J Trop Med Hyg,* 3**,** 19-50.

STADLER, K., ALLISON, S. L., SCHALICH, J. & HEINZ, F. X. 1997. Proteolytic Activation of Tick-Borne Encephalitis Virus by Furin. *J Virol,* 71**,** 8475-8481.

STANLEY, W. M. 1935. Isolation of a Crystalline Protein Possessing the Properties of Tobacco-Mosaic Virus. *Science,* 81**,** 644-645.

STEELE, K. E., LINN, M. J., SCHOEPP, R. J., KOMAR, N., GEISBERT, T. W., MANDUCA, R. M., CALLE, P. P., RAPHAEL, B. L., CLIPPINGER, T. L., LARSEN, T., SMITH, J., LANCIOTTI, R. S., PANELLA, N. A. & MCNAMARA, T. S. 2000. Pathology of fatal West Nile virus infections in native and exotic birds during the 1999 outbreak in New York City, New York. *Vet Pathol,* 37**,** 208-224.

STEVENS, T. M. & SCHLESINGER, R. W. 1965. Studies on the nature of dengue viruses: I. Correlation of particle density, infectivity, and RNA content of type 2 virus. *Virology,* 27**,** 103-112.

STIASNY, K., ALLISON, S. L., MARCHLER-BAUER, A., KUNZ, C. & HEINZ, F. X. 1996. Structural Requirements for Low-pH-Induced Rearrangements in the Envelope Glycoprotein of Tick-Borne Encephalitis Virus. *J Virol,* 70**,** 8142-8147.

STIASNY, K., ALLISON, S. L., SCHALICH, J. & HEINZ, F. X. 2002. Membrane interactions of the tick-borne encephalitis virus fusion protein E at low pH. *J Virol,* 76**,** 3784-3790.

STIASNY, K., BRESSANELLI, S., LEPAULT, J., REY, F. A. & HEINZ, F. X. 2004. Characterization of a membrane-associated trimeric low-pH-induced Form of the class II viral fusion protein E from tick-borne encephalitis virus and its crystallization. *J Virol,* 78**,** 3178-3183.

STIASNY, K. & HEINZ, F. X. 2004. Effect of membrane curvature-modifying lipids on membrane fusion by tick-borne encephalitis virus. *J Virol,* 78**,** 8536-8542.

STIASNY, K., KOESSL, C. & HEINZ, F. X. 2003. Involvement of lipids in different steps of the flavivirus fusion mechanism. *J Virol,* 77**,** 7856-7862.

STIMPSON, H. E. M., TORET, C. P., CHENG, A. T., PAULY, B. S. & DRUBIN, D. G. 2009. Early-arriving Syp1p and Ede1p function in endocytic site placement and formation in budding yeast. *Mol Biol Cell,* 20**,** 4640-4651.

STOCKS, C. E. & LOBIGS, M. 1995. Posttranslational signal peptidase cleavage at the flavivirus C-prM junction in vitro. *J Virol,* 69**,** 8123-8126.

STOLLAR, V. 1969. Studies on the nature of dengue viruses: IV. The structural proteins of type 2 dengue virus. *Virology,* 39**,** 426-438.

STOLLAR, V., SCHLESINGER, R. W. & STEVENS, T. M. 1967. Studies on the nature of dengue viruses: III. RNA synthesis in cells infected with type 2 dengue virus. *Virology,* 33**,** 650-658.

STOLLAR, V., STEVENS, T. M. & SCHLESINGER, R. W. 1966. Studies on the nature of dengue viruses: II. Characterization of viral RNA and effects of inhibitors of RNA synthesis. *Virology,* 30**,** 303-312.

STOWELL, M. H., MARKS, B., WIGGE, P. & MCMAHON, H. T. 1999. Nucleotide-dependent conformational changes in dynamin: evidence for a mechanochemical molecular spring. *Nat Cell Biol,* 1**,** 27-32.

SUEN, W. W., PROW, N. A., HALL, R. A. & BIELEFELDT-OHMANN, H. 2014. Mechanism of West Nile virus neuroinvasion: a critical appraisal. *Viruses,* 6**,** 2796-2825.

SULTANA, H., FOELLMER, H. G., NEELAKANTA, G., OLIPHANT, T., ENGLE, M., LEDIZET, M., KRISHNAN, M. N., BONAFÉ, N., ANTHONY, K. G., MARASCO, W. A., KAPLAN, P., MONTGOMERY, R. R., DIAMOND, M. S., KOSKI, R. A. & FIKRIG, E. 2009. Fusion loop peptide of the West Nile virus envelope protein is essential for pathogenesis and is recognized by a therapeutic cross-reactive human monoclonal antibody. *J Immunol,* 183**,** 650-660.

SUMIYOSHI, H., MORI, C., FUKE, I., MORITA, K., KUHARA, S., KONDOU, J., KIKUCHI, Y., NAGAMATU, H. & IGARASHI, A. 1987. Complete nucleotide sequence of the Japanese encephalitis virus genome RNA. *Virology,* 161**,** 497-510.

SUN, J., YU, Y. & DEUBEL, V. 2012. Japanese encephalitis virus NS1' protein depends on pseudoknot secondary structure and is cleaved by caspase during virus infection and cell apoptosis. *Microbes Infect,* 14**,** 930-940.

SUNDBORGER, A., SODERBLOM, C., VORONTSOVA, O., EVERGREN, E., HINSHAW, J. E. & SHUPLIAKOV, O. 2011. An endophilin-dynamin complex promotes budding of clathrin-coated vesicles during synaptic vesicle recycling. *J Cell Sci,* 124**,** 133-143.

SUTHAR, M. S., BRASSIL, M. M., BLAHNIK, G., MCMILLAN, A., RAMOS, H. J., PROLL, S. C., BELISLE, S. E., KATZE, M. G. & GALE, M. 2013a. A systems biology approach reveals that tissue tropism to West Nile virus is regulated by antiviral genes and innate immune cellular processes. *PLoS Pathog,* 9**,** e1003168.

SUTHAR, M. S., DIAMOND, M. S. & GALE, M. 2013b. West Nile virus infection and immunity. *Nat Rev Microbiol,* 11**,** 115-128.

SVITKIN, Y. V., LYAPUSTIN, V. N., LASHKEVICH, V. A. & AGOL, V. I. 1978. A comparative study on translation of flavivirus and picornavirus RNAs in vitro. *FEBS Letters,* 96**,** 211-215.

SVITKIN, Y. V., LYAPUSTIN, V. N., LASHKEVICH, V. A. & AGOL, V. I. 1984. Differences between translation products of tick-borne encephalitis virus RNA in cell-free systems from Krebs-2 cells and rabbit reticulocytes: Involvement of membranes in the processing of nascent precursors of flavivirus structural proteins. *Virology,* 135**,** 536-541.

SVITKIN, Y. V., UGAROVA, T. Y., CHERNOVSKAYA, T. V., LYAPUSTIN, V. N., LASHKEVICH, V. A. & AGOL, V. I. 1981. Translation of tick-borne encephalitis virus (flavivirus) genome in vitro: Synthesis of two structural polypeptides. *Virology,* 110**,** 26-34.

SWEET, B. H. & SABIN, A. B. 1954. Properties and antigenic relationships of hemagglutinins associated with the dengue viruses. *J Immunol,* 73**,** 363-373.

SWEITZER, S. M. & HINSHAW, J. E. 1998. Dynamin undergoes a GTP-dependent conformational change causing vesiculation. *Cell,* 93**,** 1021-1029.

TAKAMATSU, Y., OKAMOTO, K., DINH, D. T., YU, F., HAYASAKA, D., UCHIDA, L., NABESHIMA, T., BUERANO, C. C. & MORITA, K. 2014. NS1' protein expression facilitates production of Japanese encephalitis virus in avian cells and embryonated chicken eggs. *J Gen Virol,* 95**,** 373-383.

TAKEGAMI, T., MIYAMOTO, H., NAKAMURA, H. & YASUI, K. 1982. Biological activities of the structural proteins of Japanese encephalitis virus. *Acta Virol,* 26**,** 312-320.

TAN, B. H., FU, J., SUGRUE, R. J., YAP, E. H., CHAN, Y.-C. & TAN, Y. H. 1996. Recombinant dengue type 1 virus NS5 protein expressed in Escherichia coli exhibits RNA-dependent RNA polymerase activity. *Virology,* 216**,** 317-325.

TANG, W.-C., LIN, R.-J., LIAO, C.-L. & LIN, Y.-L. 2014. Rab18 facilitates dengue virus infection by targeting fatty acid synthase to sites of viral replication. *J Virol,* 88**,** 6793-6804.

TASSANEETRITHEP, B., BURGESS, T. H., GRANELLI-PIPERNO, A., TRUMPFHELLER, C., FINKE, J., SUN, W., ELLER, M. A., PATTANAPANYASAT, K., SARASOMBATH, S., BIRX, D. L., STEINMAN, R. M., SCHLESINGER, S. & MAROVICH, M. A. 2003. DC-SIGN (CD209) mediates dengue virus infection of human dendritic cells. *J Exp Med,* 197**,** 823-829.

TAY, M. Y. F., FRASER, J. E., CHAN, W. K. K., MORELAND, N. J., RATHORE, A. P., WANG, C., VASUDEVAN, S. G. & JANS, D. A. 2013. Nuclear localization of dengue virus (DENV) 1-4 non-structural protein 5; protection against all 4 DENV serotypes by the inhibitor Ivermectin. *Antiviral Res,* 99**,** 301-306.

TAYLOR, R. M., HURLBUT, H. S., DRESSLER, H. R., SPANGLER, E. W. & THRASHER, D. 1953. Isolation of West Nile virus from Culex mosquitoes. *J Egypt Med Assoc,* 36**,** 199-208.

TEO, C. S. H. & CHU, J. J.-H. 2014. Cellular vimentin regulates construction of dengue virus replication complexes through interaction with NS4A protein. *J Virol,* 88**,** 1897-1913.

TERAO, S., YILMAZ, G., STOKES, K. Y., RUSSELL, J., ISHIKAWA, M., KAWASE, T. & GRANGER, D. N. 2008. Blood cell-derived RANTES mediates cerebral microvascular dysfunction, inflammation, and tissue injury after focal ischemia-reperfusion. *Stroke,* 39**,** 2560-2570.

THEPPARIT, C. & SMITH, D. R. 2004. Serotype-specific entry of dengue virus into liver cells: identification of the 37-kilodalton/67-kilodalton high-affinity laminin receptor as a dengue virus serotype 1 receptor. *J Virol,* 78**,** 12647-12656.

THONGTAN, T., WIKAN, N., WINTACHAI, P., RATTANARUNGSAN, C., SRISOMSAP, C., CHEEPSUNTHORN, P. & SMITH, D. R. 2012. Characterization of putative Japanese encephalitis virus receptor molecules on microglial cells. *J Med Virol,* 84**,** 615-623.

THURNER, C., WITWER, C., HOFACKER, I. L. & STADLER, P. F. 2004. Conserved RNA secondary structures in Flaviviridae genomes. *J Gen Virol,* 85**,** 1113-1124.

TIGABU, B., JUELICH, T., BERTRAND, J. & HOLBROOK, M. R. 2009. Clinical evaluation of highly pathogenic tick-borne flavivirus infection in the mouse model. *J Med Virol,* 81**,** 1261-1269.

TIGABU, B., JUELICH, T. L. & HOLBROOK, M. R. 2010. Comparative Analysis of Immune Responses to Russian Spring-Summer Encephalitis and Omsk Hemorrhagic Fever Viruses in Mouse Models. *Virology,* 408**,** 57-63.

TILGNER, M., DEAS, T. S. & SHI, P.-Y. 2005. The flavivirus-conserved penta-nucleotide in the 3' stem-loop of the West Nile virus genome requires a specific sequence and structure for RNA synthesis, but not for viral translation. *Virology,* 331**,** 375-386.

TIO, P. H., JONG, W. W. & CARDOSA, M. J. 2005. Two dimensional VOPBA reveals laminin receptor (LAMR1) interaction with dengue virus serotypes 1, 2 and 3. *Virol J,* 2**,** 25.

TRENT, D. W. 1977. Antigenic characterization of flavivirus structural proteins separated by isoelectric focusing. *J Virol,* 22**,** 608-618.

TRENT, D. W. & QURESHI, A. A. 1971. Structural and nonstructural proteins of Saint Louis encephalitis virus. *J Virol,* 7**,** 379-388.

TRENT, D. W., SWENSEN, C. C. & QURESHI, A. A. 1969. Synthesis of Saint Louis encephalitis virus ribonucleic acid in BHK-21-13 cells. *J Virol,* 3**,** 385-394.

TUMBAN, E., MAES, N. E., SCHIRTZINGER, E. E., YOUNG, K. I., HANSON, C. T., WHITEHEAD, S. S. & HANLEY, K. A. 2013. Replacement of conserved or variable sequences of the mosquito-borne dengue virus 3' UTR with homologous sequences from Modoc virus does not change infectivity for mosquitoes. *J Gen Virol,* 94**,** 783-788.

TUMBAN, E., MITZEL, D. N., MAES, N. E., HANSON, C. T., WHITEHEAD, S. S. & HANLEY, K. A. 2011. Replacement of the 3' untranslated variable region of mosquito-borne dengue virus with that of tick-borne Langat virus does not alter vector specificity. *J Gen Virol,* 92**,** 841-848.

UCHIL, P. D. & SATCHIDANANDAM, V. 2003a. Architecture of the flaviviral replication complex. Protease, nuclease, and detergents reveal encasement within double-layered membrane compartments. *J Biol Chem,* 278**,** 24388-24398.

UCHIL, P. D. & SATCHIDANANDAM, V. 2003b. Characterization of RNA synthesis, replication mechanism, and in vitro RNA-dependent RNA polymerase activity of Japanese encephalitis virus. *Virology,* 307**,** 358-371.

UMAREDDY, I., CHAO, A., SAMPATH, A., GU, F. & VASUDEVAN, S. G. 2006. Dengue virus NS4B interacts with NS3 and dissociates it from single-stranded RNA. *J Gen Virol,* 87**,** 2605-2614.

UNGEWICKELL, E., UNGEWICKELL, H., HOLSTEIN, S. E., LINDNER, R., PRASAD, K., BAROUCH, W., MARTIN, B., GREENE, L. E. & EISENBERG, E. 1995. Role of auxilin in uncoating clathrin-coated vesicles. *Nature,* 378**,** 632-635.

UPANAN, S., KUADKITKAN, A. & SMITH, D. R. 2008. Identification of dengue virus binding proteins using affinity chromatography. *J Virol Methods,* 151**,** 325-328.

URBANOWSKI, M. D. & HOBMAN, T. C. 2013. The West Nile Virus Capsid Protein Blocks Apoptosis Through a Phosphatidylinositol 3-Kinase-Dependent Mechanism. *J Virol,* 87**,** 872-881.

VAN DER MOST, R. G., CORVER, J. & STRAUSS, J. H. 1999. Mutagenesis of the RGD motif in the yellow fever virus 17D envelope protein. *Virology,* 265**,** 83-95.

VAN DER SCHAAR, H. M., RUST, M. J., CHEN, C., VAN DER ENDE-METSELAAR, H., WILSCHUT, J., ZHUANG, X. & SMIT, J. M. 2008. Dissecting the cell entry pathway of dengue virus by single-particle tracking in living cells. *PLoS Pathog,* 4**,** e1000244.

VAN DUIJL-RICHTER, M. K. S., HOORNWEG, T. E., RODENHUIS-ZYBERT, I. A. & SMIT, J. M. 2015. Early Events in Chikungunya Virus Infection-From Virus Cell Binding to Membrane Fusion. *Viruses,* 7**,** 3647-3674.

VAN DYKE, R. W. 1993. Acidification of rat liver lysosomes: quantitation and comparison with endosomes. *Am J Physiol,* 265**,** C901-17.

VAN DYKE, R. W. 1996. Acidification of lysosomes and endosomes. *Subcell Biochem,* 27**,** 331-360.

VEGA-ALMEIDA, T. O., SALAS-BENITO, M., DE NOVA-OCAMPO, M. A., DEL ANGEL, R. M. & SALAS-BENITO, J. S. 2013. Surface proteins of C6/36 cells involved in dengue virus 4 binding and entry. *Arch Virol,* 158**,** 1189-1207.

VOLK, D. E., BEASLEY, D. W. C., KALLICK, D. A., HOLBROOK, M. R., BARRETT, A. D. T. & GORENSTEIN, D. G. 2004. Solution structure and antibody binding studies of the envelope protein domain III from the New York strain of West Nile virus. *J Biol Chem,* 279**,** 38755-38761.

VON LINDERN, J. J., ARONER, S., BARRETT, N. D., WICKER, J. A., DAVIS, C. T. & BARRETT, A. D. T. 2006. Genome analysis and phylogenetic relationships between east, central and west African isolates of Yellow fever virus. *J Gen Virol,* 87**,** 895-907.

VORNDAM, A. V., MATHEWS, J. H., BARRETT, A. D. T., ROEHRIG, J. T. & TRENT, D. W. 1993. Molecular and biological characterization of a non-glycosylated isolate of St Louis encephalitis virus. *J Gen Virol,* 74**,** 2653-2660.

VOSSMAN, S., WIESELER, J., KERBER, R. & KÜMMERER, B. M. 2015. A basic cluster in the N terminus of yellow fever virus NS2A contributes to infectious particle production. *J Virol,* 89**,** 4951-4965.

WAGSTAFF, K. M., SIVAKUMARAN, H., HEATON, S. M., HARRICH, D. & JANS, D. A. 2012. Ivermectin is a specific inhibitor of importin α/β-mediated nuclear import able to inhibit replication of HIV-1 and dengue virus. *Biochem J,* 443**,** 851-856.

WAHALA, W. M. P. B., KRAUS, A. A., HAYMORE, L. B., ACCAVITTI-LOPER, M. A. & DE SILVA, A. M. 2009. Dengue virus neutralization by human immune sera: role of envelope protein domain III-reactive antibody. *Virology,* 392**,** 103-113.

WAN, S.-W., LU, Y.-T., HUANG, C.-H., LIN, C.-F., ANDERSON, R., LIU, H.-S., YEH, T.-M., YEN, Y.-T., WU-HSIEH, B. A. & LIN, Y.-S. 2014. Protection against dengue virus infection in mice by administration of antibodies against modified nonstructural protein 1. *PLoS One,* 9**,** e92495.

WEBSTER, L. T. 1938. Japanese B Encephalitis Virus: Its Differentiation from St. Louis Encephalitis Virus and Relationship to Louping Ill Virus. *J Exp Med,* 67**,** 609-618.

WEBSTER, L. T. & FITE, G. L. 1934. St. Louis Encephalitis. *Science,* 79**,** 254-255.

WEBSTER, L. T., FITE, G. L., CLOW, A. D. & MUENCH, H. 1935. Experimental Studies on Encephalitis IV. Specific Inactivation of Virus by Sera from Persons Exposed to Encephalitis, St. Louis Type, 1933 with a Note on the Evaluation of the Results of Mouse Tests of Sera. *J Exp Med,* 62**,** 827-847.

WECKSTRÖM, P. & NYHOLM, M. 1965. Electron Microscopy of a Tick-Borne Encephalitis Virus. *Nature,* 205**,** 211-212.

WEI, H.-Y., JIANG, L.-F., FANG, D.-Y. & GUO, H.-Y. 2003. Dengue virus type 2 infects human endothelial cells through binding of the viral envelope glycoprotein to cell surface polypeptides. *J Gen Virol,* 84**,** 3095-3098.

WEINBREN, M. P. 1955. The occurrence of West Nile virus in South Africa. *S Afr Med J,* 29**,** 1092-1097.

WEISS, D., CARR, D., KELLACHAN, J., TAN, C., PHILLIPS, M., BRESNITZ, E., LAYTON, M. & GROUP, W. N. V. O. R. W. 2001. Clinical findings of West Nile virus infection in hospitalized patients, New York and New Jersey, 2000. *Emerging Infect Dis,* 7**,** 654-658.

WENGLER, G., BEATO, M. & WENGLER, G. 1979. In Vitro Translation of 42 S Virus-Specific RNA from Cells Infected with the Flavivirus West Nile Virus. *Virology,* 96**,** 516-529.

WENGLER, G. & CASTLE, E. 1986. Analysis of structural properties which possibly are characteristic for the 3'-terminal sequence of the genome RNA of flaviviruses. *J Gen Virol,* 67**,** 1183-1188.

WENGLER, G., CASTLE, E., LEIDNER, U., NOWAK, T. & WENGLER, G. 1985. Sequence analysis of the membrane protein V3 of the flavivirus west nile virus and of its gene. *Virology,* 147**,** 264-274.

WENGLER, G. & WENGLER, G. 1981. Terminal sequences of the genome and replicative-from RNA of the flavivirus West Nile virus: absence of poly(A) and possible role in RNA replication. *Virology,* 113**,** 544-555.

WENGLER, G. & WENGLER, G. 1989a. An analysis of the antibody response against West Nile virus E protein purified by SDS-PAGE indicates that this protein does not contain sequential epitopes for efficient induction of neutralizing antibodies. *J Gen Virol,* 70**,** 987-992.

WENGLER, G. & WENGLER, G. 1989b. Cell-Associated West Nile Flavivirus is Covered with E+pre-M Protein Heterodimers Which Are Destroyed and Reorganized by Proteolytic Cleavage during Virus Release. *J Virol,* 63**,** 2521-2526.

WENGLER, G. & WENGLER, G. 1991. The carboxy-terminal part of the NS 3 protein of the West Nile flavivirus can be isolated as a soluble protein after proteolytic cleavage and represents an RNA-stimulated NTPase. *Virology,* 184**,** 707-715.

WENGLER, G. & WENGLER, G. 1993. The NS 3 nonstructural protein of flaviviruses contains an RNA triphosphatase activity. *Virology,* 197**,** 265-273.

WENGLER, G., WENGLER, G. & GROSS, H. J. 1978. Studies on virus-specific nucleic acids synthesized in vertebrate and mosquito cells infected with flaviviruses. *Virology,* 89**,** 423-437.

WERME, K., WIGERIUS, M. & JOHANSSON, M. 2008. Tick-borne encephalitis virus NS5 associates with membrane protein scribble and impairs interferon-stimulated JAK-STAT signalling. *Cell Microbiol,* 10**,** 696-712.

WESTAWAY, E. G. 1973. Proteins Specified by Group B Togaviruses in Mammalian Cells During Productive Infections. *Virology,* 51**,** 454-465.

WESTAWAY, E. G. 1975. The Proteins of Murray Valley Encephalitis Virus. *J Gen Virol,* 27**,** 283-292.

WESTAWAY, E. G. 1977. Strategy of the flavivirus genome: Evidence for multiple internal initiation of translation of proteins specified by Kunjin virus in mammalian cells. *Virology,* 80**,** 320-335.

WESTAWAY, E. G. 1980. Replication of Flaviviruses. *In:* SCHLESINGER, R. W. (ed.) 1st ed. New York: Academic Press.

WESTAWAY, E. G. 1987. Flavivirus Replication Strategy. *Adv Virus Res,* 33**,** 45-90.

WESTAWAY, E. G., KHROMYKH, A. A. & MACKENZIE, J. M. 1999. Nascent flavivirus RNA colocalized in situ with double-stranded RNA in stable replication complexes. *Virology,* 258**,** 108-117.

WESTAWAY, E. G., MACKENZIE, J. M., KENNEY, M. T., JONES, M. K. & KHROMYKH, A. A. 1997. Ultrastructure of Kunjin virus-infected cells: colocalization of NS1 and NS3 with double-stranded RNA, and of NS2B with NS3, in virus-induced membrane structures. *J Virol,* 71**,** 6650-6661.

WESTAWAY, E. G., MCKIMM, J. L. & MCLEOD, L. G. 1977. Heterogeneity Among Flavivirus Proteins Separated in Slab Gels. *Arch Virol,* 53**,** 305-312.

WESTAWAY, E. G. & REEDMAN, B. M. 1969. Proteins of the group B arbovirus Kunjin. *J Virol,* 4**,** 688-693.

WESTAWAY, E. G., SCHLESINGER, R. W., DALRYMPLE, J. M. & TRENT, D. W. 1980. Nomenclature of Flavivirus-Specific Proteins. *Intervirology,* 14**,** 114-117.

WESTAWAY, E. G. & SHEW, M. 1977. Proteins and glycoproteins specified by the flavivirus Kunjin. *Virology,* 80**,** 309-319.

WHITEHEAD, S. S., HANLEY, K. A., BLANEY, J. E., GILMORE, L. E., ELKINS, W. R. & MURPHY, B. R. 2003. Substitution of the structural genes of dengue virus type 4 with those of type 2 results in chimeric vaccine candidates which are attenuated for mosquitoes, mice, and rhesus monkeys. *Vaccine,* 21**,** 4307-4316.

WHO. 2015. *Dengue and Severe Dengue* [Online]. Geneva: World Health Organization. Available: http://www.who.int/mediacentre/factsheets/fs117/en/ [Accessed 21 Jul 2015 2015].

WICHIT, S., JITTMITTRAPHAP, A., HIDARI, K. I. P. J., THAISOMBOONSUK, B., PETMITR, S., UBOL, S., AOKI, C., ITONORI, S., MORITA, K., SUZUKI, T., SUZUKI, Y. & JAMPANGERN, W. 2011. Dengue virus type 2 recognizes the

carbohydrate moiety of neutral glycosphingolipids in mammalian and mosquito cells. *Microbiol Immunol,* 55**,** 135-140.

WIGGE, P., KÖHLER, K., VALLIS, Y., DOYLE, C. A., OWEN, D., HUNT, S. P. & MCMAHON, H. T. 1997. Amphiphysin heterodimers: potential role in clathrin-mediated endocytosis. *Mol Biol Cell,* 8**,** 2003-2015.

WILLIAMS, P. 1883. Second Report by Special Committee on "Louping-Ill" and "Braxy". *Trans Highland Ag Soc Scot,* 15**,** 176-201.

WILLIAMS, P. 1897. Louping Ill: Further Researches into the Causation and Prevention of Louping-Ill or Trembling in Sheep. *Trans Highland Ag Soc Scot,* 11**,** 278-290.

WILSON, J. R., DE SESSIONS, P. F., LEON, M. A. & SCHOLLE, F. 2008. West Nile virus nonstructural protein 1 inhibits TLR3 signal transduction. *J Virol,* 82**,** 8262-8271.

WONG, D., DOROVINI-ZIS, K. & VINCENT, S. R. 2004. Cytokines, nitric oxide, and cGMP modulate the permeability of an in vitro model of the human blood-brain barrier. *Exp Neurol,* 190**,** 446-455.

WOODSON, S. E., FREIBERG, A. N. & HOLBROOK, M. R. 2013. Coagulation factors, fibrinogen and plasminogen activator inhibitor-1, are differentially regulated by yellow fever virus infection of hepatocytes. *Virus Res,* 175**,** 155-159.

WORK, T. H., HURLBUT, H. S. & TAYLOR, R. M. 1953. Isolation of West Nile virus from hooded crow and rock pigeon in the Nile delta. *Proc Soc Exp Biol Med,* 84**,** 719-722.

WORK, T. H., HURLBUT, H. S. & TAYLOR, R. M. 1955. Indigenous wild birds of the Nile Delta as potential West Nile virus circulating reservoirs. *Am J Trop Med Hyg,* 4**,** 872-888.

WRIGHT, P. J., BOWDEN, D. S. & WESTAWAY, E. G. 1977. Unique peptide maps of the three largest proteins specified by the flavivirus Kunjin. *J Virol,* 24**,** 651-661.

WRIGHT, P. J. & WESTAWAY, E. G. 1977. Comparisons of the peptide maps of Kunjin virus proteins smaller than the envelope protein. *J Virol,* 24**,** 662-672.

WU, M.-F., CHEN, S.-T., YANG, A.-H., LIN, W.-W., LIN, Y.-L., CHEN, N.-J., TSAI, I.-S., LI, L. & HSIEH, S.-L. 2013. CLEC5A is critical for dengue virus-induced inflammasome activation in human macrophages. *Blood,* 121**,** 95-106.

XIE, X., GAYEN, S., KANG, C., YUAN, Z. & SHI, P.-Y. 2013. Membrane topology and function of dengue virus NS2A protein. *J Virol,* 87**,** 4609-4622.

YANG, M.-R., LEE, S. R., OH, W., LEE, E.-W., YEH, J.-Y., NAH, J.-J., JOO, Y.-S., SHIN, J., LEE, H.-W., PYO, S. & SONG, J. 2008. West Nile virus capsid protein induces p53-mediated apoptosis via the sequestration of HDM2 to the nucleolus. *Cell. Microbiol.,* 10**,** 165-176.

YANG, S.-H., LIU, M.-L., TIEN, C.-F., CHOU, S.-J. & CHANG, R.-Y. 2009a. Glyceraldehyde-3-phosphate dehydrogenase (GAPDH) interaction with 3' ends of Japanese encephalitis virus RNA and colocalization with the viral NS5 protein. *J. Biomed. Sci.,* 16**,** 40.

YANG, T.-C., SHIU, S.-L., CHUANG, P.-H., LIN, Y.-J., WAN, L., LAN, Y.-C. & LIN, C.-W. 2009b. Japanese encephalitis virus NS2B-NS3 protease induces caspase 3 activation and mitochondria-mediated apoptosis in human medulloblastoma cells. *Virus Res,* 143**,** 77-85.

YE, Q., LI, X.-F., ZHAO, H., LI, S.-H., DENG, Y.-Q., CAO, R.-Y., SONG, K.-Y., WANG, H.-J., HUA, R.-H., YU, Y.-X., ZHOU, X., QIN, E.-D. & QIN, C.-F. 2012. A single nucleotide mutation in NS2A of Japanese encephalitis-live vaccine virus (SA14-14-2) ablates NS1' formation and contributes to attenuation. *J Gen Virol,* 93**,** 1959-1964.

YIANG, G.-T., CHEN, Y.-H., CHOU, P.-L., CHANG, W.-J., WEI, C.-W. & YU, Y.-L. 2013. The NS3 protease and helicase domains of Japanese encephalitis virus trigger cell death via caspase-dependent and -independent pathways. *Mol Med Rep,* 7**,** 826-830.

YON, C., TERAMOTO, T., MUELLER, N., PHELAN, J., GANESH, V. K., MURTHY, K. H. M. & PADMANABHAN, R. 2005. Modulation of the nucleoside triphosphatase/RNA helicase and 5'-RNA triphosphatase activities of Dengue virus type 2 nonstructural protein 3 (NS3) by interaction with NS5, the RNA-dependent RNA polymerase. *J Biol Chem,* 280**,** 27412-27419.

YOSHII, K., SUNDEN, Y., YOKOZAWA, K., IGARASHI, M., KARIWA, H., HOLBROOK, M. R. & TAKASHIMA, I. 2014. A critical determinant of

neurological disease associated with highly pathogenic tick-borne flavivirus in mice. *J Virol,* 88**,** 5406-5420.

YOSHINAKA, Y. & HOTTA, S. 1971. Purification of arboviruses grown in tissue culture. *Proc Soc Exp Biol Med,* 137**,** 1047-1053.

YOU, S. & PADMANABHAN, R. 1999. A novel in vitro replication system for Dengue virus. Initiation of RNA synthesis at the 3'-end of exogenous viral RNA templates requires 5'- and 3'-terminal complementary sequence motifs of the viral RNA. *J Biol Chem,* 274**,** 33714-33722.

YOUN, S., LI, T., MCCUNE, B. T., EDELING, M. A., FREMONT, D. H., CRISTEA, I. M. & DIAMOND, M. S. 2012. Evidence for a genetic and physical interaction between nonstructural proteins NS1 and NS4B that modulates replication of West Nile virus. *J Virol,* 86**,** 7360-7371.

YOUNG, L. B., MELIAN, E. B. & KHROMYKH, A. A. 2013. NS1' colocalizes with NS1 and can substitute for NS1 in West Nile virus replication. *J Virol,* 87**,** 9384-9390.

YOUNG, P. R., BLETCHLY, C. & MACKENZIE, J. S. 1993. Antigenic and Structural Analysis of the Dengue Virus Glycoprotein, NS1. *In:* UREN, M. F. (ed.) *Proceedings of the 6th Symposium on Arbovirus Research in Australia.* Brisbane: Queensland Institute of Medical Research.

YU, I.-M., ZHANG, W., HOLDAWAY, H. A., LI, L., KOSTYUCHENKO, V. A., CHIPMAN, P. R., KUHN, R. J., ROSSMANN, M. G. & CHEN, J. 2008. Structure of the immature dengue virus at low pH primes proteolytic maturation. *Science,* 319**,** 1834-1837.

YU, L., TAKEDA, K. & MARKOFF, L. 2013. Protein-protein interactions among West Nile non-structural proteins and transmembrane complex formation in mammalian cells. *Virology,* 446**,** 365-377.

YUSOF, R., CLUM, S., WETZEL, M., MURTHY, H. M. & PADMANABHAN, R. 2000. Purified NS2B/NS3 serine protease of dengue virus type 2 exhibits cofactor NS2B dependence for cleavage of substrates with dibasic amino acids in vitro. *J Biol Chem,* 275**,** 9963-9969.

ZHAN, C., ZHAO, L., CHEN, X., LU, W.-Y. & LU, W. 2013. Total Chemical Synthesis of Dengue 2 Virus Capsid Protein via Native Chemical Ligation: Role of the Conserved Salt-Bridge. *Bioorg Med Chem,* 21**,** 3443-3449.

ZHANG, B., DONG, H., STEIN, D. A., IVERSEN, P. L. & SHI, P.-Y. 2008. West Nile virus genome cyclization and RNA replication require two pairs of long-distance RNA interactions. *Virology,* 373**,** 1-13.

ZHANG, S., BOVSHIK, E. I., MAILLARD, R., GROMOWSKI, G. D., VOLK, D. E., SCHEIN, C. H., HUANG, C. Y. H., GORENSTEIN, D. G., LEE, J. C., BARRETT, A. D. T. & BEASLEY, D. W. C. 2010. Role of BC loop residues in structure, function and antigenicity of the West Nile virus envelope protein receptor-binding domain III. *Virology,* 403**,** 85-91.

ZHANG, S., LI, L., WOODSON, S. E., HUANG, C. Y. H., KINNEY, R. M., BARRETT, A. D. T. & BEASLEY, D. W. C. 2006. A mutation in the envelope protein fusion loop attenuates mouse neuroinvasiveness of the NY99 strain of West Nile virus. *Virology,* 353**,** 35-40.

ZHANG, S., VOGT, M. R., OLIPHANT, T., ENGLE, M., BOVSHIK, E. I., DIAMOND, M. S. & BEASLEY, D. W. C. 2009. Development of resistance to passive therapy with a potently neutralizing humanized monoclonal antibody against West Nile virus. *JID,* 200**,** 202-205.

ZHANG, W., CHIPMAN, P. R., CORVER, J., JOHNSON, P. R., ZHANG, Y., MUKHOPADHYAY, S., BAKER, T. S., STRAUSS, J. H., ROSSMANN, M. G. & KUHN, R. J. 2003a. Visualization of membrane protein domains by cryo-electron microscopy of dengue virus. *Nat Struct Biol,* 10**,** 907-912.

ZHANG, X., SHENG, J., PLEVKA, P., KUHN, R. J., DIAMOND, M. S. & ROSSMANN, M. G. 2013. Dengue structure differs at the temperatures of its human and mosquito hosts. *PNAS,* 110**,** 6795-6799.

ZHANG, Y., CORVER, J., CHIPMAN, P. R., ZHANG, W., PLETNEV, S. V., SEDLAK, D., BAKER, T. S., STRAUSS, J. H., KUHN, R. J. & ROSSMANN, M. G. 2003b. Structures of immature flavivirus particles. *EMBO J,* 22**,** 2604-2613.

ZHAO, Y., SOH, T. S., ZHENG, J., CHAN, K. W. K., PHOO, W. W., LEE, C. C., TAY, M. Y. F., SWAMINATHAN, K., CORNVIK, T. C., LIM, S. P., SHI, P.-Y., LESCAR, J., VASUDEVAN, S. G. & LUO, D. 2015. A crystal structure of the

Dengue virus NS5 protein reveals a novel inter-domain interface essential for protein flexibility and virus replication. *PLoS Pathog,* 11**,** e1004682.

ZHU, Y.-Z., CAO, M.-M., WANG, W.-B., WANG, W., REN, H., ZHAO, P. & QI, Z.-T. 2012. Association of heat-shock protein 70 with lipid rafts is required for Japanese encephalitis virus infection in Huh7 cells. *J Gen Virol,* 93**,** 61-71.

ZOU, G., PUIG-BASAGOITI, F., ZHANG, B., QING, M., CHEN, L., PANKIEWICZ, K. W., FELCZAK, K., YUAN, Z. & SHI, P.-Y. 2009a. A single-amino acid substitution in West Nile virus 2K peptide between NS4A and NS4B confers resistance to lycorine, a flavivirus inhibitor. *Virology,* 384**,** 242-252.

ZOU, G., ZHANG, B., LIM, P.-Y., YUAN, Z., BERNARD, K. A. & SHI, P.-Y. 2009b. Exclusion of West Nile virus superinfection through RNA replication. *J Virol,* 83**,** 11765-11776.

ZOU, J., LEE, L. T., WANG, Q. Y., XIE, X., LU, S., YAU, Y. H., YUAN, Z., GEIFMAN SHOCHAT, S., KANG, C., LESCAR, J. & SHI, P.-Y. 2015a. Mapping the Interactions between the NS4B and NS3 proteins of dengue virus. *J Virol,* 89**,** 3471-3483.

ZOU, J., XIE, X., LEE, L. T., CHANDRASEKARAN, R., REYNAUD, A., YAP, L., WANG, Q. Y., DONG, H., KANG, C., YUAN, Z., LESCAR, J. & SHI, P.-Y. 2014. Dimerization of flavivirus NS4B protein. *J Virol,* 88**,** 3379-3391.

ZOU, J., XIE, X., WANG, Q. Y., DONG, H., LEE, M. Y., KANG, C., YUAN, Z. & SHI, P.-Y. 2015b. Characterization of dengue virus NS4A and NS4B protein interaction. *J Virol,* 89**,** 3455-3470.

ZUO, Z., LIEW, O. W., CHEN, G., CHONG, P. C. J., LEE, S. H., CHEN, K., JIANG, H., PUAH, C. M. & ZHU, W. 2009. Mechanism of NS2B-mediated activation of NS3pro in dengue virus: molecular dynamics simulations and bioassays. *J Virol,* 83**,** 1060-1070.

Vita

Alexander McAuley was born in Newport, UK on the 28th June 1987 to John and Philippa McAuley. Prior to emigrating to the United States in 2009, Alex completed his undergraduate Master of Biology degree in Molecular and Cellular Biology with honours. During the course of his undergraduate studies, Alex was afforded the opportunity to spend a year as a placement student at the Health Protection Agency at Porton Down, where he worked to characterise the human immune response to the UK anthrax vaccine.

Whilst at UTMB, Alex has trained at BSL-3 and BSL-4, and is an approved mentor at each of the biosafety levels. He has received predoctoral fellowships from both the James W. McLaughlin Endowment Fund and the Jeane B. Kempner Fund. He has additionally been awarded two Zhou Sisters Great Expectations Awards, and an American Society for Virology travel award.

In 2014, Alex married a rather charming Texan called Kristen, and they are planning to move to Vancouver, Canada next year to allow Alex to pursue a postdoctoral position at the University of British Columbia working to characterise host determinants of West Nile virus infection.

EDUCATION

MBiol, July 2009, University of Bath, Bath, Somerset, United Kingdom

PUBLICATIONS

Research Papers

McAuley, A. J., Torres, M., Plante, J. A., Huang, C., Bente, D. A., Beasley, D. W. C. (2015) Generation and Characterization of Flavivirus Receptor-Binding Domain Chimaeras. *J Virol* (Paper Submitted)

McAuley, A. J., Sawatsky, B. M., Beasley, D. W. C., Bente, D. A. (2015) Cross-Neutralization of Tick-Borne Flaviviruses Following Tick-Borne Encephalitis Vaccination or Infection (Paper in Preparation)

McAuley, A. J. & Beasley, D. W. C. (2015) Propagation and Titration of West Nile Virus on Vero Cells. *Methods Mol Biol* (Book Chapter Accepted)

Kortekaas, J., Vloet, R. P. M., **McAuley, A. J.**, Shen, X., Bosch, B. J., de Vries, L., Moormann, R. J. M., Bente, D. A. (2015) Crimean-Congo Hemorrhagic Fever Virus Subunit Vaccines Induce High Levels of Neutralizing Antibodies but No Protection in STAT01 Knockout Mice. *Vector-Borne Zoonotic Dis* (In Press)

Arasli, M., Ozsurekci, Y., Eladi, N., **McAuley, A. J.**, Karadag Oncel, E., Tekin, I. O., Kaya, A., Icagasioglu, F. D., Caglayik, D. Y., Korukluoglu, G., Kokturk, F., Bakir, M., Bente, D. A., Ceyhan, M. (2015) Elevated Chemokine Levels During Adult but not Pediatric Crimean-Congo Hemorrhagic Fever. *J Clin Virol* **66**:76-82

Nuckols, J. T., **McAuley, A. J.**, Huang, Y.-J., Horne, K. M., Higgs, S. J., Davey, R. A., Vanlandingham, D. L. (2014) pH-Dependent Entry of Chikungunya Virus Fusion into Mosquito Cells. *Virol J* 11(**1**):215

Kim, D.-Y., Atasheva, S., **McAuley, A. J.**, Plante, J. A., Frolova, E. I., Beasley, D. W. C., Frolov, I. (2014) Enhancement of Protein Expression by Alphavirus Replicons by Designing Self-Replicating Subgenomic RNAs. *PNAS* 111**(29)**:10708-10713

Sawatsky, B. M., **McAuley, A. J.**, Holbrook, M. R., Bente, D. A. (2014) Comparative Pathogenesis of Alkhumra Hemorrhagic Fever and Kyasanur Forest Disease Viruses in a Mouse Model. *PLoS Negl Trop Dis* 8**(6)**:e2934

Nuckols, J. T., Ziegler, S. A., Huang, Y.-J., **McAuley, A. J.**, Vanlandingham, D. L., Klowden, M. J., Spratt, H., Davey, R. A., Higgs, S. J. (2013) Infection of *Aedes albopictus* with Chikungunya Virus Rectally Administered by Enema. *Vector-Borne Zoonotic Dis* 13**(2)**:103-110

Bowick, G. C. & **McAuley, A. J.** (2011) Meta-Analysis of High Throughput Datasets Reveals Cellular Responses Following Haemorrhagic Fever Virus Infection. *Viruses* 3**(5)**:613-619

Review Papers

Beasley, D. W. C., **McAuley, A. J.**, Bente, D. A. (2015) Yellow Fever Virus: Genetic and Phenotypic Diversity and Implications for Detection, Prevention and Therapy. *Antiviral Res* 115:48-70

Bente, D. A., Forrester, N., Watts, D., **McAuley, A. J.**, Whitehouse, C., Bray, M. (2013) Natural History and Genetic Diversity of Crimean-Congo Hemorrhagic Fever Virus. *Antiviral Res* 100**(1)**:159-189

Bowick, G. C. & **McAuley, A. J.** (2011) Vaccine and Adjuvant Design for Emerging Viruses: Mutations, Deletions, Segments and Signalling. *Bioengineered Bugs* 2**(3)**:129-135

Presentations

McAuley, A. J., Bente, D. A., Beasley, D. W. C. (2015) Generation and Characterisation of Flavivirus Receptor-Binding Domain Chimaeras [oral presentation]. *Presented at:* American Society for Virology 34th Annual Meeting, 10-15 July 2014, University of Western Ontario, London, ON, Canada

McAuley, A. J., Bente, D. A., Beasley, D. W. C. (2014) Generation and Characterisation of Flavivirus Receptor-Binding Domain Chimaeras [poster]. *Presented at:* American Society for Virology 33rd Annual Meeting, 21-24 June 2014, Colorado State University, Fort Collins, CO, USA

Permanent address: 810 Ferry Road Apt 203, Galveston, TX 77550

This dissertation was typed by the author